

REMARKS

The Applicants respectfully request reconsideration of the present application in view of the foregoing amendments and in view of the reasons that follow.

I. Amendments to the claims

Claims 24 and 33 are currently being amended. The claim amendments do not add new matter. Exemplary support for the amended claims can be found in the specification at page 6, lines 17-35.

This amendment adds, changes and/or deletes claims in this application. A detailed listing of all claims that are, or were, in the application, irrespective of whether the claim(s) remain under examination in the application, is presented, with an appropriate defined status identifier.

After amending the claims as set forth above, claims 24-34 are now pending in this application.

II. Claim rejections – 35 U.S.C. § 101/112, first paragraph, lack of utility, enablement

Claims 24-34 are rejected under 35 U.S.C. § 101 and 35 U.S.C. § 112, first paragraph, as allegedly lacking utility. The office action asserts that “since the claimed invention is not supported by either a specific and substantial asserted utility or a well established utility for the reasons set forth in the previous Office Action (23 January 2006), one skilled in the art clearly would not know how to use the claimed invention.” The Applicants respectfully traverse this ground for rejection. Independent claims 24 and 33 have been amended; as such, the claims are now “supported by either a specific and substantial utility or a well established utility.”

As is well appreciated, it is acceptable for an applicant to rely on post-filing date publications from other research groups to relate experimental data in lieu of experiments performed by the Applicants to substantiate an assertion of utility. Accordingly, a BLAST sequence alignment (Exhibit A) is provided, which identifies a third-party database entry that is 100% identical in sequence to the amino acid sequence of SEQ ID NO: 28. This entry, submitted by researchers who are not “concerned parties,” reference a post filing date publication that substantiates a utility for the claimed human transmembrane protein of SEQ ID NO: 28, which is encoded by polynucleotide SEQ ID NO: 57.

The publication, Grasberger and Refetoff, *J. Biol. Chem.*, 281(27):18269-18272 (2006), (“Grasberger, *et al.*” Exhibit B), describes the characterization of a protein termed dual oxidase maturation factor 2 (“DUOXA2”). DUOXA2 is SEQ ID NO 28. (*See* sequence presented in Grasberger, *et al.* at 18270 and Exhibit A). DUOXA2 (SEQ ID NO: 28) is an endoplasmic reticulum (“ER”) transmembrane protein which functions to promote endoplasmic reticulum exit and protein maturation of cellular proteins such as dual oxidase 2, “DUOX2.” (*Id.* at 18270-71). The Specification at page 6, lines 16-35, describes endoplasmic reticulum transmembrane proteins which function in protein maturation and transport. (Specification at 6, lines 16-35). Thus, the Office Action assertions that “very little information is given in the instant Specification about a specific function for the HTMP protein,” and that “the claimed HTMP nucleic acid [and protein] is probably not a member of any of the protein families listed in the Specification,” are incorrect. (Office Action at 4).

Further, in transporting DUOX2 to cell membranes, SEQ ID NO:28 has been shown to play a role in the production of thyroid hormone. (Grasberger, *et al.* at 18269). Thyroid hormone has been known to play a role in some smooth muscle disorders, such as some types of cardiovascular disease, and has also been implicated in reproductive and neurological disorders. (*See e.g.* , Buccino, *et al.* , *Influence of the Thyroid State*, J. Clin. Investigation, 46(10):1669-1682 (1967), Exhibit C; Wharton, G.K., *Unrecognized Hypothyroidism*, Can. Med. Assn. J., April, 371-376 (1939), Exhibit D; Martin, *et al.* , *Peripheral Neuropathy in Hypothyroidism – an Association with Spurious Polycythaemia (Gaisbock’s Syndrome)*, J. Royal Soc. Med., 76:187-189 (1983), Exhibit E; Semple, *et al.*, *Hypothyroidism Presenting*

with Hyperprolactinaemia, British Med. J., 286:1200-1201 (1983), Exhibit F; Inuwa, *et al.*, *Morphometric Study on the Uterine Horn and Thyroid Gland in Hypothyroid, and Thyroxine Treated Hypothyroid Rats*, J. Anat., 188:383-393 (1996), including a review of hypothyroidism and reproductive consequences in the introduction, Exhibit G). Thus, detection of aberrant SEQ ID NO: 28 activity or expression is likely indicative of aberrant thyroid levels; as noted in the specification, detection, diagnosis and treatment of smooth muscle, reproductive and neurological disorders may be achieved. (See Specification at page 8 lines 21-24; pages 36 and 37). Additionally, SEQ ID NO:28 has been implicated as a possible cause of hypothyroidism. (Grasberger, *et al.* at 18269).

Accordingly, the Office Action assertions that there is “no nexus between the HTMP and any disease” and that “significant experimentation would be required of the skilled artisan to specifically characterize the protein and search of possible diseases caused by mutation of the HTMP protein” are also incorrect. (Office Action at 5). As such, the claimed invention may be used as described in the specification to detect, diagnose, characterize and treat disease by detecting the presence, absence and/or amount of SEQ ID NO: 57 and variants thereof (*e.g.*, gene mutations, mRNA abnormalities, etc.), or SEQ ID NO: 28 and variants thereof. (See *e.g.*, specification at page 45 lines 5-7, 34-35 and lines 27-29).

Thus, the peptide encoded by SEQ ID NO: 28 and the nucleic acid which encodes this peptide, SEQ ID NO: 57, have a credible, specific and substantial utility.

For at least the reasons stated above, reconsideration and withdrawal of the rejection under 35 U.S.C. § 101 and § 112 first paragraph, for lack of utility and enablement is requested.

III. Claim Rejection – 35 U.S.C. § 112, first paragraph – written description

The Office Action asserts that claims 24, 27-30 and 33 are rejected under 35 U.S.C. § 112, first paragraph, as allegedly “containing subject matter which was not described in the specification in such a way as to reasonably convey to one skilled in the relevant art that the inventor, at the time the application was filed, had possession of the claimed invention.” (Office Action at 8). The Office Action asserts that “Applicants have not described or shown

possession of all polypeptides 95% homologous to SEQ ID NO: 28, that are functionally equivalent to SEQ ID NO: 28.” *Id.* The Office Action further asserts that the Applicants have not described “a representative number of species that have 95% homology to SEQ ID NO: 28, such that it is clear that they were in possession of a genus of polypeptides functionally similar to SEQ ID NO: 28.” The Applicants respectfully traverse the rejection.

The claims have been amended to include the following functional language: “wherein the polypeptide functions to promote protein exit from the endoplasmic reticulum and protein maturation.” The specification fully supports the amended claims and one skilled in the art would determine that the inventors had possession of the claimed invention at the time of filing.

“What is conventional or well known to one of ordinary skill in the art need not be disclosed in detail,” and “if a skilled artisan would have understood the inventor to be in possession of the claimed invention at the time of filing, even if every nuance of the claims is not explicitly described in the specification, then the adequate description requirement is met.” (MPEP § 2163.II.A.3). Here, it would have been routine—conventional—for one of skill in the art to perform assays to simply determine whether a transmembrane protein that has 95% homology to SEQ ID NO: 28 functions to promote protein exit from the ER and protein maturation.

For example, host cells (*e.g.*, HeLa cells) could be transfected with a “target protein” which requires the activity of SEQ ID NO: 28 to exit the ER or for maturation. An exemplary target protein is the dual oxigenase 2 protein, “DUOX2” (as described in Grasberger, *et al.* at 18269 and 18271). Without a transmembrane protein such as SEQ ID NO: 28, the target protein remains in the ER; it is not transported to the plasma membrane or to other regions of the cell and thus cannot be detected on the outside of the cell or in other regions of the cell. And, without SEQ ID NO: 28, a target protein such as DUOX2 cannot mature and cannot effectively perform its function, (*e.g.*, generate H₂O₂, Grasberger, *et al.* at 18271). A co-transfection with the transmembrane protein (*e.g.*, a peptide having 95% homology to SEQ ID NO: 28) and the target protein can be performed. This can be followed by an assay for 1) the presence of the target protein on the plasma membrane or in non-ER regions of the cell, 2)

the mature protein, and/or 3) the mature protein function. One of skill in the art could then easily determine whether the transmembrane protein functioned to promote exit of the target protein from the ER and protein maturation. Additionally or alternatively, ER preparations of host cells transfected with the target protein alone and host cells transfected with both the target protein and the transmembrane protein could be performed by methods known in the art (e.g., Sigma Endoplasmic Reticulum Isolation Kit, SIGMA, St. Louis, Missouri; *see also* Dallner, *Isolation of Rough and Smooth Microsomes – General*, Methods in Enzymol., 31:191-201 (1974), Exhibit H; Adelman, *et al.*, *Non-destructive Separation of Rat Liver Rough Microsomes into Ribosomal and membranous Components*, Methods in Enzymol., 31:2011-215 (1974), Exhibit I; Schenkman, *et al.*, *Preparation of Microsomes with Calcium*, Methods in Enzymol., 52:83-89 (1978), Exhibit J). Then, the presence, absence and amount of the target protein in the ER could be evaluated to determine whether the transmembrane protein functioned to promote exit of the target from the ER and protein maturation.

Because it would be conventional or well known to one of ordinary skill in the art to perform assays to simply test for the specific function of the transmembrane protein, the specification as filed fully supports the amended claims reciting a polypeptide that has at least about 95% sequence identity to the amino acid of SEQ ID NO: 28. As such, reconsideration and withdrawal of the rejection is respectfully requested.

IV. Claim Rejection – 35 U.S.C. § 112, second paragraph

The Office Action asserts that claim 33 is rejected under 35 U.S.C. § 112, second paragraph, for allegedly being indefinite. The Office Action notes that “[a]mending the claim to recite ‘the polynucleotide of SEQ ID NO 57’ would overcome this rejection.” (Office Action at 10). Claim 33 has been amended as suggested by the Office Action. As such, reconsideration and withdrawal of the rejection under 35 U.S.C. §112, second paragraph, is requested.

V. Conclusion

The present application is now in condition for allowance. Favorable reconsideration of the application as amended is respectfully requested.

The Examiner is invited to contact the undersigned by telephone if it is felt that a telephone interview would advance the prosecution of the present application.

The Commissioner is hereby authorized to charge any additional fees which may be required regarding this application under 37 C.F.R. §§ 1.16-1.17, or credit any overpayment, to Deposit Account No. 19-0741. Should no proper payment be enclosed herewith, as by a check or credit card payment form being in the wrong amount, unsigned, post-dated, otherwise improper or informal or even entirely missing, the Commissioner is authorized to charge the unpaid amount to Deposit Account No. 19-0741.

If any extensions of time are needed for timely acceptance of papers submitted herewith, the Applicants hereby petition for such extension under 37 C.F.R. § 1.136 and authorize payment of any such extensions fees to Deposit Account No. 19-0741.

Respectfully submitted,

Date 11-20-06

By Stephanie H. Vavra

FOLEY & LARDNER LLP
Customer Number: 22428

Stephanie H. Vavra
Attorney for the Applicants
Registration No. 45,178
Telephone: (414-319-7305)
Facsimile: (414-297-4900)



results of BLAST

EXHIBIT A

BLASTP 2.2.15 [Oct-15-2006]

Reference:

Altschul, Stephen F., Thomas L. Madden, Alejandro A. Sch  ffer, Jinghui Zhang, Zheng Zhang, Webb Miller, and David J. Lipman (1997), "Gapped BLAST and PSI-BLAST: a new generation of protein database search programs", Nucleic Acids Res. 25:3389-3402.

Reference:

Sch  ffer, Alejandro A., L. Aravind, Thomas L. Madden, Sergei Shavirin, John L. Spouge, Yuri I. Wolf, Eugene V. Koonin, and Stephen F. Altschul (2001), "Improving the accuracy of PSI-BLAST protein database searches with composition-based statistics and other refinements", Nucleic Acids Res. 29:2994-3005.

RID: 1162490617-30379-65363355407.BLASTQ4

Database: All non-redundant GenBank CDS translations+PDB+SwissProt+PIR+PRF excluding environmental samples
4,099,826 sequences; 1,413,990,101 total letters

If you have any problems or questions with the results of this search please refer to the [BLAST FAQs](#)
[Taxonomy reports](#)

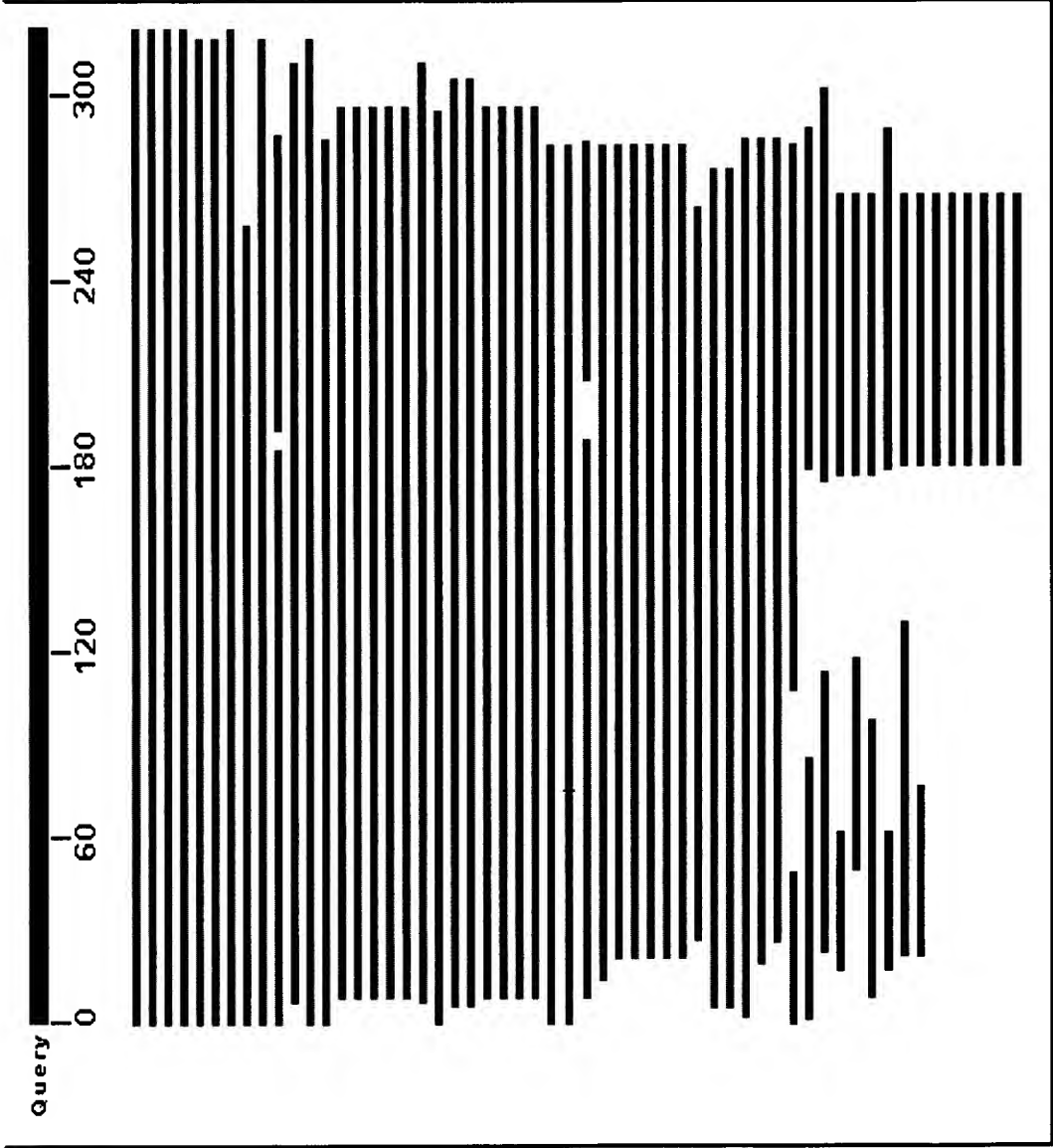
Query=
Length=320

Distribution of 93 Blast Hits on the Query Sequence

Mouse-over to show define and scores, click to show alignments

Color key for alignment scores

<40	40-50	50-80	80-200	>=200
-----	-------	-------	--------	-------



Distance tree of results [NEW](#)

Sequences producing significant alignments:

gi 94961770 gb ABF48256.1 	dual oxidase activator 2 [Homo sapien	646	0.0	UG
--	---	---------------------	---------------------	--------------------

gi 98986325 ref NP_997464.2 	dual oxidase activator 2 [Homo sapi	643	0.0	U G
gi 109080940 ref XP_001111110.1 	PREDICTED: similar to Numb-i...	616	4e-175	G
gi 74000506 ref XP_851517.1 	PREDICTED: similar to Numb-inter...	522	7e-147	U G
gi 13385246 ref NP_080053.1 	Numb-interacting protein 2 [Mus ...	508	1e-142	U G
gi 62645690 ref XP_575222.1 	PREDICTED: similar to Numb-inter...	507	3e-142	G
gi 76627905 ref XP_592260.2 	PREDICTED: similar to Numb-inter...	505	1e-141	G
gi 76627903 ref XP_876867.1 	PREDICTED: similar to Numb-inter...	444	3e-123	G
gi 12843239 dbj BAB25910.1 	unnamed protein product [Mus musculu	379	1e-103	U G
gi 114656759 ref XP_001146826.1 	PREDICTED: dual oxidase activat	367	3e-100	G
gi 62645692 ref XP_230527.2 	PREDICTED: similar to Numb-inter...	348	1e-94	G
gi 94366864 ref XP_001003392.1 	PREDICTED: similar to Numb-inter	347	4e-94	G
gi 76627911 ref XP_608616.2 	PREDICTED: similar to Numb-interact	343	6e-93	G
gi 94961772 gb ABF48257.1 	dual oxidase activator 1 [Homo sapien	342	2e-92	U G
gi 46485465 ref NP_653166.2 	Numb-interacting protein [Homo s...	342	2e-92	U G
gi 114656781 ref XP_001162743.1 	PREDICTED: Numb-interacting ...	341	3e-92	G
gi 114656785 ref XP_001162967.1 	PREDICTED: Numb-interacting ...	341	3e-92	G
gi 73999955 ref XP_544660.2 	PREDICTED: similar to Numb-inter...	341	3e-92	U G
gi 21703790 ref NP_663370.1 	Numb-interacting protein 1 [Mus ...	332	2e-89	U G
gi 68392693 ref XP_693410.1 	PREDICTED: similar to Numb-interact	292	2e-77	G
gi 50415464 gb AAH77555.1 	MGC83502 protein [Xenopus laevis]	278	2e-73	U G
gi 112418659 gb AAI22089.1 	Unknown (protein for MGC:147630) [Xe	274	5e-72	G
gi 109080942 ref XP_001111148.1 	PREDICTED: similar to Numb-inte	263	6e-69	G
gi 16552420 dbj BAB71304.1 	unnamed protein product [Homo sap...	261	3e-68	U G
gi 114656789 ref XP_001162827.1 	PREDICTED: Numb-interacting ...	260	5e-68	G
gi 73999957 ref XP_860877.1 	PREDICTED: similar to Numb-inter...	258	3e-67	U G
gi 50752733 ref XP_425055.1 	PREDICTED: similar to CDNA sequence	254	4e-66	G
gi 50752731 ref XP_425054.1 	PREDICTED: similar to CDNA sequence	244	3e-63	G
gi 47220524 emb CAG05550.1 	unnamed protein product [Tetraodon n	190	7e-47	G
gi 91079842 ref XP_970783.1 	PREDICTED: similar to CG4482-PA,...	157	6e-37	U G
gi 108876501 gb EAT40726.1 	conserved hypothetical protein [Aede	149	1e-34	G
gi 19921356 ref NP_609733.1 	moladietz CG4482-PA, isoform A [...	145	3e-33	U G
gi 58392116 ref XP_319114.2 	ENSANGP00000006016 [Anopheles ga...	143	1e-32	G
gi 54645694 gb EAL34432.1 	GA18214-PA [Drosophila pseudoobscura]	143	1e-32	G
gi 66513371 ref XP_393580.2 	PREDICTED: similar to moladietz ...	142	3e-32	G

gi 91088357 ref XP_971705.1	PREDICTED: similar to CG4482-PA,...	126	U G	1e-27
gi 72013586 ref XP_801771.1	PREDICTED: similar to ENSANGP000...	121	G	5e-26
gi 115738140 ref XP_001177754.1	PREDICTED: similar to ENSANG...	121	G	5e-26
gi 39591661 emb CAE71238.1	Hypothetical protein CBG18111 [Caeno	110		9e-23
gi 25149497 ref NP_498886.2	C06E1.3 [Caenorhabditis elegans]...	106	U G	1e-21
gi 25375307 pir A88533	hypothetical protein C06E1.3 - Caenorhab	103	U G	1e-20
gi 24584366 ref NP_723890.1	moladietz CG4482-PB, isoform B [...	99.4	U G	2e-19
gi 76627901 ref XP_876772.1	PREDICTED: similar to Numb-inter...	97.8	G	6e-19
gi 104781029 ref YP_607527.1	hypothetical protein PSEEN1884 ...	42.7	G	0.023
gi 67157078 ref ZP_00418440.1	Protein-disulfide reductase [A...	39.7		0.19
gi 69260554 ref ZP_00608077.1	Sulfatase [Magnetococcus sp. M...	39.3		0.25
gi 54024138 ref YP_118380.1	hypothetical protein nfa21700 [N...	38.5	G	0.42
gi 62180329 ref YP_216746.1	MFS superfamily, nitrite extrusi...	37.7	G	0.72
gi 16765106 ref NP_460721.1	nitrite extrusion protein [Salmo...	37.7	G	0.72
gi 16760121 ref NP_455738.1	nitrite extrusion protein (nitri...	37.7	G	0.72
gi 66045306 ref YP_235147.1	Protein of unknown function DUF2...	37.4	G	0.95
gi 91210447 ref YP_540433.1	nitrite extrusion protein [Esche...	37.0	G	1.2
gi 82776568 ref YP_402917.1	nitrite extrusion protein [Shige...	37.0	G	1.2
gi 30062747 ref NP_836918.1	nitrate transport protein nark [...	37.0	G	1.2
gi 26247549 ref NP_753589.1	Nitrite extrusion protein 1 [Esc...	37.0	G	1.2
gi 15801454 ref NP_287471.1	nitrite extrusion protein [Esche...	37.0	G	1.2
gi 42104 emb CAA48933.1	nark [Escherichia coli]	37.0		1.2
gi 15830982 ref NP_309755.1	nitrite extrusion protein [Esche...	37.0	G	1.2
gi 75230215 ref ZP_00716716.1	COG2223: Nitrate/nitrite transpor	37.0		1.2
gi 75242028 ref ZP_00725822.1	COG2223: Nitrate/nitrite trans...	37.0		1.2
gi 75190277 ref ZP_00703544.1	COG2223: Nitrate/nitrite transpor	37.0		1.2
gi 16129186 ref NP_415741.1	nitrate/nitrite transporter [Esc...	37.0	G	1.2
gi 26989040 ref NP_744465.1	ABC transporter, permease protei...	36.6	G	1.6
gi 116623359 ref YP_825515.1	protein of unknown function DUF...	36.6	G	1.6
gi 115372120 ref ZP_01459431.1	vitamin K epoxide reductase f...	36.2		2.1
gi 94413278 ref ZP_01293166.1	hypothetical protein PaerP_010...	36.2		2.1
gi 15598054 ref NP_251548.1	hypothetical protein PA2858 [Pse...	36.2	G	2.1
gi 84326345 ref ZP_00974372.1	COG3127: Predicted ABC-type tr...	36.2		2.1
gi 84320398 ref ZP_00968776.1	COG3127: Predicted ABC-type tr...	36.2		2.1
gi 82738301 ref ZP_00901136.1	ABC transporter, permease prot...	36.2		2.1
gi 114769129 ref ZP_01446755.1	inner-membrane translocator [...	35.8		2.8
gi 92912133 ref ZP_01280769.1	ATPase, E1-E2 type:Copper-tran...	35.8		2.8

gi 28869466 ref NP_792085.1	permease, putative [Pseudomonas ...	35.8	2.8	G
gi 88803929 ref ZP_011119449.1	hypothetical protein RB2501_03...	35.8	2.8	
gi 69290299 ref ZP_00619002.1	NLP/P60:SLT [Kineococcus radio...	35.8	2.8	
gi 116617574 ref YP_817945.1	permease of the major facilitat...	35.8	2.8	G
gi 107102407 ref ZP_01366325.1	hypothetical protein PaerPA_0...	35.4	3.6	
gi 54026538 ref YP_120780.1	putative nitrite extrusion prote...	35.4	3.6	G
gi 116062235 dbj BAA79067.2	hypothetical protein [Aeropyrum per	35.0	4.7	
gi 83769792 dbj BAE59927.1	unnamed protein product [Aspergillus	35.0	4.7	
gi 14600492 ref NP_147008.1	hypothetical protein APE0156 [Aerop	35.0	4.7	G
gi 115443030 ref XP_001218322.1	conserved hypothetical prote...	34.7	6.1	G
gi 113942881 ref ZP_01428585.1	protein of unknown function D...	34.7	6.1	
gi 113936404 ref ZP_01422297.1	Glycosyl transferase, family ...	34.7	6.1	
gi 21219547 ref NP_625326.1	ABC transport system integral me...	34.7	6.1	G
gi 88711067 ref ZP_01105155.1	hypothetical protein FB2170_03...	34.7	6.1	
gi 87309448 ref ZP_01091583.1	hypothetical protein DSM3645_2...	34.7	6.1	
gi 91781984 ref YP_557190.1	Putative glycosyltransferase [Bu...	34.3	8.0	G
gi 70728684 ref YP_258433.1	signaling repeat/GGDEF domain/EA...	34.3	8.0	G
gi 68448684 gb AA96807.1	unknown [Monkeypox virus] >gi 6844...	34.3	8.0	
gi 18202585 sp Q60457 SOAT1 CRIGR	Sterol O-acyltransferase 1 ...	34.3	8.0	
gi 83747811 ref ZP_00944845.1	LivG [Ralstonia solanacearum U...	34.3	8.0	

Alignments

Get selected sequences

Select all

Deselect all

Distance tree of results

> ☐ gi|94961770|gb|ABF48256.1| **UG** dual oxidase activator 2 [Homo sapiens]
Length=320

Score = 646 bits (1666), Expect = 0.0
Identities = 320/320 (100%), Positives = 320/320 (100%), Gaps = 0/320 (0%)

Query	1	MTLWNGVLPFYQPQRHAAGFSVPLLIIVILVFLAALAAASFLILPGIRGHSRWFVLVRVLLS	60
		MTLWNGVLPFYQPQRHAAGFSVPLLIIVILVFLAALAAASFLILPGIRGHSRWFVLVRVLLS	
Sbjct	1	MTLWNGVLPFYQPQRHAAGFSVPLLIIVILVFLAALAAASFLILPGIRGHSRWFVLVRVLLS	60
Query	61	LFIGAEIVAVHFSAEWFGVTNTNTSYKAFSAARVTARVGLLVGLEGINITLTGTPVHQL	120
		LFIGAEIVAVHFSAEWFGVTNTNTSYKAFSAARVTARVGLLVGLEGINITLTGTPVHQL	
Sbjct	61	LFIGAEIVAVHFSAEWFGVTNTNTSYKAFSAARVTARVGLLVGLEGINITLTGTPVHQL	120

Query	121	NETIDYNEQFTWRLKENYAAEYANALEKGLPDPVLYLAEKFTPSSPCGLYHQYHLAGHYA	180
Sbjct	121	NETIDYNEQFTWRLKENYAAEYANALEKGLPDPVLYLAEKFTPSSPCGLYHQYHLAGHYA	180
Query	181	SATLWVAFCFWLLSNVLLSTPAPLYGGLALLTTGAFALFGVFALASISSVPLCPLRLGSS	240
Sbjct	181	SATLWVAFCFWLLSNVLLSTPAPLYGGLALLTTGAFALFGVFALASISSVPLCPLRLGSS	240
Query	241	ALTTQYGAAFWVTLATGVLCLFLGGAVVSLQYVRPSALRTLDDQSAKDCSQERGGSPLIL	300
Sbjct	241	ALTTQYGAAFWVTLATGVLCLFLGGAVVSLQYVRPSALRTLDDQSAKDCSQERGGSPLIL	300
Query	301	GDPLHKQAALPDLKCITTNL	320
Sbjct	301	GDPLHKQAALPDLKCITTNL	320

> [gi|98986325|ref|NP_997464.2|](#) **UG** dual oxidase activator 2 [Homo sapiens]
Length=320

Score = 643 bits (1658), Expect = 0.0
Identities = 319/320 (99%), Positives = 319/320 (99%), Gaps = 0/320 (0%)

Query	1	MTLWNGVLPFYQPQRHAAAGFSVPLLIIVILVFLAASFLILPGIRGHSRWFVLVRVLLS	60
Sbjct	1	MTLWNGVLPFYQPQRHAAAGFSVPLLIIVILVFLAASFLILPGIRGHSRWFVLVRVLLS	60
Query	61	LFIGAEIVAVHFSAEWFVGTNTNTSYKAFSAARVTARVGLLVGLEGINITLTGTPVHQL	120
Sbjct	61	LFIGAEIVAVHFSAEWFVGTNTNTSYKAFSAARVTARV LLVGLEGINITLTGTPVHQL	120
Query	121	NETIDYNEQFTWRLKENYAAEYANALEKGLPDPVLYLAEKFTPSSPCGLYHQYHLAGHYA	180
Sbjct	121	NETIDYNEQFTWRLKENYAAEYANALEKGLPDPVLYLAEKFTPSSPCGLYHQYHLAGHYA	180
Query	181	SATLWVAFCFWLLSNVLLSTPAPLYGGLALLTTGAFALFGVFALASISSVPLCPLRLGSS	240
Sbjct	181	SATLWVAFCFWLLSNVLLSTPAPLYGGLALLTTGAFALFGVFALASISSVPLCPLRLGSS	240
Query	241	ALTTQYGAAFWVTLATGVLCLFLGGAVVSLQYVRPSALRTLDDQSAKDCSQERGGSPLIL	300
Sbjct	241	ALTTQYGAAFWVTLATGVLCLFLGGAVVSLQYVRPSALRTLDDQSAKDCSQERGGSPLIL	300
Query	301	GDPLHKQAALPDLKCITTNL	320

Sbjct 301 GDPLHKQAALPDLKCITTNL
320 GDPLHKQAALPDLKCITTNL

> [gi|109080940|ref|XP_001111110.1|](#) **G** PREDICTED: similar to Numb-interacting protein 2 [Macaca mulatta]
Length=320

Score = 616 bits (1589), Expect = 4e-175
Identities = 303/320 (94%), Positives = 312/320 (97%), Gaps = 0/320 (0%)

Query 1	MTLWNGVLPFYQPQRHAAGFSVPLLIVILVFLAASFLLLILPGIRGHSRWFVLRVLLS	60
	MTLWNGVLPFYQPQRHAAGFSVPLLIVILVFLAASFLLLILPGIRGHSRWFVLRVLLS	
Sbjct 1	MTLWNGVLPFYQPQRHAAGFSVPLLIVILVFLAASFLLLILPGIRGHSRWFVLRVLLS	60
Query 61	LFIGAEIVAVHFSAEWFGVTNTNTSYKAFSAARVTARVGLLVGLEGINITLTGTPVHQL	120
	LFIGAEIVAVHFSAEWFGVTNTNTSYKAFSAARVTARVGLLVGLEGINITLTGTPVHQL	
Sbjct 61	LFIGAEIVAVHFSAEWFGVTNTNTSYKAFSAARVTARVGLLVGLEGINITLTGTPVHQL	120
Query 121	NETIDYNEQFTWRLKENYAAEYANALEKGLPDPVLYLAEKFTPSSPCGLYHQYHLAGHYA	180
	NETIDYNEQFTWRLKENYAAEYANALEKGLPDPVLYLAEKFTPSSPCGLYHQYHLAGHYA	
Sbjct 121	NETIDYNEQFTWRLRDNYAAEYANALEKGLPNPVLAEKFTPSSPCGLYHQYRLAGHYA	180
Query 181	SATLWVAFCFWLLSNVLLSTPAPLYGGLALLTTGAFALFGVFALASISSVPLCPLRLGSS	240
	SATLWVAFCFWLLSNVLLSTPAPLYGGLALLTTGAFALFG+FA ASISSVPLCPLRLGS+	
Sbjct 181	SATLWVAFCFWLLSNVLLSTPAPLYGGLALLTTGAFALFGIFAFASISSVPLCPLRLGSA	240
Query 241	ALTTQYGAAFWVTLATGVLCLFLGGAVVSLQYVRPSALRTLDDQSAKDCSQERGGSPLIL	300
	LT QYGAAFWVTLATG+LCLFLGGAVVSL YVRPSALRTLDDQSA+DCSQ +GGSPILIL	
Sbjct 241	VLTAQYGAAFWVTLATGILCLFLGGAVVSLHYVRPSALRTLDDQSAEDCSQAKGGSPLIL	300
Query 301	GDPLHKQAALPDLKCITTNL	320
	G+PLHKQAALPDLK ITTNL	
Sbjct 301	GNPLHKQAALPDLKFITTNL	320

> [gi|74000506|ref|XP_851517.1|](#) **U** **G** PREDICTED: similar to Numb-interacting protein 2 [Canis familiaris]
Length=320

Score = 522 bits (1345), Expect = 7e-147
Identities = 266/321 (82%), Positives = 279/321 (86%), Gaps = 2/321 (0%)

Query 1	MTLWNGVLPFYQPQRHAAGFSVPLLIVILVFLAASFLLLILPGIRGHSRWFVLRVLLS	60
	MTLWNG L FYPQPRHA GFSVPLLIVILVFLAASFLLLILPGIRGHSRWFVLRVLLS	

```

Sbjct 1 MTLWNGELSFYQPRHAPGFSVPLLVILVFLAASFLILPGIRGHSRWFVLVRVLLS 60
Query 61 LFIGAEIVAVHFSAEWFGVTNTNTSYKAFSAARVTARVGLLVLEGINITLTGTPVHQL 120
        LFIGAEIVAV+FSA+W VG +NTNTSYKAFSAARV+A VGL +GLEGINITLTGTPVHQL
Sbjct 61 LFIGAEIVAVNFSAQSVGGINTNTNTSYKAFSAARVSAHVGLHIGLEGINITLTGTPVHQL 120

Query 121 NETIDYNEQFTWRLKENYAAEYANALEKGLPDPVLYLAEKFTPPSSPCGLYHQYHLAGHYA 180
        NETIDYNE F WRL ENYAAEY +ALEKGLPDPVLYLAEKFTPPSSPCGLY QY LAGH+A
Sbjct 121 NETIDYNEHFKWRLGENYAAEYWDALEKGLPDPVLYLAEKFTPPSSPCGLYRQYRLAGHFA 180

Query 181 SATLWVAFCFWLLSNVLLSTPAPLYGGLALLTTGAFALGFVAFALASISSVPLCPLRLGSS 240
        SA LWVAFCFWLLSN LLS P PL+GGLALLT GAFALF FA ASISSVPLCPLRLGSS
Sbjct 181 SAALWVAFCFWLLSNALLSMPVPLHGLLALLTAGAFALFSTFAFASISSVPLCPLRLGSS 240

Query 241 ALTTQYGAAFWVTLATGVLCLFLGGAVVSLQYVRPSALRTLILDQSAKDC-SQERGGSPLI 299
        LTT YGAAFWVTLATG+LCL LG AVVSL Y RPSALRT LDQS K+ SQ +G PLI
Sbjct 241 TLTTYGAAFWVTLATGILCLLGLGAVVSLHYSRPSALRTFLDQSVKNYGSQVKGSLPLI 300

Query 300 LGDPLHKQALPDLKCITTNL 320
        L +PLHKQ DL +TNL
Sbjct 301 LNNPLHKQFGALDL-TTSTNL 320

```

> [gi|13385246|ref|NP_080053.1|](#) **U G** Numb-interacting protein 2 [Mus musculus]
[gi|128583339|dbj|BAB31281.1|](#) **U G** unnamed protein product [Mus musculus]
[gi|21411408|gb|AAH31111.1|](#) **U G** RIKEN cDNA 9030623N16 gene [Mus musculus]
Length=320

Score = 508 bits (1309), Expect = 1e-142
Identities = 250/318 (78%), Positives = 270/318 (84%), Gaps = 1/318 (0%)

```

Query 1 MTLWNGVLPFYQPQRHAAAGFSVPLLVILVFLAASFLILPGIRGHSRWFVLVRVLLS 60
        MT W+GVLPFYQPQRHAA FSVPLLVILVFL+LAASFL ILPGIRGHSRWFVLVRVLLS
Sbjct 1 MTAWDGVLPFYQPQRHAAAGFSVPLLVILVFLSAAASFLFILPGIRGHSRWFVLVRVLLS 60

Query 61 LFIGAEIVAVHFSAEWFGVTNTNTSYKAFSAARVTARVGLLVLEGINITLTGTPVHQL 120
        LFIGAEIVAVHFS +WFGV V TNTSYKAFS +RV VGL VGL G+NITL GTP QL
Sbjct 61 LFIGAEIVAVHFSGDWFGVGRVWNTNTSYKAFSPSRVQVHVHVLHVLGAGVNITLRGTPRQQL 120

Query 121 NETIDYNEQFTWRLKENYAAEYANALEKGLPDPVLYLAEKFTPPSSPCGLYHQYHLAGHYA 180
        NETIDYNE+FTWRL E+Y EY +ALEKGLPDPVLYLAEKFTPPSSPCGLYHQYHLAGHYA
Sbjct 121 NETIDYNERFTWRLNEDYTKEYVHALEKGLPDPVLYLAEKFTPPSSPCGLYHQYHLAGHYA 180

```

Query 181 SATLWVAFCFWLLSNVLLSTPAPLYGGLALLTTGAFALFGVFALASISSVPLCPLRLGSS 240
 +ATLWVAFCFW+++N LLS PAPLYGGLALLTTGAF LFGVFA ASISSVPLC RLGS+
 Sbjct 181 AATLWVAFCFWIIANALLSMPAPLYGGLALLTTGATFLFGVFASISSVPLCHFRLGSA 240

Query 241 ALTTQYGAAFWVTLATGVLCLFLGGAVVSLQYVRPSALRLLDQSAKDCS-QERGGSPLI 299
 LT YGA+FW+TLATG+L L LGGAVV L Y RPSALR+ LD S KDCS Q +G SPL
 Sbjct 241 VLTPYYGASFVTLATGILSLLGGLVILHYTRPSALRSFLDLSVKDCSNQAKGNSPLT 300

Query 300 LGDPLHKQAALPDLKCIT 317
 L +P H+Q PDL T
 Sbjct 301 LNNPQHEQLKSPDLNITT 318

> [gi|62645690|ref|XP_575222.1|](#) **G** PREDICTED: similar to Numb-interacting protein 2 [Rattus norvegicus]
[gi|109470732|ref|XP_001080999.1|](#) **G** PREDICTED: similar to Numb-interacting protein 2 [Rattus norvegicus]
 Length=320

Score = 507 bits (1305), Expect = 3e-142
 Identities = 249/318 (78%), Positives = 267/318 (83%), Gaps = 1/318 (0%)

Query 1 MTLWNGVLPFYQPQRHAAAGFSVPLLIIVLVFLAASFLILPGIRGHSRWFVLRVLLS 60
 MT W+GVLPFYQPQRHAAAGFSVPLLIIVLVFL+LAASFL ILPGIRGHSRWFVLRVLLS
 Sbjct 1 MTAWDGVLPFYQPQRHAAAGFSVPLLIIVLVFLSAAASFLILPGIRGHSRWFVLRVLLS 60

Query 61 LFIGAEIVAVHFSAEWFGVTNTNTSYKAFSAARVTARVGLLVGLEGINITLTGTPVHQL 120
 LFIGAEIVAVHFS +WFGV V TNTSYKAFS +RV VGL VGLEG+NITL GTP+ QL
 Sbjct 61 LFIGAEIVAVHFSGDWFGVRVNTNTSYKAFSTSRVQVHVGLHVGLGVNITLRTGTPMQQL 120

Query 121 NETIDYNEQFTWRLKENYAAEYANALEKGLDPVLYLAEKFTPSPPCGLYHQYHLAGHYA 180
 NETIDYNEQFTWRL E+Y EY ALEKGLDPVLYLAEKFT+SPCGLYHQYH AGHYA
 Sbjct 121 NETIDYNEQFTWRLNEDYTKYVQALEKGLDPVLYLAEKFTPNNSPCGLYHQYHAGHYA 180

Query 181 SATLWVAFCFWLLSNVLLSTPAPLYGGLALLTTGAFALFGVFALASISSVPLCPLRLGSS 240
 ATLWVAFCFW+++N LLS PAPLYGGLALL TGAF LF VFA ASISSVPLC RLGS+
 Sbjct 181 GATLWVAFCFWIIANALLSMPAPLYGGLALLITGATFLFSVFASISSVPLCHFRLGSA 240

Query 241 ALTTQYGAAFWVTLATGVLCLFLGGAVVSLQYVRPSALRLLDQSAKDCS-QERGGSPLI 299
 ALT YGA+FWVTLATG+L L LGG VV L Y RPS LR LLDQ+ KDCS Q G S I
 Sbjct 241 ALTPHYGASFVTLATGILSLLGGLVILHYTRPSVLRALLDQNVKDCSNQADGNSHFI 300

Query 300 LGDPLHKQAALPDLKCIT 317
 L +P H+Q+ PDL T
 Sbjct 301 LDNPQHRQSKTPDLNVT 318

> [gi|76627905|ref|XP_592260.2|](#) **G** PREDICTED: similar to Numb-interacting protein 2 isoform 1 [Bos taurus]
Length=320

Score = 505 bits (1300), Expect = 1e-141
Identities = 255/321 (79%), Positives = 270/321 (84%), Gaps = 2/321 (0%)

Query	1	MTLWNGVLPFPYQPRHAAGFSVPLLIIVILVFLAALAAASFLILPGIRGHSRWFVLVRVLLS	60
		MTLWNGVLPFPYQPRHAAG SVPLLIIVILVFL LAASFLILPGIRGHSRWFVLVRVLLS	
Sbjct	1	MTLWNGVLPFPYQPRHAAGLSVPLLIIVILVFLAALAAASFLILPGIRGHSRWFVLVRVLLS	60
Query	61	LFIGAEIVAVHFSAEWFGVTNTNTSYKAFSAARVTARVGLLVLEGINITLTGTPVHQL	120
		LFIGAEIVA HFSAEW VG+V+T TSYKAFS RV A VGL VGLEG+NITLTG PV QL	
Sbjct	61	LFIGAEIVAAHFSAEWSVGSVSTKTSYKAFSVERVRAHVGLHVLEGVNITLTGNPVQQL	120
Query	121	NETIDYNEQFTWRLLKENYAAEYANALEKGLDPVLYLAEKFTPSSPCGLYHQYHLAGHYA	180
		NETIDYNEQF WR +NYA YA ALE+GLP+PVLYLAEKFTPSSPCG+Y QY LAGHYA	
Sbjct	121	NETIDYNEQFIWRFGQNYAGAYAEALERGLPNPVLYLAEKFTPSSPCGVYRQYRLAGHYA	180
Query	181	SATLWVAFCFWLLSNVLLSTPAPLYGGLALLTTGAFALFGVFALASISSVPLCPLRLGSS	240
		SATLWVAFCFWLLSN+LLS P P YGGL LL TGAFALF VFA ASISSVPLC LR+GSS	
Sbjct	181	SATLWVAFCFWLLSNMLLSMPVPHYGGLTLITGAFALFSVFAFASISSVPLCQLRVGSS	240
Query	241	ALTTQYGAAFWVTLATGVLCFLGGAUVSLQYVRPSALRTLDDQSAKDC-SQERGGSPLI	299
		LTT YGAAFW+TLATGVLC LG AV+SL Y RPSALR L+ S D S +G SPLI	
Sbjct	241	ELTTHYGAAFWITLATGVLCLLGAAVLSLHYARPSALRLFLEGSVNDLESPTKGSSPLI	300
Query	300	LGDPLHKQAALPDLKCITTNL	320
		L +PLHKQ DL I+TNL	
Sbjct	301	LSNPLHKQFKTSDL-TISTNL	320

> [gi|76627903|ref|XP_876867.1|](#) **G** PREDICTED: similar to Numb-interacting protein 2 isoform 3 [Bos taurus]
Length=294

Score = 444 bits (1141), Expect = 3e-123
Identities = 217/257 (84%), Positives = 227/257 (88%), Gaps = 0/257 (0%)

Query	1	MTLWNGVLPFPYQPRHAAGFSVPLLIIVILVFLAALAAASFLILPGIRGHSRWFVLVRVLLS	60
		MTLWNGVLPFPYQPRHAAG SVPLLIIVILVFL LAASFLILPGIRGHSRWFVLVRVLLS	

```

Sbjct 1      MTLWNGVLPFYQPQRHAAAGLSVPLLIIVILVFLVLAASFLILPGIRGHSRWFVLVRVLLS 60
Query 61      LFIGAEIVAVHFSAEWFGVTNTNTSYKAFSAARVTARVGLLVGLEGINITLTGTPVHQL 120
          LFIGAEIVA HFSAEW VG+V+T TSYKAFS RV A VGL VGLEG+NITLTG PV QL
Sbjct 61      LFIGAEIVAAHFSAEWSVSTKTSYKAFSVERVRAHVGLHVGLGVNITLTGNPVQQL 120
Query 121     NETIDYNEQFTWRLKENYAAEYANALEKGLPDPVLYLAEKFTPPSSPCGLYHQYHLAGHYA 180
          NETIDYNEQF WR +NYA YA ALE+GLP+PVLVLAEKFTPPSSPCG+Y QY LAGHYA
Sbjct 121     NETIDYNEQFIWRFGONYAGAYAEALERGLPNPVLVLAEKFTPPSSPCGVYRQYRLAGHYA 180
Query 181     SATLWVAFCFWLLSNVLLSTPAPLYGGLALLTTGAFALFGVFALASISSVPLCPLRLGSS 240
          SATLWVAFCFWLLSN+LLS P P YGGL LL TGAFALF VFA ASISSVPLC LR+GSS
Sbjct 181     SATLWVAFCFWLLSNMLLSMPVPHYGGLTLLITGAFALFSVFAFASISSVPLCQLRVGSS 240
Query 241     ALTTQYGAAFWVTLATG 257
          LTT YGAAFW+TLATG
Sbjct 241     ELTTYGAAFWITLATG 257

```

> [gi|12843239|dbj|BAB25910.1](#) **U G** unnamed protein product [Mus musculus]
Length=320

Score = 379 bits (972), Expect = 1e-103
Identities = 209/326 (64%), Positives = 232/326 (71%), Gaps = 17/326 (5%)

```

Query 1      MTLWNGVLPFYQPQRHAAAGFSVPLLIIVILVFLAASFLILPGIRGHSRWFVLVRVLLS 60
          MT W+GVLPFYQPQRHAA FSVPLLIIVILVFL+LAASFL ILPGIRGHSRWFVLVRVLLS
Sbjct 1      MTAWDGVLPFYQPQRHAAASFVPLLIIVILVFLSLAASFLFILPGIRGHSRWFVLVRVLLS 60
Query 61      LFIGAEIVAVHFSAEWFGVTNTNTSYKAFSAARVTARVGLLVGLEGINITLTGTPVHQL 120
          LFIGAEIVAVHFS +WV V TNTSYKAFS +RV VGL VGL G+NITL GTP QL
Sbjct 61      LFIGAEIVAVHFSGDWFEVETNTSYKAFSPSRVQVHVGLHVGLAGVNITLRTGTPRQQL 120
Query 121     NETIDYNEQFTWRLKENYAAEYANALEKGLPDPVLYLAEKFTPPSSPCGLYHQYHLAGHYA 180
          NETIDYNE+FTWRL E+Y EY +A EKGLPDPVLYLAEKFTPPSSPCGLYHQYHL GHYA
Sbjct 121     NETIDYNERFTWRLNEDYTYKEYVHAFEKGLPDPVLYLAEKFTPPSSPCGLYHQYHLPGHYA 180
Query 181     SATLWVAFCFWLLSNVLLSTPAPLYGGLALLTTGAFALFGVFALASI-----SSVPL 232
          +ATLWV LL + A L+ L G + AL + +++PL
Sbjct 181     AATLWVGIL--LLDH--RQCAALHARPTLRLRGLFAHHRCLRALRCLRFLRDLDFQRAALPL 235
Query 233     CPLRLGSSALTTQYGAAFWVTLATGVLCFLGGAVVSLQYVRPSALRTLDDQSAKDCS-Q 291
          P AL + +TLATG+L L LGGAV L Y RPSALR+ LD S KDCS Q
Sbjct 236     PPWLRLRLHALLRR---LLLLTLATGILSLLLGGAVVILHYTRPSALRSFLDLSVKDCSNQ 292

```

Query 292 ERGGSPLILGDPDLHKQAALPDLKCIT 317
+G SPL L +P H+Q PDL T
Sbjct 293 AKGNSPLTLNPNQHEQLKSPDLNITT 318

> [gi|114656759|ref|XP_001146826.1|](#)  PREDICTED: dual oxidase activator 2 [Pan troglodytes]
Length=202


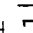
Score = 367 bits (943), Expect = 3e-100
Identities = 184/202 (91%), Positives = 184/202 (91%), Gaps = 17/202 (8%)

Query 1 MTLWNGVLPFPYQPRHAAGFSVPLLIIVILVFLAASFLLIILPGIRGHSRWFVLRVLLS 60
MTLWNGVLPFPYQPRHAAGFSVPLLIIVILVFLAASFLLIILPGIRGHSRWFVLRVLLS
Sbjct 1 MTLWNGVLPFPYQPRHAAGFSVPLLIIVILVFLAASFLLIILPGIRGHSRWFVLRVLLS 60

Query 61 LFIGAEIVAVHFSAEWFGVTNTNTSYKAFSAARVTARVGLLVGLEGINITL----- 112
LFIGAEIVAVHFSAEWFGV VNTNTSYKAFSAARVTARVGLLVGLEGINITL
Sbjct 61 LFIGAEIVAVHFSAEWFGVGRVNTNTSYKAFSAARVTARVGLLVGLEGINITLTVARSPTA 120

Query 113 -----TGTPVHQLNETIDYNEQFTWRLKENYAAEYANALEKGLPDPVLYLAEKFTP 163
TGTPVHQLNETIDYNEQFTWRLKENYAAEYANALEKGLPDPVLYLAEKFTP
Sbjct 121 GSPMSPHPPTGTPVHQLNETIDYNEQFTWRLKENYAAEYANALEKGLPDPVLYLAEKFTP 180

Query 164 SSPCGLYHQYHLAGHYASATLW 185
SSPCGLYHQYHLAGHYASATLW
Sbjct 181 SSPCGLYHQYHLAGHYASATLW 202

> [gi|62645692|ref|XP_230527.2|](#)  PREDICTED: similar to Numb-interacting protein 1 [Rattus norvegicus]
[gi|109470734|ref|XP_001081001.1|](#)  PREDICTED: similar to Numb-interacting protein 1 [Rattus norvegicus]
Length=340

Score = 348 bits (894), Expect = 1e-94
Identities = 172/302 (56%), Positives = 217/302 (71%), Gaps = 0/302 (0%)

Query 8 LPFYQPRHAAGFSVPLLIIVILVFLAASFLLIILPGIRGHSRWFVLRVLLSLFIGAEI 67
LPFY P+ L ++I +FL +F++ILPGIRG +R FWL+RV+ SLFIGA I
Sbjct 8 LPFYTGPKPTFPMDTTLAVIITIFLTALVTFIIILPGIRGKTRFLWLLRVVTSFIGAVI 67

Query 68 VAVHFSAEWFGVTNTNTSYKAFSAARVTARVGLLVGLEGINITLTGTPVHQLNETIDYN 127
+AV+FS+EW VG +NTNT+YKAFS RV+ VGL +GL G+NITLTGTPV QLNETI+YN
Sbjct 68 LAVNFSSEWSVGHINTNTTYKAFSPKRVSVHVGLQIGLGLNITLTGTPVQQLNETINYN 127

```

Query 128 EQFTWRLKENYAAEYANALEKGLPDPVLYLAEKFTSPSPCGLYHQYHLAGHYASATLWVA 187
          E+FTWRL ++YA EYA ALEKGLPDPVLYLAEKF P SPCGLY+QY LAGHYASA LWVA
Sbjct 128 EEFTRWRLGKSYAEYAKALEKGLPDPVLYLAEKFAPRSPCGLYNQYRLAGHYASAMLWVA 187

Query 188 FCFWLLSNVLLSTPAPLYGGLALLTTGAFALFGVFALASISSVPLCPLRLGSSALTTQYG 247
          F WLL+NV+LS P +YGG LL TG F L +F + +S+ CPLRLG++ L T +G
Sbjct 188 FLCWLLANVMLSMPVLVYGGHMLLATGLFQLLALFFFSMTTSLMSCPLRLGTAVLYTHHG 247

Query 248 AAFWVTLATGVLCLFLGGAVVSLQYVRPSALRTLTDQSAKDCSQERGGSPILLGDPLHKQ 307
          AFW+TLATG+LC+ LG + ++P L+ L + S++D E G L P ++
Sbjct 248 PAFWITLATGLLCILLGLVMVAHRMQPHRLKALFNLSSEDPMLEWGSEEGLLSPHYRS 307

Query 308 AA 309
          A
Sbjct 308 IA 309

```

> [gi|94366864|ref|XP_001003392.1](#) | **G** PREDICTED: similar to Numb-interacting protein 2 [Mus musculus]
Length=258

```

Score = 347 bits (890), Expect = 4e-94
Identities = 192/318 (60%), Positives = 207/318 (65%), Gaps = 63/318 (19%)

Query 1 MTLWNGVLPFYQPQRHAAGFSVPLLIIVLVFLAASFLILPGIRGHSRWFVLVRVLLS 60
          MT W+GVLPFYQPQRHAA FSVPLLIIVLVFL+LAASFLLPGLRHSRWFVLVRVLLS
Sbjct 1 MTAWDGVLPFYQPQRHAASFSVPLLIIVLVFLSAAFLFILPGIRGHSRWFVLVRVLLS 60

Query 61 LFIGAEIVAVHFSAEWFVGTVTNTSYKAFSAARVTARVGLLVGLEGINITLTGTPVHQL 120
          LFIGAEIVAVHFS +WFGV V TNTSYKAFS +RV VGL VGL G+NITL GTP QL
Sbjct 61 LFIGAEIVAVHFSGDWFGVGRVWNTNTSYKAFSPSRVQVHVGLHVGLAGVNITLRTGTPRQQL 120

Query 121 NETIDYNEQFTWRLKENYAAEYANALEKGLPDPVLYLAEKFTSPSPCGLYHQYHLAGHYA 180
          NETIDYNE+FTWRL E+Y EY +ALEKGLPDPVLYLAEKFTSPSPCGLYHQYH
Sbjct 121 NETIDYNERFTWRLNEDYTKYVHALEKGLPDPVLYLAEKFTSPSPCGLYHQYH----- 174

Query 181 SATLWVAFCFWLLSNVLLSTPAPLYGGLALLTTGAFALFGVFALASISSVPLCPLRLGSS 240
          L G +A A+ LCP S
Sbjct 175 -----LAGHYAAAT-----LCPSVFPPS 192

Query 241 ALTTQGAAFWVTLATGVLCLFLGGAVVSLQYVRPSALRTLTDQSAKDCS-QERGGSPLI 299
          G+L L LGGAVV L Y RPSALR+ LD S KDCS Q +G SPL
Sbjct 193 G-----AGILSLLGGAVVILHYTRPSALRSFLDLSVKDCSNQAKGNSPLT 238

```

Query 300 LGDPLHKQAALPDLKCIT 317
 L +P H+Q PDL T
 Sbjct 239 LNNPQHEQLKSPDLNITT 256

> [gi|76627911|ref|XP_608616.2|](#) **G** PREDICTED: similar to Numb-interacting protein [Bos taurus]
 Length=337

Score = 343 bits (880), Expect = 6e-93
 Identities = 168/286 (58%), Positives = 209/286 (73%), Gaps = 1/286 (0%)

Query 1 MTLWNGVLPFYQPQRHAAGFSVPLLIVILVFLAALAAASFLILPGIRGHSRWFVLRVLLS 60
 M + PFY P+ L +++ +FL +F++ILPGIRG R FW++RV+ S
 Sbjct 1 MAAFHTFPFYAGPKPTFTDTTAVIVAIFLTSLVTFTIIILPGIRGKMLRFLRVVTS 60

Query 61 LFIGAEIVAVHFSAEWFGTVNTNTSYKAFSAARVTARVGLLVGLEGINITLTGTPVHQL 120
 LFIGA I+AV+FS+EW VG V+TNTSYKAFS+ ++A VGL +GL G+NITLTGTPV QL
 Sbjct 61 LFIGAVILAVNFSSEWSVGQVSTNTSYKAFSSQWISANVGLQIGLGGVNITLTGTPVQQL 120

Query 121 NETIDYNEQFTWRLLKENYAAEYANALEKGLPDPVLYLAEKFTPSSPCGLYHQYHLAGHYA 180
 NETIDYNE+FTWRL ENYA EYANALEKGLPDPVLYLAEKFTP SPCGL+ QY LAGHY
 Sbjct 121 NETIDYNEEFTWRLLGENYAAEYANALEKGLPDPVLYLAEKFTPHSPCGLHGQYRLAGHYT 180

Query 181 SATLWVAFCFWLLSNVLLSTPAPLYGGLALLTTGAFALFGVFALASISSV-PLCPLRLGS 239
 SA LWAF WLL+NV+LS P +YGG LL TG F L G+ ++ +S+ P CPLRLG+
 Sbjct 181 SAMLWVAFLCWLLANVMLMPVLVYGGHMLLATGLFQLLGLLFFSTATSLTPPCPLRLGA 240

Query 240 SALTTOYGAAFWVTLATGVLCFLGGAVVSLQYVRPSALRTLDDQS 285
 + L T G A+W+TL TG+LC+ LG A+V ++P L+ QS
 Sbjct 241 ATLHTRGPAYWITLTGLLCVLLGLAMVVAHRMQPHRLKAFFSQS 286

> [gi|94961772|gb|ABF48257.1|](#) **UG** dual oxidase activator 1 [Homo sapiens]
 Length=343

Score = 342 bits (876), Expect = 2e-92
 Identities = 173/294 (58%), Positives = 213/294 (72%), Gaps = 8/294 (2%)

Query 9 PFYQPQRHAAGFSVPLLIVILVFLAALAAASFLILPGIRGHSRWFVLRVLLSLFIGAEIV 68
 PFY P+ L +I++FL A+F++ILPGIRG +R FWL+RV+ SLFIGA I+
 Sbjct 9 PFYAGPKPTFPMDTTLASIIMIFLTALATFIVILPGIRGKTRLFWLLRVVTSLSFIGAAIL 68

Query 69 AVHFSAEWFGTVNTNTSYKAFSAARVTARVGLLVGLEGINITLTGTPVHQLNETIDYNE 128

	AV+FS+EW VG V+TNTSYKAFS+ ++A +GL VGL G+NITLTGTPV QLNETI+YNE	128
Sbjct	69 AVNFSSEWSVGQVSTNTSYKAFSSEWISADIGLQVGLGGVNITLTGTPVQQLNETINYN	
Query	129 QFTWRLKENYAAEYANALEKGLPDPVLYLAEKFTTPSSPCGLYHQYHLAGHYASATLWVAF	188
	+FTWRL ENYA EYA ALEKGLPDPVLYLAEKFTT SPCGLY QY LAGHY SA LWVAF	
Sbjct	129 EFTWRLGENYAAEYAKALEKGLPDPVLYLAEKFTTPRSPCGLYRQYRLAGHYTSAMLWVAF	188
Query	189 CFWLLSNVLLSTPAPLYGGLALLTTGAFALFGV--FALASISSVPLCPLRLGSSALTTQY	246
	WLL+NV+LS P +YGG LL TG F L + F++A+ + P CPL LG+S L T +	
Sbjct	189 LCWLLANVMSMPVLVYGGYMLLATGIFQLLALLFFSMATSLTSP-CPLHLGASVLHTHH	247
Query	247 GAAFWVTLATGVLCLFLGGAVVSLQYVRPSALRTLDDQSAK-----DCSQERGG	295
	G AFW+TL TG+LC+ LG A+ ++P L+ +QS + S E GG	
Sbjct	248 GPAFWITLTGLLCVLLGLAMAVAHMQPHRLKAFFNQSVDEDPMLEWSPEEGG	301

> [gi|46485465|ref|NP_653166.2|](#) **UG** Numb-interacting protein [Homo sapiens]
[gi|20987584|gb|AAH29819.1|](#) **UG** Dual oxidase maturation factor 1 [Homo sapiens]
 Length=483

Score = 342 bits (876), Expect = 2e-92
 Identities = 173/294 (58%), Positives = 213/294 (72%), Gaps = 8/294 (2%)

Query	9 PFYQPRHAAGFSVPLLIVILVFLALAAASFLILPGIRGSRFWLVRVLLSLFIGAEIV	68
	PFY P+ L +I++FL A+F++ILPGIRG +R FWL+RV+ SLFIGA I+	
Sbjct	9 PFYAGPKPTFPMDTTLASIIIMIFLTALATFIVILPGIRKTRFLWLLRVVTSFIGAAIL	68
Query	69 AVHFSAEWFVGTVNTNTSYKAFSAARVTARVGLLVGLEGINITLTGTPVHQLNETIDYNE	128
	AV+FS+EW VG V+TNTSYKAFS+ ++A +GL VGL G+NITLTGTPV QLNETI+YNE	
Sbjct	69 AVNFSSEWSVGQVSTNTSYKAFSSEWISADIGLQVGLGGVNITLTGTPVQQLNETINYN	128
Query	129 QFTWRLKENYAAEYANALEKGLPDPVLYLAEKFTTPSSPCGLYHQYHLAGHYASATLWVAF	188
	+FTWRL ENYA EYA ALEKGLPDPVLYLAEKFTT SPCGLY QY LAGHY SA LWVAF	
Sbjct	129 EFTWRLGENYAAEYAKALEKGLPDPVLYLAEKFTTPRSPCGLYRQYRLAGHYTSAMLWVAF	188
Query	189 CFWLLSNVLLSTPAPLYGGLALLTTGAFALFGV--FALASISSVPLCPLRLGSSALTTQY	246
	WLL+NV+LS P +YGG LL TG F L + F++A+ + P CPL LG+S L T +	
Sbjct	189 LCWLLANVMSMPVLVYGGYMLLATGIFQLLALLFFSMATSLTSP-CPLHLGASVLHTHH	247
Query	247 GAAFWVTLATGVLCLFLGGAVVSLQYVRPSALRTLDDQSAK-----DCSQERGG	295
	G AFW+TL TG+LC+ LG A+ ++P L+ +QS + S E GG	
Sbjct	248 GPAFWITLTGLLCVLLGLAMAVAHMQPHRLKAFFNQSVDEDPMLEWSPEEGG	301

> [gi|114656781|ref|XP_001162743.1|](#) **G** PREDICTED: Numb-interacting protein isoform 1 [Pan troglodytes]
[gi|114656783|ref|XP_510370.2|](#) **G** PREDICTED: Numb-interacting protein isoform 8 [Pan troglodytes]
 Length=509

Score = 341 bits (874), Expect = 3e-92
 Identities = 173/294 (58%), Positives = 212/294 (72%), Gaps = 8/294 (2%)

Query	9	PFYQPRHAAGFSVPLLIIVLFLALAAASFLILPGIRGHSRWFVLVRVLLSLFIGAEIV	68
		PFY P+ L +I++FL A+F++ILPGIRG R FWL+RV+ SLFIGA I+	
Sbjct	9	PFYAGPKPTFPMDTTLASIIMIFLTALATFIVILPGIRGKMLFWLLRVVTSIFGAAIL	68
Query	69	AVHFSAEWFVGTNTNTSYKAFSAARVTARVGLLVGLEGINITLTGTPVHQLNETIDYNE	128
		AV+FS+EW VG V+TNTSYKAFS+ ++A +GL VGL G+NITLTGTPV QLNETI+YNE	
Sbjct	69	AVNFSSEWSVGQVSTNTSYKAFSSEWISADIGLQVGLGGVNITLTGTPVQQLNETINYN	128
Query	129	QFTWRLKENYAAEYANALEKGLPDPVLYLAEKFTPPSPCGLYHQYHLAGHYASATLWVAF	188
		+FTWRL ENYA EYA ALEKGLPDPVLYLAEKFTTP SPCGLY QY LAGHY SA LWVAF	
Sbjct	129	EFTWRLGENYAAEYAKALEKGLPDPVLYLAEKFTTPSPCGLYRQYRLAGHYTSAMLWVAF	188
Query	189	CFWLLSNVLLSTPAPLYGGLALLTTGAFALFGV--FALASISSVPLCPLRLGSSALTTQY	246
		WLL+NV+LS P +YGG LL TG F L + F++A+ + P CPL LG+S L T +	
Sbjct	189	LCWLLANVMLSMPVLVYGGVMLLATGIFQLLALLFFSMATSLTSP-CPLHLGASVLHTHH	247
Query	247	GAAFVWTLATGVLCLFLGGAVVSLQYVRPSALRTLDDQSAK-----DCSQERGG	295
		G AFW+TL TG+LC+ LG A+ ++P L+ +QS + S E GG	
Sbjct	248	GPAFWITLTGTLGCVLLGLAMAVAHMQPHRLKAFFNQSVDEDPMLEWSPEEGG	301

> [gi|114656785|ref|XP_001162967.1|](#) **G** PREDICTED: Numb-interacting protein isoform 6 [Pan troglodytes]
[gi|114656787|ref|XP_001163002.1|](#) **G** PREDICTED: Numb-interacting protein isoform 7 [Pan troglodytes]
 Length=343

Score = 341 bits (874), Expect = 3e-92
 Identities = 173/294 (58%), Positives = 212/294 (72%), Gaps = 8/294 (2%)

Query	9	PFYQPRHAAGFSVPLLIIVLFLALAAASFLILPGIRGHSRWFVLVRVLLSLFIGAEIV	68
		PFY P+ L +I++FL A+F++ILPGIRG R FWL+RV+ SLFIGA I+	
Sbjct	9	PFYAGPKPTFPMDTTLASIIMIFLTALATFIVILPGIRGKMLFWLLRVVTSIFGAAIL	68
Query	69	AVHFSAEWFVGTNTNTSYKAFSAARVTARVGLLVGLEGINITLTGTPVHQLNETIDYNE	128
		AV+FS+EW VG V+TNTSYKAFS+ ++A +GL VGL G+NITLTGTPV QLNETI+YNE	
Sbjct	69	AVNFSSEWSVGQVSTNTSYKAFSSEWISADIGLQVGLGGVNITLTGTPVQQLNETINYN	128

```

Query 129 QFTWRLKENYAAEYANALEKGLDPDPVLYLAЕКFTPPSPCGLYHQYHLAGHYASATLWVAF 188
+FTWRL ENYA EYA ALEKGLDPDPVLYLAЕКFTP SPCGLY QY LAGHY SA LWVAF
Sbjct 129 EFTWRLGENYAAEYAKALEKGLDPDPVLYLAЕКFTPPSPCGLYRQYRLAGHYTSAMLWVAF 188

Query 189 CFWLLSNVLLSTPAPLYGGLALLTTGAFALFGV--FALASISSVPLCPLRLGSSALTTOY 246
WLL+NV+LS P +YGG LL TG F L + F++A+ + P CPL LG+S L T +
Sbjct 189 LCWLLANVMSMPVLVYGGYMLLATGIFQLLALLFFSMATSLTSP-CPLHLGASVLHTHH 247

Query 247 GAAFVWTLATGVLCLFLGGAVVSLQYVRPSALRTLDDQSAK-----DCSQERGG 295
G AFW+TL TG+LC+ LG A+ ++P L+ +QS + S E GG
Sbjct 248 GPAFWITLTGLLCVLLGLAMAVAHRMQPHRLKAFFNQSVDEDPMLEWSPEEG 301

```

> [gi|73999955|ref|XP_544660.2|](#) **UG** PREDICTED: similar to Numb-interacting protein isoform 3 [Canis familiaris]
Length=342

Score = 341 bits (874), Expect = 3e-92
Identities = 170/293 (58%), Positives = 212/293 (72%), Gaps = 6/293 (2%)

```

Query 9 PFYPQPRHAAGFSVPLLIVLFLALAAASFLILPGIRGHSRWFVLRVLLSLFIGAEIV 68
PFY + L ++I +FL +F++ILPGIRG R FWL+RV+ SLFIGA I+
Sbjct 9 PFYTGKPIFPMDTTLAVIIAIFLTALVTIIILPGIRGKMLRFLVLRVVTSLFIGAVIL 68

Query 69 AVHFSAEWFVGTNTNTSYKAFSAARVTARVGLLVLEGINITLTGTPVHQINETIDYNE 128
AV+FS+EWFG V+TNTSYKAFS+ + A VGL VGL G+NITLTGTPV QLNETI+YNE
Sbjct 69 AVNFSSEWFGVQVSTNTSYKAFSSEWIRADVGLQVGLGGVNITLTGTPVQQLNETINYN 128

Query 129 QFTWRLKENYAAEYANALEKGLDPDPVLYLAЕКFTPPSPCGLYHQYHLAGHYASATLWVAF 188
+FTWRL ENYA EYA LEKGLDPDPVLYLAЕКFTP+SPCGL+ QY LAGHY SA LWVAF
Sbjct 129 EFTWRLGENYAAEYAKGLEKGLDPDPVLYLAЕКFTPNPCGLHGQYRLAGHYTSAMLWVAF 188

Query 189 CFWLLSNVLLSTPAPLYGGLALLTTGAFALFGVFALASISSV-PLCPLRLGSSALTTOY 247
WLL+NV+LS P +YGG LL TG F + G+ ++ +S+ P CPLRLG+++L T +G
Sbjct 189 LCWLLANVMSMPVLVYGGYMLLATGIFQMLGLLFFSTATSLTSPCPLRLGTASLHTHG 248

Query 248 AAFVWTLATGVLCLFLGGAVVSLQYVRPSALRTLDDQS-----AKDCSQERGG 295
AFW+TL TG+LC+ LG A+ + P L+ +QS A + + E GG
Sbjct 249 PAFWITLTGLLCVLLGLAMAVAHRIHPQLKAFFNQSTGEDPALEWNPEEG 301

```

> [gi|21703790|ref|NP_663370.1|](#) **UG** Numb-interacting protein 1 [Mus musculus]

[gi|18043595|gb|AAH19755.1|](#)  Dual oxidase maturation factor 1 [Mus musculus]
Length=341

Score = 332 bits (850), Expect = 2e-89
Identities = 168/303 (55%), Positives = 210/303 (69%), Gaps = 1/303 (0%)

Query 8 LPFYQPRHAAGFSVPLLIIVLFLAALAAFLLLPGIRGHSRWFVLRVLLSLFIGAEI 67
LPFY + L ++I +FL +F++ILPGIRG +R FWL+RV+ SLFIGA I
Sbjct 8 LPFYTGKPTFPMDTTLAVIITIFLTALVTFIILPGIRGKTRLFWLLRVVTSLFIGAVI 67

Query 68 VAVHFSAEWFGVTNTNTSYKAFSAARVTARVGLLVGLEGINITLTGTPVHQINETIDYN 127
+AV+FS+EW VG VN NT+YKAFS V+ VGL +GL G+NIT TGTPV QLNETI+YN
Sbjct 68 LAVNFSSEWSVGHVNANTTYKAFSPKWSDVGLQIGLGGVNITFTGTPVQQINETINYN 127

Query 128 EQFTWRLKENYAAEYANALEKGLDPVLYLEAEKFTSPSSPCGLYHQYHLAGHYASATLWVA 187
E F WRL +YA EYA ALEKGLDPVLYLEAEKFTP SPCGLY+QY LAGHYASA LWVA
Sbjct 128 EFAFWRLGRSYAEYAKALEKGLDPVLYLEAEKFTSPRSPCCGLYNQYRLAGHYASAMLWVA 187

Query 188 FCFWLLSNVLLSTPAPLYGGLALLTTGAFALFGVFALASISS-VPLCPLRLGSSALTTQY 246
F WLL+NV+LS P +YGG LL TG F L +F + +S + CPLRLG++ L T +
Sbjct 188 FLCWLLANVMLSMPVLVYGGHMLLATGLFQLLALFFFSMTTSLISPCPLRLGTAVLHTHH 247

Query 247 GAAFWVTLATGVLCLFLGGAVVSLQYVRPSALRLLDQSAKDCSQERGGSPLILGDPLHK 306
G AFW+TLATG+LC+ LG + ++P L+ + S++D E G L P ++
Sbjct 248 GPAFWITLATGLLCILLGLVMVAHRMQPHRLKAFFNLSSDPVLEWGSEEGLLSPHYR 307

Query 307 QAA 309
A
Sbjct 308 SIA 310

>  [gi|68392693|ref|XP_693410.1|](#)  PREDICTED: similar to Numb-interacting protein 2 [Danio rerio]
Length=329

Score = 292 bits (747), Expect = 2e-77
Identities = 144/298 (48%), Positives = 194/298 (65%), Gaps = 6/298 (2%)

Query 1 MTLWNGVLPFYQPQRHAAGFSVPLLIIVLFLAALAAFLLLPGIRGHSRWFVLRVLLS 60
MT ++G+ PFYP R ++ LL+ ILVF LA SFL ILPGIRG SRWFV+ R+ +S
Sbjct 1 MTFYDGIYPFYPLQSRPFMINISLLVAILVFSVLAVSFLFILPGIRGSRWFWMFRIFIS 60

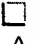

Query 61 LFIGAEIVAHFSAEWFVGTNTNTSYKAFSAARVTARVGLLVGLEGINITLTGTPVHQL 120
LFIG +V ++F+ +W V NT+YK+FS A V+A VGL VGL GINITL G PV Q+

```

Sbjct 61  LFIGVVLVNLFTGDWAEARVKANTTYKSFSTAVVSAEVGLHVGLYGINITLKGEPTQI 120
Query 121  NETIDYNEQFTWRLKENYAAEYANALEKGLPDPVLYLAEKFTPPSSPCGLYHQYHLAGHYA 180
      NETI+YNE  +W  + +Y +ALE+GLP+P+LY+AEKFT +S CGL +QY  + +A
Sbjct 121  NETINYNEIISW--SSSVDEQYGDALERGLPNPILYIAEKFTYNSACGLIYQYSYARFA 178

Query 181  SATLWVAFCFWLLSNVLLSTPAPLYGGLALLTTGAFALFGVFALASISSVPLCPLRLGSS 240
      SA LW AFC WLL+NN+L S P LY G ++ T AF F V + ++I +V C  +GS
Sbjct 179  SANLWTAFCWLLANILFSPVILYAGYMMIATAAFAIFFSVASFSTIYNVSPCDFSIGSE 238

Query 241  ALTTQYGAAFVTLATGVLCLFLGGAVVSLQYVRPSALRTL-----LDQSAKDCSQERG 294
      AL T Y +FW+ LATG+LC +G VV L + P+ +R +D +C + G
Sbjct 239  ALRTDYSHSFWLALATGLLCAVIGLLVLLDCLFARMREAFSVGVDDDECCADEG 296

>  gi|50415464|gb|AAH77555.1|  MGC83502 protein [Xenopus laevis]
Length=308

Score = 278 bits (712), Expect = 2e-73
Identities = 131/304 (43%), Positives = 197/304 (64%), Gaps = 6/304 (1%)

Query 7  VLPFPQPRHAAGFSVPLLIVILVFLALAAASFLILPGIRGSRWFLVRVLLSLFIGAE 66
      + PFYPQPR F ++ +I++ + A +F++ILPGIRG SR WL+R+L SLFIGA
Sbjct 5  IFPFPQPRTPFKFDTKIIEIIICIVTACTFIIILPGIRKRSIWLLRILTSFIGAV 64

Query 67  IVAVHFSAEWFGTVNTNTSYKAFSAARVTARVGLLVLEGINITLTGTPVHQLNETIDY 126
      I+AV+F+++W +GT+ T YK+FS + + A +GL +GL+G+NITL G P +QLNETI+Y
Sbjct 65  ILAVNFTSDWEMGTITATTVYKSFSSHMLNASIGLWIGLKGLNITLIGNPEYQLNETINY 124

Query 127  NEQFTWRLKENYAAEYANALEKGLPDPVLYLAEKFTPPSSPCGLYHQYHLAGHYASATLWV 186
      NE+F W + Y +ALE+GLP P++Y+AEKFT SS CGL+ QY ++ +Y+S +W+
Sbjct 125  NEEFAWESANQFETSYKDALERGLPFPVIVYAEKFTISSDCGLFQQYCISTYYSSGIMWI 184

Query 187  AFCFWLLSNVLLSTPAPLYGGLALLTTGAFALFGVFALASISSVPLCPLRLGSSALTQY 246
      AFC W+L NVL S P LYG + T L + + AS+ P+C ++ G+S L T +
Sbjct 185  AFCSWILYNVLFSPVILYGIYMMFVTAICMLVSLISFASVRKAPVCNIQFGNSILKTHF 244

Query 247  GAAFWVTLATGVLCFLGGAVVSLQYVRPSALRTL-----DQSAKDCSQERGGSPLIL 300
      G ++W++L TG+LCL + ++ L +P L+ + D S K ++E S L L
Sbjct 245  GVSYWLSLITGLLCLIIISLVLLFLYKTPKVLQIFSYGEEEDLSNKSENEEHSSVLSL 304


Query 301  GDPL 304
      + L
Sbjct 305  NEIL 308

```

> [gi|112418659|gb|AAI22089.1|](#) Unknown (protein for MGC:147630) [Xenopus tropicalis]
Length=308

Score = 274 bits (700), Expect = 5e-72
Identities = 130/304 (42%), Positives = 193/304 (63%), Gaps = 6/304 (1%)

Query	7	VLPFYQPRHAAGFSVPLLIIVILVFLAALAAASFLILPGIRGHSRWFVLRVLLSLFIGAE	66
		+ PFYQPR + F ++ +I++ + A +F++ILPGIRG SR WL R+L SLFIGA	
Sbjct	5	IFPFYQPRTSFKFDTKIIEIIIIICIVTACTFIILPGIRGKRSIWLFRILTSFIGAV	64
Query	67	IVAVHFSAEWFGVTNTNTSYKAFSAARVTARVGLLVGLEGINITLTGTPVHQLNETIDY	126
		I+AV+F+++W G V T YK+FS + + A +GL +GL+G+NITL G PV+QLNETI+Y	
Sbjct	65	ILAVNFTSDWETGIVTATTVYKSFHSHMLNASIGLWIGKGVNITLIGNPVYQLNETINY	124
Query	127	NEQFTWRLKENYAAEYANALEKGLDPVLVLAEEKFTPPSPCGLYHQYHLAGHYASATLWV	186
		NE+F W + Y + LE+GLP P+LY+AEKFT +SPCGL+ QY ++ +Y+S +WV	
Sbjct	125	NEEFAWESANQFDKNYKDGRLGLPYPILYVAEKFTINSPCGLFQOYCISTYYSSSEIMWV	184
Query	187	AFCFWLLSNVLLSTPAPLYGGLALLTTGAFAFGVFALASISSVPLCPLRLGSSALTTQY	246
		AF W+L NVL S P LYG + T L + + AS+ P+C + G++ L T +	
Sbjct	185	AFGSWILYNVLFMPVILYGICMMFVTAICMLVSLISFASVRQAPVCNIHFGNAVLTKEF	244
Query	247	GAAFVWTLATGVLCLFLGGAVVSLQYVRPSALRTL-----DQSAKDCSQERGGSPLIL	300
		G ++W++L TG+ CL + ++ L +P +R + D S K ++E S L L	
Sbjct	245	GVSYWLSLVTGLFLCLIVSLVLLFLYKTPKVIRLIFSYPEEEDLSDKSENEEHSSALS	304
Query	301	GDPL 304	
		+ L	
Sbjct	305	NEML 308	

> [gi|109080942|ref|XP_001111148.1|](#)  PREDICTED: similar to Numb-interacting protein [Macaca mulatta]
Length=298

Score = 263 bits (673), Expect = 6e-69
Identities = 142/293 (48%), Positives = 172/293 (58%), Gaps = 51/293 (17%)

Query	9	PFYQPRHAAGFSVPLLIIVILVFLAALAAASFLILPGIRGHSRWFVLRVLLSLFIGAEIV	68
		PFY P+ +I++FL A+F++ILPGIRG +R FWL+RV+ LFIGA I+	
Sbjct	9	PFYAGPKPTFPMDTTSATIIIMIFLTALATFIVILPGIRGKTRLFWLLRVVVTGLFIGAAIL	68

Query 69 AVHFSAEWFVGTVNTNTSYKAFSAARVTARVGLLVGLEGINITLTGTPVHQNLNETIDYNE 128
 Sbjct 69 -----GTPV QLNETI+YNE 83

Query 129 QFTWRLKENYAAEYANALEKGLPDPVLYLAEEKFTPSSPCGLYHQYHLAGHYASATLWVAF 188
 +FTWRL ENYA EY A+EKGLPDPVLYLAEEKFTP SPCGLY QYHLAGHYASA LWVAF
 Sbjct 84 EFTWRLGENYAAEYTKAMEKGLPDPVLYLAEEKFTPGSPCGLYRQYHLAGHYASAMLWVAF 143

Query 189 CFWLLSNVLLSTPAPLYGGLALLTTGAFALFG-VFALASISSVPLCPLRLGSSALTTQY 247
 WLL+NV+LS P +YGG LL TG F L +F + S P CPL LG+S L T +G
 Sbjct 144 LCWLLANVMSMPVLVYGGYMLLATGIFQLLALLFFSMATSLTPPCPLHLGASVLHTHHG 203

Query 248 AAFWVTLATGVLCLFLGGAVVLSQYVRPSALRLLDQSAK-----DCSQERGG 295
 AFW+TL TG+LC+ LG A+V ++P L+ +QS + S E GG
 Sbjct 204 PAFWITLTTGLLCVLLGLAMVVAHRMQPHRLKAFFNQSVDEDPMLEWSPEEGG 256

> [gi|16552420|dbj|BAB71304.1](#) **U G** unnamed protein product [Homo sapiens]
[gi|18089176|gb|AAH20841.1](#) **U G** DUOX1 protein [Homo sapiens]
 Length=298

Score = 261 bits (667), Expect = 3e-68
 Identities = 143/294 (48%), Positives = 175/294 (59%), Gaps = 53/294 (18%)

Query 9 PFYQPQRHAAGFSVPLLIVILVFLALAAASFLILPGIRGSRFWLVRVLLSLFIGAEIV 68
 PFY P+ L +I++FL A+F++ILPGIRG +R FWL+RV+ SLFIGA I+
 Sbjct 9 PFYAGPKPTFPMDTTLASIIIMFLTALATFIVILPGIRGKTRLFWLLRVVTSFIGAAIL 68

Query 69 AVHFSAEWFVGTVNTNTSYKAFSAARVTARVGLLVGLEGINITLTGTPVHQNLNETIDYNE 128
 GTPV QLNETI+YNE
 Sbjct 69 -----GTPVQQLNETININE 83

Query 129 QFTWRLKENYAAEYANALEKGLPDPVLYLAEEKFTPSSPCGLYHQYHLAGHYASATLWVAF 188
 +FTWRL ENYA EYA ALEKGLPDPVLYLAEEKFTP SPCGLY QY LAGHY SA LWVAF
 Sbjct 84 EFTWRLGENYAAEYAKALEKGLPDPVLYLAEEKFTPRSPCGLYRQYRLAGHYTSAMLWVAF 143

Query 189 CFWLLSNVLLSTPAPLYGGLALLTTGAFALFGV--FALASISSVPLCPLRLGSSALTTQY 246
 WLL+NV+LS P +YGG LL TG F L + F++A+ + P CPL LG+S L T +
 Sbjct 144 LCWLLANVMSMPVLVYGGYMLLATGIFQLLALLFFSMATSLTSP-CPLHLGASVLHTHH 202

Query 247 GAAFVTLATGVLCLFLGGAVVLSQYVRPSALRLLDQSAK-----DCSQERGG 295
 G AFW+TL TG+LC+ LG A+ ++P L+ +QS + S E GG
 Sbjct 203 GPAFWITLTTGLLCVLLGLAMVVAHRMQPHRLKAFFNQSVDEDPMLEWSPEEGG 256

> [gi|114656789|ref|XP_001162827.1|](#) **G** PREDICTED: Numb-interacting protein isoform 2 [Pan troglodytes]
[gi|114656791|ref|XP_001162868.1|](#) **G** PREDICTED: Numb-interacting protein isoform 3 [Pan troglodytes]
[gi|114656793|ref|XP_001162900.1|](#) **G** PREDICTED: Numb-interacting protein isoform 4 [Pan troglodytes]
[gi|114656795|ref|XP_001162937.1|](#) **G** PREDICTED: Numb-interacting protein isoform 5 [Pan troglodytes]
 Length=298

Score = 260 bits (665), Expect = 5e-68
 Identities = 143/294 (48%), Positives = 174/294 (59%), Gaps = 53/294 (18%)

Query	9	PFYPQPRHAAGFSVPLLIIVLFLALAAASFLILPGIRHSRWFVLRVLLSLFIGAEIV	68
		PFY P+ L +I++FL A+F++ILPGIRG R FWL+RV+ SLFIGA I+	
Sbjct	9	PFYAGPKPTFPMDDTTLASIIIMIFLTALATFIVILPGIRGKMRFLWLLRVVTSLSFIGAAIL	68
Query	69	AVHFSAEWFVGTVNTNTSYKAFSAARVTVRVGLLVGLEGINITLTGTPVHQNLNETIDYNE	128
		GTPV QLNETI+YNE	
Sbjct	69	-----GTPVQQNLNETINYNE	83
Query	129	QFTWRLLKENYAAEYANALEKGLPDPVLYLAEKFTSPSPCGLYHQYHLAGHYASATLWVAF	188
		+FTWRL ENYA EYA ALEKGLPDPVLYLAEKFTP SPCGLY QY LAGHY SA LWVAF	
Sbjct	84	EFTWRLGENYAEYAKALEKGLPDPVLYLAEKFTSPSPCGLYRQYRLAGHYTSAMLWVAF	143
Query	189	CFWLLSNVLLSTPAPLYGGLALLTTGAFALFGV--FALASISSVPLCPLRLGSSALTTOY	246
		WLL+NV+LS P +YGG LL TG F L + F++A+ + P CPL LG+S L T +	
Sbjct	144	LCWLLANVMSMPVLVYGGYMLLATGIFQLLALLFFFSMATSLTSP-CPLHLGASVLHTHH	202
Query	247	GAAFVWTLATGVLCFLGGAVVSLQYVRPSALRTLDDQSAK-----DCSQERGG	295
		G AFW+TL TG+LC+ LG A+ ++P L+ +QS + S E GG	
Sbjct	203	GPAFWITLTGLLCVLLGLAMAVAHMQPHRLKAFFNQSVDEDPMLEWSPEEGG	256

> [gi|739999957|ref|XP_860877.1|](#) **U** **G** PREDICTED: similar to Numb-interacting protein 1 isoform 4 [Canis familiaris]
 Length=297

Score = 258 bits (658), Expect = 3e-67
 Identities = 138/293 (47%), Positives = 174/293 (59%), Gaps = 51/293 (17%)

Query	9	PFYPQPRHAAGFSVPLLIIVLFLALAAASFLILPGIRHSRWFVLRVLLSLFIGAEIV	68
		PFY + L ++I +FL +F++ILPGIRG R FWL+RV+ SLFIGA I+	
Sbjct	9	PFYTGHKPIFPMDTTLAVIIAIFLTALVTFIILPGIRGKMRFLWLLRVVTSLSFIGAVIL	68


```


Query 69  AVHFAEWFVGTNTNTSYKAFSAARVTARVGLLVGLEGINITLTGTPVHQNLNETIDYNE 128
Sbjct 69  -----GTPVQQLNETINYNE 83

Query 129  QFTWRLKENYAAEYANALEKGLDPVLYLAEKFTPSSPCGLYHQYHLAGHYASATLWVAF 188
+FTWRL ENYA EYA LEKGLDPDPVLYLAEKFT+SPCGL+ QY LAGHY SA LWVAF
Sbjct 84  EFTWRLGENYAAEYAKGLEKGLDPDPVLYLAEKFTPNSPCGLHGQYRLAGHYTSAMLWVAF 143

Query 189  CFWLLSNVLLSTPAPLYGGLALLTTGAFALFGVFALASISSV-PLCPLRLGSSALTYYG 247
WLL+NV+LS P +YGG LL TG F + G+ ++ +S+ P CPLRLG+++L T +G
Sbjct 144  LCWLLANVMSMPVLVYGGHMLLATGIFQMLGLLFFSTATSLTPSCPLRLGTASLTHHG 203

Query 248  AAFWVTLATGVLCFLFGGAVVSLQYVRPSALRTLDDQS-----AKDCSQERGG 295
AFW+TL TG+LC+ LG A+ + P L+ +QS A + + E GG
Sbjct 204  PAFWITLTGLLCVLLGLAMAVAHRIHPQRLKAFFNQSTGEDPALEWNPEEG 256

```

>gi|50752733|ref|XP_425055.1|  PREDICTED: similar to CDNA sequence BC019755 [Gallus gallus]
Length=316

Score = 254 bits (649), Expect = 4e-66
Identities = 128/283 (45%), Positives = 173/283 (61%), Gaps = 11/283 (3%)

```

Query 1  MTLWNGVLPFYQPQRHAAAGFSVPLLVILVFLAALASFLILPGIRGHSRWFVLRVLLS 60
MTLW+G PFYP F I+ VFL++ + ++ILPGIRG R FWL+RV+ S
Sbjct 1  MTLWDGSPFPYPGTNACFPDFTTWAIIASVFLSVLITSIILPGIRGKRLFWLLRVVTS 60

Query 61  LFIGAEIVAVHFAEWFVGTNTNTSYKAFSAARVTARVGLLVGLEGINITLTGTPVHQ 120
LFIGA ++ + F+ +W G V N SYK+FS A V A +GL +GL G+NITL G PV+Q+
Sbjct 61  LFIGAVLTIQFTRDWESGWVTANISYKFSRAMVNANIGLHIGLAGVNITLVGNPNVQV 120

Query 121  NETIDYNEQFTWRLKENYAAEYANALEKGLDPVLYLAEKFTPSSPCGLYHQYHLAGHYA 180
NETI+YNE F W +Y Y+ LEKGLP P+LY+AEKFT SPC ++ QY ++ YA
Sbjct 121  NETINYNEHFAWSFDADYDHSYSEGLEKGLPSPILYVAEKFTTQSPCNVHRQYRISSCYA 180

Query 181  SATLWVAFCFWLLSNVLLSTPAPLYGGLALLTTGAFALFGVFALASISSVPLCPLRLGSS 240
S TLW+A C WL+S +L S P LYGG LL T A LF + ++ + + LG +
Sbjct 181  SITLWMALCTWLISILLFSPVLLYGGYMLLLTAALMLFSLFFVTVDAP---GVHLGPT 237

Query 241  ALTTQYGAAFWVTLATGVLCFLFGGAVVSLQYVRPSALRTLDD 283
L+T +G+LCL LG V+ L V P L+ + +
Sbjct 238  HLST-----LCVSGLLCLLLGLGIVILNSVHPQKLVFN 272

```

> [gi|50752731|ref|XP_425054.1|](#) **G** PREDICTED: similar to CDNA sequence BC019755 [Gallus gallus]
Length=602

Score = 244 bits (624), Expect = 3e-63
Identities = 113/233 (48%), Positives = 153/233 (65%), Gaps = 4/233 (1%)

Query	51	WFWLVRVLLSLFIGAEIVAVHFSAEWFGVTNTNTSYKAFSAARVTARVGLLVLEGINI	110
		W L+ LF+ V F+ +W G V NTSYK+FS A V +GL VGL G+NI	
Sbjct	335	WSPALTLIELFLSV---VQFTGDWESGWVTANTSYKSFSCAVNVNDIGLHVGLAGVNI	390
Query	111	TLTGTPVHQLNETIDYNEQFTWRLKENYAAEYANALEKGLDPVLYLAEKFTTPSSPCGLY	170
		TL G PV+Q+NETI+YNE F W +Y Y LEKGLP P+LY+AEKFT SPC ++	
Sbjct	391	TLVGNPVNQVNETINYNHEHFAWSFDADYDHSYGEKGLPSPILYVAEKFTTQSPCNVH	450
Query	171	HQYHLAGHYASATLWVAFCFWLLSNVLLSTPAPLYGGLALLTTGAFALFGVFALASISSV	230
		QY ++ HYASA+LWVAF W L+SN+L STP +YGG +L TGAF +F + + +++ +	
Sbjct	451	RQYRISSHYASASLWVAFCTWLISNMLFSTPVLVYGGYMILFTGAFMIFSLLSFSTVRNS	510
Query	231	PLCPLRLGSSALTTOYGAAFWVTLATGVLCFLGGAVVSQYVRPSALRTLDD	283
		+CP++ G+++L YG +FW+TLA G+LC G VV+L Y P L+T D	
Sbjct	511	LVCPIQFGTTSLWISYGGFWLTLAVGLLCFVAGITVVALHYFNPELLKTFDD	563

Score = 80.5 bits (197), Expect = 1e-13
Identities = 39/75 (52%), Positives = 52/75 (69%), Gaps = 0/75 (0%)

Query	1	MTLWNGVLPFYQPQRHAAAGFSVPLLLIVILVFLALAAASFLILLPGIRGSRWFVLRVLLS	60
		MTL++G+ PFY Q R + F V +IV++VFL LA++FLLI+PGIRG R +W+VR L S	
Sbjct	138	MTLFDGIYPFYLQQRKSFVDVSTIIIVIVFLMLASTFLLIIPGIRGRVRLYWMVRALFS	197
Query	61	LFIGAEIVAVHFSAE	75
		L +G IV V E	
Sbjct	198	LMVGVIIVVVTLCLE	212

> [gi|47220524|emb|CAG05550.1|](#) unnamed protein product [Tetraodon nigroviridis]
Length=296

Score = 190 bits (483), Expect = 7e-47
Identities = 107/207 (51%), Positives = 125/207 (60%), Gaps = 29/207 (14%)

Query	9	PFYQPRHAAAGFSVPLLLIVILVFLALAAASFLILLPGIRGH-----	48
-------	---	---	----

```

Sbjct 1 PFYP R + FS LL +ILVFL LA S LLILPGIRG 60
        PFYPPQRTSFIFSGRLLTIILVFLLLALLLILPGIRKVVSGFQRQPNNSLGLHLHL
Query 49 -----SRFWLVRVLLSLFFIGAEIVAVHFSAEWFGVTNTNTSYKAFSAARVTARVGL 101
        R FW+ R+LLS+FIGA IVA++F+ +W + T +YK+FS+A VTA VGL
Sbjct 61 SPSSPSCQRLFWMFRIILSIFIGAVIVALNFTTRDAEARMTTTAAAYKSFSSAVVTAEVGL 120

Query 102 LVGLEGINITLTGTPVHQLNETIDYNEQFTWRLKENYAAEYANALEKGLPDPVLYLAEKF 161
        VGL GIN+TL GTP QLNETIDYNE FTW EY ALE+GLP+P+LY+AEKF
Sbjct 121 HVGLYGINVTLKGTPAVQLNETIDYNEMFTWH--GTVEEYEEALERGLPNPILYVAEKF 178

Query 162 TPSSPCGLYHQYHLAGHYASATLWVAF 188
        T S C L QY G ASATLW F
Sbjct 179 TRSGACRLVSQYRYPGRCASATLWYTF 205

```

>gi|91079842|ref|XP_970783.1| **UG** PREDICTED: similar to CG4482-PA, isoform A [Tribolium castaneum]
Length=406

Score = 157 bits (397), Expect = 6e-37
Identities = 96/273 (35%), Positives = 143/273 (52%), Gaps = 9/273 (3%)

```

Query 15 RHAAGFSVPLLIVILVFLALAAASFLILPGIRGHSRWFVLRVLLSLFFIGAEIVAVHFS 74
        R A V L+ + +F L +FL+I PGIR R+ V LSLF+GA I+ F +
Sbjct 22 RTAVTGDVTLITFLTIFSTLYVAFLLIIFPGIR-KERFTTFFAVTSLFVGATILVTLFGS 80

Query 75 EWFVGTNTNTSYKAFSAARVTARVGLLVGLEGINITLTGTPVHQLNETIDYNEQFTWRL 134
        W V T + ++Y+AFS ++++ +G+ VGL +NITL + H ID+NEQF W
Sbjct 81 AHWATASIVSTYRAFSITDKLSSNIGVVVGLRHVNITLQASGGHNWTSIDIDFNEQFLWIN 140

Query 135 KENYAAEYANALEKGLPDPVLYLAEKFTPSSPCGLY--HQYHLAGHYASATLWVAFCFWL 192
        + + A+ +GLP P+L +AE FT GL QY AG+YA LW +F W+
Sbjct 141 SDQMGSFREAMVRGLPFPILTVAEYFTMGQE-GLSWGQYRAAGYAIIMLWTSFSVWI 199

Query 193 LSNVLLSTPAPLYGGLALLTTGAFALFGVFALASISSVPLCPL--RLGSSALTTQYGA 250
        L N++L P YG + L+TT F L A +P PL + S L +G +
Sbjct 200 LMNMLIV-VPRYGAV-LMTTCGFLLLAT-ACGYFGLLPETPLVHVHIEGSTLHFSFGWCY 256

Query 251 WVTLATGVLCFLGGA VSVLQYVRPSALRTLDD 283
        W+ L G +CL G + L+ + P + T+L+
Sbjct 257 WLVLIAGSICLLSGVIITVLEIIFPHSFSTILE 289

```

> [gi|108876501|gb|EAT40726.1|](#) conserved hypothetical protein [Aedes aegypti]
Length=421

Score = 149 bits (377), Expect = 1e-34
Identities = 95/269 (35%), Positives = 139/269 (51%), Gaps = 14/269 (5%)

Query 22 VPLLIVILVFLAALAAASFLLLILPGIRGHSRWFVLVRVLLSLFAGAEIVAVHFSAEWFGTV 81
V ++ V ++F + +FL+I PG+R ++ V LSLF+G I+ + W V
Sbjct 29 VSIVAVCVLFATIVLAFLVIFPGVR-KQKFTTTTITLSLFFVGLVILVTRLGSGWHVAQS 87

Query 82 NTNTSYKAFSAARVTARVGLLVGLEGINITLTGTPV-HQLNETIDYNEQFTWRLKENYAA 140
YKAFS ++ AR+G +GL INITL PV + ID+NE+F+W +
Sbjct 88 TIVAPYKAFSREKLPARLGAHIGLMHINITLAALPVGNWSTPDIDFNERFSWNQANDMGN 147

Query 141 EVANALEKGLDPDVLXLAEKFTPSPCGLY-HQYHLAGHYASATLWVAFCFWLLSNVLLS 199
Y NAL++GLP P+L +AE F+ + QY AG+YAS LW +F WLL N+LL
Sbjct 148 SYKNALQRLGPLYPILTVAEYFSLGQGFANGQYRAAGYYASILLWASFASWLLMNL-- 206

Query 200 TPAPLYGGLALLTTGAFALGFVAFALASISSVPLCPLR-----LGSSALTTQYGAAFWVT 254
P YG + TGA L G ASI + P R + ++ + G FW+ L
Sbjct 207 VAVPRYGAYTMTLTGAL-LIG----ASIGYSQMLPKRPLTIFIEGGRISFRLGWCFLVL 261

Query 255 ATGVLCFLGGAVVSLQYVRPSALRTLDD 283
G+LCL +G + + V P T+L+
Sbjct 262 IAGILCLSVGLIISIIDLVPWPHRFSTILE 290

> [gi|19921356|ref|NP_609733.1|](#) [UG](#) moladietz CG4482-PA, isoform A [Drosophila melanogaster]
[gi|116007332|ref|NP_001036362.1|](#) [G](#) moladietz CG4482-PD, isoform D [Drosophila melanogaster]
[gi|116007334|ref|NP_001036363.1|](#) [G](#) moladietz CG4482-PC, isoform C [Drosophila melanogaster]
[gi|16769350|gb|AAL28894.1|](#) [UG](#) LD27791p [Drosophila melanogaster]
[gi|22946509|gb|AAF53425.2|](#) [G](#) CG4482-PA, isoform A [Drosophila melanogaster]
[gi|41058061|gb|AAR99096.1|](#) [UG](#) RE74613p [Drosophila melanogaster]
[gi|113194986|gb|ABI31316.1|](#) [G](#) CG4482-PD, isoform D [Drosophila melanogaster]
[gi|113194987|gb|ABI31317.1|](#) [G](#) CG4482-PC, isoform C [Drosophila melanogaster]
Length=474

Score = 145 bits (365), Expect = 3e-33
Identities = 86/264 (32%), Positives = 131/264 (49%), Gaps = 4/264 (1%)

Query 22 VPLLIVILVFLAALAAASFLLLILPGIRGHSRWFVLVRVLLSLFAGAEIVAVHFSAEWFGTV 81

```

      V ++ V ++F      +FL+I PG+R ++      V LSLF+G I+      + W V
Sbjct 29 VSIVAVSVLFATFYVAFLVIFPGVR-KQKFTTTFSTVTLSLFVGLVILITRLGSAWHVAHA 87



Query 82 NTNTSYKAFSAARVTARVGLLVGLEGINITLTGTPV-HQLNETIDYNEQFTWRLKENYAA 140
      YKAFS ++ AR+G +GL +N+TLT P+ + IDYNE+FTW + +A
Sbjct 88 TIIAPYKAFSREKLPARIGTHIGLHMVNVTLTAPIGNWTTPDDIDYNERFTWEGANDMSA 147

Query 141 EYANALEKGLPDPVLYLAEKFTPSSPCGLY-HQYHLAGHYASATLWVAFCFWLLSNVLLS 199
      Y +AL++GLP P+L +AE F+      + QY AG++AS LW + WLL N+LL
Sbjct 148 NYRHALQRLGPPILTVAEYFSLGREGFSWGGQYRAAGYFASIMLWASLASWLLMNL-- 206

Query 200 TPAPLYGGLALLTTGAFALFGVFALASISSVPLCPLRLGSSALTTQYGAAFWVTLATGVL 259
      P YG TGA +      +      + L L L +G +W+ L G+L
Sbjct 207 IAVPRYGAYMKALTGALLVCTTVGYHCLLPKRPLSIHLEGGRLFEHFGWCYWLVLVAGIL 266

Query 260 CLFLGGAVVSLQYVRPSALRTLDD 283
      C G + + V P T+L+
Sbjct 267 CFIAGVLISIIDLVMPHTFSTVLE 290

```

> [gi|58392116|ref|XP_319114.2|](#)  ENSANGP00000006016 [Anopheles gambiae str. PEST]
[gi|55236197|gb|EAA13920.2|](#)  ENSANGP00000006016 [Anopheles gambiae str. PEST]
Length=374

```

Score = 143 bits (360), Expect = 1e-32
Identities = 86/264 (32%), Positives = 135/264 (51%), Gaps = 4/264 (1%)

Query 22 VPLLIVILVFLAALASFLILPGIRGHSRWFVLVRVLLSLFIGAEIVAVHFSAEWFGTV 81
      V ++ V ++F + +FL+I PG+R ++      V LSLF+G I+      + W V
Sbjct 29 VSIVAVCVMFATVYLAFLVIFPGVR-KQKFTTFTTTLTLFVGLVILVSRGSGWHVAQS 87

Query 82 NTNTSYKAFSAARVTARVGLLVGLEGINITLTGTPV-HQLNETIDYNEQFTWRLKENYAA 140
      Y+AFS ++ AR+G +GL INITLT P+ + ID+NE+F+W +
Sbjct 88 TIVAPYRAFSREKLPARIGAHIGLHMHINITLTALPLGNWTTPDDIDFNERFSWNQANDMGN 147

Query 141 EYANALEKGLPDPVLYLAEKFTPSSPCGLY-HQYHLAGHYASATLWVAFCFWLLSNVLLS 199
      Y +AL++GLP P+L +AE F+      + QY AG+YAS LW +F WLL N+LL
Sbjct 148 SYRDALQRLGPPILTVAEYFSLGQEGFAWGGQYRAAGYASILLWASFAAWLLMNL-- 206

Query 200 TPAPLYGGLALLTTGAFALFGVFALASISSVPLCPLRLGSSALTTQYGAAFWVTLATGVL 259
      P YG + TGA +      +S+      + + + + G F++ L GVL
Sbjct 207 VAVPRYGAYTMTLTGALLIGASIGYSSMLPKRPLTIVIEGARIDFHLGWCFCYLVLIAGVL 266

```

Query 260 CLFLGAVVSLQYVRPSALRTLDD 283
 C +G + + V P T+L+
 Sbjct 267 CFAIGLVISIIDLVPHPHFSTILE 290

> [gi|54645694|gb|EAL34432.1|](#) GA18214-PA [Drosophila pseudoobscura]
 Length=467

Score = 143 bits (360), Expect = 1e-32
 Identities = 88/265 (33%), Positives = 133/265 (50%), Gaps = 6/265 (2%)


Query 22 VPLLIVILVFLAALAAASFLILPGIRGHSRWFVLVRVLLSLFIGAEIVAVHFSAEWFGTV 81
 V ++ V ++F +FL+I PG+R ++ V LSLF+G I+ + W V
 Sbjct 29 VSIVAVSVLFATFYVAFVLVFPGVR-KQKFTTFTSTVTLSTLVGLVILITRLGSAWHVAHA 87

Query 82 NTNTSYKAFSAARVTARVGLLVGLEGINITLTGTPV-HQLNETIDYNEQFTWRLKENYAA 140
 YKAFS ++ AR+G +GL +N+TLT P+ + IDYNE+F W + +A
 Sbjct 88 TIIAPYKAFSREKLPARIGTHIGLMHVNVTLTAIPIGNYTPPDIDYNERFMWEGATDMSA 147

Query 141 EYANALEKGLPDPVLYLAEKFTPSSPCGLY-HQYHLAGHYASATLWVAFCFWLLSNVLLS 199
 Y +AL++GLP P+L +AE F+ + QY AG++AS LW + WLL N+LL
 Sbjct 148 NYRHALQRLPFPILTVAEYFSLGREGFSGGQYRAAGYFASIMLWSSLASWLLMNLLL- 206

Query 200 TPAPLYGGLALLTTGAFALFGVFAL-ASISSVPLCPLRLGSSALITQYGAAFWVTLATGV 258
 P YG TGA + + PLC + L L +G +W+ L G+
 Sbjct 207 IAVPRYGAYMKALTGALLVCTTVGYHCLLPKRPLC-IYLEGGRLEFHFHGWYWLVLVAGI 265

Query 259 LCLFLGGAVVSLQYVRPSALRTLDD 283
 LC G + + V P T+L+
 Sbjct 266 LCFIAGVLISIIDLVPHPHTFSTVLE 290

> [gi|66513371|ref|XP_393580.2|](#)  PREDICTED: similar to moladietz CG4482-PA, isoform A [Apis mellifera]
 Length=387

Score = 142 bits (357), Expect = 3e-32
 Identities = 88/266 (33%), Positives = 135/266 (50%), Gaps = 8/266 (3%)

Query 22 VPLLIVILVFLAALAAASFLILPGIRGHSRWFVLVRVLLSLFIGAEIVAVHFSAEWFGTV 81
 VPL+IV +VF + +FL+I PGIR R+ + V LSLF+GA I + + W +
 Sbjct 29 VPLVIVFVWFGTIFTAFLVIFPGIR-KERFSTFLTITLSTLVGASIQVAQYQSSWHTSSA 87

Query 82 NTNTSYKAFSAARVTARVGLLVGLEGINITLTGTPVHQ-LNETIDYNEQFTWRLKENYAA 140

```

      ++Y AFS + A +G +GL INIT P + + ++YNE+F WR +
Sbjct 88 TIVSTYSAFSRQKTAEEIGGYIGLMHINITYRLLPSSENPMDDVEYNERFWWRSTGEMTS 147

Query 141 EYANALEKGLPDPVLYLAEKFT-PSSPCGLYHQYHLAGHYASATLWVAFCFWLLSNVLLS 199
      + AL +G P P++ LAE F+ +Y AG+YAS LW +F W + N+LL
Sbjct 148 AFKQALNQAGPFPPIVSLAEYFSLHQEGFSWGSKYRQAGYYASLMLWTSFASWAMNLLLI 207

Query 200 TPAPLYGGLALLTTGAFALFGVFALASISSVPLCPL--RLGSSALTTQYGAAFWVTLATG 257
      P YG ++ TG L + L + +P PL + S L G +W+ L G
Sbjct 208 V-VPRYGAYGMIFTGICML--ITNLVYWALLPCEPLIAHVDGSILAFNLGWNWLVLLAG 264

Query 258 VLCLFLGGAVVSLQYVRPSALRTLDD 283
      + CLF G + ++ + P T+L+
Sbjct 265 IGCLFAGVVITAIDMIFPHQFSTILE 290

```

> [gi|91088357|ref|XP_971705.1|](#) **U****G** PREDICTED: similar to CG4482-PA, isoform A [Tribolium castaneum]
 Length=375

Score = 126 bits (317), Expect = 1e-27
 Identities = 81/250 (32%), Positives = 125/250 (50%), Gaps = 16/250 (6%)

```

Query 28 ILVFLALAASFLLLILPGIRGHSRWFVLRVLLSLFIGAEIVAVHFSAEWFGVTNNTSY 87
      I F+ L S L++LP V + L IG ++ +F EW VG + T T Y
Sbjct 32 IAAFIILLSLVLLPTSSLKKTCLCFVEITTLTIGLLLLLGNFGQEWEGVGHILTRTPY 91



Query 88 KAFAARVTARVGLLVGLEGINITLTG--TPVHQLNETIDYNEQFTWRLKE----- 136
      KA S+A + A +GL +GL +N+TL P + E I+YNE+F+W +
Sbjct 92 KAGSSAEINASIGLKIGLRVNVTLKSDQNPPNLAREIINYNERNFSTWDQDRLGFGPFA 151

Query 137 -NYAAEYANALEKGLPDPVLYLAEKFTSPSPCGLYHQ-YHLAGHYASATLWVAFCFWLLS 194
      + E+ A +GLP P+L++ E F + + Y AG Y+ LW AF WL++
Sbjct 152 GHLQQEFAAQYRGLPTPILWVVEYFVIDGEGFRFGRFYRTAGWYSHVALWCAFCWLVA 211

Query 195 NVLLSTPAPLYGGLALLTTGAFAL-FGVFALASISSVPLCPLRLGSSALTTQYGAAFWVT 253
      +LL LYGG L GA L + L + +PL + +TT++G ++W+T
Sbjct 212 -LLLFRSVILYGGYCLAACGALQLTANLIWLVRNPIPLV-VPFEDGTITTRFGLSYWIT 269

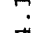
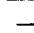
Query 254 LATGVLCFL 263
      A+G+LCL +
Sbjct 270 FASGILCLVI 279

```

> [gi|72013586|ref|XP_801771.1|](#)  PREDICTED: similar to ENSANGP00000006016 isoform 2 [Strongylocentrotus purpuratus]
[gi|115944173|ref|XP_001176848.1|](#)  PREDICTED: similar to ENSANGP00000006016 isoform 1 [Strongylocentrotus purpuratus]
 Length=430

Score = 121 bits (303), Expect = 5e-26
 Identities = 88/295 (29%), Positives = 138/295 (46%), Gaps = 34/295 (11%)

Query	6	GVLFPYQPRHAAGFSVPLLIVLVFLAALAAFLILPGIRHSRWFVLRVLLSLFIGA	65
		G+ +YP + A V + I F+ SF++ILPGIRG R + VR+ +SLFIGA	
Sbjct	12	GLPTYPPNKTAVTADVLEIGFIFAFVIAFFSFIVILPGIRGMQRCYSFVRITISLFIGA	71
Query	66	EIVAVHFSAEWFGTVN-TNTSYKAFSAARV-TARVGLLVGLEGINITL---TGTPVHQL	120
		I+ + EW ++ T YKAFS + A + + +GL +NITL + V	
Sbjct	72	GIMLSLWGQEWKAEHLHGIETYYKAFSYYEIIHDADIEVKIGLSVNITLKAPANSLSVEHP	131
Query	121	NETIDYNEQFTW-----RLKENYAAEYANALEKGLDPVLYLAEKFT-PSSPCGL	169
		+E IDYNE+F + R E+ A G P PVL++AE FT	
Sbjct	132	DEVIDYNERFHFYGGQGRGGRFGRINREFREAQWSGKPYVPLWIAEYFTLDGEDIRW	191
Query	170	YHQYHLAGHYASATLWVAFCFWLLSNVLLSTPAPLYGGLALLTTGAFALFGVFALASISS	229
		Y +AG+YA +W++F W+L+N+L ++ GA+ L ++	
Sbjct	192	GRSYRMAGYYAYIMVWLSFPLWILANILF-----FMVIRNGAYFLIMTGGSLLTAN	242
Query	230	VPLCPLRLGSS-----ALTQYGAAFWVTLATGVLCFLGGA VSLQYVRP	275
		V +R GS L G +FW+ + G++ + G V+++ Y+ P	
Sbjct	243	VLYATIRYGSELKIPFAAHHVLEFHKGPSFWLCMVAGLISVICGFIVLAMDIYP	297

> [gi|115738140|ref|XP_001177754.1|](#)  PREDICTED: similar to ENSANGP00000006016 [Strongylocentrotus purpuratus]
[gi|115944171|ref|XP_001176989.1|](#)  PREDICTED: similar to ENSANGP00000006016 isoform 2 [Strongylocentrotus purpuratus]
 Length=438

Score = 121 bits (303), Expect = 5e-26
 Identities = 88/295 (29%), Positives = 138/295 (46%), Gaps = 34/295 (11%)

Query	6	GVLFPYQPRHAAGFSVPLLIVLVFLAALAAFLILPGIRHSRWFVLRVLLSLFIGA	65
		G+ +YP + A V + I F+ SF++ILPGIRG R + VR+ +SLFIGA	
Sbjct	12	GLPTYPPNKTAVTADVLEIGFIFAFVIAFFSFIVILPGIRGMQRCYSFVRITISLFIGA	71


```

Query 66 EIVAVHFSAEWFGVTN-TNTSYKAFSAARV-TARVGLLVGLEGINITL---TGTPVHQL 120
      I+ + EW ++ T YKAFS + A + + +GL +NITL + V
Sbjct 72 GIMLSLWGQEWKAEHLGIIETYYKAFSYEEIHDADIEVKIGLNSVNITLKAPANSLVEHP 131

Query 121 NETIDYNEQFTW-----RLKENYAAEYANALEKGLPDPVLYLAEKFT-PSSPCGL 169
      +E IDYNE+F + R E+ A G P PVL++AE FT
Sbjct 132 DEVIDYNERHFHYGGQGRGGRFGRINREFREAQWQKPYPLWIAEYFTLGDGDIRW 191

Query 170 YHQYHLAGHYASATLWVAFCFWLLSNVLLSTPAPLYGGLALLTTGAFALFGVFALASISS 229
      Y +AG+YA +W++F W+L+N+L ++ GA+ L ++
Sbjct 192 GRSYRMAGYYAYIMVWLSFPLWILANILF-----FMVIRNGAYFLIMTGGSLLTAN 242

Query 230 VPLCPLRLGSS-----ALTTOYGAAFWVTTLATGVLCFLGGA VVSLOQYVRP 275
      V +R GS L G +FW+ + G++ + G V+++ Y+ P
Sbjct 243 VLYATIRYGSELKIPFAAHVLEFHKGPSFWLCMVAGLISVICGFIVLAMDIYP 297

```

> [gi|39591661|emb|CAE71238.1|](#) Hypothetical protein CBG18111 [Caenorhabditis briggsae]
 Length=397

Score = 110 bits (275), Expect = 9e-23
 Identities = 88/301 (29%), Positives = 137/301 (45%), Gaps = 23/301 (7%)

```

Query 3  LWNVLPFYQPRHAA--GFSVPLLIVILVFLALAAASFLILPGIRGHSRWFVLVRVLLS 60
      LW G P +AA F++ ++ VFL ++LLILPG+R R V +L
Sbjct 2  LWFGGNPSPSDYPNAAIPNFMHAFVIFSFLIPFIAYLLILPGVR-RKRVIITVTYVLM 60

Query 61  LFIGAEIVAVHFSAEWFGVTNTNTSYKAFSAARVTARVGLLVGLEGINITLTGTPVHQL 120
      L +GA ++A W G T ++ S R+ A++G+ +GL+ +N+TL +
Sbjct 61  LVVGASLIASLILPCWASGNQMIYTOQFRGHSNERILAKIGVEIGLQKVNVTLKFERLLSS 120

Query 121 NETID-----YNEQFTWRLKENYAAEYANALEKGLPDPVLYLAEKFTPSSPCGLY-H 171
      ++ + YNE F + A + LE GLP P+L + E F+ +
Sbjct 121 SDVLPGSDMTELYNEGFDISGISSMAEALHHGLENGLPYPMLSVLEYFSLNQDAFDWGR 180

Query 172 QYHLAGHYASATLWVAFCFWLLSNVLLSTPAPLYGGLALLTTGAFALFGVFALASISSVP 231
      Y +AGHY +A +W AF W LS VLL P ++L TG L +S
Sbjct 181 HYRVAGHYTNAAVWFAFACWCLSVLLFL-LPHNAYKSILATGISCLVLLSP-- 237

Query 232 LCPLRLGSSA-----LTTQYGAAFWVTTLATGVLCFLGGA VVSLOQYVRPSALRTLDDQ 284
      C LR+ + LT + F++ A G+LC+ G + ++ R L T LD
Sbjct 238 -CELRIAFGTENFERVDLTATFSFCFYLI FAMGILCVLCGLGVCCEHWRIYTLSTFLDA 296

Query 285 S 285

```

S
Sbjct 297 S 297

> [gi|25149497|ref|NP_498886.2|](#) [UG](#) C06E1.3 [Caenorhabditis elegans]
[gi|21542476|sp|P34298|YKQ3 CAEEL](#) [G](#) Hypothetical protein C06E1.3
[gi|20198766|gb|AAA27934.2|](#) [G](#) Hypothetical protein C06E1.3 [Caenorhabditis elegans]
Length=397

Score = 106 bits (265), Expect = 1e-21
Identities = 82/283 (28%), Positives = 130/283 (45%), Gaps = 23/283 (8%)

Query 20 FSVPLLVILVFLAALAAASFLLLILPGIRGHSRWFVLVRVLLSLFIGAEIVAVHFSAEWFG 79
F++ ++ VFL ++LILPG+R R V +L L +G ++A W G

Sbjct 21 FNMHAFVIFSFLIPLIAYILILPGVR-RKRVTVTYVLMVAVGGALIASLIYPCWASG 79

Query 80 TVNTNTSYKAFSAARVTARVGLLVGLEGINITLTGTPVHQLNETID-----YNEQFT 131
+ T ++ S R+ A++G+ +GL+ +N+TL + N+ + YNE F

Sbjct 80 SQMIYTQFRGHSNERILAKIGVEIGLQKVNVTLKFERLLSSNDVLPGSDMTELYNEGFD 139

Query 132 WRLKENYAAEYANALEKGLDPVLYLAEKFTSPSPCGLY-HQYHLAGHYASATLWVAFCF 190
+ A + LE GLP P+L + E F+ + + Y +AGHY A +W AF

Sbjct 140 ISGISSMAEALHHGLENGLPYPMLSVLEYSFSLNQDSFDWGRHYRVAGHYTHAAIWFAFAC 199

Query 191 WLLSNVL-LSTPAPLYGGLALLTTGAFALFGVFALASISSVPLCLRIGSSA-----L 242
W LS VL L P Y ++L TG L +S C LR+ + L

Sbjct 200 WCLSVVLMFLPHNAY--KSILATGISCLIACLVYLLSP---CELRIAFGTGENFERVDL 254

Query 243 TTQYGAAFVWVTLATGVLCLFLGGAVVSLQYVRPSALRTLDDQS 285
T + F++ A G+LC+ G + ++ R L T LD S

Sbjct 255 TATFSFCFYLIFAIGILCVLCGLGICEHWRIYTLSTFLDAS 297

> [gi|25375307|pir||A88533](#) hypothetical protein C06E1.3 - Caenorhabditis elegans
Length=383

Score = 103 bits (257), Expect = 1e-20
Identities = 81/276 (29%), Positives = 126/276 (45%), Gaps = 23/276 (8%)

Query 27 VILVFLAALAAASFLLLILPGIRGHSRWFVLVRVLLSLFIGAEIVAVHFSAEWFGVTNTNTS 86
+ VFL ++LILPG+R R V +L L +G ++A W G+ T

Sbjct 14 IFSVFLIPLIAYILILPGVR-RKRVTVTYVLMVAVGGALIASLIYPCWASGSQMIYTQ 72

```

Query 87 YKAFAARVTARVGLLVGLEGINITLTGTPVHQNLNETID-----YNEQFTWRLKENY 138
++ S R+ A++G+ +GL+ +N+TL + N+ + YNE F +
Sbjct 73 FRGHSNERILAKIGVEIGLKQVNVTLKFERLLSNDVLPGSDMTELYNEGFDISGISM 132

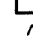

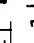
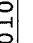
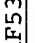
Query 139 AAEEYANALEKGLPDPVLYLAEKFTPPSSPCGLY-HQYHLAGHYASATLWVAFCFWLLSNVL 197
A + LE GLP P+L + E F+ + + Y +AGHY A +W AF W LS VL
Sbjct 133 AEALHGLENGLPYPMLSVLEYFSLNQDSFDWGRHYRVAGHYTHAAIWFAFACWCLSVVL 192

Query 198 -LSTPAPLYGGLALLTTGAFALFGVFALASISSVPLCPLRLGSSA-----LTTQYGAA 249
L P Y ++L TG L +S C LR+ + LT +
Sbjct 193 MLFLPHNAY--KSILATGISCLIACLVYLLSP---CELRIAGTGFENFVRLTATFSFC 247

Query 250 FWVTLATGVLCLFLGGAVVSQYVRPSALRTLDDQS 285
F++ A G+LC+ G + ++ R L T LD S
Sbjct 248 FYLIFAIGILCVLCGLGIGICEHWRIYTLSTFLDAS 283

```

```

>  gi|24584366|ref|NP_723890.1|  U G moladietz CG4482-PB, isoform B [Drosophila melanogaster]
gi|116007336|ref|NP_001036364.1|  G moladietz CG4482-PE, isoform E [Drosophila melanogaster]
gi|7298189|gb|AAF53424.1|  G CG4482-PB, isoform B [Drosophila melanogaster]
gi|113194988|gb|ABI31318.1|  G CG4482-PE, isoform E [Drosophila melanogaster]
Length=363

```

Score = 99.4 bits (246), Expect = 2e-19
 Identities = 58/178 (32%), Positives = 86/178 (48%), Gaps = 3/178 (1%)

```



Query 108 INITLTGTPVHQNLNET-IDYNEQFTWRLKENYAAEYANALEKGLPDPVLYLAEKFTPPSSP 166
+N+TLT P+ IDYNE+FTW + +A Y +AL++GLP P+L +AE F+
Sbjct 3 VNVTLTAIPIGNWTPPDIDYNERFTWEGANDMSANYRHALQRLPFPILTVAEYFSLGRE 62

Query 167 CGLY-HQYHLAGHYASATLWVAFCFWLLSNVLLSTPAPLYGGLALLTTGAFALFGVFALA 225
+ QY AG++AS LW + WLL N+LL P YG TGA +
Sbjct 63 GFSWGGQYRAAGYFASIMLWASLASWLLMNL--IAVPRYGAYMKALTGALLVCTTVGYH 121

Query 226 SISSVPLCPLRLGSSALTTQYGAFTVTLATGVLCLFLGGAVVSQYVRPSALRTLDD 283
+ + L L +G +W+ L G+LC G + + V P T+L+
Sbjct 122 CLLPKRPLSIHLEGGRLFEHFGWCYWLVLVAGILCFIAGVLISIIDLVPHTFSTVLE 179

```

```

>  gi|76627901|ref|XP_876772.1|  G PREDICTED: similar to Numb-interacting protein isoform 2 [Bos
taurus]
Length=100

```

Score = 97.8 bits (242), Expect = 6e-19
 Identities = 47/49 (95%), Positives = 47/49 (95%), Gaps = 0/49 (0%)

Query 1 MTLWNGVLPFPQPRHAAGFSVPLLIVLVFLAALAAAFLLILPGIRGHS 49
 MTLWNGVLPFPQPRHAAG SVPLLIVLVFL LAAAFLLILPGIRGHS
 Sbjct 1 MTLWNGVLPFPQPRHAAGLSVPLLIVLVFLVLAASFFLLILPGIRGHS 49

> [gi|104781029|ref|YP_607527.1|](#) **G** hypothetical protein PSEEN1884 [Pseudomonas entomophila L48]
[gi|95110016|emb|CAK14721.1|](#) **G** conserved hypothetical protein; putative membrane protein [Pseudomonas]
 Length=835

Score = 42.7 bits (99), Expect = 0.023
 Identities = 42/111 (37%), Positives = 54/111 (48%), Gaps = 5/111 (4%)

Query 179 YASATLWAFCFWLLSNVLLSTPAPLYGGL-ALLTTGAFAFGVFALASISSVPLCPRL 237
 Y +A L + W LS LL T A L GGL A L GA L G+ +L + + P RL
 Sbjct 401 YGAALLALGLIMWRLSDLLLTTFALLGGGLIAALLGALLLGLRSLRLLADAPLPWRL 460

Query 238 GSSALTTQYGAAFWVTLATGVLCLFLGGAVVSLQYVRPSALRTLDDQSAKD 288
 G L AA TLA G++ L +G +V+L +R L T Q KD
 Sbjct 461 GLGQLLRHPLAAAGQTLAFGLILLAMG--LVAL--LRAELDDTWOQLPKD 507

> [gi|67157078|ref|ZP_00418440.1|](#) Protein-disulfide reductase [Azotobacter vinelandii AvOP]
[gi|67085755|gb|EAM05227.1|](#) Protein-disulfide reductase [Azotobacter vinelandii AvOP]
 Length=928

Score = 39.7 bits (91), Expect = 0.19
 Identities = 43/132 (32%), Positives = 57/132 (43%), Gaps = 12/132 (9%)

Query 175 LAGHYASATLWAFCFWLLSNVLLS--TPAPLYGGLALLTTGAFAFG---VFALASISS 229
 LAG+ +LW A +LS++L+S APL G L +++ AL G +FAL
 Sbjct 625 LAGNTRGGSLLWGAAVLGVLSLLVSPCVSAPLAGALLYISSSGDALGGGLKLFALGLGMG 684

Query 230 VPLCPRLGSSALTTQYGAAFWVTLATGVLCLFLGGAVVSLQYVRPSALRTLDDQSAKDC 289
 PL G AL + G + V + L L AV L+ V P L L S
 Sbjct 685 APLVLFAGGGALLPRSG-PWMVVVRNFAFGVLLLA VAVWLLERVLPGLALALWGSL--- 740


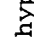
Query 290 SQERGGSPILIG 301
 GG L IG
 Sbjct 741 ---AGGVALFLG 749

> [gi|69260554|ref|ZP_00608077.1|](#) Sulfatase [Magnetococcus sp. MC-1]
[gi|68245385|gb|EAN27511.1|](#) Sulfatase [Magnetococcus sp. MC-1]
 Length=532

Score = 39.3 bits (90), Expect = 0.25
 Identities = 30/87 (34%), Positives = 44/87 (50%), Gaps = 7/87 (8%)

Query 2 TLWNGVLPFPQPRHAAGFSVPLLIVLFLAALAAASFLLLPGIRGHSRWFVLRVLLSL 61
 T ++GVL YP +H AGF V L++ FL L S L +L G R + ++LS
 Sbjct 26 TFFSGVLQVYPWQOH-AGFFVSLVAYS AFLVLLFSLLSLLFGORSVA----IFMLILSA 80


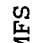
Query 62 FIG--AEIVAVHFSAEWFGTVNTNTS 86
 FIG ++ V + T+ TN S
 Sbjct 81 FIGYFSDNFGVIIDRDMLQNTLETNLS 107

> [gi|54024138|ref|YP_118380.1|](#)  hypothetical protein nfa21700 [Nocardia farcinica IFM 10152]
[gi|54015646|dbj|BAD57016.1|](#)  hypothetical protein [Nocardia farcinica IFM 10152]
 Length=271

Score = 38.5 bits (88), Expect = 0.42
 Identities = 32/95 (33%), Positives = 46/95 (48%), Gaps = 6/95 (6%)

Query 24 LLIVILVFLAALASFL----LILPGIRG-HSRWFVLRVLLSLFIGAEIVAVHFSAEWV 78
 LL V+ V LA+A SFL + + G R +R F V ++ F+ V VH EW +
 Sbjct 150 LLGVSVLLAVAISFLGLFAVTMIGFRVVETRGFRVTYQIVGTFLAGLFVPVHLFPEW-L 208

Query 79 GTVNTNTSYKAFSAARVTARVGLLVGLEGINITLT 113
 TV T + A A V G +VGL+ + + T
 Sbjct 209 RTVANATPFPAMLQAPVDVLSGRVVGLDAVQVVGT 243

> [gi|62180329|ref|YP_216746.1|](#)  MFS superfamily, nitrite extrusion protein [Salmonella enterica subsp. enterica serovar Choleraesuis str. SC-B67]
[gi|62127962|gb|AAx65665.1|](#)  MFS superfamily, nitrite extrusion protein [Salmonella enterica subsp. enterica serovar Choleraesuis str. SC-B67]
 Length=477

Score = 37.7 bits (86), Expect = 0.72
 Identities = 32/103 (31%), Positives = 47/103 (45%), Gaps = 21/103 (20%)

Query 177 GH-YASATLWV-----AFCFWLL-SNVLLSTPAPLYGGLALLTTGAFALFGVFALASI 227
 GH AS LW+ AFC W+L S V ++ P + F +F L ++
 Sbjct 42 GHRVASRNLWISVPCLLLAFCVWMLFSAVAVNLPKVGFN-----FTTDQLFMLTAL 92

Query 228 SSVPLCPLRLGSSALTTQYGAAFWVTLATGVL---CLFLGGAV 267
 SV LR+ S + +G W +TG+L C++LG AV
 Sbjct 93 PSVSGALLRPYPYFMVPLFGGRRWTAFTSTGILIVPCVWLGFV 135

> [gi|16765106|ref|NP_460721.1|](#) nitrite extrusion protein [Salmonella typhimurium LT2]
[gi|16420294|gb|AAL20680.1|](#) MFS superfamily nitrite extrusion protein [Salmonella typhimurium LT2]
 Length=465

Score = 37.7 bits (86), Expect = 0.72
 Identities = 32/103 (31%), Positives = 47/103 (45%), Gaps = 21/103 (20%)

Query 177 GH-YASATLWV-----AFCFWLL-SNVLLSTPAPLYGGLALLTTGAFALFGVFALASI 227
 GH AS LW+ AFC W+L S V ++ P + F +F L ++
 Sbjct 30 GHRVASRNLWISVPCLLLAFCVWMLFSAVAVNLPKVGFN-----FTTDQLFMLTAL 80

Query 228 SSVPLCPLRLGSSALTTQYGAAFWVTLATGVL---CLFLGGAV 267
 SV LR+ S + +G W +TG+L C++LG AV
 Sbjct 81 PSVSGALLRPYPYFMVPLFGGRRWTAFTSTGILIVPCVWLGFV 123

> [gi|16760121|ref|NP_455738.1|](#) nitrite extrusion protein (nitrite facilitator) [Salmonella enterica subsp. enterica serovar Typhi str. CT18]
[gi|29142108|ref|NP_805450.1|](#) nitrite extrusion protein [Salmonella enterica subsp. enterica serovar Typhi Ty2]
[gi|56413313|ref|YP_150388.1|](#) nitrite extrusion protein (nitrite facilitator) [Salmonella enterica subsp. enterica serovar Paratyphi A str. ATCC 9150]
[gi|25296684|pir||AG0648](#) nitrite extrusion protein (nitrite facilitator) [imported] -
 Salmonella enterica subsp. enterica serovar Typhi (strain CT18)
[gi|16502415|emb|CAD08370.1|](#) nitrite extrusion protein (nitrite facilitator) [Salmonella enterica subsp. enterica serovar Typhi]
[gi|29137737|gb|AAO69299.1|](#) nitrite extrusion protein [Salmonella enterica subsp. enterica serovar Typhi Ty2]
[gi|56127570|gb|AAV77076.1|](#) nitrite extrusion protein (nitrite facilitator) [Salmonella enterica subsp. enterica serovar Paratyphi A str. ATCC 9150]

Length=465

Score = 37.7 bits (86), Expect = 0.72
Identities = 32/103 (31%), Positives = 47/103 (45%), Gaps = 21/103 (20%)

Query 177 GH-YASATLWV-----AFCFWLL-SNVLLSTPAPLYGGLALLTTGAFALFGVFALASI 227
GH AS LW+ AFC W+L S V ++ P + F +F L ++
Sbjct 30 GHRVASRNLWISVPCILLAFVCVWMLFSAVAVNLPKVGFN-----FTTDQLFMLTAL 80

Query 228 SSVPLCLRLGSSALTTQYGAAFWVTLATGVL---CLFLGGAV 267
SV LR+ S + +G W +TG+L C++LG AV
Sbjct 81 PSVSGALLRVPYSFMVPLFGGRRWTAFSTGILIVPCVWLGFV 123

> [gi|66045306|ref|YP_235147.1|](#) **G** Protein of unknown function DUF214:Fimbrial assembly [Pseudomonas syringae pv. syringae B728a]

[gi|63256013|gb|AAY37109.1|](#) **G** Protein of unknown function DUF214:Fimbrial assembly [Pseudomonas syringae pv. syringae B728a]
Length=838

Score = 37.4 bits (85), Expect = 0.95
Identities = 36/111 (32%), Positives = 51/111 (45%), Gaps = 5/111 (4%)

Query 179 YASATLWVAFCFWLLSNVLLSTPAPLYGGL-ALLTTGAFALFGVFALASISSVPLCPRL 237
Y +A L + W LS L+ T A L GG+ A L G+ L + +L + S P RL
Sbjct 401 YGAALLALGLIMWRLSLDLVLTFFALLGGGIVAALLGSLLLALNSLRLLSGASLPWRL 460



Query 238 GSSALTTQYGAAFWVTLATGVLCLFLGGAVVSLQYVRPSALRTLDDQSAKD 288
G L AA +LA G++ L +G + +R L T +Q KD
Sbjct 461 GLGQLLRYPPLAAAGQSLAFGLILLSMG----LIALLRGELLDTWQNQLPKD 507

> [gi|91210447|ref|YP_540433.1|](#) **G** nitrite extrusion protein [Escherichia coli UTI89]
[gi|91072021|gb|ABE06902.1|](#) **G** nitrite extrusion protein [Escherichia coli UTI89]
Length=465

Score = 37.0 bits (84), Expect = 1.2
Identities = 30/99 (30%), Positives = 45/99 (45%), Gaps = 20/99 (20%)

Query 180 ASATLWV-----AFCFWLL-SNVLLSTPAPLYGGLALLTTGAFALFGVFALASISSVP 231
AS LW+ AFC W+L S V ++ P + F +F L ++ SV
Sbjct 36 ASRNLWISVPCILLAFVCVWMLFSAVAVNLPKVGFN-----FTTDQLFMLTALPSVS 86



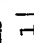



Query 232 LCPLRLGSSALTTQYGAAFWVTLATGVL---CLFLGGAV 267
 LR+ S + +G W +TG+L C++LG AV
 Sbjct 87 GALLRVPYSFMVPIFGGRRWTAFTSTGILIIPCVWLGFAY 125

> [gi|82776568|ref|YP_402917.1|](#)  nitrite extrusion protein [Shigella dysenteriae Sd197]
[gi|81240716|gb|ABB61426.1|](#)  nitrite extrusion protein [Shigella dysenteriae Sd197]
 Length=463

Score = 37.0 bits (84), Expect = 1.2
 Identities = 30/99 (30%), Positives = 45/99 (45%), Gaps = 20/99 (20%)

Query 180 ASATLWV-----AFCFWLL-SNVLLSTPAPLYGGLALLTTGAFALFGVFALASISSVP 231
 AS LW+ AFC W+L S V ++ P + F +F L ++ SV
 Sbjct 34 ASRNLWISVPCLLLLAFCVWMLFSAVAVNLPKVGFN-----FTTDQLFMLTALPSVS 84

Query 232 LCPLRLGSSALTTQYGAAFWVTLATGVL---CLFLGGAV 267
 LR+ S + +G W +TG+L C++LG AV
 Sbjct 85 GALLRVPYSFMVPIFGGRRWTAFTSTGILIIPCVWLGFAY 123

> [gi|30062747|ref|NP_836918.1|](#)  nitrate transport protein nark [Shigella flexneri 2a str. 2457T]
[gi|56479859|ref|NP_707132.2|](#)  nitrate transport protein nark [Shigella flexneri 2a str. 301]
[gi|110805230|ref|YP_688750.1|](#)  nitrite extrusion protein [Shigella flexneri 5 str. 8401]
[gi|30040995|gb|AAP16725.1|](#)  nitrate transport protein nark [Shigella flexneri 2a str. 2457T]
[gi|56383410|gb|AAN42839.2|](#)  nitrate transport protein nark [Shigella flexneri 2a str. 301]
[gi|110614778|gb|ABF03445.1|](#)  nitrite extrusion protein [Shigella flexneri 5 str. 8401]
 Length=463

Score = 37.0 bits (84), Expect = 1.2
 Identities = 30/99 (30%), Positives = 45/99 (45%), Gaps = 20/99 (20%)

Query 180 ASATLWV-----AFCFWLL-SNVLLSTPAPLYGGLALLTTGAFALFGVFALASISSVP 231
 AS LW+ AFC W+L S V ++ P + F +F L ++ SV
 Sbjct 34 ASRNLWISVPCLLLLAFCVWMLFSAVAVNLPKVGFN-----FTTDQLFMLTALPSVS 84

Query 232 LCPLRLGSSALTTQYGAAFWVTLATGVL---CLFLGGAV 267
 LR+ S + +G W +TG+L C++LG AV
 Sbjct 85 GALLRVPYSFMVPIFGGRRWTAFTSTGILIIPCVWLGFAY 123

> [gi|26247549|ref|NP_753589.1|](#) [G](#) Nitrite extrusion protein 1 [Escherichia coli CFT073]
[gi|26107951|gb|AAN80151.1|AE016760.10](#) [G](#) Nitrite extrusion protein 1 [Escherichia coli CFT073]
 Length=465

Score = 37.0 bits (84), Expect = 1.2
 Identities = 30/99 (30%), Positives = 45/99 (45%), Gaps = 20/99 (20%)

Query 180 ASATLWV-----AFCFWLL-SNVLLSTPAPLYGGLALLTTGAFALFGVFALASISSVP 231
 AS LW+ AFC W+L S V ++ P + F +F L ++ SV
 Sbjct 36 ASRNLWISVPCLLLAFCVWMLFSAVAVNLPKVGFN-----FTTDQLFMLTALPSVS 86

Query 232 LCPLRLGSSALTTQYGAAFWVTLATGVL---CLFLGGAV 267
 LR+ S + +G W +TG+L C++LG AV
 Sbjct 87 GALLRVPYSFMVPIFGRRWTAFSTGILIIPCWLGFV 125

> [gi|15801454|ref|NP_287471.1|](#) [G](#) nitrite extrusion protein [Escherichia coli O157:H7 EDL933]
[gi|12514941|gb|AAG56083.1|AE005339.10](#) [G](#) nitrite extrusion protein [Escherichia coli O157:H7 EDL933]
 Length=463

Score = 37.0 bits (84), Expect = 1.2
 Identities = 30/99 (30%), Positives = 45/99 (45%), Gaps = 20/99 (20%)

Query 180 ASATLWV-----AFCFWLL-SNVLLSTPAPLYGGLALLTTGAFALFGVFALASISSVP 231
 AS LW+ AFC W+L S V ++ P + F +F L ++ SV
 Sbjct 34 ASRNLWISVPCLLLAFCVWMLFSAVAVNLPKVGFN-----FTTDQLFMLTALPSVS 84

Query 232 LCPLRLGSSALTTQYGAAFWVTLATGVL---CLFLGGAV 267
 LR+ S + +G W +TG+L C++LG AV
 Sbjct 85 GALLRVPYSFMVPIFGRRWTAFSTGILIIPCWLGFV 123

> [gi|42104|emb|CAA48933.1|](#) narK [Escherichia coli]
 Length=347

Score = 37.0 bits (84), Expect = 1.2
 Identities = 30/99 (30%), Positives = 45/99 (45%), Gaps = 20/99 (20%)

Query 180 ASATLWV-----AFCFWLL-SNVLLSTPAPLYGGLALLTTGAFALFGVFALASISSVP 231
 AS LW+ AFC W+L S V ++ P + F +F L ++ SV
 Sbjct 34 ASRNLWISVPCLLLAFCVWMLFSAVAVNLPKVGFN-----FTTDQLFMLTALPSVS 84

Query 232 LCPLRLGSSALTTQYGAAFWVTLATGVL---CLFLGGAV 267
 LR+ S + +G W +TG+L C++LG AV
 Sbjct 85 GALLRVPYSFMVPIFGGRRWTAFTSTGILIIPCVMWLGFAV 123

> [gi|15830982|ref|NP_309755.1|](#) [G](#) nitrite extrusion protein [Escherichia coli O157:H7 str. Sakai]
[gi|13361193|dbj|BAB35151.1|](#) [G](#) nitrite extrusion protein [Escherichia coli O157:H7 str. Sakai]
 Length=463

Score = 37.0 bits (84), Expect = 1.2
 Identities = 30/99 (30%), Positives = 45/99 (45%), Gaps = 20/99 (20%)

Query 180 ASATLWV-----AFCFWLL-SNVLLSTPAPLYGGLALLTTGAFALFGVFALASISSVP 231
 AS LW+ AFC W+L S V ++ P + F +F L ++ SV
 Sbjct 34 ASRNLWISVPCLLLAFCVWMLFSAVANLPKVGFN-----FTTDQLFMLTALPSVS 84

Query 232 LCPLRLGSSALTTQYGAAFWVTLATGVL---CLFLGGAV 267
 LR+ S + +G W +TG+L C++LG AV
 Sbjct 85 GALLRVPYSFMVPIFGGRRWTAFTSTGILIIPCVMWLGFAV 123

> [gi|75230215|ref|ZP_00716716.1|](#) COG2223: Nitrate/nitrite transporter [Escherichia coli B7A]
 Length=463

Score = 37.0 bits (84), Expect = 1.2
 Identities = 30/99 (30%), Positives = 45/99 (45%), Gaps = 20/99 (20%)

Query 180 ASATLWV-----AFCFWLL-SNVLLSTPAPLYGGLALLTTGAFALFGVFALASISSVP 231
 AS LW+ AFC W+L S V ++ P + F +F L ++ SV
 Sbjct 34 ASRNLWISVPCLLLAFCVWMLFSAVANLPKVGFN-----FTTDQLFMLTALPSVS 84

Query 232 LCPLRLGSSALTTQYGAAFWVTLATGVL---CLFLGGAV 267
 LR+ S + +G W +TG+L C++LG AV
 Sbjct 85 GALLRVPYSFMVPIFGGRRWTAFTSTGILIIPCVMWLGFAV 123

> [gi|75242028|ref|ZP_00725822.1|](#) COG2223: Nitrate/nitrite transporter [Escherichia coli F11]
[gi|110641455|ref|YP_669185.1|](#) [G](#) nitrite extrusion protein [Escherichia coli 536]
[gi|110343047|gb|ABG69284.1|](#) [G](#) nitrite extrusion protein [Escherichia coli 536]
 Length=463

Score = 37.0 bits (84), Expect = 1.2

Identities = 30/99 (30%), Positives = 45/99 (45%), Gaps = 20/99 (20%)

Query 180 ASATLWV-----AFCFWLL-SNVLLSTPAPLYGGLALLTTGAFALFGVFALASISSVP 231
 AS LW+ AFC W+L S V ++ P + F +F L ++ SV
 Sbjct 34 ASRNLWISVPCLLLAFCVWMLFSAVANLPCVGFN-----FTTDQLFMLTALPSVS 84

Query 232 LCPLRLGSSALTTQYGAAFWVTLATGVL---CLFLGGAV 267
 LR+ S + +G W +TG+L C++LG AV
 Sbjct 85 GALLRVPYSFMVPIFGRRWTAFTSTGILIIPCVMWLGFAV 123

> [gi|75190277|ref|ZP_00703544.1|](#) COG2223: Nitrate/nitrite transporter [Escherichia coli E24377A]
 Length=461



Score = 37.0 bits (84), Expect = 1.2

Identities = 30/99 (30%), Positives = 45/99 (45%), Gaps = 20/99 (20%)

Query 180 ASATLWV-----AFCFWLL-SNVLLSTPAPLYGGLALLTTGAFALFGVFALASISSVP 231
 AS LW+ AFC W+L S V ++ P + F +F L ++ SV
 Sbjct 34 ASRNLWISVPCLLLAFCVWMLFSAVANLPCVGFN-----FTTDQLFMLTALPSVS 84

Query 232 LCPLRLGSSALTTQYGAAFWVTLATGVL---CLFLGGAV 267
 LR+ S + +G W +TG+L C++LG AV
 Sbjct 85 GALLRVPYSFMVPIFGRRWTAFTSTGILIIPCVMWLGFAV 123




> [gi|16129186|ref|NP_415741.1|](#) [G](#) nitrate/nitrite transporter [Escherichia coli K12]
[gi|74312436|ref|YP_310855.1|](#) [G](#) nitrite extrusion protein [Shigella sonnei Ss046]
[gi|75179178|ref|ZP_00699196.1|](#) COG2223: Nitrate/nitrite transporter [Shigella boydii BS512]
[gi|75195376|ref|ZP_00705446.1|](#) COG2223: Nitrate/nitrite transporter [Escherichia coli HS]
[gi|75212660|ref|ZP_00712658.1|](#) COG2223: Nitrate/nitrite transporter [Escherichia coli B171]
[gi|75235265|ref|ZP_00719502.1|](#) COG2223: Nitrate/nitrite transporter [Escherichia coli E110019]
[gi|75257132|ref|ZP_00728668.1|](#) COG2223: Nitrate/nitrite transporter [Escherichia coli E22]
[gi|75511743|ref|ZP_00734372.1|](#) COG2223: Nitrate/nitrite transporter [Escherichia coli 53638]
[gi|82544322|ref|YP_408269.1|](#) [G](#) nitrite extrusion protein [Shigella boydii Sb227]
[gi|83569301|ref|ZP_00920757.1|](#) COG2223: Nitrate/nitrite transporter [Shigella dysenteriae 1012]
[gi|83587367|ref|ZP_00925995.1|](#) COG2223: Nitrate/nitrite transporter [Escherichia coli 101-1]
[gi|89108071|ref|AP_001851.1|](#) nitrate/nitrite transporter [Escherichia coli W3110]
[gi|127835|sp|P10903|NARK_ECOLI](#) Nitrite extrusion protein 1 (Nitrite facilitator 1)
[gi|42091|emb|CAA34126.1|](#) nark [Escherichia coli]
[gi|1651617|dbj|BAA36091.1|](#) nitrate/nitrite transporter [Escherichia coli W3110]
[gi|1787475|gb|AAC74307.1|](#) [G](#) nitrate/nitrite transporter [Escherichia coli K12]

gi|73855913|gb|AAZ88620.1|  nitrite extrusion protein [Shigella sonnei Ss046]
 gi|81245733|gb|ABB66441.1|  nitrite extrusion protein [Shigella boydii Sb227]
 gi|115512565|gb|ABJ00640.1| nitrate/nitrite transporter NarK [Escherichia coli APEC O1]
 gi|226457|prf|1513219A narK gene
 Length=463

Score = 37.0 bits (84), Expect = 1.2
 Identities = 30/99 (30%), Positives = 45/99 (45%), Gaps = 20/99 (20%)

Query 180 ASATLWV-----AFCFWLL-SNVLLSTPAPLYGGLALLTTGAFALGFVAFALASISSVP 231
 AS LW+ AFC W+L S V ++ P + F +F L ++ SV
 Sbjct 34 ASRNLWISVPCLLLAFCVWMLFSAVANLPKVGFN-----FTTDQLFMLTALPSVS 84




Query 232 LCPLRLGSSALTTQYGAAFWVTLATGVL---CLFLGGAV 267
 LR+ S + +G W +TG+L C++LG AV
 Sbjct 85 GALLRVPYSFMVPIFGGRRWTAFTSTGILIIPCVMWLGFAV 123

>  gi|26989040|ref|NP_744465.1|  ABC transporter, permease protein, putative [Pseudomonas putida
 KT2440]
 gi|24983865|gb|AAN67929.1|AE016425.6  ABC transporter, permease protein, putative [Pseudomonas putida
 KT2440]
 Length=832

Score = 36.6 bits (83), Expect = 1.6
 Identities = 39/111 (35%), Positives = 51/111 (45%), Gaps = 5/111 (4%)

Query 179 YASATLWVAFCFWLLSNVLLSTPAPLYGGL-ALLTTGAFALGFVAFALASISSVPLCPRL 237
 Y +A L + W LS LL T A L GGL A L G L G+ +L + + RL
 Sbjct 398 YGAALLALGLIMWRLSLDLLLTFALLGGGLVAALLLGGLLLLGLRSLRQLLAGAPLTWRL 457

Query 238 GSSALTTQYGAAFWVTLATGVLCLFLGGAVVSLQYVRPSALRTLDDQSAKD 288
 G L AA LA G++ L + A+V+L +R L T Q KD
 Sbjct 458 GLGQLLRHPTAAAGQALAFGLILLAM--ALVAL--LRAELDDTWQAQLPKD 504

>  gi|116623359|ref|YP_825515.1|  protein of unknown function DUF214 [Solibacter usitatus Ellin6076]
 gi|116226521|gb|ABJ85230.1|  protein of unknown function DUF214 [Solibacter usitatus Ellin6076]
 Length=840

Score = 36.6 bits (83), Expect = 1.6
 Identities = 30/96 (31%), Positives = 48/96 (50%), Gaps = 8/96 (8%)

Query 192 LLSNVLLSTPA-PLYGGLALLTTGAFALFGVFALASISSVPLCPLRLGSSALTTQYGAAF 250
 L+S +++ T L GG++ L FA +G+ L + P+ L S G AF
 Sbjct 339 LVSQLVVETVVVSLGGISGLV---FAWWGIRVLMGLLPKRAIPIDLNLSPDWRVLGFAF 395

Query 251 WVTLATGVLCFLFGGAVVSLQYVRPSALRTLILDQSA 286
 +L TG+LC G V +LQ RP+ + L +++A
 Sbjct 396 LASLVTGLLC----GLVPALQSTRPNLVTALKNETA 427

> [gi|115372120|ref|ZP_01459431.1|](#) vitamin K epoxide reductase family [Stigmatella aurantiaca DW4/3-1]
[gi|115370822|gb|EAU69746.1|](#) vitamin K epoxide reductase family [Stigmatella aurantiaca DW4/3-1]
 Length=551

Score = 36.2 bits (82), Expect = 2.1
 Identities = 39/153 (25%), Positives = 53/153 (34%), Gaps = 32/153 (20%)

Query 102 LVLEGINITLTGTPVHQLNETIDYNEQFTWRLKENYAAEYANALEKGLPDPVLYLAEKF 161
 L+ L T+ G H ET+ +N F R+ E + G+P L L
 Sbjct 145 LLTLRAGGATVCGVSEHVNCETV-WNSPFASRVHELF-----GIPVAGLGLLWGI 193

Query 162 TPSSPCGLYHQYHLAGHYASATLWVAFCFWLLSNVLLSTPAPLYGGLALLTTGAFALFGV 221
 ++ GLY + GH T P GL L +
 Sbjct 194 VATALAGLYVAWRSGH-----TVRPAVNGLRRLTAAAGVVSTVI 232

Query 222 FALASISSVPLCPLRLGSSALTTQYGAAFWVTL 254
 FA S S LCP LG+ AL + A W+ L
 Sbjct 233 FAGVSAGSGVLCPTCLGTVALVIAFAAVAWLGL 265

> [gi|94413278|ref|ZP_01293166.1|](#) hypothetical protein PaerP_01004978 [Pseudomonas aeruginosa PA7]
 Length=833

Score = 36.2 bits (82), Expect = 2.1
 Identities = 32/84 (38%), Positives = 38/84 (45%), Gaps = 1/84 (1%)

Query 179 YASATLWVAFCFWLLSNVLLSTPAPLYGGL-ALLTTGAFALFGVFALASISSVPLCPLRL 237
 YA A L+ W LS L T A L GGL A L GA L G+ L + P RL
 Sbjct 401 YACALLAAGLIMWRLSLDLKLTALLGGGLVATLGAIGALLLGLNGLRRLARASLPWRL 460

Query 238 GSSALTTQYGAAFWVTLATGVLC 261
 G L AA +LA G++ L
 Sbjct 461 GLGQLLRHPLAAAGQSLAFGLILL 484

> [gi|15598054|ref|NP_251548.1|](#) **G** hypothetical protein PA2858 [Pseudomonas aeruginosa PAO1]
[gi|9948946|gb|AAG06246.1|AE004712.6](#) **G** conserved hypothetical protein [Pseudomonas aeruginosa PAO1]
 Length=830

Score = 36.2 bits (82), Expect = 2.1
 Identities = 32/84 (38%), Positives = 38/84 (45%), Gaps = 1/84 (1%)

Query 179 YASATLWVAFCFWLLSNVLLSTPAPLYGGL-ALLTTGAFALFGVFALASISSVPLCPLRL 237
 YA A L + W LS L T A L GGL A L GA L G+ L + P RL
 Sbjct 398 YACALLALGLIMWRLSLDLKLTLLALLGGGLVATLVGALLLLGLNGLRRALARASLPWRL 457

Query 238 GSSALTTQYGAAFWVTLATGVLC L 261
 G L AA +LA G++ L
 Sbjct 458 GLGQLLRHPLAAAGQSLAFGLILL 481

> [gi|84326345|ref|ZP_00974372.1|](#) COG3127: Predicted ABC-type transport system involved in lysophospholipase
 L1 biosynthesis, permease component [Pseudomonas
 aeruginosa 2192]
 Length=833

Score = 36.2 bits (82), Expect = 2.1
 Identities = 32/84 (38%), Positives = 38/84 (45%), Gaps = 1/84 (1%)

Query 179 YASATLWVAFCFWLLSNVLLSTPAPLYGGL-ALLTTGAFALFGVFALASISSVPLCPLRL 237
 YA A L + W LS L T A L GGL A L GA L G+ L + P RL
 Sbjct 401 YACALLALGLIMWRLSLDLKLTLLALLGGGLVATLVGALLLLGLNGLRRALARASLPWRL 460

Query 238 GSSALTTQYGAAFWVTLATGVLC L 261
 G L AA +LA G++ L
 Sbjct 461 GLGQLLRHPLAAAGQSLAFGLILL 484

> [gi|84320398|ref|ZP_00968776.1|](#) COG3127: Predicted ABC-type transport system involved in lysophospholipase
 L1 biosynthesis, permease component [Pseudomonas
 aeruginosa C3719]
 Length=736

Score = 36.2 bits (82), Expect = 2.1
 Identities = 32/84 (38%), Positives = 38/84 (45%), Gaps = 1/84 (1%)

Query 179 YASATLWVAFCFWLLSNVLLSTPAPLYGGL-ALLTTGAFALFGVFALASISSVPLCPRL 237
YA A L + W LS L T A L GGL A L GA L G+ L + P RL
Sbjct 304 YACALLALGLIMWRLSLDLKLTLLALLGGGLVATLVLGALLLGLNGLRRLARASLPWRL 363

Query 238 GSSALTTQYGAAFWVTTLATGVLC 261
G L AA +LA G++ L
Sbjct 364 GLGQLLRHPLAAAGQSLAFGLILL 387

> [gi|82738301|ref|ZP_00901136.1|](#) ABC transporter, permease protein, putative [Pseudomonas putida F1]
[gi|82714582|gb|EAP49661.1|](#) ABC transporter, permease protein, putative [Pseudomonas putida F1]
Length=832

Score = 36.2 bits (82), Expect = 2.1
Identities = 39/111 (35%), Positives = 51/111 (45%), Gaps = 5/111 (4%)

Query 179 YASATLWVAFCFWLLSNVLLSTPAPLYGGL-ALLTTGAFALFGVFALASISSVPLCPRL 237
Y +A L + W LS LL T A L GGL A L G L G+ +L + + RL
Sbjct 398 YGAALLALGLIMWRLSLDLKLTLLALLGGGLVATLVLGALLLGLNGLRRLARASLPWRL 457

Query 238 GSSALTTQYGAAFWVTTLATGVLCFLGGAVVSLQYVRPSALRTLDDQSAKD 288
G L AA LA G++ L + A+V+L +R L T Q KD
Sbjct 458 GLGQLLRHPMAAAGQALAFGLILLAM--ALVAL--LRAELDDTWQAQLPKD 504

> [gi|114769129|ref|ZP_01446755.1|](#) inner-membrane translocator [alpha proteobacterium HTCC2255]
[gi|114550046|gb|EAU52927.1|](#) inner-membrane translocator [alpha proteobacterium HTCC2255]
Length=307

Score = 35.8 bits (81), Expect = 2.8
Identities = 19/77 (24%), Positives = 37/77 (48%), Gaps = 0/77 (0%)

Query 208 LALLTTGAFALFGVFALASISSVPLCPRLGSSALTTQYGAAFWVTTLATGVLCFLGGAV 267
L L++ G +FGV L +++ L + ++A + +FW+ L ++ + G +
Sbjct 20 LFLMSAGTLVFGVMGLINLAHGSLYMIGAFAAAAIASWTGSFWLGLVASLMAAAIAGVI 79

Query 268 VSLQYVRPSALRTLDDQ 284
V + +R R LDQ
Sbjct 80 VEIVIRRLYKRDHLDQ 96

> [gi|92912133|ref|ZP_01280769.1|](#) ATPase, E1-E2 type:Copper-translocating P-type ATPase:Heavy metal translocating P-type ATPase [Mycobacterium sp. JLS]
[gi|92430634|gb|EAS89976.1|](#) ATPase, E1-E2 type:Copper-translocating P-type ATPase:Heavy metal translocating P-type ATPase [Mycobacterium sp. JLS]
 Length=780

Score = 35.8 bits (81), Expect = 2.8
 Identities = 40/145 (27%), Positives = 63/145 (43%), Gaps = 30/145 (20%)

Query 188 FCFWLLSNVLLSTPAPLYGGL-----ALLTTGAFALFGVFALASISSV--PLCPLRLG 238

F +W +++ L+ P ++ A L G + + +L ++S+ L L LG

Sbjct 148 FTYQWASLTAAAPVVVWAAWPFHRAAWANLRHGTATMDTLISLGTVSFAFLWSLYALFLG 207

Query 239 SSA-----LTTQYGA--FWVTLATGVLCLFLGGAVVSLQYVRPS--ALRTLDDQ 284



S+ L +GAA ++ +A GV L G + R + ALR LLD

Sbjct 208 SAGTPGMKHPFAFTLAPSHGAANIYLEVAAGVTTFILAGRYFEKRSKRQAGAAALRALLDL 267

Query 285 SAKDCSQERGS-----PLILGD 302

AKD S RGG+ L++GD

Sbjct 268 GAKDVSVLRGGTETKIAIEELVVG D 292

> [gi|28869466|ref|NP_792085.1|](#)  permease, putative [Pseudomonas syringae pv. tomato str. DC3000]
[gi|28852707|gb|AAO55780.1|](#)  permease, putative [Pseudomonas syringae pv. tomato str. DC3000]
 Length=838

Score = 35.8 bits (81), Expect = 2.8
 Identities = 35/111 (31%), Positives = 51/111 (45%), Gaps = 5/111 (4%)

Query 179 YASATLWVAFCFWLLSNVLLSTPAPLYGG-LALLTTGAFALFGVFALASISSVPLCPLRL 237

Y +A L + W LS L+ T A L GG +A L G+ L + +L + + P RL

Sbjct 401 YGAALLAALGLIMWRLSLDLVLTFTALLGGVVAALILGSLLLALNSLRRLLAGASLPWRL 460

Query 238 GSSALTTQYGAAFWVTLATGVLCLFLGGAVVSLQYVRPSALRTLDDQSAKD 288

G L AA +LA G++ L +G + +R L T +Q KD

Sbjct 461 GLGQLLRYPLAAAGQSLAFGLILLSMG----LIALLRGELLDTWQNQLPKD 507

> [gi|88803929|ref|ZP_01119449.1|](#) hypothetical protein RB2501_03745 [Robiginitalea biformata HTCC2501]
[gi|88784808|gb|EAR15977.1|](#) hypothetical protein RB2501_03745 [Robiginitalea biformata HTCC2501]
 Length=460

Score = 35.8 bits (81), Expect = 2.8

Identities = 16/45 (35%), Positives = 29/45 (64%), Gaps = 0/45 (0%)

Query 18 AGFSVPLLIVLFLAALAAFLLLPGIRGHSRWFVLVRVLLSLF 62
AGF+ +L+ +++ LA + +LI GI+ ++ F L+ VLL L+
Sbjct 187 AGFAGTILLTVVIALAASYGIILIFQGIKSQAKQFLLIAVLLLY 231

> [gi|69290299|ref|ZP_00619002.1|](#) NLP/P60:SLT [Kineococcus radiotolerans SRS30216]
[gi|67985309|gb|EAM73262.1|](#) NLP/P60:SLT [Kineococcus radiotolerans SRS30216]
Length=368

Score = 35.8 bits (81), Expect = 2.8
Identities = 24/72 (33%), Positives = 34/72 (47%), Gaps = 3/72 (4%)

Query 221 VFALASISSVPLCPLRLGSSALTTQYGAAFVVTLATGVLCFLGGAVVSLQYVRPSALRT 280
V ++ + P+ RLG++A TT GA L TGV A + YVRP++L +
Sbjct 180 VVKISKVWETPMTIRRLGAAAATTAGAGVAAALLTGVGAT---SAADTSSYVRPASLSS 236

Query 281 LLDQSAKDCSQE 292
SAK E
Sbjct 237 ASSASAKSAPYE 248

> [gi|116617574|ref|YP_817945.1|](#) [G](#) permease of the major facilitator superfamily [Leuconostoc mesenteroides
subsp. mesenteroides ATCC 8293]
[gi|116096421|gb|ABJ61572.1|](#) [G](#) permease of the major facilitator superfamily [Leuconostoc mesenteroides
subsp. mesenteroides ATCC 8293]
Length=462

Score = 35.8 bits (81), Expect = 2.8
Identities = 24/66 (36%), Positives = 34/66 (51%), Gaps = 2/66 (3%)

Query 204 LYGGLALLTTGAFALFGVFALASISSVPLCPLRLGSS--ALTTQYGAAFVVTLATGVLC 261
L GG ++ GA FG S+SSVP+ G+S + TT Y AA + LA G++
Sbjct 357 LTGGFMVIQIGAGFWFGNNMTYSVSSVPVEFQSSGNSIFSATTNYSAAVGIALAAGIIAT 416

Query 262 FLGGAV 267
F A+
Sbjct 417 FQKQAI 422



> [gi|107102407|ref|ZP_01366325.1|](#) hypothetical protein PaerPA_01003469 [Pseudomonas aeruginosa
PACS2]

Length=833

Score = 35.4 bits (80), Expect = 3.6
Identities = 31/84 (36%), Positives = 38/84 (45%), Gaps = 1/84 (1%)

Query 179 YASATLWVAFCFWLLSNVLLSTPAPLYGGL-ALLTTGAFALFGVFALASISSVPLCPLRL 237
YA A L + W LS L T A L GGL A L GA L G+ L + P RL
Sbjct 401 YACALLALGLIMWRLSLDLKLTALLGGGLVATLVGALLLLGLNGLRRALARASLPWRL 460

Query 238 GSSALTTQYGAAFWVTLATGVLC L 261
G L AA ++A G++ L
Sbjct 461 GLGQLLRHPLAAAGQSMAGLL L 484

> [gi|54026538|ref|YP_120780.1](#)  putative nitrite extrusion protein [Nocardia farcinica IFM 10152]
[gi|54018046|dbj|BAD59416.1](#)  putative nitrite extrusion protein [Nocardia farcinica IFM 10152]
Length=494

Score = 35.4 bits (80), Expect = 3.6
Identities = 26/75 (34%), Positives = 32/75 (42%), Gaps = 2/75 (2%)

Query 193 LSNVLLSTPAPLYGGLALLTTGAFAL--FGVFALASISSVPLCPLRLGSSALTTQYGAAF 250
+SN LL T P G AL FA+ FG A + S+ L LG + Q G
Sbjct 92 VSNALLTSTPTLVGAALRIPYTFIPAIPRFGGRAFTAFSAAMLLVPTLGLAWFVNQPGTPM 151

Query 251 WVTLATGVLCFLGG 265
WV + L F GG
Sbjct 152 WVFVLAALAGFGG 166

> [gi|116062235|dbj|BAA79067.2](#)  hypothetical protein [Aeropyrum pernix K1]
Length=386

Score = 35.0 bits (79), Expect = 4.7
Identities = 27/95 (28%), Positives = 46/95 (48%), Gaps = 2/95 (2%)

Query 193 LSNVLLSTPAP--LYGGLALLTTGAFALFGVFALASISSVPLCPLRLGSSALTTQYGAAF 250
+SN +L P GLA+ L VF+ A+ ++ L P+ + +AL T G
Sbjct 78 ISNHVLGAGPEVYLTGLAVSAASGIFLTTVFSTATSIALGLEPVMVPAALITLLGVLL 137


Query 251 WVTLATGVLCFLGGAVVSLQYVRPSALRTLDDQS 285
+TL T ++ + L VS V P+ L +++D +
Sbjct 138 VLTLLTWIIIVMLLRGLGVSPDNVMPAILTSIIDMA 172

> [gi|83769792|dbj|BAE59927.1|](#) unnamed protein product [Aspergillus oryzae]
Length=516

Score = 35.0 bits (79), Expect = 4.7
Identities = 24/69 (34%), Positives = 36/69 (52%), Gaps = 6/69 (8%)

Query 50 RFWLVRVLLSLFIGAEIVAVHFSAEWFGVTNTNTSYKAFSAARVTARVGLLVGLEGIN 109
R W+V ++ + FIGA I VH V V SY ++A+ V+A + L + G
Sbjct 410 RLHWIPIIGTFFIGAGIFYVH-----LVTQVYLVDSTYLYAASAVSAELALRC-VFGAT 463



Query 110 ITLTGTPVH 118
I L GTP++
Sbjct 464 IPLAGTPLY 472

> [gi|14600492|ref|NP_147008.1|](#)  hypothetical protein APE0156 [Aeropyrum pernix K1]
Length=363

Score = 35.0 bits (79), Expect = 4.7
Identities = 27/95 (28%), Positives = 46/95 (48%), Gaps = 2/95 (2%)

Query 193 LSNVLLSTPAP--LYGGLALLTTGAFALFGVFALASISSVPLCPLRLGSSALTTQYGAAF 250
+SN +L P GLA+ L VF+ A+ ++ L P+ + +AL T G
Sbjct 55 ISNHVLGGAGPEVYLTGLAVSAASGIFLTTVFSTATSIALGLEPVMVMPAALITLLGVLL 114

Query 251 WVTLATGVLCFLGGAUVSLQYVRPSALRTLDDQS 285
+TL T ++ + L VS V P+ L +++D +
Sbjct 115 VLTLLTWIIIVMLRLGLVSPDNVMPAILTSIIDMA 149

> [gi|115443030|ref|XP_001218322.1|](#)  conserved hypothetical protein [Aspergillus terreus NIH2624]
[gi|114188191|gb|EAU29891.1|](#)  conserved hypothetical protein [Aspergillus terreus NIH2624]
Length=1604

Score = 34.7 bits (78), Expect = 6.1
Identities = 23/90 (25%), Positives = 41/90 (45%), Gaps = 1/90 (1%)

Query 9 PFYQPRAAGFSVPLLIVLFLALAAASFLILPGIRGHSRWFVLRVLLSLFIGAEIV 68
P+ PR A +V L L L L + +F ++LP + +++ + GAE
Sbjct 1391 PYVQSPRAYAGTVSALTSGLRLLYIGMAFAIVLPSLFALIMELYILVPAHTYLGAEETH 1450

Query 69 AVHFAEWFVGTNTNTSYKAFSAARVTAR 98
+HF +W +G + + K F+ R T+R
Sbjct 1451 VIHFVQDWTGLGVLYVQMAIK-FALWRSTSR 1479

> [gi|113942881|ref|ZP_01428585.1|](#) protein of unknown function DUF125, transmembrane [Salinispora tropica CNB-440]
[gi|113905730|gb|EAU24564.1|](#) protein of unknown function DUF125, transmembrane [Salinispora tropica CNB-440]
Length=259

Score = 34.7 bits (78), Expect = 6.1
Identities = 28/71 (39%), Positives = 35/71 (49%), Gaps = 16/71 (22%)

Query 215 AFALFGVFALASISSVPLCLRLGSSALTTQYGAAFWVTLATGVLCFLGAVVSLQYVR 274
+F F V AL VPL P LGS++L W+ L G LFL GA+V+ R
Sbjct 180 SFVCFVSGAL-----VPLLPYLLGSTL-----WLALGVGGFLFLAGAIVARFTSR 226



Query 275 P---SALRLLL 282
P + LR LL
Sbjct 227 PWSAGLRQLL 237

> [gi|113936404|ref|ZP_01422297.1|](#) Glycosyl transferase, family 39 [Caulobacter sp. K31]
[gi|113729165|gb|EAU10242.1|](#) Glycosyl transferase, family 39 [Caulobacter sp. K31]
Length=568

Score = 34.7 bits (78), Expect = 6.1
Identities = 36/116 (31%), Positives = 49/116 (42%), Gaps = 13/116 (11%)

Query 182 ATLWVAFCFWLLSNVLLSTPAPLYGGLA----LLTTGAF-----ALFGVFALASISSVP 231
A L A C W + +L L GG+ LL+T AF AL G LA + +
Sbjct 105 AMLAAACAWGAAALLGPRTGLLAGILGATLLLSTEAFLAKTDAALCGFTTLAMAALMR 164

Query 232 LCPLRLGSSALTTQYGAAFWVTLATGVLCFLGAVVSLQYVRPSALRLLDQSAK 287
+ L +T AFWV LA GVL + G V + V + L D+ A+
Sbjct 165 IYAAHLNGGTITRTWTKLAFWVGLAMGVL---IKGPVGLMVVVLSSLMLALWDRKAR 217

> [gi|21219547|ref|NP_625326.1|](#)  ABC transport system integral membrane protein [Streptomyces coelicolor A3(2)]
[gi|8894820|emb|CAB96016.1|](#)  putative ABC transport system integral membrane protein [Streptomyces coelicolor A3(2)]

Length=855

Score = 34.7 bits (78), Expect = 6.1
 Identities = 33/96 (34%), Positives = 45/96 (46%), Gaps = 3/96 (3%)

Query 193 LSNVLLSTPAPLYGGLALLTTGAFALFGVFALAS---ISSVPLCPLRLGSSALTTQYGAA 249
 L VLLS L G A+LT AF + G A A+ + VPL LR + L +
 Sbjct 432 LVGVLLSPSVWLAGLGAVLTAAFFVVLGPVASATAVRVLGVPLDRLRGVTGGLARRNALR 491

Query 250 FVWTLATGVLCLFLGGAVVSLQVVRPSALRTLDDQS 285
 A L +G AVVSL V ++L+ +DQ+
 Sbjct 492 SPKRTAATAGALMIGVAVVSLFTVFGASLKATMDQT 527

> [gi|88711067|ref|ZP_01105155.1|](#) hypothetical protein FB2170_03115 [Flavobacteriales bacterium HTCC2170]
[gi|88710008|gb|EAR02240.1|](#) hypothetical protein FB2170_03115 [Flavobacteriales bacterium HTCC2170]
 Length=448

Score = 34.7 bits (78), Expect = 6.1
 Identities = 16/45 (35%), Positives = 30/45 (66%), Gaps = 0/45 (0%)

Query 18 AGFSVPLLIIVLFLAALAAFLILPGIRGHSRWFVLRVLLSLF 62
 +GF++ LLI +++ LA + + +LI I+ ++ F L+ VLL L+
 Sbjct 187 SGFAINLLITVVIALAASVAIILFQRIKSPAKFLLLIAVLLLLY 231



> [gi|87309448|ref|ZP_01091583.1|](#) hypothetical protein DSM3645_24140 [Blastopirellula marina DSM 3645]
[gi|87287756|gb|EAQ79655.1|](#) hypothetical protein DSM3645_24140 [Blastopirellula marina DSM 3645]
 Length=189

Score = 34.7 bits (78), Expect = 6.1
 Identities = 28/98 (28%), Positives = 43/98 (43%), Gaps = 17/98 (17%)

Query 172 QYHLAGHYASATLWVAF--CFWLLSNVLLSTPAPL---YGGIALITTGAFALFGVFALAS 226
 QY L+ +A + A WL +L S+ PL + G L+ GA+
 Sbjct 56 QYELSIVWAGPIVGAALPVTIWLAMRLRSSHEPLAFAFFAGFCLANGAY----- 105



Query 227 ISSVPLCPLRLGSSALTTQYGAAFVWTLATGVLCLFLG 264
 + + L P+ G +A Q G + W+ GV+CL LG

Sbjct 106 LGAAILTPV--GDAAEILQLGGSLWMLALFGVICPLG 141

> [gi|91781984|ref|YP_557190.1|](#)  Putative glycosyltransferase [Burkholderia xenovorans LB400]
[gi|91685938|gb|ABE29138.1|](#)  Putative glycosyltransferase [Burkholderia xenovorans LB400]
 Length=450

Score = 34.3 bits (77), Expect = 8.0
 Identities = 31/119 (26%), Positives = 50/119 (42%), Gaps = 21/119 (17%)

Query	94	RVTARVGLLVGLEGINITLTGTPVHQNLNETIDYNEQFTWRLLKENYAA-EYANALEKGLPD	152
		+ TA + +L+ G + + P + Y E WR+ E YA+ Y + G+	
Sbjct	19	KYTAEMAVLLADRGHEVRVVCAPPY-----YPE---WRVSEGYASWRVQHETRDGV--	66
Query	153	PVLYLAEKFTPSSPCGLYHQVHLAGHYASA-----TLWVAFCFWLLSNVLLSTPAPL	204
		++ A + PS P GL HLA A++ LW L++ L+ PA L	
Sbjct	67	-AVWRAPLWVPSRPSGLKRMHLATFAATSLPLLAQALWRPHAVMLIAPTLMCAPASL	124

> [gi|70728684|ref|YP_258433.1|](#)  signaling repeat/GGDEF domain/EAL domain protein [Pseudomonas fluorescens Pf-5]
[gi|68342983|gb|AA90589.1|](#)  signaling repeat/GGDEF domain/EAL domain protein [Pseudomonas fluorescens Pf-5]
 Length=759

Score = 34.3 bits (77), Expect = 8.0
 Identities = 29/110 (26%), Positives = 54/110 (49%), Gaps = 3/110 (2%)

Query	23	PLLVILVFLAASF--LLILPGIR-GHSRWFVLRVLLSLFIGAEIVAVHFSAEWFG	79
		PLL+ + V +A+A S LL+ +R G + L++ SL +GA IV +HF+ W +	
Sbjct	158	PLLMALSVIVAIACSLAALLSRHLREGSGMFHQLLKYASSLVLGAAIVLMHFTGIWAMT	217
Query	80	TVNTNTSYKAFSAARVTARVGLLVGLEGINITLTGTPVHQNLNETIDYNEQ	129
		V S A + + ++GL + + I +G ++ + + E+	
Sbjct	218	LVLPAAGSLPAPATSDGHLQLGLTLSAIVLLIIGSGISAALADKKLQHKR	267

> [gi|68448684|gb|AA96807.1|](#) unknown [Monkeypox virus]
[gi|68448869|gb|AA96992.1|](#) unknown [Monkeypox virus]
[gi|68449287|gb|AA97407.1|](#) unknown [Monkeypox virus]
[gi|68449472|gb|AA97592.1|](#) unknown [Monkeypox virus]
[gi|68449486|gb|AA97605.1|](#) unknown [Monkeypox virus]

gi|68449671|gb|AAAY97790.1| unknown [Monkeypox virus]
Length=121

Score = 34.3 bits (77), Expect = 8.0
Identities = 32/112 (28%), Positives = 44/112 (39%), Gaps = 17/112 (15%)

Query 153 PVLYLEAEKFTSPSSPCGLYHQYHLAGHYASATLWVAFCFWLLSNVLLSTPAPLYGGLA--- 209

PVL LA F GL L H L++ F LL ++ L++ Y

Sbjct 10 PVLILASMF---GSIGLIFALTLRHEHPLNLYILCGFTLLESITLASVVTFFYDARIVMQ 66

Query 210 --LTTGAFALFGVFALASISSVPLCLRLGSSALTTQYGAAFWVTLATGVL 259

+LTT F + L S + S L T AAFW+ + +GVL

Sbjct 67 AFMLTTAVFLALTTYTLQS-----KRDFSCLVTGLFAAFWILILSGVL 109

> gi|18202585|sp|Q60457|SOAT1_CRIGR Sterol O-acyltransferase 1 (Cholesterol acyltransferase 1) (Acyl
coenzyme A:cholesterol acyltransferase 1) (ACAT-1)

gi|1408466|gb|AAC52670.1| ACAT

Length=546

Score = 34.3 bits (77), Expect = 8.0
Identities = 16/55 (29%), Positives = 29/55 (52%), Gaps = 4/55 (7%)

Query 23 PLLIVILVFLAALAAASFLILPGIRGHSRWFVLVRLLSLFIGAEIVAVHFSAEWF 77

P+L V+ +F +A +F++ R W + V SLF+G ++ +S EW+

Sbjct 469 PVLFLVMFFGMAFNFIWN----DSRKRPINIMVWASFLGHGVILCFYSQEWY 519

> gi|83747811|ref|ZP_00944845.1| LivG [Ralstonia solanacearum UW551]

gi|83725583|gb|EAP72727.1| LivG [Ralstonia solanacearum UW551]

Length=608

Score = 34.3 bits (77), Expect = 8.0
Identities = 32/100 (32%), Positives = 41/100 (41%), Gaps = 7/100 (7%)

Query 184 LWVAFCFWLLSNVLLSTPA-----PLYGGLALLTTGAFALFGVFALASISSVPLCLRL 237

L VAF L +L TP G +L+ G L GV L S L

Sbjct 23 LTVAFVIVLALLPVLPTPEFWITLLNYIGLSLVALGLVLLTGVGGLTSFGQAQAFVGLGA 82

Query 238 GSSA-LTTQYGAAFWVTLATGVLCLFLGGAVVSLQYVRPS 276

S+A LTTQYG + W+ L G+ V+ L +R S

Sbjct 83 YSTAYLTTQYGLSPWIGLLAGLAITMASAYVIGLITMRMS 122

Get selected sequences

Select all

Deselect all

Distance tree of results

Database: All non-redundant GenBank CDS translations+PDB+SwissProt+PIR+PRF excluding environmental samples

Posted date: Nov 1, 2006 5:52 PM

Number of letters in database: 1,413,990,101

Number of sequences in database: 4,099,826

Lambda K H
0.325 0.139 0.438

Gapped
Lambda K H
0.267 0.0410 0.140

Matrix: BLOSUM62

Gap Penalties: Existence: 11, Extension: 1

Number of Sequences: 4099826

Number of Hits to DB: 89282072

Number of extensions: 3664871

Number of successful extensions: 13026

Number of sequences better than 10: 8

Number of HSP's better than 10 without gapping: 0

Number of HSP's gapped: 13161

Number of HSP's successfully gapped: 8

Length of query: 320

Length of database: 1413990101

Length adjustment: 131

Effective length of query: 189

Effective length of database: 876912895

Effective search space: 165736537155

Effective search space used: 165736537155

T: 11

A: 40



X1: 15 (7.0 bits)

X2: 38 (14.6 bits)

X3: 64 (24.7 bits)

S1: 40 (20.0 bits)

S2: 77 (34.3 bits)



PubMed

Protein

Nucleotide

for

Genome

Structure

PMC

Search

Protein

GenPept

Show

20

Send to

Clear

Limits

Preview/Index

History

Clipboard

Display

GenPept

Show

20

Send to

Refresh

Range: from

begin

to

end

Features:

+

Refresh

☐ 1: [ABF48256](#). Reports dual oxidase acti...[gi:94961770]

Features Sequence

LOCUS ABF48256 320 aa linear PRI 03-JUL-2006
DEFINITION dual oxidase activator 2 [Homo sapiens].
ACCESSION ABF48256
VERSION ABF48256.1 GI:94961770
DBSOURCE accession [DQ489734.1](#)
KEYWORDS .
SOURCE Homo sapiens (human)
ORGANISM [Homo sapiens](#)
Eukaryota; Metazoa; Chordata; Craniata; Vertebrata; Euteleostomi;
Mammalia; Eutheria; Euarchontoglires; Primates; Haplorrhini;
Catarrhini; Hominidae; Homo.
REFERENCE 1 (residues 1 to 320)
AUTHORS Grasberger,H. and Refetoff,S.
TITLE Identification of the maturation factor for dual oxidase: Evolution of an eukaryotic operon equivalent
JOURNAL J. Biol. Chem. 281 (27), 18269-18272 (2006)
PUBMED [16651268](#)
REFERENCE 2 (residues 1 to 320)
AUTHORS Grasberger,H.
TITLE Direct Submission
JOURNAL Submitted (11-APR-2006) Medicine, University of Chicago, 5841 South Maryland Ave., Chicago, IL 60637, USA
COMMENT Method: conceptual translation supplied by author.
FEATURES Location/Qualifiers
source 1..320
/organism="Homo sapiens"
/db_xref="taxon:9606"

```

      /map="DUOX1/DUOX2 intergenic region"
      /tissue_type="thyroid gland"
      1..320
      /product="dual oxidase activator 2"
      1..320
      /coded_by="DQ489734.1:133..1095"
      /note="shared promoter region with DUOX2"

ORIGIN
    1 mtlwnvglpf ypqprhaagf svpllivlv flalaasfl1 ilpgirghsr wfwlvrvlls
    61 lfigaeivav hfsaewfvt vntntsykaf saarvtarvg llvglegini tltgtpvhql
    121 netidyneqf twrlkenyaa eyanalekgl pdpvlylaek ftpsspcgly hgyhlaghya
    181 satlwafcf wllsnvllst paplyggglal lttgafalfg vfalasissv plcplrlgss
    241 alttqygaaf wtlatgvlc lfiggavvsl qyvrrpsalrt lldqsakdcs qerggsplil
    301 gdplhkqaal pdlkcittnl
//
```

[Disclaimer](#) | [Write to the Help Desk](#)
[NCBI](#) | [NLM](#) | [NIH](#)

Sep 27 2006 15:22:06

This material may be protected by Copyright law (Title 17 U.S. Code)

Identification of the Maturation Factor for Dual Oxidase

EVOLUTION OF AN EUKARYOTIC OPERON EQUIVALENT^{*†‡}

Received for publication, April 24, 2006

Published, JBC Papers in Press, May 1, 2006, DOI 10.1074/jbc.C600095200

Helmut Grasberger[†] and Samuel Refetoff^{‡§¶}From the Departments of [†]Medicine, [‡]Pediatrics, and [§]Committee on Genetics, University of Chicago, Chicago, Illinois 60637

Dual oxidase 2 (DUOX2), an NADPH:O₂ oxidoreductase flavoprotein, is a component of the thyroid H₂O₂ generator crucial for hormone synthesis at the apical membrane. Mutations in *DUOX2* produce congenital hypothyroidism in humans. However, no functional DUOX-based NADPH oxidase has ever been reconstituted at the plasma membrane of transfected cells. It has been proposed that DUOX retention in the endoplasmic reticulum (ER) of heterologous systems is due to the lack of an unidentified component required for functional maturation of the enzyme. By data mining of a massively parallel signature sequencing tissue expression data base, we identified an uncharacterized gene named DUOX maturation factor (*DUOXA2*) arranged head-to-head to and co-expressed with *DUOX2*. A paralog (*DUOXA1*) was similarly linked to *DUOX1*. The genomic rearrangement leading to linkage of ancient *DUOX* and *DUOXA* genes could be traced back before the divergence of echinoderms. We demonstrate that co-expression of *DUOXA2*, an ER-resident transmembrane protein, allows ER-to-Golgi transition, maturation, and translocation to the plasma membrane of functional DUOX2 in a heterologous system. The identification of *DUOXA* genes has important implications for studies of the molecular mechanisms controlling DUOX expression and the molecular genetics of congenital hypothyroidism.

Generation of H₂O₂ at the apical membrane of thyroid follicular cells is essential for iodination of thyroglobulin by thyroid peroxidase and constitutes the rate-limiting step of thyroid hormone synthesis. Dual oxidases (DUOX1 and DUOX2)² appear to constitute the catalytic core of the H₂O₂ generator (1, 2). They are large homologs of the phagocyte gp91^{phox}/Nox2 NADPH-dependent oxidase with an N-terminal extension comprising a peroxidase-like domain. Although the crucial role of *DUOX2* in thyroid hormonogenesis has been substantiated by reports of severe congenital hypothyroidism in patients with biallelic nonsense mutations (3), the understanding of structure, function, and regulation of DUOX has remained limited. The major obstacle for molecular studies of DUOX is the lack of a suitable heterologous cell system for DUOX-based functional NADPH oxidase expression. Transfected cells completely retain DUOX in the endoplasmic reticulum (ER) (4–8), suggesting that an unidentified component, essential for DUOX maturation, may be specifically expressed in tissues containing the functional enzyme.

^{*} This work was supported in part by National Institutes of Health Grants DK15070 and DK20595. The costs of publication of this article were defrayed in part by the payment of page charges. This article must therefore be hereby marked "advertisement" in accordance with 18 U.S.C. Section 1734 solely to indicate this fact.

^{†‡} The on-line version of this article (available at <http://www.jbc.org>) contains supplemental Figs. 15–35 and Table 4S.

The nucleotide sequence(s) reported in this paper has been submitted to the GenBank™/EBI Data Bank with accession number(s) DQ489734 and DQ489735.

¹ To whom correspondence should be addressed: Dept. of Medicine, The University of Chicago, 5841 S. Maryland Ave., MC3090, Chicago, IL 60637. Tel.: 773-702-9273; Fax: 773-702-6940; E-mail: hgrasber@uchicago.edu.

² The abbreviations used are: DUOX, dual (domain) oxidase; BLAST, basic local alignment search tool; DPI, diphenyleneiodonium; EGFP, enhanced green fluorescent protein; ER, endoplasmic reticulum; EST, expressed sequence tag; HA, hemagglutinin; MPSS, massively parallel signature sequencing; ORF, open reading frame; PNGase F, N-glycosidase F; Endo H, endoglycosidase H; contig, group of overlapping clones.

EXPERIMENTAL PROCEDURES

EXHIBIT B

Data Mining and Computational Analysis—Massively parallel signature sequencing (MPSS) data (9) were obtained from the NCBI Gene Expression Omnibus repository (www.ncbi.nlm.nih.gov/geo/; records GSE1747 and GPL1443). A thyroid specificity score, as defined by Jongeneel *et al.* (9), was calculated for signatures with frequency >100 tags per million (~30 mRNA copies/cell) in the thyroid/parathyroid library. Tags with scores >−1 were mapped to the human genome assembly using BLAST. *DUOXA* homologs were identified by tBLASTn searches against the NCBI nr data base and trace archive and BLAT queries (at genome.ucsc.edu/) against assembled whole genome sequences. Orthologs were operationally defined as reciprocal best BLAST hits. Gene structures were deduced by spliced alignment maintaining maximum homolog similarity of the open reading frames (ORFs) and consensus splice junctions. Cladograms were constructed from ClustalX alignments (BLOSUM weight matrix, excluding gaps) using the Jones, Taylor, and Thornton (JTT) substitution model in PHYLIP 2.4.4 (10). SignalP 3.0 (11) and Phobius (12) were used to analyze signal peptides, transmembrane helices, and topology.

Northern Blot Analysis—A human multiple tissue Northern blot (Origene) was hybridized with *DUOXA2* (125–470 of DQ489734) and *DUOXA1* (1244–1623 of BC020841) probes.

Heterologous Expression of *DUOX2* and *DUOXA2* Constructs—cDNA was synthesized with Superscript reverse transcriptase (Invitrogen) by oligo(dT) priming of total RNA from a normal human thyroid gland. The *DUOX2* and *DUOXA2* ORFs were amplified using native *Pfu* polymerase (Stratagene) and cloned into pcDNA3.1 (Invitrogen). Epitope-tagged constructs and fusions with enhanced green fluorescent protein (EGFP) were prepared by replacement or splicing-by-overlap extension using specifically designed primers. All constructs were verified by sequencing. HeLa cells were cultured and transfected as described (13).

Confocal Laser Scanning Microscopy—Indirect immunofluorescence of permeabilized cells has been described previously (13). For surface staining, cells were incubated with rat anti-HA clone 3F10 and/or mouse anti-c-myc clone 9E10 (both from Roche Applied Science) at 1 µg/ml in Hank's buffered saline solution/10 mM Hepes, pH 7.4, 1% bovine serum albumin at 4 °C. Rabbit anti-calnexin was obtained from StressGen. Images were captured on a Nikon Eclipse E800 equipped with PCM2000.

Analysis of N-Glycosylation—Postnuclear supernatants (in 50 mM Tris/HCl, pH 8.0, 150 mM NaCl, and proteinase inhibitors) were adjusted to 0.5% SDS, 0.4 mM dithiothreitol and denatured, at room temperature, for 30 min. Samples were deglycosylated with N-glycosidase F (PNGase F) and endoglycosidase H (Endo H) (both from New England Biolabs) according to manufacturer's recommendations, followed by SDS-PAGE under reducing conditions and Western blotting as described (13).

Measurement of H₂O₂ Generation—Release of H₂O₂ was determined by reaction with cell-impermeable 10-acetyl-3,7-dihydroxyphenoxazine (14) (Amplex Red reagent, Invitrogen) in the presence of excess peroxidase, producing fluorescent resorufin. Briefly, cell monolayers were incubated, with or without 10 µM diphenyleneiodonium (DPI), in Dulbecco's phosphate-buffered saline supplemented with 50 µM Amplex Red reagent and 0.1 unit/ml horseradish peroxidase for 1 h at 37 °C. Relative fluorescence units (excitation/emission: 535/595) were corrected for Amplex Red oxidation in wells containing non-transfected cells and converted into H₂O₂ concentrations using a calibration curve. *Renilla* luciferase activity from co-transfected pRL-Tk plasmid (Promega) was used as internal control as described (13).

RESULTS AND DISCUSSION

Identification of Novel Genes in the *DUOX1/2* Intergenic Region—We used MPSS data for 32 normal human tissues (9) to identify novel transcripts with predominant expression in thyroid gland. One of the extracted tags mapped to an uncharacterized locus (LOC405753) oriented head-to-head to *DUOX2* in the ~16-kbp *DUOX1/2* intergenic region. For reasons outlined below, we called the corresponding gene DUOX maturation factor 2 (*DUOXA2*).³

Based on human-mouse homology (Riken clone 9030623N16Rik), and supported by contig assembly of expressed sequence tags (ESTs), it comprises six

³ The gene name and symbol have been approved by the HUGO Gene Nomenclature Committee.

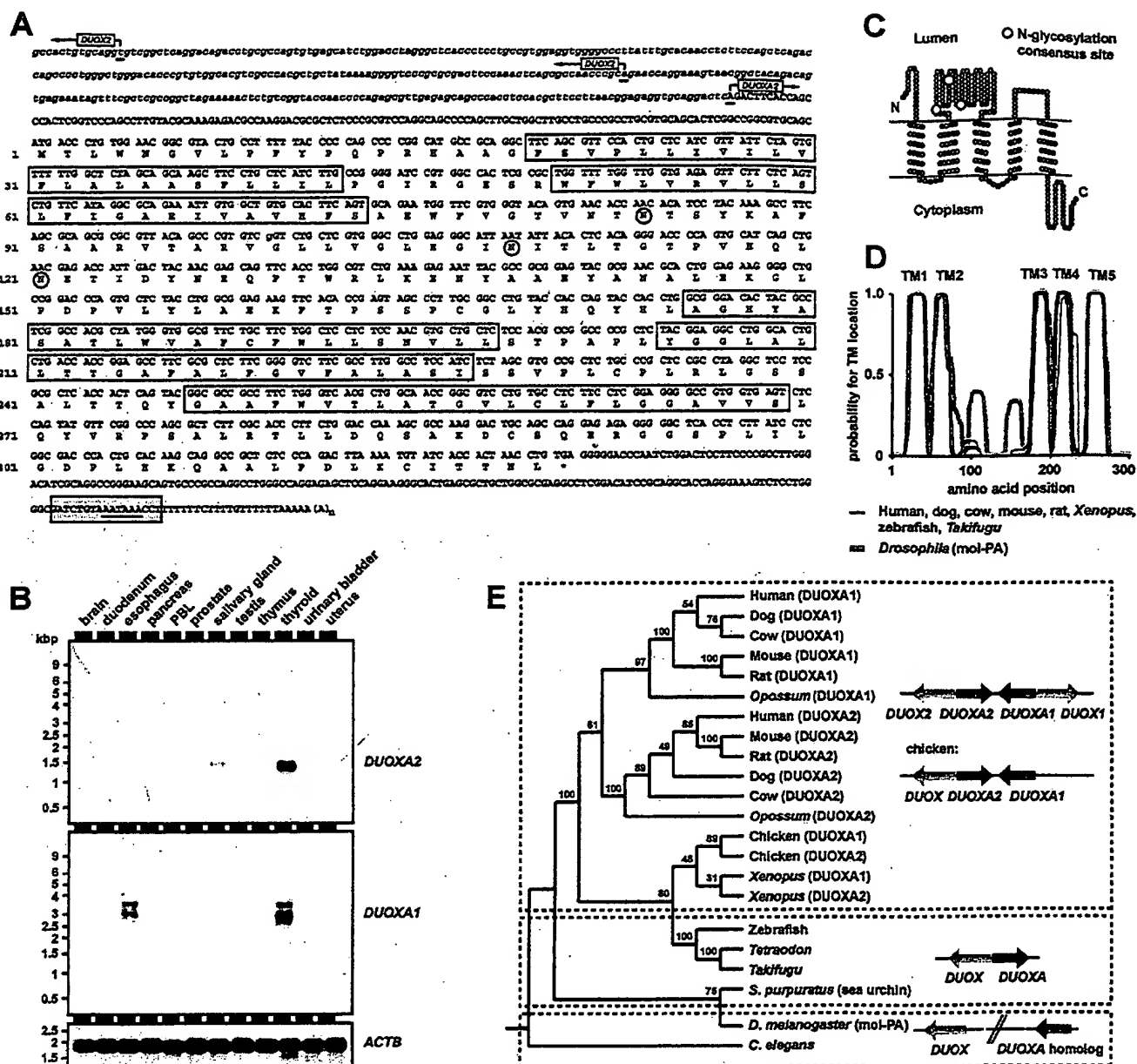


FIGURE 1. Identification of novel genes in the *DUOX1/DUOX2* intergenic region. A, sequence of *DUOX2* cDNA and 5'-flanking region. The GC-rich region upstream of the tentative *DUOX2* transcriptional start site (arrow) is in lowercase italics. The predicted membrane-spanning helices and N-glycosylation sites are marked by open boxes and circles, respectively. The shaded box indicates the MPSS signature extracted by data base mining, which also contains the 3'-polyadenylation signal (underlined). Arrows in the upstream genomic region indicate the transcriptional start sites of *DUOX2* on the opposite strand, as previously determined by 5'-rapid amplification of cDNA ends (23) and as evidenced by EST B1045475. B, multiple tissue Northern blot analysis for *DUOX2* and *DUOX1*. C, strongly favored topology model for *DUOX2*, depicting five membrane-integral regions including a reverse signal anchor with external N terminus (type III). Identical topology was predicted for the *DUOX1* paralogs. D, plot of the residue-wise posterior probability for transmembrane location in *DUOX2*. Data were calculated with the hidden Markov model-based predictor Phobius (12). Note the potential for two additional membrane-spanning regions in the *Drosophila* homolog (mol-PA). E, maximum likelihood protein cladogram illustrating the relationship of *DUOX1* and *DUOX2* homologs (multiple protein alignment shown in Fig. 3S in the on-line supplement). Bootstrapping values for 100 replicates are shown at the nodes. The schematic to the right summarizes the results of the microsynteny analysis. In *Caenorhabditis elegans*, *DUOX1* homolog and *duox* are on distinct chromosomes; in *D. melanogaster*, they are on the same chromosome, but ~14 Mbp apart. Note that for clarity evolutionary recent tandem duplications of the protosomal *duox* loci are not shown.

exons, confirmed by reverse transcription-PCR amplification from human thyroid tissue (GenBank™ accession number DQ489734). The putative transcription start site defined by clone DKFZp686C04213 maps to a GpC rich region (Fig. 1A). This site is 135 bp from the 5' terminus of a spliced *DUOX2* EST (B1045475) on the opposite strand. A single polyadenylation signal (Fig. 1A) is supported by all mapped 3' ESTs. We confirmed a specific transcript of the expected size (1.3 kbp) by Northern blot analysis (Fig. 1B), which also validated the MPSS-based expression profiling: *DUOX2* mRNA was by far most abundant in thyroid, with lower levels in salivary glands reflecting the known expression profile of *DUOX2* (1, 2, 15).

The *DUOX2* ORF is initiated within a Kozak consensus (gcagcATGa) and spans all six exons. The encoded 320-amino acid protein was strongly pre-

dicted to comprise five membrane-integral regions, including a reverse signal anchor with external N terminus (type III) (Fig. 1C). The three NX(S/T) consensus sites for N-glycosylation are clustered within an extended external loop connecting the second and third transmembrane helices.

We identified a single *DUOX2* paralog in the human genome. We will refer to this locus, annotated as "homolog of *Drosophila* Numb-interacting protein," as *DUOX1*. It is immediately adjacent, in tail-to-tail orientation to *DUOX2* and extends, via untranslated exons, into the *DUOX1* promoter region. *DUOX1* mRNA was predominantly expressed in thyroid gland and, at lower level, in esophagus (Fig. 1B). Two transcripts of ~2.9 and ~3.5 kbp were detected, compatible with alternative splicing of 5'-untranslated exons and the use of alternative 3'-polyadenylation signals (data not shown). The *DUOX1*

ORF was confirmed by sequencing from human thyroid cDNA (GenBankTM accession number DQ489735).

By spliced alignment, we deduced the gene structures of all *DUOX* homologs in 10 other vertebrate whole genome assemblies. The splicing sites of all structures were conserved at the single codon level (exon alignment shown in Fig. 2S in the on-line supplement). Remarkably, the bidirectional *DUOX/DOXA* arrangement was conserved throughout the vertebrate lineage (Fig. 1E, accession numbers of genomic contigs available in Table 4S in the on-line supplement). Teleosts have a single *DUOX/DOXA* arrangement, which has undergone tandem duplication to an inverted repeat (*DUOX2/DOXA2/DOXA1/DOXA1*) before the amphibian divergence. Analyzing unassembled genomic contigs, we mapped the evolutionary event leading to the bidirectional association of *DUOX* and *DOXA* before the divergence of echinoderms, since linkage of the loci was present in *Strongylocentrotus purpuratus*. Thus, conserved microsynteny in deuterostomes was a strong predictor for cooperation between *DUOX* and *DOXA*.

The protostomes *C. elegans* and *D. melanogaster* lack a *DOXA* homolog in the vicinity of their respective *duox* loci. They do, however, each harbor a single ancient *DOXA* homolog. For instance, *Drosophila moladietz* (*mol*) encodes a 474-amino acid protein that exhibits 39% amino acid identity over 256 amino acids with human *DOXA1*.

Functional Rescue of *DUOX2* by *DOXA2*—To test whether *DOXA2* can reconstitute *DUOX2* activity in a heterologous system, we expressed either *DUOX2*, *DOXA2*, or both in HeLa cells and measured H_2O_2 released into the culture medium. Transfection of either *DUOX2* or *DOXA2* alone did not result in increased H_2O_2 generation compared with nontransfected cells, confirming previous results for *DUOX2* (2, 4). Remarkably, co-transfection of *DUOX2* with *DOXA2* rescued *DUOX2* activity as indicated by the significant amounts of H_2O_2 released from the cells (Fig. 2A). The H_2O_2 release triggered by *DUOX2/DOXA2* co-transfection was completely blocked by the flavoprotein inhibitor DPI (Fig. 2A).

Co-expression of *DOXA2* Permits ER-Exit of *DUOX2* and Plasma Membrane Targeting via the Secretory Pathway—Lack of *DUOX2* activity in heterologous systems has been associated with absence of *DUOX2* at the plasma membrane (4). To directly test whether reconstitution of active *DUOX2* by *DOXA2* is indeed due to translocation of *DUOX2* to the plasma membrane, we HA-tagged *DUOX2* at its extracellular domain (HA-*DUOX2*; tag inserted between Asp²⁷ and Ala²⁸). Non-permeabilized cells showed strong anti-HA plasma membrane signals in cells co-transfected with HA-*DUOX2* and *DOXA2* (Fig. 2B). Untransfected cells, or cells transfected with either *DOXA2* or HA-*DUOX2* alone, were devoid of surface fluorescence (Fig. 2B and data not shown).

To determine whether *DOXA2*-induced surface expression of *DUOX2* involved ER-to-Golgi transition of *DUOX2*, we analyzed the maturation of *DUOX2* N-glycan moieties using specific glycosidases. Whereas all N-glycans are cleavable by PNGase F, the ER-derived high-mannose type N-glycans become resistant to Endo H once they have been modified by Golgi-localized enzymes. HA-*DUOX2* expressed in HeLa cells migrated as a single band on SDS-PAGE and was sensitive to full deglycosylation by Endo H, consistent with published data (4). In contrast, co-transfection with *DOXA2* resulted in the appearance of a second *DUOX2* species with slightly decreased mobility and complete resistance to deglycosylation by Endo H (Fig. 2C). These findings resembled those previously obtained with endogenous *DUOX2* protein (4, 5, 16), indicating that expression of *DUOX2* in our reconstituted system involved normal maturation of *DUOX2* within the secretory pathway.

Characterization of *DOXA2* as ER-resident Protein—*DOXA2* could be an integral part of a *DUOX2* complex, endowing a holocomplex with the ability to exit the ER and reach the plasma membrane. We, therefore, determined whether myc-tagged *DOXA2* alone or in combination with *DUOX2* would be detectable at the plasma membrane. Of several constructs tested, only *DOXA2* with N- (myc-*DOXA2*) or C-terminal (*DOXA2*-myc/His) attached myc tags were fully functional in rescuing *DUOX2* activity as assessed by H_2O_2 generation and HA-*DUOX2* plasma membrane targeting (data not shown). However, neither myc-*DOXA2* nor *DOXA2*-myc/His was detectable at the plasma membrane (data not shown), although they had the expected size on Western blot analysis (Fig. 3A) and intracellularly co-localized with HA-*DUOX2* (Fig. 3B).

To exclude that this was due to a discrepancy between the modeled and actual *DOXA2* membrane topology or due to masking of the N-terminal epitope tag, we fused EGFP/myc to the C terminus of *DOXA2* (an N-terminal fusion was not functional). As shown in Fig. 3C, *DOXA2*-EGFP/myc did

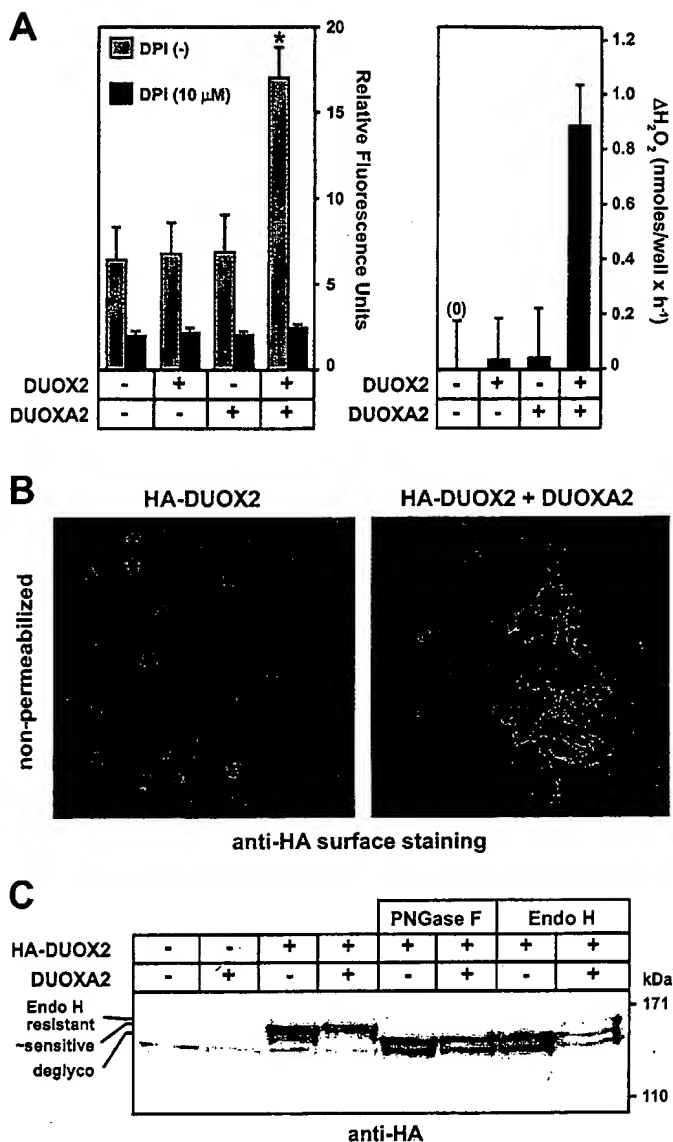


FIGURE 2. Co-expression of *DOXA2* promotes ER release, Golgi modification, and surface expression of functional *DUOX2* in a heterologous system. A, H_2O_2 generation in HeLa cells transfected with the indicated constructs. Total amount of DNA per transfection was kept constant by adjusting with empty vector. * $p < 10^{-7}$ versus single transfections ($n = 10$). B, *DUOX2* is targeted to the plasma membrane in cells co-expressing *DOXA2*. Surface expression of *DUOX2* (red) was detected by indirect immunofluorescence via an HA tag in the extracellular peroxidase-like domain of *DUOX2*. DNA is stained with Hoechst 33342 (blue). C, co-expression of *DOXA2* results in the appearance of a higher molecular weight *DUOX2* band with Endo H-resistant N-glycans, suggesting modification within the Golgi complex.

not co-localize with HA-*DUOX2* at the plasma membrane, the latter delineated by anti-HA surface staining. The intracellular distribution of *DOXA2*-EGFP/myc (and of *DOXA2*-myc/His) showed a similar distribution pattern as the ER-marker calnexin (Fig. 3D).

To further corroborate that *DOXA2* is indeed an ER-resident protein, we analyzed the maturation of *DOXA2*-myc/His N-glycosylation in cells co-expressing HA-*DUOX2*. We found that the N-glycans of *DOXA2*-myc/His were exclusively of the high-mannose type (Fig. 3E). In contrast, detection of HA-*DUOX2* in the same samples demonstrated, again, that about half of *DUOX2* protein had been subject to Golgi modification of its glycosylation (data not shown, compare Fig. 2C). Collectively, these results indicate that *DOXA2* is not an integral part of a *DUOX2* enzyme complex at the plasma membrane but an ER-resident protein promoting ER exit and maturation of *DUOX2*. It should be noted that N-glycosylation of *DOXA2* supports our topology model (Fig. 1C), since the apparent molecular weight of the N-glycan moieties (~ 10 kDa) indicates N-glycosylation of all three consensus sites.

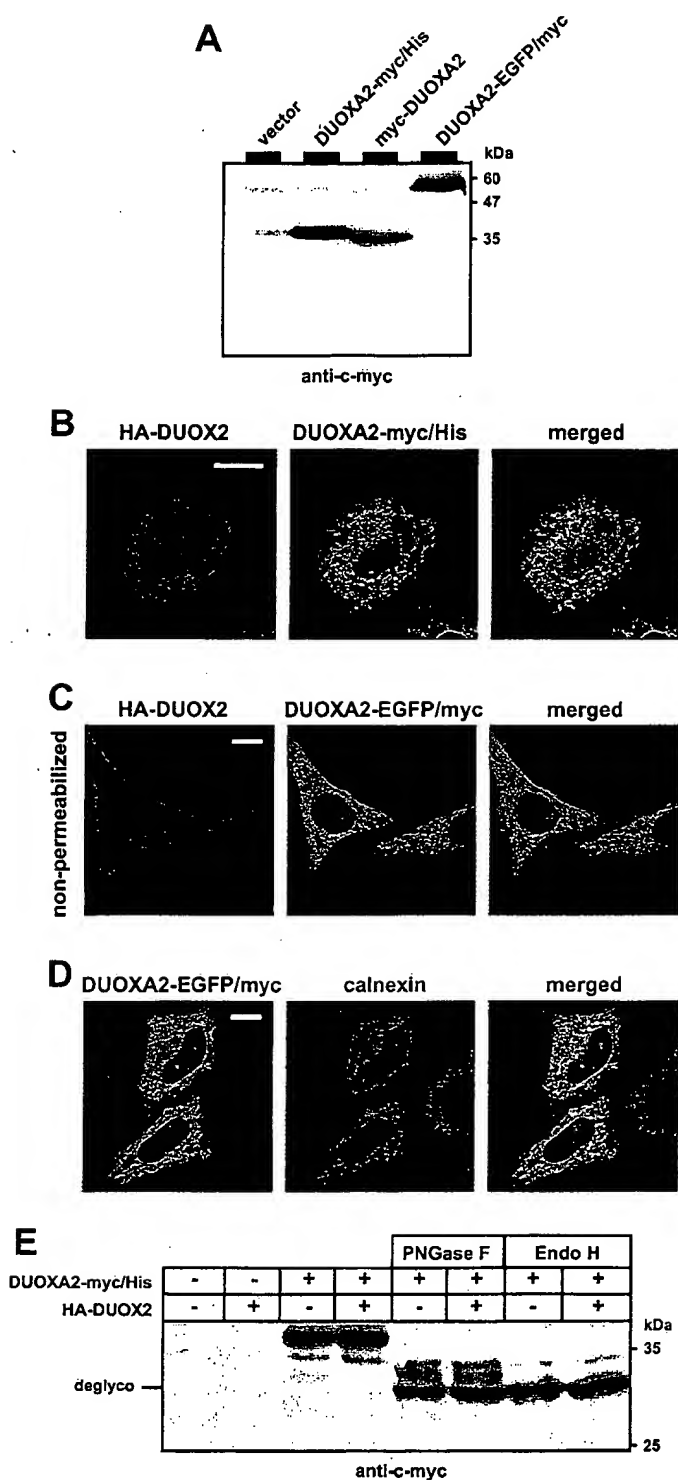


FIGURE 3. Characterization of DUOX2 as ER-resident protein. A, Western blot analysis of myc-tagged DUOX2 constructs. B, confocal microscopy reveals intracellular colocalization of DUOX2-myc/His with HA-DUOX2 in permeabilized cells. C, DUOX2-EGFP/myc allows functional rescue of HA-DUOX2 (visualized by surface staining) but does not co-localize with HA-DUOX2 at the plasma membrane. D, intracellular distribution of DUOX2-EGFP/myc compared with endogenous calnexin. E, DUOX2-myc/His N-glycan moieties are not subject to Golgi modification in cells co-expressing HA-DUOX2. Scale bars in B–D represent 10 μ m.

An Evolutionary Perspective on the Physiological Role of DUOXA—The *DUOX1/DUOX2* transcriptional unit is an excellent example of bidirectional transcription of tightly linked genes that are not structurally related but are involved in the same pathway, an arrangement considered equivalent to a prokaryotic operon (17). In contrast to the organization in deuterostomes, the

two protosomal *DUOX*A-homologs analyzed were not genetically linked to *duox*; in fruit flies, there is also evidence for a distinct functional speciation. The *Drosophila* *DUOX*A-homolog (*mol*) encodes a plasma membrane protein (mol-PA) implicated in the polarized recruitment of a cytosolic signal mediator (Numb) to the plasma membrane (18). That mol-PA may not cooperate with *Drosophila* Duox is also suggested by the distinct phenotypes caused by deficiency of *mol* (memory loss; listed as CG4482 in Ref 19) or *Drosophila* *duox* (defective gut immunity) (20). Remarkably, this functional divergence relates to a distinct topology prediction of the region likely crucial for functional speciation of mol-PA and DUOX. In DUOX, the second and third transmembrane helices are connected by an extended luminal loop consistent with N-glycosylation of DUOX2 (Figs. 1C and 3E). In mol-PA, the equivalent region harbors a binding motif crucial for recruitment of Numb (18), which, therefore, would have to be cytosolic. Analysis of the residue-wise posterior probabilities for a given state (inside/outside/transmembrane) in the 1-best Phobius topology models indeed supports such a scenario of distinct membrane topologies: the profile of transmembrane probabilities in mol-PA, but not vertebrate DUOX, indicates the potential for two additional membrane-spanning helices (Fig. 1D), which would flank the Numb-binding motif resulting in its cytosolic exposure.

If, as we propose, DUOX expression in *Drosophila* does not require *mol*, what could have been the advantage of a *DUOX1/DUOX2* system that caused its maintenance in deuterostomes over more than 500 million years (21) of divergent evolution? For unexplained reasons, in sea urchin eggs (22) and likewise in follicular thyroid cells (4), the bulk of DUOX protein is not detected at the cell surface but in intracellular compartments, which could provide a stimulus-recruitable pool. Thus, from an evolutionary perspective, the emergence of *DUOX*A may have provided an additional level of DUOX regulation, specifically, the control of DUOX translocation to the plasma membrane. The ability to reconstitute active DUOX enzyme will provide the tool to investigate the molecular mechanisms underlying DUOX expression in diverse model systems.

REFERENCES

- Dupuy, C., Ohayon, R., Valent, A., Noel-Hudson, M. S., Deme, D., and Virion, A. (1999) *J. Biol. Chem.* **274**, 37265–37269
- De Deken, X., Wang, D., Many, M. C., Costagliola, S., Libert, F., Vassart, G., Dumont, J. E., and Miot, F. (2000) *J. Biol. Chem.* **275**, 23227–23233
- Moreno, J. C., Bikker, H., Kempers, M. J., van Trotsenburg, A. S., Baas, F., de Vijlder, J. J., Vulsma, T., and Ris-Stalpers, C. (2002) *N. Engl. J. Med.* **347**, 95–102
- De Deken, X., Wang, D., Dumont, J. E., and Miot, F. (2002) *Exp. Cell Res.* **273**, 187–196
- Morand, S., Chaaroui, M., Kaniewski, J., Deme, D., Ohayon, R., Noel-Hudson, M. S., Virion, A., and Dupuy, C. (2003) *Endocrinology* **144**, 1241–1248
- Morand, S., Agnandji, D., Noel-Hudson, M. S., Nicolas, V., Buisson, S., Macon-Lemaitre, L., Gnidehou, S., Kaniewski, J., Ohayon, R., Virion, A., and Dupuy, C. (2004) *J. Biol. Chem.* **279**, 30244–30251
- Wang, D., De Deken, X., Milenkovic, M., Song, Y., Pirson, I., Dumont, J. E., and Miot, F. (2005) *J. Biol. Chem.* **280**, 3096–3103
- Ameziane-El-Hassani, R., Morand, S., Boucher, J. L., Frapart, Y. M., Apostolou, D., Agnandji, D., Gnidehou, S., Ohayon, R., Noel-Hudson, M. S., Francon, J., Lalaoui, K., Virion, A., and Dupuy, C. (2005) *J. Biol. Chem.* **280**, 30046–30054
- Jongeneel, C. V., Delorenzi, M., Iseli, C., Zhou, D., Haudenschield, C. D., Khrebukova, I., Kuznetsov, D., Stevenson, B. J., Strausberg, R. L., Simpson, A. J., and Vasicsek, T. J. (2005) *Genome Res.* **15**, 1007–1014
- Guindon, S., and Gascuel, O. (2003) *Syst. Biol.* **52**, 696–704
- Bendtsen, J. D., Nielsen, H., von Heijne, G., and Brunak, S. (2004) *J. Mol. Biol.* **340**, 783–795
- Kall, L., Krogh, A., and Sonnhammer, E. L. (2004) *J. Mol. Biol.* **338**, 1027–1036
- Grasberger, H., Ringkarnont, U., Lefrançois, P., Abramowicz, M., Vassart, G., and Refetoff, S. (2005) *Mol. Endocrinol.* **19**, 1779–1791
- Zhou, M., Diwu, Z., Panchuk-Voloshina, N., and Haugland, R. P. (1997) *Anal. Biochem.* **253**, 162–168
- Geiszt, M., Witta, J., Baffi, J., Lekstrom, K., and Leto, T. L. (2003) *FASEB J.* **17**, 1502–1504
- El Hassani, R. A., Benfantes, N., Caillou, B., Talbot, M., Sabourin, J. C., Belotte, V., Morand, S., Gnidehou, S., Agnandji, D., Ohayon, R., Kaniewski, J., Noel-Hudson, M. S., Bidart, J. M., Schlumberger, M., Virion, A., and Dupuy, C. (2005) *Am. J. Physiol.* **288**, G933–G942
- Gavalas, A., Dixon, J. E., Brayton, K. A., and Zalkin, H. (1993) *Mol. Cell. Biol.* **13**, 4784–4792
- Qin, H., Percival-Smith, A., Li, C., Jia, C. Y., Gloor, G., and Li, S. S. (2004) *J. Biol. Chem.* **279**, 11304–11312
- Dubnau, J., Chiang, A. S., Grady, L., Barditch, J., Gossweiler, S., McNeil, J., Smith, P., Buldoc, F., Scott, R., Certa, U., Broger, C., and Tully, T. (2003) *Curr. Biol.* **13**, 286–296
- Ha, E. M., Oh, C. T., Bae, Y. S., and Lee, W. J. (2005) *Science* **310**, 847–850
- Douzery, E. J., Snell, E. A., Baptiste, E., Delsuc, F., and Philippe, H. (2004) *Proc. Natl. Acad. Sci. U. S. A.* **101**, 15386–15391
- Wong, J. L., Creton, R., and Wessel, G. M. (2004) *Dev. Cell* **7**, 801–814
- Pachucki, J., Wang, D., Christophe, D., and Miot, F. (2004) *Mol. Cell. Endocrinol.* **214**, 53–62

Influence of the Thyroid State on the Intrinsic Contractile Properties and Energy Stores of the Myocardium *

ROBERT A. BUCCINO, JAMES F. SPANN, JR., PETER E. POOL, EDMUND H. SONNENBLICK, AND EUGENE BRAUNWALD

(From the Cardiology Branch, National Heart Institute, Bethesda, Maryland)

Abstract. The intrinsic contractile properties of isolated cat papillary muscles and myocardial high energy phosphate stores were examined at three levels of thyroid activity and correlated with hemodynamic measurements in the intact animal. In addition, the relationship of thyroid state to endogenous norepinephrine stores and myocardial responsiveness to certain inotropic interventions were studied. In muscles from hyperthyroid cats, the velocity of shortening and the rate of tension development were markedly augmented, while duration of active state was decreased, compared to euthyroid muscles. These findings occurred in the presence and absence of intact norepinephrine stores and over a wide range of temperature and contraction frequency. The opposite changes occurred in muscles from hypothyroid cats. Isometric tension was slightly higher in muscles from hyperthyroid and lower in muscles from hypothyroid cats. The inotropic response to both norepinephrine and strophanthidin varied inversely with the level of thyroid state and allowed all three groups of muscles to reach a common ceiling of isometric tension regardless of thyroid state. Creatine phosphate and adenosine triphosphate stores were intact at all three levels of thyroid state. Thus, the level of thyroid activity profoundly affects the intrinsic contractile state of cardiac muscle, independent of both norepinephrine stores and alterations in high energy phosphate stores, and, in addition, modifies the responsiveness of cardiac muscle to inotropic agents.

Introduction

It is well known that alterations in thyroid activity result in profound changes in cardiovascular function. It has been shown, or it is generally believed, that cardiac index, heart rate, mean systolic ejection rate, and the response to sympathetic stimuli are elevated in hyperthyroidism, while peripheral vascular resistance, arterio-mixed venous O_2 difference, and the response to digitalis glycosides are reduced (1-5). The opposite changes have been noted in myxedema. In the intact organism, these alterations in cardiovascular function have been interpreted as secondary

to the changes in peripheral metabolic requirements (1, 2), in peripheral vascular resistance (3), and in the autonomic nervous system (2, 6) induced by the abnormal thyroid state. However, the possibility exists that thyroid hormone exerts a more direct effect on the intrinsic contractile properties of the myocardium and that the changes in the circulation result, at least in part, from such a direct effect. Furthermore, assessment of myocardial energy stores is essential in relation to studies of contractility, since considerable evidence has accumulated to indicate an effect of thyroid hormone on oxidative phosphorylation (7).

Accordingly, the aim of the present investigation was to determine the effects of hyper- and hypothyroidism on: (a) the intrinsic contractile properties of the myocardium in the presence and

* Received for publication 29 March 1967 and in revised form 9 June 1967.

Address requests for reprints to Dr. Eugene Braunwald, Cardiology Branch, National Heart Institute, Bethesda, Md. 20014.

absence of intact norepinephrine stores; (b) the contractile responses of the myocardium to various inotropic stimuli; and (c) the high energy phosphate stores in the myocardium. The recent development of methods for detailed and quantitative analysis of mechanical characteristics of isolated cat papillary muscle (8), removed from the nervous, humoral, and metabolic influences that exist *in vivo*, and the ability to compare the function of muscles obtained from different groups of animals (9), permit critical examination of these problems. In addition, although interpretation of many previous studies of myocardial high energy phosphate stores in altered thyroid states (10-14) was limited by the extreme lability of these energy stores, recent modifications of biopsy and analytic techniques have made possible the accurate assessment of these stores *in vivo* (15, 16).

The basic experimental plan was to compare the behavior of muscles obtained from three groups of cats: (a) untreated, i.e., euthyroid; (b) hypothyroid; and (c) hyperthyroid. Two additional groups of animals were studied to define the relationship between norepinephrine stores and hyperthyroidism; one group was subjected to catecholamine depletion with reserpine, administered before and concurrent with induction of the hyperthyroid state, and the other was treated with the same schedule of reserpine alone. The intrinsic contractile properties of isolated heart muscle were examined in papillary muscles and the effects of certain inotropic interventions were studied. To correlate the intrinsic function of the isolated myocardium with cardiovascular function in the intact organism, we performed cardiac catheterization and hemodynamic studies.

The results of these studies indicate that the intrinsic contractile state of cardiac muscle and its responsiveness to inotropic agents are profoundly affected by the level of thyroid state. Also it was found that these changes do not result from alterations in myocardial high energy phosphate stores and are not dependent upon intact norepinephrine stores.

Methods

Right ventricular papillary muscles were isolated from 24 normal cats, 13 cats given a single intraperitoneal injection of radioactive ^{131}I (1 mc/kg) 3 months previously, 13 cats subjected to intraperitoneal injection of *l*-thyrox-

ine (1 mg/kg per day) for 8-17 days, six cats pretreated with reserpine (0.5 mg/kg per day) for 2 days and then treated concurrently with maintenance reserpine (0.02 mg/kg per day) and *l*-thyroxine (1 mg/kg per day) for an additional 8-13 days, and six cats treated only with reserpine in the same amounts. Before sacrifice, serum was obtained for determination of protein-bound iodine and cholesterol and right heart catheterization was performed. The animals were anesthetized with intravenous pentobarbital (10-25 mg/kg); arterial pressure and blood samples were obtained through a polyethylene catheter inserted into the abdominal aorta via the femoral artery, while right ventricular pressure and mixed venous blood were obtained through a catheter inserted into the right ventricle from the external jugular vein. The electrocardiogram was monitored, pressures were measured by Statham pressure transducers (P23Db, Statham Instruments, Inc., Los Angeles, Calif.), and all signals were recorded on a multichannel oscillograph. Cardiac output was determined by the indicator dilution technique, with the injection of indocyanine dye into the right ventricle and the withdrawal of blood through a cuvette densitometer from the aorta. Oxygen consumption was calculated as the product of the cardiac output and the arterio-mixed venous oxygen difference and corrected for unit surface area according to the equation developed for the cat by Bartorelli and Gerola, $m^2 = 0.087 \text{ kg}^{2/3}$ (17).

After the hemodynamics study, intermittent positive pressure ventilation was provided via a tracheostomy and care was taken to assure adequate oxygenation and a stable hemodynamic state. The chest was opened widely and biopsies of right and left ventricular myocardium for measurement of high energy phosphate stores were obtained with a 6 inch mastoid rongeur. Myocardial specimens, weighing an average of 22 mg, were frozen in liquid nitrogen within 0.5 sec. The sample from the second ventricle to be biopsied was analyzed only if obtained within 3 sec of the first biopsy. Biopsies were transventricular and the right ventricle was sampled first in most cases.

After the biopsies, the hearts were rapidly extirpated and right ventricular papillary muscles were removed immediately and suspended in a bath containing oxygenated Krebs' solution. The technique and apparatus utilized to study mechanical function of isolated papillary muscles have been described in detail (8). In brief, the papillary muscle was held at its lower nontendinous end by a spring-loaded clip, forming the end of a rigid pin penetrating the bottom of a bath and attached directly to a Statham (GI-4-250) force transducer. The tendinous end of the muscle was attached to a lever mounted on a rigid Palmer stand (D12, C. F. Palmer, Ltd., London, England), arranged so that both isotonic and isometric contractions could be studied. Papillary muscles were stimulated with square wave DC impulses of 9 msec duration and a voltage 10-25% greater than threshold, delivered through field electrodes placed parallel to the long axis of the muscle. Shortening, tension, and the stimulus artifact were recorded at a paper speed of 100 mm/sec on a mul-

TABLE I
Hemodynamic and biochemical determinations at three levels of thyroid activity

	PBI	Cholesterol	Heart rate	Cardiac index	Stroke index	Mean systolic ejection rate	A-V O ₂ difference	Oxygen consumption
	$\mu\text{g}/100\text{ ml}$	$\text{mg}/100\text{ ml}$	beats/min	$\text{ml}/\text{min per kg}$	$\text{ml}/\text{kg per beat}$	$\text{ml}/\text{kg per sec}$	$\text{vol } \%$	$\text{ml}/\text{min per m}^2$
Hypothyroid	$1.2 \pm 0.2^*$ (15)	$124.3 \pm 13.1^\dagger$ (15)	$160 \pm 9^\S$ (9)	$113 \pm 9^\dagger$ (9)	$0.78 \pm 0.10^\dagger$ (9)	$3.0 \pm 0.4^*$ (5)	$4.9 \pm 0.2^\dagger$ (9)	$91 \pm 10^\dagger$ (9)
Euthyroid	4.3 ± 0.2 (24)	101.2 ± 10.0 (24)	212 ± 19 (7)	124 ± 18 (7)	0.63 ± 0.09 (7)	5.2 ± 0.3 (7)	5.6 ± 0.4 (7)	115 ± 16 (7)
Hyperthyroid	$>25^*$ (12)	$49.1 \pm 7.3^*$ (12)	$245 \pm 5^\dagger$ (5)	$212 \pm 28^\S$ (5)	$0.81 \pm 0.09^\dagger$ (4)	$9.8 \pm 1.0^*$ (3)	$6.9 \pm 0.7^\dagger$ (4)	$222 \pm 28^*$ (4)

PBI, protein-bound iodine; A-V, arteriovenous.

Values represent mean \pm standard error of the mean with the number of animals for each determination indicated in parentheses.

* $P = <0.01$ when compared to euthyroid.

$^\dagger P = >0.05$ when compared to euthyroid.

$^\S P = <0.05$ when compared to euthyroid.

tichannel oscillograph, and the rate of tension development, time to peak tension, and velocity of shortening were determined from these recordings. In order to

compare the mechanical function of papillary muscles of different sizes, we corrected tension for cross-sectional area and expressed it in grams per square millimeter and expressed velocity of shortening in terms of muscle lengths per second.

Temperature was maintained at 30°C and frequency of contraction at 12/min, except when the effects of changes in these two variables were studied specifically. Responsiveness to cardiac glycosides was studied by measuring the maximum active tension 20 min after the addition of strophanthidin to individual preparations to achieve final concentrations of 0.01, 0.10, 0.25, 0.50, and 1.00 $\mu\text{g}/\text{ml}$. In separate muscles, the responsiveness to *l*-norepinephrine was similarly studied at 5-min intervals with concentrations of 10^{-10} to 10^{-6} mole/liter, without washout between additions of the catecholamine.

Right ventricular norepinephrine concentration was measured spectrophotofluorometrically by the trihydroxy-indole method as described in detail elsewhere (18). Myocardial biopsies for high energy phosphate determinations were stored in liquid nitrogen. On the day of assay, each tissue was pulverized at -50°C as previously described (16) and perchloric acid extracts were prepared. Creatine phosphate (CP) and inorganic phosphate (P_i) were determined by the phosphomolybdate method of Fiske and Subbarow (19) as modified by Furchgott and De Gubareff (15). Creatine concentrations were measured by the α -naphthol-diacetyl method of Ennor and Rosenberg (20, 21), and adenosine triphosphate (ATP) by a modification of the firefly luminescence method of Strehler and McElroy (22). Modifications of these procedures have been described previously in detail (16). To avoid possible errors involved in weighing small tissues in the frozen state, we calculated sample weights by the determination of creatine concentration in two separately obtained samples of the right ventricle and the creatine content of the biopsy sample as previously described (16).

Statistical analyses were performed utilizing Student's unpaired *t* test to compare the mean values in muscles

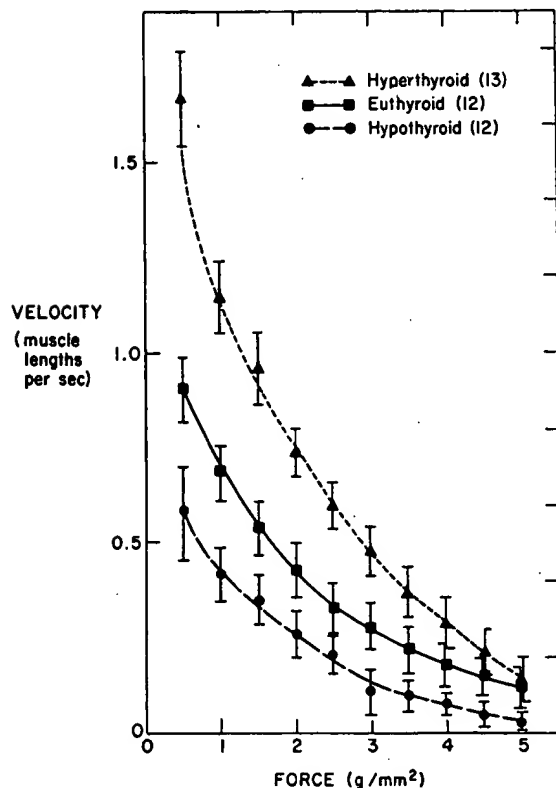


FIG. 1. THE AVERAGE FORCE-VELOCITY RELATIONSHIP FOR PAPILLARY MUSCLES FROM HYPERTHYROID, EUTHYROID, AND HYPOTHYROID CATS. Initial velocity of shortening is normalized in terms of muscle lengths per second, and load, corrected for cross-sectional area of individual muscles, is expressed in g/mm^2 . Brackets represent \pm SEM.

from hyperthyroid and hypothyroid cats with those of euthyroid cats. Differences between groups were considered to be statistically significant when $P < 0.01$ and probably significant when $0.01 < P < 0.05$.

Results

I. Characterization of thyroid state

A. Protein-bound iodine and serum cholesterol. Serum protein-bound iodine was significantly elevated in the hyperthyroid and reduced in the hypothyroid cats; serum cholesterol was significantly reduced in the hyperthyroid cats and slightly, but not significantly, elevated in the hypothyroid cats (Table I).

B. Hemodynamic measurements. In the hyperthyroid animals, cardiac index, mean systolic ejection rate, and total O_2 consumption were all significantly elevated above normal while in the hypothyroid cats the heart rate and mean systolic ejection rate were reduced significantly below the values observed in the euthyroid animals (Table I).

II. Myocardial mechanics

A. Analysis of isotonic contractions. Maximum velocity of isotonic shortening (V_{\max}) was found to vary directly with the level of the thyroid state (Fig. 1); at the lightest load studied (0.5 g/mm^2), V_{\max} averaged 0.90 ± 0.08 muscle lengths/sec in the muscles from 12 euthyroid cats and was significantly lower ($P < 0.01$) in the muscles obtained from 12 hypothyroid cats (0.58 ± 0.12 muscle lengths/sec) and significantly higher ($P < 0.01$) in the muscles from 13 hyperthyroid cats (1.67 ± 0.12 muscle lengths/sec). Expressed in terms of Hill's equation (23), these curves can be analyzed as displaced hyperbolae (24) and the constants a and b and the actual V_{\max} of the Hill equation may be calculated (Fig. 2). The ratio a/P_0 , which characterizes the steepness of the force-velocity curve, was not greatly altered by changes in thyroid state, while b , the velocity constant, and calculated V_{\max} which equals $(P_0/a)b$, were directly related to the level of thyroid activity.

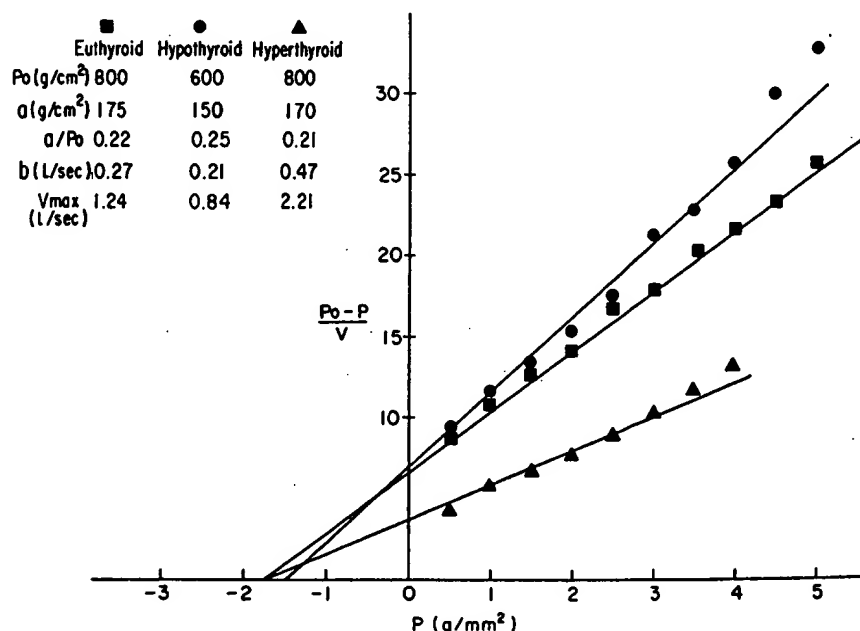


FIG. 2. CONSTANTS OF THE HILL EQUATION OBTAINED BY LINEARIZATION OF THE DATA SHOWN IN FIG. 1. The Hill equation, $(P + a)V = (P_0 - P)b$, may be rearranged to the form of a linear equation, $P_0 - P/V = 1/b(P + a)$, where P =load, V =velocity of shortening, P_0 =maximum isometric force, and a and b are constants which may be derived from the force-velocity curve. Substituting the values from Fig. 1, the relations shown in Fig. 2 are obtained. The slope of the line equals $1/b$, and the intercept on the y axis equals a in the Hill equation. The values thus obtained are shown in the insert of the figure.

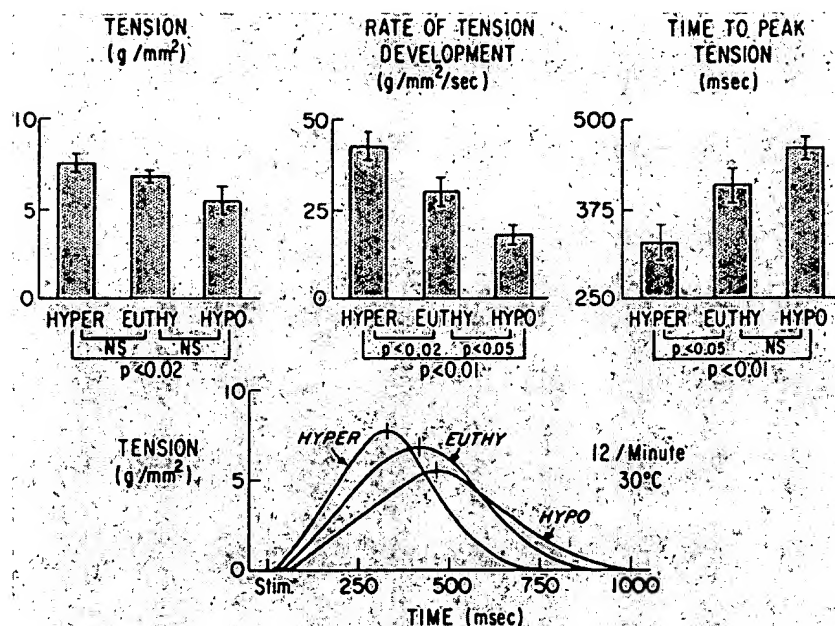


FIG. 3. ISOMETRIC TENSION EXAMINED IN RELATION TO TIME AND ANALYZED IN TERMS OF ITS COMPONENT FACTORS AS A FUNCTION OF LEVEL OF THYROID STATE. Tension represents maximum active tension, measured at the peak of the length-active tension curve. Rate of tension development was measured as the maximum slope of the tension curve, and time to peak tension was measured from the stimulus. Tension curves in the lower panel represent average data, as presented in columns of the upper panel, for muscles from 11 hyperthyroid, 8 euthyroid, and 13 hypothyroid cats. NS = $P > 0.05$.

B. Analysis of isometric contractions. The compliance of the papillary muscle was unchanged by alterations in the level of thyroid state as shown by the essentially identical length-resting tension curves in the muscles from all three groups of cats. At L_{max} , i.e. the muscle length at which active tension was maximal, resting tension averaged 1.9 ± 0.6 g/mm² in the muscles obtained from the 7 hyperthyroid cats, 2.3 ± 0.4 g/mm² in the muscles obtained from the 12 euthyroid cats, and 2.5 ± 0.3 g/mm² in the muscles obtained from the 11 hypothyroid cats. These values did not differ significantly from one another nor were there differences in resting tension among the three groups of muscles at other portions of the length-resting tension curve.

Active tension at the peak of the length-active tension curve averaged 6.8 ± 0.3 g/mm² in the muscles from 24 euthyroid animals, 7.7 ± 0.5 g/mm² in the muscles from 11 hyperthyroid animals, and 5.4 ± 0.7 g/mm² in the muscles from 13 hypothyroid animals. Although the hyper- and hypothyroid groups did not differ significantly from

the euthyroid, the maximum isometric tension in the hyperthyroid muscles was significantly ($P < 0.02$) greater than that in the hypothyroid group.

When tension was explained as a function of time and analyzed in terms of the rate of tension development and the time from stimulus to peak tension, it was observed that the level of thyroid state affects the contractile performance of the isometrically contracting muscle to a much greater extent than is indicated by the relatively small changes in peak tension (Fig. 3). Time to peak tension varied inversely with the level of thyroid state, averaging 458 ± 16 , 406 ± 22 , and 326 ± 28 msec, and the rate of tension development varied directly, averaging 17.6 ± 2.8 , 29.8 ± 3.9 , and 44.6 ± 3.6 g/mm² per sec, for the hypothyroid, euthyroid, and hyperthyroid groups, respectively, measured at 30°C and 12 contractions/min.

Variations in temperature from 21° to 37°C and variations in the frequency of contraction from 6 to 48/min resulted in directionally similar changes in the time to peak tension and the rate of tension development in muscles from each group of ani-

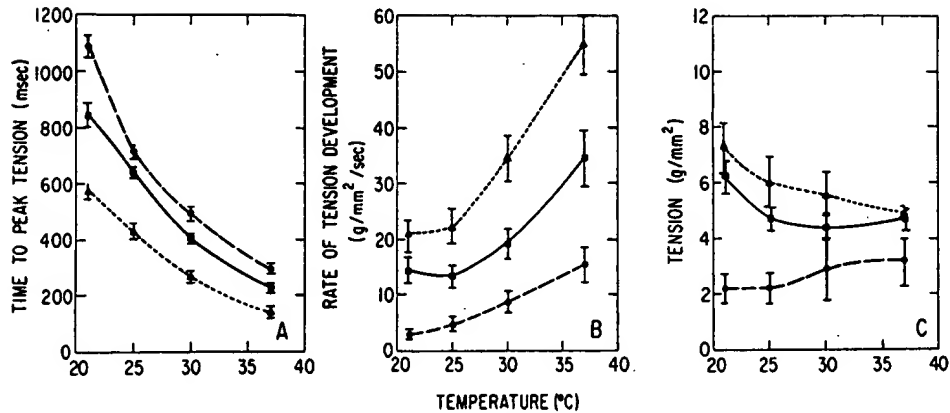


FIG. 4. TIME TO PEAK TENSION (A), RATE OF TENSION DEVELOPMENT (B), AND TENSION (C) MEASURED AT VARIOUS TEMPERATURES IN 8 MUSCLES FROM HYPERTHYROID CATS (▲), 10 FROM EUTHYROID CATS (■), AND 5 FROM HYPOTHYROID CATS (●).

mals (Figs. 4 and 5). Consequently, the differences in time to peak tension and rate of tension development observed at 30°C and 12 contractions/min among the three groups pertained to the entire range of temperature and frequency studied.

Absolute tension represents the interaction between the rate of tension development and the time to peak tension. As temperature was raised in muscles obtained from hyperthyroid and euthyroid cats, at a constant frequency (12/min), time to peak tension was shortened relatively more than the rate of tension development was augmented, so that tension fell (Fig. 4C). On the other hand, in muscles removed from hypothyroid cats, the reciprocal changes in the rate of tension development and time to peak tension were of similar

relative magnitude, so that the resultant tension showed little change as temperature was varied between 21° and 37°C. When temperature was maintained constant (at 30°C) and frequency of contraction increased from 6 to 48/min, the time to peak tension declined (Fig. 5A) while the rate of tension development was augmented in all three groups of muscles (Fig. 5B). In the muscles removed from the euthyroid and hypothyroid cats, the rate of tension development rose proportionately more than the time to peak tension declined and, as a consequence, tension increased as frequency was elevated. On the other hand, in the muscles removed from hyperthyroid cats, the augmentation in the rate of tension development was not as great as in the

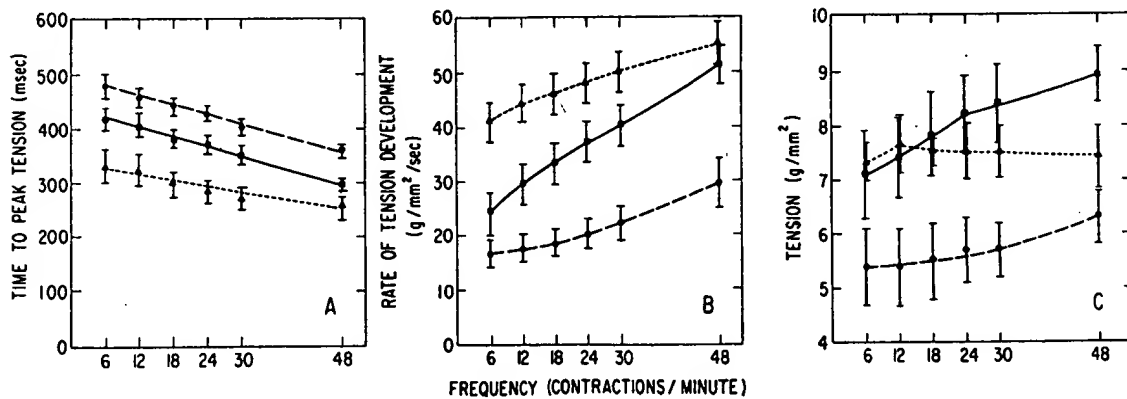


FIG. 5. TIME TO PEAK TENSION (A), RATE OF TENSION DEVELOPMENT (B), AND TENSION (C) MEASURED AT VARIOUS CONTRACTION FREQUENCIES IN MUSCLES FROM 11 HYPERTHYROID CATS (▲), 8 EUTHYROID CATS (■), AND 12 HYPOTHYROID CATS (●).

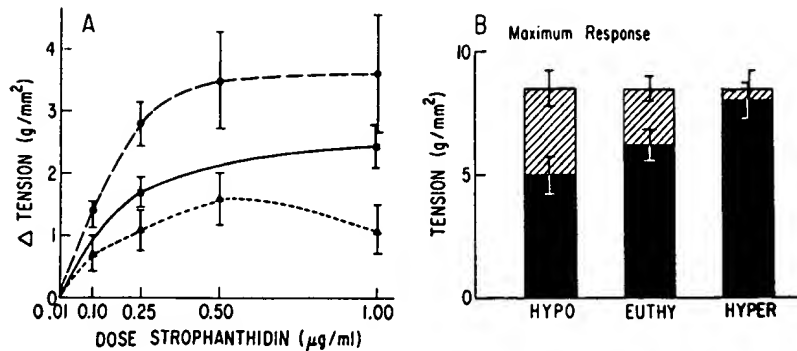


FIG. 6. THE EFFECTS OF A CARDIAC GLYCOSIDE, STROPHANTHIDIN, ON ISOMETRIC TENSION AT 30°C AND 12 CONTRACTIONS/MIN IN PAPILLARY MUSCLES FROM 7 HYPERTHYROID CATS (\blacktriangle), 12 EUTHYROID CATS (\blacksquare), AND 8 HYPOTHYROID CATS (\bullet). The average increment in tension is plotted as a function of strophanthidin concentration (A) and the maximum response is shown with respect to initial tension (B) for each group of muscles. Initial tension, indicated by the solid columns, represents the control before addition of strophanthidin. Maximum response, indicated by the broken portion of each column, represents the average of the maximum increment in tension produced by strophanthidin in each muscle.

other two groups and thus no change in tension occurred (Fig. 5C).

III. Responsiveness to cardiac glycosides

As shown in Fig. 6A, muscles obtained from hyperthyroid cats exhibited a smaller contractile

response and those from hypothyroid cats a greater response than muscles from euthyroid cats. With the largest concentration of strophanthidin (1 μ g/ml), the increments in tension averaged 1.1 ± 0.4 g/mm² for the hyperthyroid muscles, a value significantly ($P < 0.05$) lower than 2.5 ± 0.3 g/mm² in the euthyroid muscles, and 3.6 ± 1.0 g/mm² in

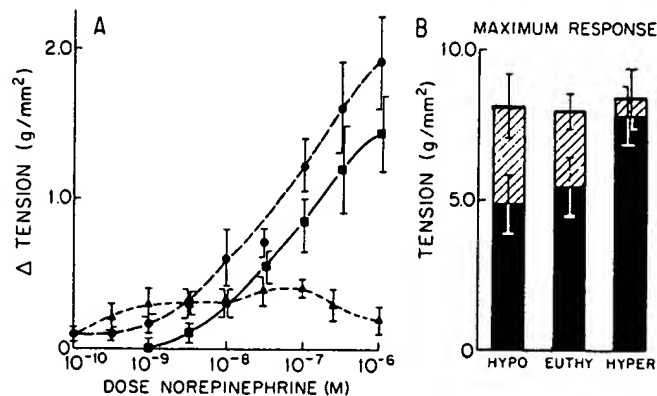


FIG. 7. THE EFFECTS OF EXOGENOUS NOREPINEPHRINE ON ISOMETRIC TENSION AT 30°C AND 12 CONTRACTIONS/MIN IN PAPILLARY MUSCLES FROM 7 HYPERTHYROID CATS (\blacktriangle), 8 EUTHYROID CATS (\blacksquare), AND 10 HYPOTHYROID CATS (\bullet). The average increment in tension is plotted as a function of norepinephrine concentration (A) and the maximum response is shown with respect to initial tension (B) for each group of muscles. Initial tension, indicated by the solid columns, represents the control before addition of norepinephrine. Maximum response, indicated by the broken portion of each column, represents the average of the maximum increment in tension produced by norepinephrine in each muscle.

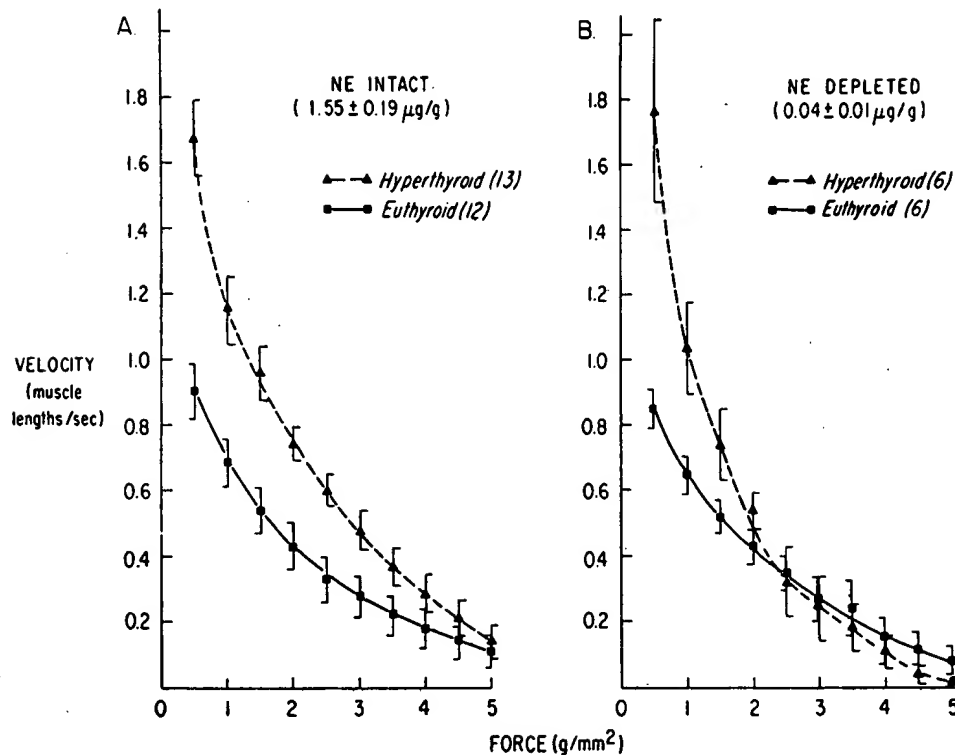


FIG. 8. (A) THE AVERAGE FORCE-VELOCITY RELATIONSHIP FOR PAPILLARY MUSCLES FROM 13 HYPERTHYROID AND 12 EUTHYROID CATS WITH INTACT CARDIAC NOREPINEPHRINE STORES. Right ventricular norepinephrine (NE) concentration is indicated in parentheses.

(B) The average force-velocity relationship for papillary muscles from six hyperthyroid and six euthyroid cats depleted of norepinephrine by reserpine. Right ventricular norepinephrine concentration is indicated in parentheses.

the hypothyroid muscles. The magnitude of the increase in force produced by strophanthidin varied inversely with the control maximum isometric tension, in such a way that the absolute levels of tension after strophanthidin were nearly identical in all three groups of muscles, averaging 8.5 ± 0.5 g/mm² in the hypothyroid group, 8.4 ± 0.5 g/mm² in the euthyroid group, and 8.6 ± 0.8 g/mm² in the hyperthyroid group (Fig. 6B).

IV. Relationship between sympathetic neurotransmitter stores and cardiac muscle function

A. Responsiveness to norepinephrine. Muscles obtained from hyperthyroid cats were not supersensitive to norepinephrine when it was added to the bath and in fact responded far less than euthyroid muscles. Although muscles obtained from hypothyroid animals appeared to respond to a greater extent than euthyroid muscles, this difference was not significant. At a concentration of

10^{-6} M norepinephrine, the increment in maximum active tension averaged 0.2 ± 0.1 , 1.4 ± 0.3 , and 1.9 ± 0.3 g/mm², for hyperthyroid, euthyroid, and hypothyroid groups, respectively (Fig. 7A). As was noted in the case of strophanthidin, the increment in tension was inversely related to the level of tension before the addition of the norepinephrine and the absolute levels of tension after norepinephrine were similar in all three groups of muscles (Fig. 7B).

B. Right ventricular norepinephrine concentration. Right ventricular norepinephrine concentration averaged 1.55 ± 0.19 , 2.13 ± 0.30 , and 1.82 ± 0.15 µg/g in the ventricles obtained from the hyperthyroid, euthyroid, and hypothyroid groups respectively; these values did not differ significantly from one another. Norepinephrine stores were essentially eliminated in the six animals treated with reserpine before and during induction of the hyperthyroid state and averaged 0.04 ± 0.01 µg/g.

C. Myocardial mechanics. The increase in the velocity of shortening observed in muscles from hyperthyroid cats with normal norepinephrine stores (Fig. 8A) was also seen in muscles from animals depleted of norepinephrine by pretreatment with reserpine (Fig. 8B); at a load of 0.5 g/mm², V_{\max} averaged 0.85 ± 0.06 muscle lengths/sec in muscles from six animals given reserpine alone and was significantly greater ($P < 0.01$), 1.76 ± 0.27 muscle lengths/sec, in the muscles from reserpine-treated hyperthyroid animals. The latter value was essentially identical with that observed in the noncatecholamine depleted muscles from hyperthyroid animals, 1.67 ± 0.12 muscle lengths/sec. Reduction of the time to peak tension and augmentation of the rate of tension development similar to that observed in muscles from hyperthyroid animals occurred in the muscles from cats pretreated and maintained on reserpine concomitant with thyroxine. Thus, time to peak tension averaged 245 ± 17 msec in muscles obtained from the reserpine-thyroxine-treated group, compared to 496 ± 18 msec in muscles obtained from reserpine-treated euthyroid animals ($P < 0.01$), while the rate of tension development averaged 32.6 ± 2.5 g/mm² per sec in the reserpine-thyroxine-treated group compared to 23.2 ± 3.5 g/mm² per sec in the reserpine-treated controls ($P < 0.05$).

V. Myocardial energy stores

Myocardial creatine phosphate concentrations did not differ significantly in either ventricle among the hyperthyroid, euthyroid, and hypothyroid groups (Table II). ATP concentrations tended to be higher in hyperthyroid and lower in hypothyroid than in euthyroid animals; this difference was significant ($P < 0.05$) with respect to the right ventricle only in hyperthyroid cats and with respect to the left ventricle only in hypothyroid cats. In both ventricles, however, ATP concentrations were slightly, though significantly higher ($P < 0.05$) in hyperthyroid as compared to hypothyroid animals.

The total high energy phosphate stores, i.e. the sum of creatine phosphate and ATP, were virtually identical in both ventricles in all three groups of cats. Inorganic phosphate concentrations were significantly lower in hypothyroid than in hyperthyroid cats ($P < 0.01$) in both ventricles, while creatine stores were significantly lower in both hyperthyroid and hypothyroid cats when compared to the euthyroid group in both ventricles ($P < 0.02$).

Discussion

The major finding of this investigation is that the thyroid state profoundly affects the intrinsic

TABLE II
Myocardial energy stores

	Right ventricle			Left ventricle		
	Hypo	Euthy	Hyper	Hypo	Euthy	Hyper
		$\mu\text{moles/g}$			$\mu\text{moles/g}$	
Cr	$12.0 \pm 0.6^*$ (14)	15.5 ± 0.6 (20)	$12.8 \pm 0.4^\dagger$ (13)	$14.2 \pm 0.8^*$ (14)	17.4 ± 0.5 (19)	$13.6 \pm 0.5^*$ (13)
CP	$7.25 \pm 0.90^\S$ (8)	7.22 ± 0.49 (17)	$6.13 \pm 0.48^\S$ (8)	$7.35 \pm 0.67^\S$ (11)	7.85 ± 0.68 (12)	$6.59 \pm 0.61^\S$ (8)
ATP	$4.83 \pm 0.32^\S$ (8)	5.13 ± 0.22 (17)	$6.00 \pm 0.41^\dagger$ (8)	$4.84 \pm 0.27^\dagger$ (11)	5.76 ± 0.31 (12)	$5.85 \pm 0.43^\S$ (8)
CP + ATP	$12.08 \pm 1.09^\S$ (8)	12.35 ± 0.52 (17)	$12.13 \pm 0.31^\S$ (8)	$12.19 \pm 0.75^\S$ (11)	13.61 ± 0.71 (12)	$12.44 \pm 0.80^\S$ (8)
P _i	$3.76 \pm 0.32^\S$ (8)	4.10 ± 0.32 (17)	$5.78 \pm 0.43^\dagger$ (8)	$3.70 \pm 0.28^*$ (11)	5.32 ± 0.38 (12)	$5.12 \pm 0.36^\S$ (8)

Cr, creatine; CP, creatine phosphate; ATP, adenosine triphosphate; P_i, inorganic phosphate.

Values represent mean \pm standard error of the mean with the number of animals for each determination indicated in parentheses.

* $P = < 0.01$ when compared to euthyroid.

$^\dagger P = < 0.05$ when compared to euthyroid.

$^\S P = > 0.05$ when compared to euthyroid.

contractile state of cardiac muscle, primarily by altering the speed of shortening of the contractile elements, as reflected by V_{\max} in isotonic contractions and by the rate of tension development in isometric contractions. This observation suggests strongly that the abnormalities in cardiovascular dynamics observed in the intact organism with hyper- or hypothyroidism (Table I) (1-4) do not result merely from the changes in the load placed upon the heart by the induced alterations in the metabolism of extracardiac tissues; but rather, it indicates that the changes observed in cardiac index, mean systolic ejection rate, and myocardial fiber-shortening rate result, at least in part, from effects on the intrinsic contractile properties of the myocardium exerted by thyroid hormone or some substance elaborated by the intact organism in response to the altered thyroid state. Moreover, these findings suggest that the inotropic properties of the heart are adjusted in a manner appropriate to meet the simultaneously induced alterations in peripheral requirements. The increased intrinsic velocity of contraction of hyperthyroid muscle helps assure an elevated cardiac output in this condition, since it permits an augmented velocity of ejection at a time when heart rate is increased. As a consequence, stroke index is maintained at a normal level, or even increased, while heart rate is augmented, resulting in a marked elevation of cardiac index (Table I).

That the thyroid state exerts only a minor effect on myocardial force development follows from the observation that the time to peak tension and the rate of tension development are affected in opposite directions by variations of thyroid state, in such a manner that resultant tension is not greatly altered. Muscles from hyperthyroid cats develop tension at a more rapid rate but for a shorter period of time than euthyroid muscles; and, conversely, muscles from hypothyroid cats develop tension at a slower rate, but this tends to be compensated for by a prolonged period of contraction. Thus, hyperthyroidism increases the intensity of the active state of the myocardium, as measured by the shift in the force-velocity curve and by increases in the rate of tension development, but simultaneously shortens the duration of active state, as reflected by abbreviation of the time to peak tension (25). These findings suggest that the thyroid state affects the contractile

state of cardiac muscle profoundly by varying the rate of interaction at contractile sites, while altering the extent of force development only to a minor degree. Consonant with this view is the finding that the constant b from the Hill equation (23), which reflects the rate with which energy leaves the muscle, also varied directly with increasing level of thyroid activity (Fig. 2).

Although time to peak tension and the rate of tension development vary inversely as the thyroid state is altered, these two parameters can, under other conditions, be affected separately. For example, we have recently observed that papillary muscle obtained from cats with right ventricular hypertrophy and failure exhibit diminished rates of development of tension as do muscles from hypothyroid animals, but exhibit no prolongation of the duration of the contraction. Therefore, unlike muscles obtained from hypothyroid animals, muscles from cats with heart failure exhibit striking reductions in the absolute levels of tension development (26). Similarly, when serotonin is administered to the isolated cat papillary muscles, the rate of tension development is augmented, as it is in muscles from cats with hyperthyroidism, but, unlike hyperthyroidism, the duration of contraction is not altered by serotonin (27). Thus, for a given increment in the rate of tension development, serotonin produces a profound increase in tension whereas hyperthyroidism does not.

From these findings, it is apparent that when tension alone is measured, large changes in the contractile state of the myocardium can be overlooked. This fact may account, at least in part, for conflicting data reported in earlier studies of this problem. Studying hypothyroid rats, Benforado and Wiggins (28) found a slight increase in tension produced by isolated ventricular strips, while Meijler (29) showed modest decreases in force development of Langendorff preparations. On the other hand, Whitehorn, Ullrick, and Anderson (30) demonstrated reductions in the maximum force developed by ventricular strips obtained from hyperthyroid rats stimulated at a frequency of 60/min. This result can be accounted for by the finding of the present study, that as the frequency of contraction is increased in cardiac muscle from hyperthyroid animals, the rate of tension development increases proportionately less than the time to peak tension is abbreviated (Fig.

5), and the net effect may be a variation in force development which does not parallel the changes in the contractile state of the myocardium, as reflected in V_{\max} .

Both temperature and frequency of contraction influence cardiac muscle obtained from hyperthyroid, euthyroid, and hypothyroid cats in similar manners, so that the differences observed among muscles obtained from the three groups of animals at any one temperature or frequency pertain to the entire range of temperature and frequency studied. It is of interest that variations of both temperature and frequency of contraction produce changes in heart muscle which are quite analogous to those induced by alterations in the thyroid state. As a consequence, when either the temperature or the frequency of contraction of hyperthyroid muscles is reduced, they behave like muscles obtained from hypothyroid animals. For example, the time to peak tension was essentially identical in muscles obtained from hyperthyroid cats studied at 21°C, from euthyroid cats studied at 26°C, and from hypothyroid cats studied at 28°C. Similarly, the time to peak tension was approximately the same in muscles from hyperthyroid cats contracting at 6/min, from euthyroid cats at 24/min, and from hypothyroid cats at 48/min.

The manner in which patients with altered thyroid states respond to cardiac glycosides has long been of interest (5, 31, 32). All workers who have examined the problem agree that both hypo- and hyperthyroid heart muscle respond to the glycoside (5, 33-35); however, analysis of the problem in patients and intact experimental animals is complicated by the facts that the absorption and the turnover of the drug (36), as well as the fraction of the cardiac output which enters the coronary circulation (37, 38), may all be influenced by alterations in the thyroid state, making it difficult to deliver a known concentration of drug to the myocardium. In an earlier study from this laboratory it was observed that the percentage increase in contractile force of the right ventricle of intact hyperthyroid dogs was only slightly, though not significantly, lower than that observed in euthyroid animals (33). In a similar preparation, Rosen and Moran noted no difference between euthyroid and hyperthyroid dogs in their inotropic response to moderate doses of ouabain,

but found that larger doses caused a smaller inotropic response in hyperthyroid than in euthyroid animals (34). Peacock and Moran reported that hyperthyroidism diminished the contractile force developed by strips of the right ventricle of rats and reduced the increment in force after the addition of ouabain to the bath (35). The findings of the present investigation are, in general, not in accord with earlier studies, since we have observed that hyperthyroidism tends to augment the intrinsic tension development of the muscle and to reduce the response at every dose of strophanthidin.

Earlier investigators observed that hypothyroid dogs exhibited a normal increment of contractile force when ouabain was administered (34) and that the contractile force of right ventricular strips removed from hypothyroid rats, although greater than normal to begin with, showed reduced response after the addition of ouabain (35). The results of the present study are again not in concert with these findings, since we have noted that intrinsic contractile tension of muscles from hypothyroid cats tends to be reduced but that the increments of tension after the addition of strophanthidin were enhanced at every dose level studied. Our findings are, however, consistent with those obtained in an earlier study from this laboratory in which intact hypothyroid dogs were shown to exhibit a markedly increased inotropic response to infused ouabain (33).

An interesting finding of the present investigation was that the maximum increment in tension produced by strophanthidin varied reciprocally with the initial intrinsic isometric tension development, the muscles with the highest intrinsic contractility (the hyperthyroid group) exhibiting the smallest response to strophanthidin and the muscles with the lowest intrinsic contractility (the hypothyroid group) exhibiting the greatest response to strophanthidin. The average maximum tensions exhibited by all three groups of muscles after strophanthidin were almost identical and appeared to be independent of the thyroid state. Since the same contractile ceiling was reached by all three groups of muscles after strophanthidin, it appears that the increment in tension in response to the glycoside depends, at least in part, upon the degree to which the initial contractile state is altered by the level of thyroid activity.

It has been suspected for many years that an

intimate relation exists between the sympathetic nervous system and the action of thyroid hormone (6). Alterations in cardiovascular function associated with hyperthyroidism resemble those produced by excess sympathetic influence and can be ameliorated by anti-adrenergic agents. Hence, these alterations have been considered to be mediated by catecholamines and not directly by thyroid hormone itself. In 1956, Brewster, Isaacs, Osgood, and King observed that the increased heart rate, oxygen consumption, cardiac index, and ventricular stroke work in hyperthyroid dogs could be abolished by epidural sympathetic blockade and then reproduced by norepinephrine infusion (39). They concluded that the hemodynamic changes of thyrotoxicosis result not from isolated activity of thyroid hormone but rather from the physiologic effects of catecholamines, particularly *l*-norepinephrine, as augmented by the thyroid hormones. Similarly, Lee, Morimoto, Bronsky, and Waldstein studied the peripheral manifestations of myxedema and thyrotoxicosis in patients and concluded that there was a synergistic relationship between thyroid hormone and the catecholamines (40). It has also been proposed that the effects on the heart of treatment with thyroxine are largely dependent upon the capacity of thyroxine to increase the catecholamine content of the heart (41). On the other hand, Van der Schoot and Moran (42) recently reported that hyperthyroidism does not potentiate, but tends to depress, the positive inotropic and chronotropic responses to catecholamines both in vivo (dogs) and in vitro (rat atria and ventricle strips); and Margolius and Gaffney found that pressor and chronotropic responses to endogenously released or exogenously administered norepinephrine in dogs were not affected by pretreatment with thyroid hormone or ^{131}I (43). Similarly, Wilson, Theilen, Hege, and Valenca showed that isoproterenol produced similar increments in heart rate and cardiac index in normal human subjects before and after triiodothyronine-induced hypermetabolism (44) and Wilson, Theilen, and Fletcher found that propranolol, in doses sufficient to block the effects of isoproterenol, did not alter the hemodynamic effects produced by triiodothyronine administration (45).

The present investigation permitted detailed analysis of the interactions of the thyroid state and the sympathetic nervous system on heart

muscle. We observed that neither hyper- nor hypothyroidism resulted in significant changes in concentration of norepinephrine in the ventricle. This finding contrasts, on the one hand with that of Goodkind, Fram, and Roberts who found that myocardial norepinephrine concentration in guinea pig ventricles was increased by hyperthyroidism and decreased by hypothyroidism (46); and, on the other hand, with that of Kurland, Hammond, and Freedberg, who found that norepinephrine concentration in rabbit ventricles was decreased by hyperthyroidism and increased by hypothyroidism (47).

Of particular interest in the present study is the observation that the changes in the intrinsic contractile state of the myocardium induced by hyperthyroidism were not dependent on cardiac norepinephrine stores. Thus, similar increases in velocity of shortening and rate of tension development were noted in muscles from hyperthyroid animals with depleted, as well as with intact, norepinephrine stores (Fig. 8). Further, papillary muscles removed from hyperthyroid cats were not supersensitive to added norepinephrine but were actually quite subsensitive, whereas muscles removed from hypothyroid cats tended to respond somewhat more than did muscles removed from euthyroid cats. Therefore, the responses to added norepinephrine resemble those to strophanthidin in that the hyperthyroid muscles, exhibiting the highest level of contractile activity before addition of the inotropic agent, demonstrated the smallest increments in tension, while the muscles with the lowest level of intrinsic activity, i.e., those obtained from hypothyroid animals, showed the greatest responses. Thus, our findings indicate that thyroid activity modifies the intrinsic myocardial contractile state independently of norepinephrine. Although the effects on the heart of increased sympathetic activity resemble those of increased thyroid activity, the combined actions appear to be additive but not synergistic.

It was of interest to determine whether the induced alterations in contractile activity observed in the intact heart and the isolated papillary muscles of hyper- and hypothyroid animals were related to alterations in myocardial high energy phosphate stores. Previously no information was available concerning energy stores in hypothyroidism, and the effects of hyperthyroidism on high

energy phosphate compounds were disputed. A number of investigators have reported marked depression of CP and ATP stores in the hearts of animals with hyperthyroidism (10-13). Piatnek-Leunissen and Olson, on the other hand, have recently reported no significant differences in CP or ATP between the hearts of normal and hyperthyroid dogs (14). In the present study we observed that the concentrations of ATP, CP, and the sum of these two compounds in the euthyroid ventricles did not differ significantly from the concentrations of these substances observed in the hearts of either hyper- or hypothyroid cats. It is recognized that the concentrations of high energy phosphate compounds reflect the steady-state conditions existing in the myocardium rather than the turnover. However, the finding of normal values indicates, on the one hand, that the depressed contractile activity characteristic of the hypothyroid heart does not result from inadequate availability of energy, and, on the other hand, that the increased contractile activity characteristic of hyperthyroidism does not deplete available energy stores.

Acknowledgments

We gratefully acknowledge the skillful technical assistance of Nancy S. Dittmore and Shirley Seagren.

References

1. Resnik, W. H., and T. R. Harrison. 1966. The high-output and low-output syndrome. In *Principles of Internal Medicine*. T. R. Harrison, R. D. Adams, I. L. Bennett, W. H. Resnik, G. W. Thorn, and M. M. Wintrobe, editors. McGraw-Hill, New York. 788.
2. Howitt, G., and D. J. Rowlands. 1967. The heart in hyperthyroidism. *Am. Heart J.* 73: 282.
3. Theilen, E. O., and W. R. Wilson. 1967. Hemodynamic effects of peripheral vasoconstriction in normal and thyrotoxic subjects. *J. Appl. Physiol.* 22: 207.
4. Ueda, H., Y. Sugishita, A. Nakanishi, I. Ito, H. Yasuda, M. Sugiura, Y. Takabatake, K. Ueda, T. Koide, and K. Ozeki. 1965. Clinical studies on the cardiac performance by means of transeptal left heart catheterization: II. Left ventricular function in high output heart diseases, especially in hyperthyroidism. *Japan. Heart J.* 6: 396.
5. Frye, R. L., and E. Braunwald. 1961. Studies on digitalis. III. The influences of triiodothyronine on digitalis requirements. *Circulation*. 23: 376.
6. Harrison, T. S. 1964. Adrenal medullary and thyroid relationships. *Physiol. Rev.* 44, 161.
7. Hoch, F. L. 1962. Biochemical actions of thyroid hormones. *Physiol. Rev.* 42: 605.
8. Sonnenblick, E. H. 1962. Force-velocity relations in mammalian heart muscle. *Am. J. Physiol.* 202: 931.
9. Spann, J. F., Jr., E. H. Sonnenblick, T. Cooper, C. A. Chidsey, V. L. Willman, and E. Braunwald. 1966. Cardiac norepinephrine stores and the contractile state of heart muscle. *Circulation Res.* 19: 317.
10. Mattonet, C. 1933. Chemischer Beitrag zur Frage der Herzmuskelschädigung durch Thyroxin. *Z. Ges. Exptl. Med.* 90: 237.
11. Berg, H. 1937. Über den Herzmuskelstoffwechsel bei Hyperthyreose und seine Beeinflussung durch Vitamin C. *Arch. Exptl. Pathol. Pharmacol.* 185: 359.
12. Schumann, H. 1939. Experimentelle Befunde zur Frage gesteigerter Thyroxinempfindlichkeit des mechanisch vermehrt belasteten Herzmuskels. *Z. Ges. Exptl. Med.* 105: 577.
13. Holland, W. C., and R. L. Klein. 1960. Chemistry of Heart Failure. Charles C Thomas, Springfield. 116.
14. Piatnek-Leunissen, D., and R. E. Olson. 1967. Cardiac failure in the dog as a consequence of exogenous hyperthyroidism. *Circulation Res.* 20: 242.
15. Furchgott, R. F., and T. De Gubareff. 1956. The determination of inorganic phosphate and creatine phosphate in tissue extracts. *J. Biol. Chem.* 223: 377.
16. Pool, P. E., and E. H. Sonnenblick. 1967. The mechanochemistry of cardiac muscle. I. The isometric contraction. *J. Gen. Physiol.* 50: 951.
17. Bartorelli, C., and A. Gerola. 1963. Tidal volume, oxygen uptake, cardiac output, and body surface in the cat. *Am. J. Physiol.* 205: 588.
18. Spann, J. F., Jr., C. A. Chidsey, P. E. Pool, and E. Braunwald. 1965. Mechanism of norepinephrine depletion in experimental heart failure produced by aortic constriction in the guinea pig. *Circulation Res.* 17: 312.
19. Fiske, C. H., and Y. Subbarow. 1929. Phosphocreatine. *J. Biol. Chem.* 81: 629.
20. Ennor, A. H., and H. Rosenberg. 1952. The determination and distribution of phosphocreatine in animal tissues. *Biochem. J.* 51: 606.
21. Ennor, A. H. 1957. Determination and preparation of N-phosphates of biological origin. In *Methods in Enzymology*. S. P. Colowick and N. O. Kaplan, editors. Academic Press Inc., New York. 3: 850.
22. Strehler, B. L., and W. D. McElroy. 1957. Assay of adenosine triphosphate. In *Methods in Enzymology*. S. P. Colowick and N. O. Kaplan, editors. Academic Press Inc., New York. 3: 871.
23. Hill, A. V. 1938. The heat of shortening and the dynamic constants of muscle. *Proc. Roy. Soc. (London), Ser. B.* 126: 136.

24. Csapo, A., and M. Goodall. 1954. Excitability, length-tension relation, and kinetics of uterine muscle contraction in relation to hormonal status. *J. Physiol. (London)*. 126: 384.
25. Sonnenblick, E. H. 1967. Active state in heart muscle. Its delayed onset and modification by inotropic agents. *J. Gen. Physiol.* 50: 661.
26. Spann, J. F., Jr., R. A. Buccino, E. H. Sonnenblick, and E. Braunwald. 1967. The contractile state of cardiac muscle obtained from animals with experimentally produced ventricular hypertrophy and heart failure. *Circulation Res.* In press.
27. Buccino, R. A., J. W. Covell, E. H. Sonnenblick, and E. Braunwald. 1967. The effects of serotonin on the contractile state of the myocardium. *Am. J. Physiol.* In press.
28. Benforado, J. M., and L. L. Wiggins. 1965. Contractility, heart rate, and response to norepinephrine of isolated rat myocardium following I^{131} -induced hypothyroidism. *J. Pharmacol. Exptl. Therap.* 147: 70.
29. Meijler, F. L. 1963. Contractility of isolated hearts from myxedematous rats. *Israel Med. J.* 22: 395.
30. Whitehorn, W. V., W. C. Ullrick, and B. R. Anderson. 1959. Properties of hyperthyroid rat myocardium. *Circulation Res.* 7: 250.
31. McIntosh, H. D., and J. J. Morris, Jr. 1965. Problems in the use of digitalis in the management of congestive heart failure. *Progr. Cardiovascular Diseases.* 7: 360.
32. Rosenberg, M. S., and J. S. Graettinger. November 1962. Digitalis intoxication-management and prevention. *Disease-A-Month.* 1.
33. Morrow, D. H., T. E. Gaffney, and E. Braunwald. 1963. Studies on digitalis VII. Influence of hyper- and hypothyroidism on the myocardial response to ouabain. *J. Pharmacol. Exptl. Therap.* 140: 324.
34. Rosen, A., and N. C. Moran. 1963. Comparison of the action of ouabain on the heart in hypothyroid, euthyroid, and hyperthyroid dogs. *Circulation Res.* 12: 479.
35. Peacock, W. F., and N. C. Moran. 1963. Influence of thyroid state on positive inotropic effect of ouabain on isolated rat ventricle strips. *Proc. Soc. Exptl. Biol. Med.* 113: 526.
36. Doherty, J. E., and W. H. Perkins. 1966. Digoxin metabolism in hypo- and hyperthyroidism. *Ann. Internal Med.* 64: 489.
37. Rowe, G. G., J. H. Huston, A. B. Weinstein, H. Tuchman, J. F. Brown, and C. W. Crumpton. 1956. The hemodynamics of thyrotoxicosis in man with special reference to coronary blood flow and myocardial oxygen metabolism. *J. Clin. Invest.* 35: 272.
38. Bing, R. J. 1951. The coronary circulation in health and disease as studied by coronary sinus catheterization. *Bull. N. Y. Acad. Med.* 27: 407.
39. Brewster, W. R., Jr., J. P. Isaacs, P. F. Osgood, and T. L. King. 1956. The hemodynamic and metabolic interrelationships in the activity of epinephrine, norepinephrine, and the thyroid hormones. *Circulation.* 13: 1.
40. Lee, W. Y., P. K. Morimoto, D. Bronsky, and S. S. Waldstein. 1961. Studies of thyroid and sympathetic nervous system interrelationships. I. The blepharoptosis of myxedema. *J. Clin. Endocrinol. Metab.* 21: 1402.
41. Lee, W. C., C. Y. Lee, and C. S. Yoo. 1965. Effects of treatment with thyroxine on the noradrenaline content of the rabbit heart. *Brit. J. Pharmacol.* 25: 651.
42. Van der Schoot, J. B., and N. C. Moran. 1965. An experimental evaluation of the reputed influence of thyroxine on the cardiovascular effects of catecholamines. *J. Pharmacol. Exptl. Therap.* 149: 336.
43. Margolius, H. S., and T. E. Gaffney. 1965. The effects of injected norepinephrine and sympathetic nerve stimulation in hypothyroid and hyperthyroid dogs. *J. Pharmacol. Exptl. Therap.* 149: 329.
44. Wilson, W. R., E. O. Theilen, J. H. Hege, and M. R. Valenca. 1966. Effects of beta-adrenergic receptor blockade in normal subjects before, during, and after triiodothyronine-induced hypermetabolism. *J. Clin. Invest.* 45: 1159.
45. Wilson, W. R., E. O. Theilen, and F. W. Fletcher. 1964. Pharmacodynamic effects of beta-adrenergic receptor blockade in patients with hyperthyroidism. *J. Clin. Invest.* 43: 1697.
46. Goodkind, M. J., D. H. Fram, and M. Roberts. 1961. Effect of thyroid hormone on myocardial catecholamine content of the guinea pig. *Am. J. Physiol.* 201: 1049.
47. Kurland, G. S., R. P. Hammond, and A. S. Freedberg. 1963. Relation of thyroid state to myocardial catecholamine concentration. *Am. J. Physiol.* 205: 1270.

UNRECOGNIZED HYPOTHYROIDISM*

By G. K. WHARTON, M.B., M.S.(MED.), F.A.C.P.

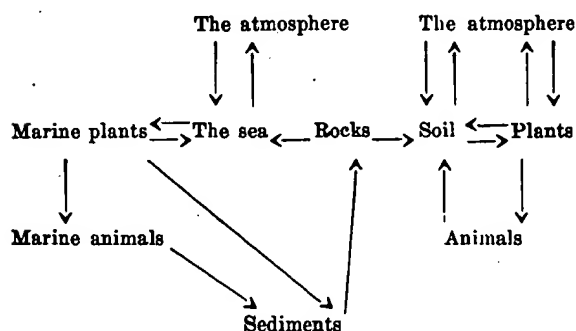
Department of Medicine, University of Western Ontario, London, Ont.

EXHIBIT D

MANY patients who could be helped by thyroid treatment are not recognized as hypothyroid. Cretinism and myxœdema are the textbook examples of the hypofunctioning thyroid gland. Very little has been written about the milder degrees and the atypical forms of deficient thyroid activity. Hypothyroidism in a mild or masked form differs so greatly from myxœdema and cretinism that constant alertness for its many and varied manifestations is demanded. This presentation is concerned with a few examples of help given by thyroid therapy in the treatment of common disorders.

PHYSIOLOGY

Iodine metabolism is closely associated with thyroid function. Lunde gives the following scheme to represent the circulation of iodine in nature.



Three chemical compounds, iodothyroglobin, diiodotyrosine, and thyroxin have been isolated from the thyroid gland. Thyroxin prepared from the gland is itself optically inactive, but dextro- and lævo-thyroxin have also been formed. While thyroxin satisfies in many respects the requirements of the active principle of thyroid gland, some of our clinical observations suggest that the two are different; probably desiccated thyroid is more complex than thyroxin and produces more bodily changes. The cells lining the acini of the thyroid gland absorb iodine from the blood, converting it into diiodotyrosine and protein combinations.

Simple goitre is a response to an absolute or relative iodine deficiency. The degree of hyperplasia is inversely related to the gland's iodine content. When hyperplasia ends in exhaustion atrophy the gland has become almost iodine-free. The majority of people in goitre belts have an enlarged thyroid, indicating an iodine deficiency at some time. If further demands are made on this depleted gland further hyperplasia or an exhaustion atrophy may ensue unless sufficient iodine is provided. Most of the pathology of the thyroid is based primarily upon simple goitre; the result may be hypothyroidism or one of the various types of hyperthyroidism.

The chief function of the thyroid gland is to regulate the speed of the metabolic processes of the body. This is accomplished largely by the thyroid hormone acting as a catalyst, sensitizing the body cells to sympathetic stimulation. The thyroid, adrenals, and sympathetic nervous system act together. The sympathetic and parasympathetic systems are antagonistic. The activity of an organ, or of even the entire individual, depends upon which is the stronger system. Thyroid activity accelerates the sympathetic system; therefore, most of the symptoms ascribed to hyperthyroidism are really an expression of hyperactivity of the sympathetic nervous system. Usually the converse is true, in that the parasympathetic system is predominant in hypothyroidism.

Oxygen consumption is increased by the action of thyroid extract on the sympathetics. The tachycardia of hyperthyroidism is caused by sympathetic sensitization in the cardiac centre in the brain as well as in muscle fibres. The thyroid hormone provides the skin with adequate amounts of water, fat, and blood, and as well regulates the activity of the sweat glands. Hypothyroidism or increased vagus activity results in hypersecretion and hypermotility; these in turn account for symptoms of spastic colon, mucus in the stool, flatulence, and constipation, unless these are counteracted by other influences. Mental activity is improved by thyroid extract; but, on the other hand,

* Read at the Sixty-ninth Annual Meeting of the Canadian Medical Association, Section of Medicine, at Halifax, N.S., June 23, 1938.

excessive mental activity is thought to precipitate hyperthyroidism. Metabolism of proteins, fats, and carbohydrates, gaseous exchange, and water balance are all increased by the thyroid hormone. Thyroid extract also acts on tissues producing an increased rate of cell differentiation, in contrast to the pituitary which hastens cell multiplication. Anæmia occurs in hypothyroidism, probably because of decreased oxygen consumption and consequently a decreased need for red cells to carry this gas.

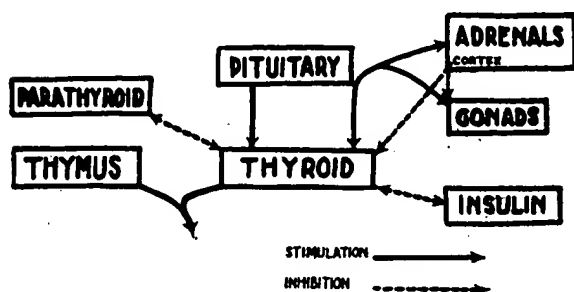


Fig. 1

The inter-relation of the thyroid and other endocrine glands is acknowledged. In one association they may be complementary, while in another they may be opposed. The pituitary gland produces a thyrotropic hormone which stimulates thyroid activity, resulting in hyperplasia of the thyroid, increased metabolism, excretion of calcium and creatinine, and an increased level of the blood iodine. Collip has described an anti-hormone about which others disagree. The thyroid has a reciprocal influence upon the adrenals and gonads which may be direct, or, more probably, indirect through the pituitary gland. Enlargement of the thyroid gland occurs with increased demands made upon it during puberty, menstruation, pregnancy, and the menopause. The adrenal cortex has, however, an inhibitory effect upon thyroid and gonads. The thyroid supplements thymic activity. The action of insulin is antagonistic to thyroid hormone which may be due to sympathetic stimulation or to increased glycogenolysis. The relation of the thyroid to the parathyroids is antagonistic because of opposite action on the sympathetic nervous system. Thyroid increases calcium and phosphorus loss from the bones without producing increased amounts in the blood such as occurs in hyperparathyroidism. These substances are lost through the urine and faeces. This review

helps us to understand some of the remote effects of hypothyroidism.

CLINICAL FINDINGS

The presence or absence of certain clinical symptoms and signs should suggest hypothyroidism to the physician. The fact that not all are found in each case suggests a fractional loss of thyroid function. Thyroid acts principally through the sympathetic nervous system and through the other ductless glands. This vast area of influence accounts for the diverse manifestations of thyroid activity. In practice the author has found the most common symptoms of hypothyroidism to be menstrual disturbances, fatigue, and gastro-intestinal upsets. The menses are usually profuse and often irregular. The blood oestrogen, tested just after menstruation, is usually excessive. Miscarriages and sterility are suggestive findings. Fatigue and the emotional disturbances so frequently associated with it occur in about two-thirds of the cases. These patients deplete their energy quickly and complain of weakness. The commonest gastro-intestinal symptoms are constipation, usually of the spastic type, and flatulence. The appetite is usually poor. Symptoms less commonly seen are migraine headaches, drowsiness, or even undue alertness and excitability.

The physical findings are few—dry skin, with a tendency to crack, eczema, acne; dry, brittle hair, and loss of the outer third of the eyebrows. In these cases underweight is as common as obesity. Anæmia is infrequently found; reflexes with slow extension are characteristic findings but seldom elicited.

LABORATORY PROCEDURES

The estimation of the basal metabolic rate has long been used as the sole criterion for thyroid activity. This test is subject to intrinsic as well as extrinsic errors. The calculation of the surface area from height and weight alone shows an error of 15 per cent. Extrinsic factors are diet, race, climate, and emotions. It is a valuable adjunct in diagnosis and a useful check on a patient already under treatment, but it measures only oxygen consumption, which is but one part of the entire thyroid activity.

Thyroid activity influences the blood cholesterol so that the latter is high in hypothyroidism and low in hyperthyroidism. The normal

concentration ranges from 150 to 180 mg. per cent. Cholesterol metabolism is influenced greatly by other factors such as pregnancy and the ingestion of certain foods. The ratio of the ester to free cholesterol is reduced in hypothyroidism, reversing the normal ratio. This reduced ratio may be seen also in liver dysfunctions. Moelig and Ainslie¹² believe that cholesterol metabolism is controlled through the pituitary gland, and the study of blood cholesterol probably reveals pituitary activity and not thyroid function. The author has not found this to be very valuable in his study of thyroid conditions.

The iodine tolerance test is analogous to the glucose tolerance test. Watson²⁰ gives 250 g. of iodine per kilogram of body weight in 15 c.c. of 0.85 per cent saline solution. Estimations of the blood iodine are made before the test and at the end of five minutes, two hours, four hours, and six hours after the ingestion of iodine. No food is given during the test. Normal persons show a retention of 9 to 23 per cent after six hours while thyrotoxic patients show none, and in hypothyroidism the percentage retention is greater than normal. The iodine-tolerance test reveals the utilization and storage of iodine within the body. Laboratory requirements, technical difficulties, and inconveniences to the patient make this test impractical as a routine procedure.

Read,¹⁴ and later other investigators, worked out formulæ based on the pulse rate and pulse pressure for estimation of the basal metabolism. Read's revised formula for basal metabolism is as follows: $(\frac{3}{4} \text{ pulse rate}) + (\frac{3}{4} \text{ pulse pressure}) - 72 = \text{B.M.R.}$ Gale's⁶ modification is as follows: $\text{B.M.R.} = \text{pulse rate} + \text{pulse pressure} - 111$. Even if basal precautions are taken in obtaining pulse rate and pulse pressure the results are open to 10 per cent error in about half of the cases. These methods are valuable bedside estimations but need to be rechecked against other tests.

Vigoroux (1888) studied the resistance of the body to a direct current, and noted changes produced by pathological conditions of the thyroid gland. Brazier¹ studied 120 cases by means of alternating current, and called the resistance factor "the impedance angle". Her conclusions were that thyrotoxicosis and thyroid feeding increase this resistance. In a later article with Grant² she showed that this

impedance angle was influenced by thyroid and thyroxin alone, and was, therefore, a more specific test than the test for the basal metabolic rate. Robertson and Wilson,¹⁶ and also Horton and his associates⁸ concluded that this test has no clinical value. The author has had no experience with this method of investigation.

The blood oestrogen normally shows a rise just before menstruation, and to a lesser extent at the mid-interval between the periods. Shute's¹⁸ test for blood oestrogen reveals excessive amounts even after menstruation is concluded in many cases of hypothyroidism. Moreover, oestrogen excess is found in many men who are hypothyroid. Indeed, the finding of an excessive amount of oestrogen at the end of menstruation, or in any man, should certainly suggest a thyroid investigation. Wheat-germ oil, thyroid, and thyroxin aid in the removal of oestrogen from the body.

The best diagnostic criterion of hypothyroidism is the patient's response to treatment with thyroid extract. Of course, the response or improvement may be secondary through some other gland. Small doses of desiccated thyroid gland, grain $\frac{1}{2}$ twice a day, will often produce the desired response, and the author has not found any ill effects from this dose if the patient is kept under observation.

MIGRAINE

Various methods of investigation and treatment have been suggested for migraine headache. Vasoconstrictor and vasodilator drugs, various hormones, drugs which act on the sympathetics and the parasympathetics, calcium and ergotamine tartrate have been used without consistent results. Christiansen⁴ considered migraine to be the result of vasomotor spasm, but did not explain the cause of this spasm. Parhon¹³ discussed the following hypotheses: (1) obstruction to duct of Munroe, (2) compression from enlarging pituitary gland, (3) allergy, and (4) endocrine imbalance. He strongly favours the last, believing that thyroid deficiency is the chief causative factor which acts through the sympathetic nervous system. Kogerer¹⁰ reports improvement in cases following thyroidectomy. Although unacquainted with the reported articles, the author saw a case (No. 1) which showed migraine at the phases of the menstrual cycle when oestrogen should be high. Oestrogen studies confirmed

the suspicion that her migraine was associated with high oestrogen. Thyroid was used with the idea of lowering the excessive oestrogen. The results were good. Wheat-germ oil also gave similar improvement although to a lesser degree. These findings suggest that high blood oestrogen may be the etiological factor. Case 3 corroborates this. Case 2 showed low thyroid, but no blood oestrogen studies were made. Further study of migraine with frequent oestrogen determinations is warranted as this would correlate the theories that hypothyroidism, ovarian dyscrasias, and pituitary dysfunctions are causative factors in the production of migraine.

ARTHRITIS

The etiology of arthritis is still obscure. Swaim and Spear¹⁹ found that 39 per cent of 200 cases studied had abnormal, usually decreased, basal metabolic rates. Klotz²⁰ reviewed the literature for the endocrine basis of arthritis and concluded that endocrine therapy, i.e., thyroid, parathyroid, and ovarian, was an important item in the management of arthritis. Case 4 suggests that thyroid deficiency background was an important factor although probably not the complete cause of her arthritis. Adequate treatment enabled her to control the progress of this disease.

ACNE VULGARIS

Bregman³ considered hyperactivity of the parasympathetic nervous system with the resultant hypersecretion of the sebaceous glands to be the basis of acne vulgaris. This dominance of the parasympathetics is seen also in hypothyroidism and probably accounts for improvement of acne vulgaris with thyroid treatment. Case 7 showed improvement with thyroid therapy. Not all cases of acne vulgaris are due to lack of thyroid, but thyroid deficiency prepares the patient for this condition.

HYPERTENSION

Hypertension, hypertrophic arthritis, and menopause often occur together. Menopause is associated with an endocrine imbalance. Hypothyroidism often occurs at this time. It seems to the author more than coincidental that essential hypertension is so often found beginning at the menopause. Case 6 showed the influence of hypothyroidism on the hyperten-

sion and the resultant improvement on thyroid treatment alone. Case 1 showed clinical improvement of a patient with early hypertension treated by thyroid therapy alone. Hall⁷ has shown arteriosclerotic change with coronary sclerosis developing after long periods of administration of acetylcholine, the active principle of the parasympathetics. In hypothyroidism the parasympathetics are dominant and this may account for the sclerotic changes associated with hypertension.

FATIGUE

Fatigue is the most frequently found symptom of hypothyroidism. Early fatigability, it is true, occurs in cases of both hyper- and hypothyroidism although from opposite causes. Thyroid deficiency slows up cellular metabolism so that there is low reserve of function in every organ. Much mental sluggishness and confusion and many emotional upsets are primarily the result of hypothyroidism and secondarily associated with psychological phenomena. These symptoms are shown in all but cases 1 and 4 of the appended case reports.

GROWTH

As far as our present knowledge is concerned, growth is controlled chiefly by the secretion of the acidophile cells of the pituitary gland. This hormone of the pituitary chiefly stimulates growth of skeleton and muscles, but also all the organs to a lesser degree. It produces an increase in the number of cells, while thyroid extract increases the rate of cell differentiation. Each cell of the body has an inherent power to grow and reproduce itself. Thymus, in some way, controls growth. The sex hormone is antagonistic to the growth hormone, and when both are injected it will nullify the effect of the growth hormone. Cancer is probably the result of imbalance of growth factors. Case 8 showed a lack of both the sex and growth hormones. Thyroid extract alone accelerated growth and sexual activity probably by means of pituitary changes.

SEXUAL MANIFESTATIONS

Thyroid extract acts directly as well as indirectly on the gonads, especially through the pituitary gland. As the result of hypothyroidism many sexual manifestations occur, such as menorrhagia, impotence, sterility, repeated abortions, or premature labour. Case 1, 2, 3,

4, 6, 7 show menorrhagia as a prominent symptom. This symptom alone should suggest lack of thyroid to the alert physician. Shute¹⁸ strongly urges more attention to this relationship of thyroid lack to menorrhagia.

CASE 1

Miss S.S., aged 50, single, nurse. Hemicranial pre- and intra-menstrual and mid-interval headaches for two to three days over a period of 30 years. "Keyed-up" and nauseated with these headaches. She had had nasal operations and dental extractions for this condition. Menses were regular and profuse.

Examination revealed blood pressure 160/114 without demonstrable cardiac enlargement, but early arteriosclerotic retinal changes, and uterine fibroids. Hemoglobin 77 per cent. Basal metabolic rate 2 plus. Blood estrogen was increased above normal at the time of the headache both just before and in the mid-period, but was negative at other periods.

Thyroid extract (P.D. & Co.), grain 1 daily for one month, gave almost complete relief of migraine, reduced the menstrual flow to about one-half, and the blood pressure became 156/86. Later she developed signs of hyperthyroidism and the thyroid was reduced to half a grain daily, but headaches returned. We gave wheat-germ oil (Kelly), also with great improvement although not complete relief of the condition. The blood pressure dropped from 160/114 to 152/72.

CASE 2

Mrs. D.G.S., aged 48, married, housewife, came in because of dizziness, fatigue and weakness. There was a history of typical migraine headache associated with profuse menses for years. Examination was essentially negative. The basal metabolic rate was minus 13.

She used thyroxin, grain 1/80, daily with complete relief of the headache and reduction of menstrual flow. Dizziness and weakness have disappeared. The patient discontinued thyroxin and had a return of the migraine. We gave thyroid extract (P.D. & Co.), grain 1, daily with complete relief.

CASE 3

The chief complaints were fatigue, lassitude, and mental confusion for over ten years, menstrual hemicranial headaches with nausea. Menstruation was every three weeks at 13 years and gradually became continuous so that hysterectomy was done at the age of 35. Many "colds"; some allergic manifestations; moderate flatulence; marked constipation.

Physical examination showed a diffusely enlarged thyroid gland and three abscessed teeth. The basal metabolic rate was minus 30. Blood estrogen was excessive.

The headaches disappeared, fatigue and mental confusion showed marked improvement on thyroid extract (P.D. & Co.), grains V, daily.

CASE 4

Mrs. E.B., aged 38, married, housewife. There had been gradual onset of arthritis in various joints for two years, worse just before menstruation. She had had tonsillectomy and some teeth removed. Chronic constipation; insomnia; moderate menorrhagia.

Physical examination showed marked swelling in various joints, with pain and crepitation on movement. A thyroid adenoma, one-half inch in diameter, was present. Hemoglobin 65 per cent. Skin dry and scaly; hair dry and brittle. The blood estrogen was normal. A basal metabolic rate was not taken.

On thyroid extract (P.D. & Co.), grains V daily, iron and a mild laxative for two months her general health improved, her skin became soft and moist, and the hair would retain a wave. Hemoglobin 85 per cent. There was a marked improvement in the amount of

swelling in the joints and a decreased amount of pain. The menstrual flow was decreased. While there still is evidence of arthritis, no premenstrual flare-up has occurred.

CASE 5

Mr. F.P., aged 35, married, tanner. He had been previously well. For 18 months he had complained of undue fatigue, irritability, poor memory, with curious subjective sensations. There was a loss in weight of 22 pounds.

Examination was essentially negative. The basal metabolic rate, minus 24.

We gave thyroid (P.D. & Co.), grains IVs daily for six weeks without any improvement and the basal metabolic rate was minus 15. We changed to thyroxin (Squibb), grain 1/80, daily. After one month's treatment he wanted to go back to work. He has been feeling well and employed regularly at hard labour for two years. His basal metabolic rate remained at minus 15 per cent.

CASE 6

Miss M.A., aged 28, single, unemployed. She developed slowly as a child and was recognized as a hypothyroid problem at 12 years. She took a small dose of thyroid until one year ago with some results, and since stopping it has become more sluggish mentally and physically. She developed "boils". She came into hospital because of oedema, especially about the face, headache, dyspnoea, weakness, and general malaise. Her menses have been irregular and excessive in amount.

The physical examination showed marked oedema; skin dry and coarse; blood pressure 185/140; reflexes of hypothyroid type. Urine analyses showed albumin with a few casts and red blood cells. Non-protein nitrogen and creatinine were normal but the Rowntree test was very low. The specific gravity volume test showed a fixed specific gravity, with equal amounts in the day and night. The urea-clearance test was 49.6 per cent normal; the iodine tolerance test showed 40 per cent in blood after six hours. The blood cholesterol was 181 mg. per cent. The basal metabolic rate was minus 21 per cent.

Placed on thyroid extract (P.D. & Co.), grains IVs daily, she showed marked improvement. After two months on this treatment she was remarkably improved physically and mentally, but her kidney function tests were about the same; albumin, grade +, but no red blood cells or casts. The basal metabolic rate was plus 2. The blood pressure was 144/98.

CASE 7

Miss M.M., aged 19, single, had had acne for years, which was worse before menstruation. She had had profuse and frequent menses for three months. She was always fatigued, had had insomnia for five years, and was nervous and emotional.

Physical examination was negative except for acne of face and chest. Hemoglobin 75 per cent. Blood estrogen excessive after end of menstruation. There was marked improvement in every way under the use of thyroid extract (P.D. & Co.), grain 1 daily.

CASE 8

W.L., aged 17, single, student. He was the largest of triplets, with normal growth until 11 years. There had been no gain in height since, but he had gained about 20 pounds. Since 14 years had been drowsy and always tired. The other living triplet is of normal size with development of pubic hair, slight beard, and sexual feelings.

This lad weighed 93 pounds and was 4 feet 11 1/4 inches tall. Penis and testes corresponded to size and not to age; no pubic or body hair. The basal metabolic rate was plus 7 per cent. Low sugar-tolerance curve. Blood estrogen, negative. The sella turcica was normal.

He was given thyroid extract (P.D. & Co.), grains $1\frac{1}{2}$, daily and began to gain in strength and weight within a month. Within three months he showed signs of pubic hair, sexual feelings, eight pounds increase in weight, and a growth of 1 inch in height.

SUMMARY

Many patients who could be helped by thyroid therapy are not recognized as hypothyroid. Standard textbooks subdivide hypothyroidism into myxœdema and cretinism, and refer to the basal metabolic rate as the significant diagnostic criterion. However, there are other important manifestations of hypothyroidism and methods of investigation based upon recent advances in the knowledge of the physiology of this gland. Endocrine factors are important in migraine, arthritis, acne vulgaris, hypertension, fatigue, growth and sexual disturbances, as these cases show.

REFERENCES

1. BRAZIER, M. A. B.: An electrical method for use in diagnosis of diseases of the thyroid gland, *The Lancet*, 1933, 2: 742.
2. BRAZIER, M. A. B. AND GRANT, F. M.: The relation of impedance angle for thyrotoxicosis to changes in basal metabolic rate, *The Lancet*, 1934, 1: 125.
3. BREGMAN, A.: New conceptions of the etiology and pathogenesis of acne vulgaris, *Arch. Dermat. & Syph.*, 1937, 36: 758.
4. CHRISTIANSEN, V.: Contributions à la patho-physiologie de la migraine, *Acta Psychiat. et Neurol.*, 1937, 12: 45.
5. COLLIP, J. B.: The anterior pituitary gland and its neuro-endocrine relationships, *Trans. Am. Neurol. Ass.*, 1935, 61: 7.
6. GALE, A. M. AND GALE, C. H.: Estimation of the basal metabolic rate, *The Lancet*, 1931, 1: 1287.
7. HALL, G. E.: Experimental heart disease, unpublished paper presented before American College of Physicians, New York City, 1938.
8. HORTON, J. W., VAURAVENSWAAY, A. C., HERTZ, S. AND THORN, G. W.: The clinical significance of electrical impedance determination in thyroid disorders, *Endocrinology*, 1936, 20: 72.
9. KLOTZ, H. P.: Existe-t-il un rhumatisme endocrinien? *Gaz. Méd. de France*, 1935, 44: 935.
10. KOGERER, H.: Migraine und Schilddrüse, *Wien. klin. Wochenschr.*, 1937, 50: 307.
11. LUNDE, G.: The geochemistry of iodine and its circulation in nature, *Chem. Rev.*, 1929, 6: 45.
12. MOELIG AND AINSLIE: (Wolf, W., *Endocrinology in Modern Practice*, Saunders, Phila., 1937, pp. 859).
13. PARHON, C. I.: Sur le traitement de la migraine, *Paris Méd.*, 1936, 150: 412.
14. READ, J. M.: Correlation of basal metabolic rate with pulse rate and pulse pressure, *J. Am. M. Ass.*, 1922, 78: 1887.
15. READ, J. M.: Basal pulse rate and pulse pressure changes accompanying variations in the basal metabolic rate, *Arch. Int. Med.*, 1924, 34: 553.
16. ROBERTSON, J. D. AND WILSON, A. T.: A combined study of the basal metabolism and impedance angle in thyrotoxicosis and myxœdema, *The Lancet*, 1934, 2: 1158.
17. SHUTE, E. V.: Resistance to proteolysis found in the blood serum of aborting women, *J. Obst. & Gyn. Brit. Emp.*, 1935, 42: 1071.
18. *Idem*: Menorrhagia and its modern treatment, *Canad. M. Ass. J.*, 1936, 35: 622.
19. SWAIM, L. T. AND SPEAR, L. M.: Studies of basal metabolism in chronic arthritis, *Boston M. & S. J.*, 1927, 198: 350.
20. WATSON, E. M.: An iodine tolerance test for investigation of thyroid function, *Endocrinology*, 1936, 20: 358.

CHORIONEPITHELIOMA FOLLOWING ECTOPIC GESTATION*

By W. A. DAFOE, F.R.C.S.(C.), M.C.O.G.

Toronto

THE possible growth of a chorionepithelioma as a sequel of hydatidiform mole has long been noted, but there has been a wide variation in the published statistics of the incidence of this complication. This variation ranges from 1 per cent (Novak) to 44 per cent (Pallasson and Violet). Brews,¹ in reporting 72 cases of hydatidiform mole in the London Hospital from 1912 to 1935, found 6 cases of chorionepithelioma (8.3 per cent). Sherman² found one case following 78 hydatidiform moles (1.3 per cent). Schumann and Voegelin³ reported 78 cases of mole with 8 followed by chorionepithelioma (10 per cent). These and other reports would lead one to believe that the incidence of chorionepithelioma following hydatidiform moles is probably less than 10 per cent. This tumour is found, of course, after full-time pregnancies and abortions, and occasionally in a teratoma of the

male sex gland. It has also been reported in a few cases of both sexes where a primary origin could not be demonstrated in the reproductive system.

The variation in the histological picture of the cellular trophoblastic layer appears to control to a great extent the clinical course of a chorionepithelioma. Marchand (1905) recognized and reported on two types, i.e., typical and atypical. In 1910 Ewing⁴ in his clear-cut manner, divided these chorionic tumours into three grades, and showed that there was a definite variation in their degree of malignancy. If Ewing's classification were carefully understood and followed possibly the figure for the incidence of the malignant variety would decrease. However, from various reports of histological and clinical studies, there still appears to be an unpredictable prognosis associated with this tumour. A biological estimation of the gonadotropic hormone in the urine is of inestimable value as confirmatory evidence in the diagnosis of chorionepi-

* A paper read at the Annual Meeting of the Canadian Gynaecological Travel Society, Toronto, October 15, 1938.

Peripheral neuropathy in hypothyroidism – an association with spurious polycythaemia (Gaisbock's syndrome)¹

Jane Martin MB BCH

G H Tomkin MD FRCP

Michael Hutchinson MB MRCP

Adelaide Hospital, Dublin 8, Eire

Summary: The neurological complications of hypothyroidism, including dementia, cerebellar ataxia, myopathy and entrapment neuropathy, are well recorded, but peripheral neuropathy has rarely been documented (Swanson *et al.* 1981). In this paper two patients are described who developed myxoedema and peripheral neuropathy. The first patient had a very rapid onset of myxoedema, and during observation he developed spurious polycythaemia (Gaisbock's syndrome) over a period of nine days.

Case reports

Case 1: A 56-year-old engineer presented in July 1980 with a five-week history of severe diarrhoea. On examination, he was slightly wasted with moderate proximal weakness. He had a coarse tremor which persisted after therapy, and was probably due to anxiety. No lid retraction, exophthalmos or goitre was observed. Pulse rate was 90/min and blood pressure 170/60 mmHg. T₄ was raised at 312 nmol/l (normal range 50–157), T₃ was raised at 7.4 nmol/l (normal range 1.5–3.0) and ¹³¹I T₄ uptake was raised at 66% (normal range 36–46%). Thyroglobulin antibodies were negative. Haemoglobin was 13.8 g/dl and haematocrit 0.398. Thyroid scan showed a homogeneous pattern.

A diagnosis of thyrotoxicosis was made, and he was treated with carbimazole, initially with improvement of all symptoms. Three months later he again became thyrotoxic (T₄ 223 nmol/l). He was treated with a 20 mCi dose of radioactive iodine, and the carbimazole was tailed off. He again improved, but three months after the radioactive iodine treatment he became very rapidly myxoedematous. T₄ dropped to 19 nmol/l and TSH rose to 47 mu/l (normal < 7.5 mu/l). Haemoglobin was 13.3 g/dl and haematocrit 0.398. He was started on L-thyroxine, but nine days later he looked ill and polycythaemic. He complained of cramps and paraesthesia in the hands and feet with clumsiness in fine movements and unsteadiness when walking. Knee and ankle reflexes were absent, and pinprick sensation was diminished in a glove and stocking distribution. Nerve conduction studies (Table 1) showed abnormalities consistent with a sensorimotor neuropathy of axonal type. The haemoglobin was 19.4 g/dl and haematocrit 0.560. Red cell volume was normal at 35.3 ml/kg (normal range 30 ± 5 ml/kg), but plasma volume was decreased at 35.45 ml/kg (normal 40–50). Serum urea, electrolytes and albumin levels were normal.

Other tests to investigate the cause of the neuropathy, including blood glucose, serum B₁₂ and serum folate levels, urinary porphobilinogen, auto-antibody screen and blood immunoglobulins, were all normal.

Six months after the onset of the myxoedema there had been some improvement in electrophysiological tests (Table 1), but 18 months after the onset of myxoedema the patient still has mild sensory symptoms, and he does not feel fit to return to work. Haemoglobin has remained at around 17 to 18 g/dl and haematocrit at 0.48 to 0.52.

Case 2: A 62-year-old woman presented with a two-year history of slowly progressive numbness of the soles of her feet followed by increasing unsteadiness. For five years her voice had been hoarse and she had had cold intolerance. Recently her skin had become dry.

¹Accepted 26 October 1982

Table 1. Nerve conduction studies

	Case 1			Case 2		
	At presentation	6 months later	Normal	At presentation	18 months later	Normal
Right sural sensory action potential:						
Amplitude (μ V)	8	10	> 6.1	—	4	> 4.2
Latency (msec)	5.6	5.8	< 4.7	—	7	< 4.9
Right median sensory action potential:						
Amplitude (μ V)				5	10	9–45
Latency (msec)				5.1	4.7	2.5–4.0
Right lateral popliteal nerve:						
Distal motor latency (msec)	4.7	5	< 7.0	5.8	5.4	< 7.0
Motor conduction velocity (m/sec)	31	42	36–64	44	44	36–64
Muscle action potential (ankle) (mV)	0.8	5	> 3.0	1.9	4	> 3.0

On examination, she appeared myxoedematous. She had weakness and impaired light touch and pinprick sensation in both feet. The gait was mildly ataxic. The thyroid gland was firm and slightly enlarged. The T4 was very low (2 nmol/l), as was the free thyroxine index (2.0; normal 8–28 pmol/l). The TSH was raised (> 50 mu/l). Serum B₁₂ and folate were normal. Nerve conduction studies (Table 1) showed abnormalities consistent with an axonal neuropathy.

The patient was treated with L-thyroxine. Five months later the serum thyroxine level (107 nmol/l) and free thyroxine (26.2 pmol/l) were normal, and the TSH level had dropped to 3.0 mu/l. The neuropathy had subjectively improved, but some distal sensory abnormalities were still present.

Nerve conduction studies 18 months after treatment (Table 1) demonstrated return to normal of the motor components, but the sensory action potential latencies in both the right median and right sural nerves were still increased.

Discussion

These two patients presented with a mild peripheral neuropathy predominantly sensory in type in association with hypothyroidism. No other cause for the neuropathy was found, and when the hypothyroidism was treated, the neurological signs improved. However, this improvement was not complete; both patients still have residual disability 18 and 36 months respectively after treatment was commenced.

Approximately 80% of patients with hypothyroidism complain of hand paraesthesia, usually due to median nerve compression in the carpal tunnel. Symmetrical sensorimotor neuropathy has been described only very rarely. Nickel *et al.* (1961) studied 25 patients with primary myxoedema: 60% had diminished peripheral sensation and 28% had objective muscle weakness. Deep tendon reflexes were absent in only one patient who was in coma. Histology of the peripheral nerves demonstrated an oedematous infiltration of the endo- and perineurium. In three cases there were degenerative changes of the myelin sheaths and axis cylinders.

The nerve conduction abnormalities in the present study, which showed absence or reduction of sensory action potentials, markedly reduced muscle action potentials and mildly prolonged latencies with mild slowing of nerve conduction velocities, are more in keeping with an axonal neuropathy than with segmental demyelination. Dyck & Lambert (1970), in an electron microscopic study of the sural nerve biopsies of two cases of hypothyroid neuropathy, demonstrated both segmental demyelination with remyelination and axis cylinder degeneration. These authors suggested that the histological findings may have resulted from either disordered Schwann cell metabolism or a disease of axis cylinders with secondary demyelination or remyelination. Shirabe *et al.* (1975) described a patient

with peripheral neuropathy who was also found to have widespread segmental demyelination.

Peripheral neuropathy is a rare complication of polycythaemia rubra vera, but secondary polycythaemia is not associated with changes in nerve conduction (Saha *et al.* 1980). We have been unable to find any reported association between myxoedema and spurious polycythaemia (an increased packed cell volume with a normal red cell mass), although there is a report of erythrocytosis (defined as a condition characterized by idiopathic proliferation of the red cell line alone) associated with a thyroid papillary carcinoma (Dallera & Gamoletti 1980). Remission in this case followed the removal of the tumour.

Our first patient is very unusual in developing polycythaemia whilst under observation. Only one other patient has been observed to develop the condition, and this was over a five-month period (Ramsay 1978). The rapid onset of the clinical features of polycythaemia with the sudden rise in haemoglobin and haematocrit over nine days was striking and remains unexplained, but may have been due to sudden decrease in plasma volume. The blood pressure is often found to be raised in these patients, but our patient did not have hypertension. The outlook for patients with this condition is not clear. Stefanini *et al.* (1978) suggested that there is a high incidence of coronary disease, cerebrovascular accidents and thromboembolic complications. Our patient so far has avoided any of these complications.

References

- Dallera F & Gamoletti R (1980) *Tumori* 66, 273-275
Dyck P J & Lambert E H (1970) *Journal of Neuropathology and Experimental Neurology* 29, 631-658
Nickel S N, Frame B, Bebin J, Tourtellotte W W, Parker J A & Ross Hughes B (1961) *Neurology (Minneapolis)* 11, 125-137
Ramsay L E (1978) *British Medical Journal* i, 1251-1252
Saha P K, Shenoy K T & Ravindran M (1980) *Indian Journal of Medical Research* 71, 801-805
Shirabe T, Tawara S, Terao A & Araki S (1975) *Journal of Neurology, Neurosurgery and Psychiatry* 38, 241-247
Stefanini M, Urbas J V & Urbas J E (1978) *Angiology* 29, 520-533
Swanson J W, Kelly J J & McConahey W (1981) *Mayo Clinic Proceedings* 56, 504-512

Lesson of the Week

EXHIBIT F

Hypothyroidism presenting with hyperprolactinaemia

C G SEMPLE, G H BEASTALL, G TEASDALE, J A THOMSON

Now that there is a specific radioimmunoassay for detecting prolactin¹ hyperprolactinaemia is recognised more frequently in women in whom it usually presents as subfertility, amenorrhoea, or galactorrhoea. It occurs less often in men with impotence and subfertility. Although hyperprolactinaemia is often due to a pituitary tumour that secretes prolactin it also occurs because of conditions such as phenothiazine or other drug therapy, polycystic ovarian disease, and disruption of the hypothalamic-pituitary dopaminergic pathways by inflammatory or neoplastic infiltrates. Thyrotrophin releasing hormone raises the serum prolactin concentration by stimulating pituitary lactotrophs,² and hypothyroidism is yet another cause of hyperprolactinaemia.³ The degree of hyperprolactinaemia seems to be proportional to the severity of hypothyroidism, so that mildly hypothyroid subjects often have a normal serum prolactin concentration.⁴

We report on six patients with hyperprolactinaemia and associated syndromes, who were initially suspected of having a tumour that secreted prolactin but the results of endocrinological tests showed that they had hyperprolactinaemia induced by hypothyroidism.

Case reports

Case 1—A 33 year old woman had had secondary amenorrhoea for 18 months. Her serum prolactin concentration had been raised at 420 mU/l and 590 mU/l (normal range 60-360 mU/l). On examination she was clinically euthyroid but because both her father and sister had hypothyroidism this diagnosis was considered and confirmed by thyroid function testing (table). She was given thyroxine treatment, and her serum prolactin concentration fell to normal soon after. She started to menstruate

Hypothyroidism may mimic syndromes that are attributed to prolactin secreting pituitary tumours

regularly and conceived six months after starting thyroxine treatment.

Case 2—A 25 year old woman was referred as a "classic" case of the galactorrhoea-amenorrhoea syndrome. She had lactated for two years after her last pregnancy, she menstruated infrequently, and her serum prolactin concentration had varied from 800 to 1900 mU/l. Clinical examination and the results of biochemical tests showed that she was hypothyroid, and she was treated with thyroxine. She began to menstruate regularly and the galactorrhoea disappeared. Her serum prolactin concentration was moderately raised (400-700 mU/l) for two years despite high normal concentrations of thyroxine and suppressed serum thyroid stimulating hormone concentrations, but after three years it was normal.

Case 3—A 24 year old woman had been referred to a neurosurgeon because of hyperprolactinaemia (580-1300 mU/l), oligomenorrhoea, and primary infertility. A clinical examination and the results of biochemical tests showed that she was hypothyroid. She was given thyroxine and her menses rapidly became regular. Despite being clinically euthyroid and having high normal serum thyroxine concentrations with suppressed serum thyroid stimulating hormone concentrations her serum prolactin concentration was raised (400-600 mU/l) for one year after treatment, but six months later it was normal though her infertility persisted.

Case 4—A 33 year old woman received thyroxine 0.1 mg/day for hypothyroidism. Because she had a two year history of amenorrhoea, galactorrhoea, and hyperprolactinaemia (900-1360 mU/l) she had been referred to a neurosurgeon. The results of endocrine assessment showed clinical and biochemical under-replacement with thyroxine. Pituitary tomography, cavernous sinogram, and computed tomography of her pituitary fossa suggested that she had an intrasellar pituitary tumour. The thyroxine dosage was increased, and she became euthyroid. A regular menstrual cycle rapidly returned and galactorrhoea disappeared. Over six months her serum prolactin concentration fell to normal, and repeat computed tomography was normal. Eighteen months after referral she conceived and delivered a healthy child after a normal pregnancy.

Case 5—A 40 year old woman who gave an eight year history of galactorrhoea was referred to a neurosurgeon because of hyperprolactinaemia (800-1270 mU/l) and he referred her for endocrine evaluation. She had had a partial thyroidectomy 13 years before for dysmorphogenetic goitre and had been prescribed replacement treatment. Nevertheless, clinical examination and biochemical test results showed that she was

Results of biochemical tests in the six patients with hypothyroidism

Case No	Thyroxine (normal 55-144 nmol/l)	Triiodothyronine (normal 0.9-2.8 nmol/l)	Thyroid stimulating hormone (normal 0-8 mU/l)	Peak prolactin (normal 0-360 mU/l)
1	23	1.5	>25	590
2	Undetectable	0.7	>50	1900
3	Undetectable	0.9	>50	1300
4	69	0.9	>50	1360
5	27	Undetectable	>50	1270
6	15	1.1	>50	3800

University Department of Medicine and Department of Pathological Biochemistry, Glasgow Royal Infirmary and Institute of Neurological Sciences, Southern General Hospital, Glasgow

C G SEMPLE, BA, MRCP, medical registrar

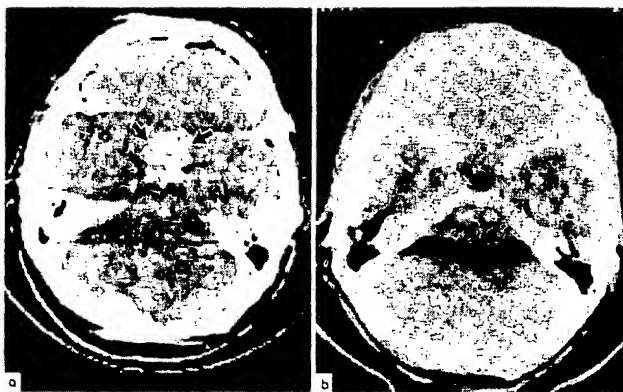
G H BEASTALL, BSC, PHD, top grade biochemist

G TEASDALE, MRCP, FRCS, professor of neurosurgery

J A THOMSON, MD, FRCP, reader in medicine

hypothyroid, and she had not taken her treatment. Thus, galactorrhoea and hyperprolactinaemia continued.

Case 6—A 53 year old man, who was known to have congenital hypothyroidism, had his eyesight checked and was found to have bilateral optic atrophy. The results of a detailed ophthalmological assessment confirmed this, showing bitemporal hemianopia. Computed tomography showed a large pituitary tumour with suprasellar extension (figure a). His serum prolactin



Computed tomography of the pituitary in the patient in case 6, showing (a) an enhanced lesion filling the suprasellar cistern; (b) disappearance of the lesion with reduced density in the pituitary fossa, suggesting intrasellar cisternal herniation.

concentration was raised (3800 mU/l); he had not taken replacement treatment for many years. He was of short stature and had dry skin but otherwise seemed clinically euthyroid. Nevertheless, the results of laboratory findings showed hypothyroidism. He was treated with gradually increasing doses of thyroxine, and prolactin concentrations returned to normal. His visual fields improved though optic atrophy persisted. A repeated computed tomographic scan showed that the suprasellar extension had resolved (figure b).

Comment

Although it is well known that menorrhagia is a common feature of hypothyroidism in women during the reproductive years it is less well recognised that hypothyroidism may lead to amenorrhoea or oligomenorrhoea sometimes associated with hyperprolactinaemia. This is clearly shown in the patients in

cases 1 to 4. Our findings do not support the view of Bigo *et al*⁴ that only severe hypothyroidism raises the serum prolactin concentration. The patient in case 1 had hyperprolactinaemia despite being clinically euthyroid, and the patient in case 4 had a raised serum prolactin concentration despite normal concentrations of thyroxine and triiodothyronine.

Now that prolactin secreting pituitary tumours are diagnosed more often and can be successfully managed either by microsurgery or by dopamine agonist treatment there is a danger that failure to recognise hypothyroidism will lead to inappropriate treatment. Hypothyroidism is likely to be overlooked when the radiological appearances (cases 4 and 6) or a visual field defect (case 6) indicate that the patient has an expanding tumour in the region of the sella. Pituitary enlargement in hypothyroidism is probably due to hypertrophy or hyperplasia of the thyrotrophs,^{4,5} or both. It is important to recognise these "feedback tumours" because they are readily reversed⁶ (case 6). Neurosurgery has appreciable risks when performed on a hypothyroid patient.

Despite the rapid correction of thyroid deficiency, the prolactin status of three of our patients (cases 2 to 4) returned only slowly to normal. This suggests either that the pituitary lactotrophs have become unusually sensitive to thyrotrophin releasing hormone or that they have developed a resistance to the usual modulating influences and continue to hypersecrete prolactin for some time after correction of the hypothalamic-pituitary-thyroid axis.

It is essential that thyroid function tests are performed on every patient with hyperprolactinaemia.

Correspondence should be addressed to: Dr C G Semple, University Department of Medicine, Royal Infirmary, Glasgow G4 0SF.

References

- Hwang P, Guyda H, Friesen H. A radioimmunoassay for human prolactin. *Proc Natl Acad Sci USA* 1971;68:1902-6.
- Friesen H, Guyda H, Tyson JE, Barbeau A. Functional evaluation of prolactin secretion: a guide to therapy. *J Clin Invest* 1972;51:706-9.
- Onishi T, Miyai K, Aono T, *et al*. Primary hypothyroidism and galactorrhoea. *Am J Med* 1977;63:373-8.
- Bigos ST, Ridgway EC, Kourides IA, Maloof F. Spectrum of pituitary alterations with mild and severe thyroid impairment. *J Clin Endocrinol Metab* 1978;46:317-25.
- Jawadi MH, Ballonoff LB, Stears JC, Katz FH. Primary hypothyroidism and pituitary enlargement. *Arch Intern Med* 1978;138:1555-7.
- Tolis G, Hoyte K, McKenzie JM, Mason B, Robb P. Clinical, biochemical, and radiological reversibility of hyperprolactinaemic galactorrhoea-amenorrhoea and abnormal sella by thyroxine in a patient with primary hypothyroidism. *Am J Obstet Gynecol* 1978;131:850-2.

(Accepted 1 December 1982)

What is the nature of "gippy tummy" and is it avoidable?

Diarrhoea, sometimes with associated constitutional disturbance, may afflict any traveller, but it is commoner in countries with generally lower standards of hygiene where it is known by a variety of affectionate and colourful cognomens apart from gippy tummy—Aden gut, Aztec two step, Basra belly, Delhi belly, Hong Kong dog, Montezuma's revenge, Tokyo trots, turista, etc. In medical publications it is called traveller's diarrhoea and is due to an enteric infection with one of a variety of organisms. Standard enteric pathogens (salmonellae, shigellae, campylobacter, giardia lamblia, or viruses) are sometimes responsible, but in most victims enterotoxigenic *Escherichia coli* is the cause. Some individuals seem more prone to the condition than others, for unknown reasons. Common sense measures to avoid infection seem wise—avoidance of salads, unpeeled fruit, and ice cream and care about sources of water—though no firm evidence

exists to show their value. The liberal use of alcohol to stimulate gastric acid secretion has many enthusiastic proponents but no controlled trial to support it. The use of clioquinol (enterovioform) affords no protection. Antibiotic prophylaxis, however, does diminish the risk. Streptotriad (one tablet twice daily for one week and one tablet daily thereafter)¹ and doxycycline 100 mg daily² both protect travellers against diarrhoea for as long as the drug is taken. Antibiotics are only justified when the likelihood of infection is sufficiently high (Mexico or Asia, for example) or if the inconvenience of an attack would be great—for instance, for a competitor in an international athletic competition.—JOHN R BENNETT, consultant physician, Kingston upon Hull.

¹ Turner AC. Traveller's diarrhoea: a survey of symptoms, occurrence, and possible prophylaxis. *Br Med J* 1967;iv:653-4.

² Sack RB, Froehlich JL, Zulich AW, *et al*. Prophylactic doxycycline for traveller's diarrhoea. *Gastroenterology* 1979;76:1368-73.

Morphometric study on the uterine horn and thyroid gland in hypothyroid, and thyroxine treated hypothyroid rats

I. INUWA AND M. A. WILLIAMS

Department of Biomedical Science, University of Sheffield, UK

(Accepted 12 September 1995)

EXHIBIT 6

ABSTRACT

A wide range of reproductive disorders such as irregular menstruation and frank infertility is found in women with hypothyroidism. Most research done on these patients has focused on steroid and gonadotropin hormone profiles, whilst there has been little work on uterine morphology. Studies on hypothyroid animals have also demonstrated increases in fetal wastage, but there have been few studies of uterine structure in the hypothyroid rat. The present study has used hypothyroid Wistar rats as a model for investigating the effects of hypothyroidism on uterine structure. Three groups of Wistar rats were studied. One was made hypothyroid with methimazole (MMI), the 2nd was also made hypothyroid with methimazole but in addition the rats were simultaneously given daily thyroxine intraperitoneally (MMI + T₄), and the 3rd was an untreated euthyroid group (control). Daily vaginal smears were obtained from rats in all 3 groups. All rats were aged 6 wk at the start of treatment and were killed after a further 6 wk. Uterine horns were removed and studied. Systematic random transverse sections were obtained from the proximal, middle, and distal regions of the horn and subjected to morphometric analysis. Difference between regions was assessed using 2-way analysis of variance. Absolute volume of endometrium in the uteri of hypothyroid rats was reduced by 45.1% ($P < 0.05$), whilst that of the muscle layer was decreased by 33.6% ($P < 0.05$). The cross-sectional area and absolute volume of the uterine horns were also reduced in hypothyroid animals ($P < 0.05$). In hypothyroid rats given thyroxine (MMI + T₄) all variables increased significantly above those of hypothyroid rats. These changes suggest that hypothyroidism has an effect on uterine structure, which demonstrably improves under exogenous thyroxine administration. The observed structural changes might well play a significant role in the reproductive difficulties observed during hypothyroidism.

Key words: Infertility; endometrium.

INTRODUCTION

Hypothyroidism is a well documented cause of subfertility and debilitating menstrual disturbance in women (Hemady et al. 1978). Hypothyroid women seldom conceive and bear children (Kennedy & Montgomery, 1978; Boyland & Drury, 1979; Montoro et al. 1981). Indeed, pregnancy in hypothyroidism is so rare that it is considered a great achievement for a hypothyroid female to conceive (Balén & Kurtz, 1990). Clinical experience has shown that a wide range of menstrual disturbance is associated with hypothyroidism, ranging from total amenorrhoea to menorrhagia (Ramsay, 1986).

Even if a hypothyroid woman does conceive, the pregnancy itself is often very difficult to maintain

successfully to term without complication. This is evidenced by a high incidence of spontaneous recurrent abortion, and of still births amongst hypothyroid pregnant women (Burrows, 1972; Ritchie, 1986). Experiments have indicated that hypothyroid animals also have difficulty in maintaining pregnancy. Studies in rats artificially made hypothyroid with propyl thiouracil have revealed increases in fetal resorption and a raised mortality at birth, as compared with control animals (Krohn & White, 1950). All these findings suggest a role for thyroid hormones in conception and maintenance of pregnancy. It is still not clear at which level of the hypothalamic–pituitary–ovarian–uterine axis altered thyroid function is most strongly expressed. Most research in man has been directed at the effects of hypothyroidism on

the serum levels of gonadotropin and steroid hormones (Distiller et al. 1975; Heyburn et al. 1986; Fish & Mariash, 1988). There have been considerably fewer studies on uterine structure in this condition (Imamura, 1982).

The present study was carried out with the aim of establishing, by morphometric methods, whether (1) there is any distinction between the structure of the rat uterine horn in various regions, and, (2) if there are effects of hypothyroidism on uterine horn structure.

MATERIALS AND METHODS

Animal model

Eighteen 6-wk-old virgin female Wistar rats were used. They weighed between 150 and 200 g at the date of use. The animals were subjected to a constant cycle of 12 h light and 12 h darkness, and the temperature was maintained at 19–21 °C, with a relative humidity of 45%–55%. The rats were fed normal rat diet (Argo Foods, Penistone). Food and water were given ad libitum. At the end of 1 wk, the rats were divided randomly into 3 groups of 6 (A, B, C).

Group A (MMI) rats were made hypothyroid by replacing their drinking water with a solution of 0.02% w/v methimazole (Sigma UK), an antithyroid agent (Kirby et al. 1992; Meisami et al. 1992; Hardy et al. 1993). According to Silver & Leonard (1985), this is the minimum concentration at which thyroid activity is completely suppressed.

Group B (MMI + T4) rats were also given the same solution of 0.02% w/v methimazole in drinking water, but in addition were given a daily intra-peritoneal injection of 5 µg thyroxine (Sigma) in 0.9% NaCl and 0.01 M NaOH.

Group C (control) rats were euthyroid animals maintained on tap water. Vaginal smears were taken daily from rats in all groups to determine the stage of

oestrus cycle, whilst all rats were weighed once weekly. The start of the experiment (day 0) was when all rats in the 3 groups were in the oestrus stage. At the end of 6 wk (42 d), the control rats were in metoestrus stage. They were therefore killed 3 d later (i.e. at the oestrus stage). Treatment was started in the other 2 groups when the rats were also in oestrus. At the end of 6 wk (42 d) of treatment, hypothyroid rats were in dioestrus stage whilst thyroxine treated hypothyroid rats were in metoestrus stage. At this point, treatment was stopped, and hypothyroid and thyroxine treated hypothyroid rats were killed 3 d later when both groups were at oestrus. The oestrus cycle itself was irregular in hypothyroid rats. The rats in each group were weighed every week up to wk 6, and then on the day they were killed. A graph of the percentage of days spent at each stage of the cycle by all the rats in individual groups was drawn (see Fig. 4). At every weight measurement, the mean for each group was calculated (see Fig. 3). The length of the uterine horns of each was measured in situ before being removed, whilst the animals were alive. The 2 lobes of the thyroid gland were also removed and weighed wet to the nearest milligram, using an electronic balance (Sauter GmbH D-7470).

Tissue processing and sampling

The whole uterus was fixed in cold 4% phosphate buffered formaldehyde (pH 7.2, 380 mOsmol) for 24 h at 4 °C. From each rat one uterine horn was randomly selected. Randomness of selection was ensured as we had no idea from which side the horn came after fixation. In any case, in an earlier pilot study using a 2-way ANOVA, we had observed that there was no significant difference in the mean volume density of compartments in the different regions of the same uterine horn, or indeed between horns in the same animal (see Table 1).

Table 1. Two-way ANOVA of *V_v* measurement of uterine horn luminal epithelium between regions of the same horn in euthyroid rats

Rat	Variation between regions			Variation within region			<i>F</i>	<i>P</i>
	SS	DF	MS	SS	DF	MS		
1	2×10^{-5}	2	1.3×10^{-5}	2.7×10^{-4}	27	1×10^{-5}	0.9	0.3
2	2×10^{-5}	2	1.1×10^{-5}	5×10^{-4}	27	2×10^{-5}	0.5	0.6
3	4×10^{-5}	2	2.3×10^{-5}	8×10^{-4}	27	3×10^{-5}	0.8	0.4
4	4.6×10^{-5}	2	2.3×10^{-5}	2.7×10^{-4}	27	1×10^{-5}	2.3	0.1
5	2.6×10^{-5}	2	1.3×10^{-5}	2.7×10^{-4}	27	1×10^{-5}	1.3	0.2
6	2.6×10^{-5}	2	1.3×10^{-5}	5×10^{-4}	27	2×10^{-5}	0.7	0.5

SS, sum of squares; DF, degree of freedom; MS, mean squares; *F* = MS between regions/MS within region.

Each uterine horn was then divided into 3 equal regions by length; proximal, middle and distal. Each region was in turn cut transversely into 2 mm lengths, and after a brief wash in phosphate buffer (pH 7.2), the pieces were dehydrated through ascending concentrations of ethanol, and finally embedded in JB4 resin (Polysciences Inc.). Two blocks per region were selected randomly (by lottery) so that a total of 6 blocks was selected per rat. Ten nonconsecutive 2 μ m random transverse sections were obtained from each block on an LKB Historange 2218 microtome using Ralph glass knife (Fig. 1). Randomness of location of sections was achieved by letting the block face be at an unknown distance from the knife edge; the block was then advanced until the first section was cut. Thereafter, sample sections were selected after every 50th section. The sections were collected with forceps and flattened by transferring them onto a water bath surface at room temperature. Sections were then collected on precleaned glass slides and air-dried before being stained with acid fuchsin and toluidine blue.

The thyroid gland was processed in similar manner to the uterine horn. Serial sections of 2 μ m thickness were cut through the whole gland and 1 section was selected after every 100 sections. The 1st section was obtained by letting the block face be at an unknown distance from the knife edge, the block then being advanced until the 1st section was cut. Thicknesses of sections were accurately measured (mean thickness, $1.81 \pm 0.07 \mu$ m) with a Vickers M86 scanning micro-interferometer (Williams, 1977).

Morphometry

The absolute volume of the thyroid gland was estimated using the Cavalieri principle (Gundersen & Jensen, 1987). Each of the selected sections of the gland was projected at $\times 13$ magnification onto a sheet of white paper bearing a square lattice (square side 10 mm, equivalent to a test point area value on the sections of 0.5917 mm^2). Tracings of the outlines of the gland were made with a pencil. The area of each section was estimated and summed over all the sample sections. This area was used to estimate the absolute volume of the gland.

The sample sections of uterine horn and thyroid gland were viewed at a final magnification of $\times 100$ under a light microscope fitted with an eyepiece reticule (Graticules Ltd). The reticule had an array of test points (areal value of one point = $2.5 \cdot 10^{-3} \text{ mm}^2$). A raster of systematic random fields of view was

obtained by advancing the slide horizontally at equal intervals, beginning from an external point at which the tissue was not in view. Thereafter, the section was moved at equal intervals whilst counting the points hitting the various components of the tissue, until the opposite edge of the section was passed. The slide was moved vertically to a new alignment and the process of field placement and counting horizontally resumed moving in the opposite direction. This procedure was carried out until the whole section had been covered. The cumulative mean volume density estimates were plotted against the number of slides, so as to determine the minimum number of sections that would give a stable estimate of volume density (Williams, 1977).

Using computer software for linear measurements, the height of epithelium of thyroid follicles were measured. On the sample sections from the thyroid gland, the height of one epithelial profile was measured in a total of 100 follicles. Using the same software, the thickness of the endometrium from the luminal surface to the stroma-muscle border on the lateral sides of the horn was measured.

Using a projecting microscope, the luminal perimeter, and section profile area of uterine horn were estimated. This was carried out by projecting the sections at a final magnification of $\times 13$ onto a sheet of white paper bearing a square lattice (square side 10 mm, equivalent to a test point area value of 0.5917 mm^2). Tracings of the outlines of the lumen and of the external surface of the horn were made with a pencil. The intersections made by the luminal tracing with the test lines were used to estimate the luminal perimeter (Smith & Guttman, 1953), whilst the numbers of points overlying the horn tracing were used to estimate section profile area. An earlier pilot experiment had confirmed that there was insignificant difference in the mean transverse profile area between the 3 regions of the horn. Thus the absolute volume of each horn of the rat was estimated from the mean profile areas of sections together with the wet length of horn.

Statistical analysis

For each data set the arithmetic means, and coefficients of variation (c.v. = standard deviation as a percentage of corresponding mean) were computed. Comparison of parameters between horn sites (proximal, middle, and distal), and within animal groups, were drawn using a 2-way ANOVA (Table 1). Differences in parameters between animal groups were analysed using the nonparametric Mann-

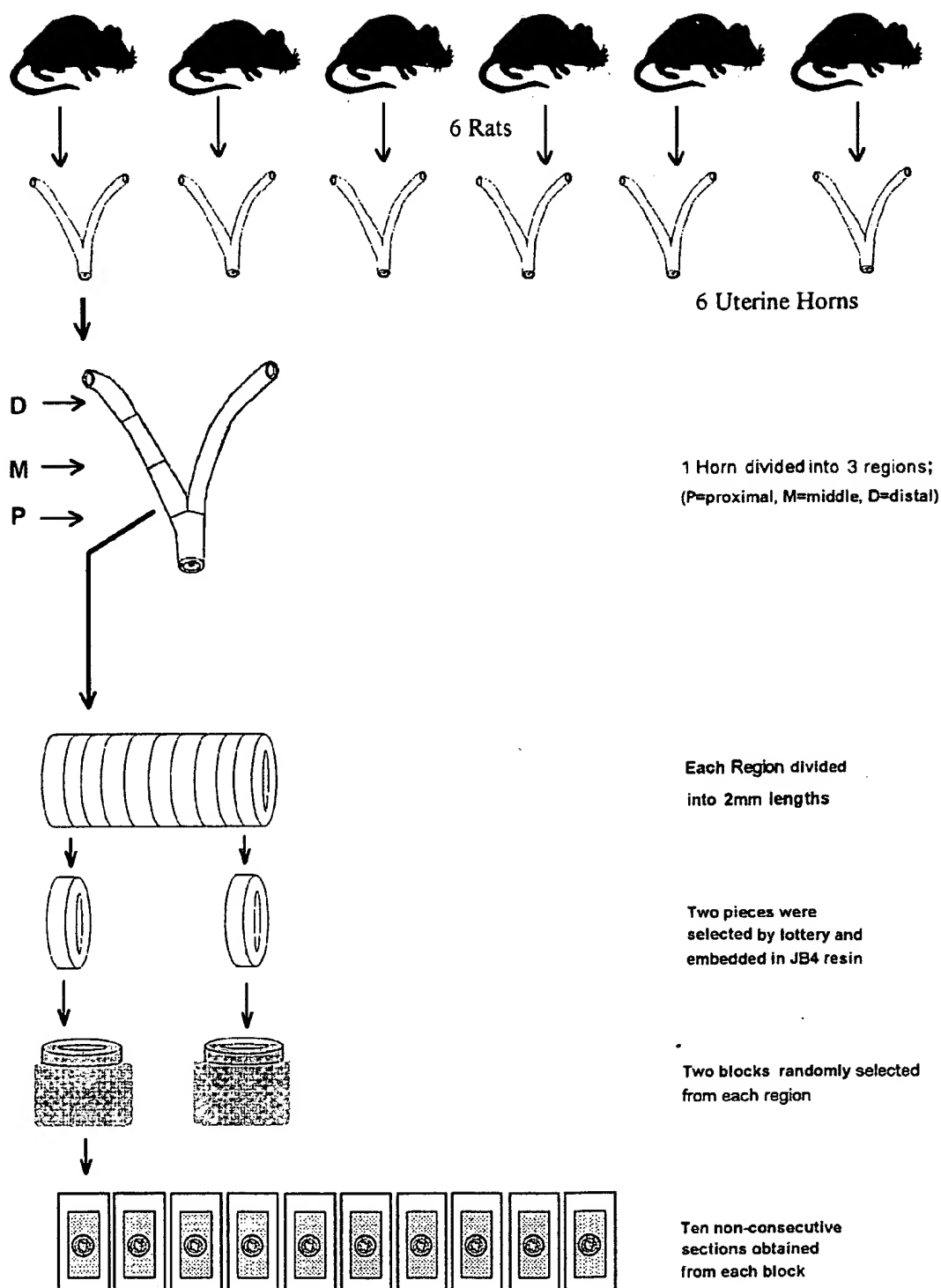


Fig. 1. Tissue sampling for morphometric study. Each uterine horn was divided into 3 equal regions, and each region further cut transversely into smaller pieces that were embedded in JB4 resin. Two blocks were randomly selected by lottery from each region making a total of 6 blocks per rat, and 10 nonconsecutive sections were obtained from each block.

Whitney U test. In each case, the null hypothesis was rejected if the probability of no difference was found to be less than 5% (i.e. $P < 0.05$). All statistical

computations were made using the statistical package Instat, version 1.15 (Graphpad Softwares, 1990) on a personal computer.

Table 2. Mean (CV%) relative and absolute volumes of different compartments of the thyroid gland in euthyroid (control), hypothyroid (MMI), and hypothyroid rats given thyroxine (MMI+T4)†

Compartment	Volume density Vv			Absolute volume (mm ³)		
	Control	MMI	MMI+T4	Control	MMI	MMI+T4
Thyroid gland	—	—	—	34.72* (8)	81.59 (5)	56.88** (8)
Epithelium	0.41* (12)	0.56 (9)	0.49** (10)	14.23* (10)	45.69 (7)	27.87** (12)
Stroma	0.36 (20)	0.39 (5)	0.38 (17)	12.5* (10)	31.82 (5)	21.61** (13)
Colloid	0.23* (10)	0.06 (10)	0.13** (21)	7.98* (12)	4.89 (8)	7.39** (13)

† Results given are group means (CV%) for 6 rats. Activity index is the ratio of volume density (Vv) of follicular epithelium to that of the lumen (colloid) of the gland. Mitotic index is the number of mitotic figures per 1000 sectioned nuclei. Control, euthyroid; MMI, hypothyroid; MMI+T4, hypothyroid rats given thyroxine; * $P < 0.05$, euthyroid vs hypothyroid; ** $P < 0.05$ hypothyroid vs hypothyroid rats given thyroxine.

RESULTS

Thyroid gland

The results of the morphological assessment of the thyroid gland are illustrated in Tables 2 and 3.

Both weight and absolute volume of the thyroid gland were increased in hypothyroid (MMI) rats. Gland weight and volume in hypothyroid rats given thyroxine (MMI+T4) were also increased, but were significantly lower as compared with the hypothyroid (MMI) rats. In hypothyroid rats the volume density and absolute volume of thyroid follicular epithelium was increased significantly as compared with those of euthyroid (control), or of hypothyroid rats given thyroxine (MMI+T4), whilst those of the lumen (colloid) were decreased significantly. The volume density of the stroma remained unchanged in all groups, although its absolute volume had increased in hypothyroid rats as a result of the overall increase in the gland volume.

Thyroid follicular epithelial height (from basement membrane to surface) increased significantly in hypothyroid rats. The epithelial height in hypothyroid rats given thyroxine (MMI+T4) was not significantly increased when compared with euthyroid rats. Numerous mitotic figures were seen in the thyroid gland of hypothyroid rats, there being significantly fewer mitotic figures in the euthyroid rats. The ratio of the volume density of follicular epithelium to that of the colloid (Activity Index) was greatly increased in hypothyroid animals. A similar ratio was obtained when absolute volumes (instead of volume density) of the 2 compartments were used (see Tables 2 and 3).

Panels A and B of Figure 2 show the structure of thyroid gland in euthyroid (control) and hypothyroid

Table 3. Morphometric indicators of thyroid function in euthyroid (control), hypothyroid (MMI), and hypothyroid rats given thyroxine (MMI+T4)†

Variable	Control	MMI	MMI+T4
Gland weight (mg)	30.8* (7)	82.5 (9)	59.75** (12)
Height of follicular epithelium (µm)	4.28* (42)	12.52 (38)	5.12** (52)
Activity index, AI (see text)	1.47* (10)	11.47 (10.7)	3.29** (18.2)
Mitotic index	0.95* (47)	16.8 (14.1)	1.65** (36.3)
Specific gravity of gland	0.901* (10)	1.03 (5.5)	1.05 (10.9)

† For explanation of abbreviations and symbols, see footnote to Table 2.

(MMI) animals. Thyroid glands in euthyroid rats have follicles of various sizes, whose walls are made up of cuboidal or squamous follicular cells, depending on the state of activity of the follicle, which surround the colloid present in the lumina. Numerous blood vessels were present in the stroma, as is typical of any endocrine gland.

In hypothyroid rats the follicular nature of the thyroid gland was disrupted. The cuboidal follicular cells had become columnar, obliterating the lumina of the thyroid follicles, and the lumen (colloid) had almost totally disappeared. There were mitotic figures amongst follicular cells, a feature not commonly seen in the gland of euthyroid animals (see Fig. 2a, b).

Changes in weights of rats and the oestrus cycle

Mean changes in weight during treatment amongst the 3 groups of rats are illustrated in Figure 3.

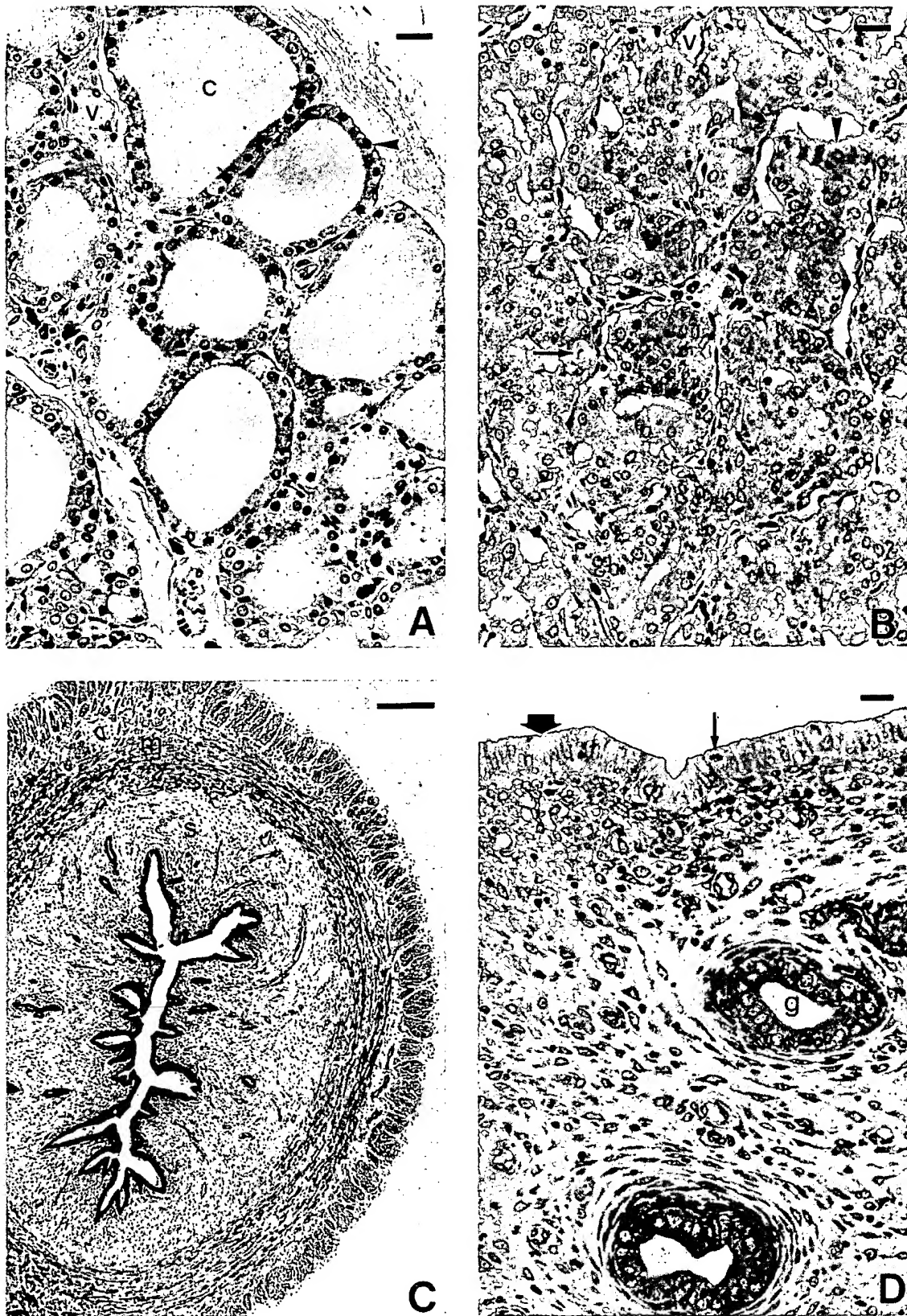
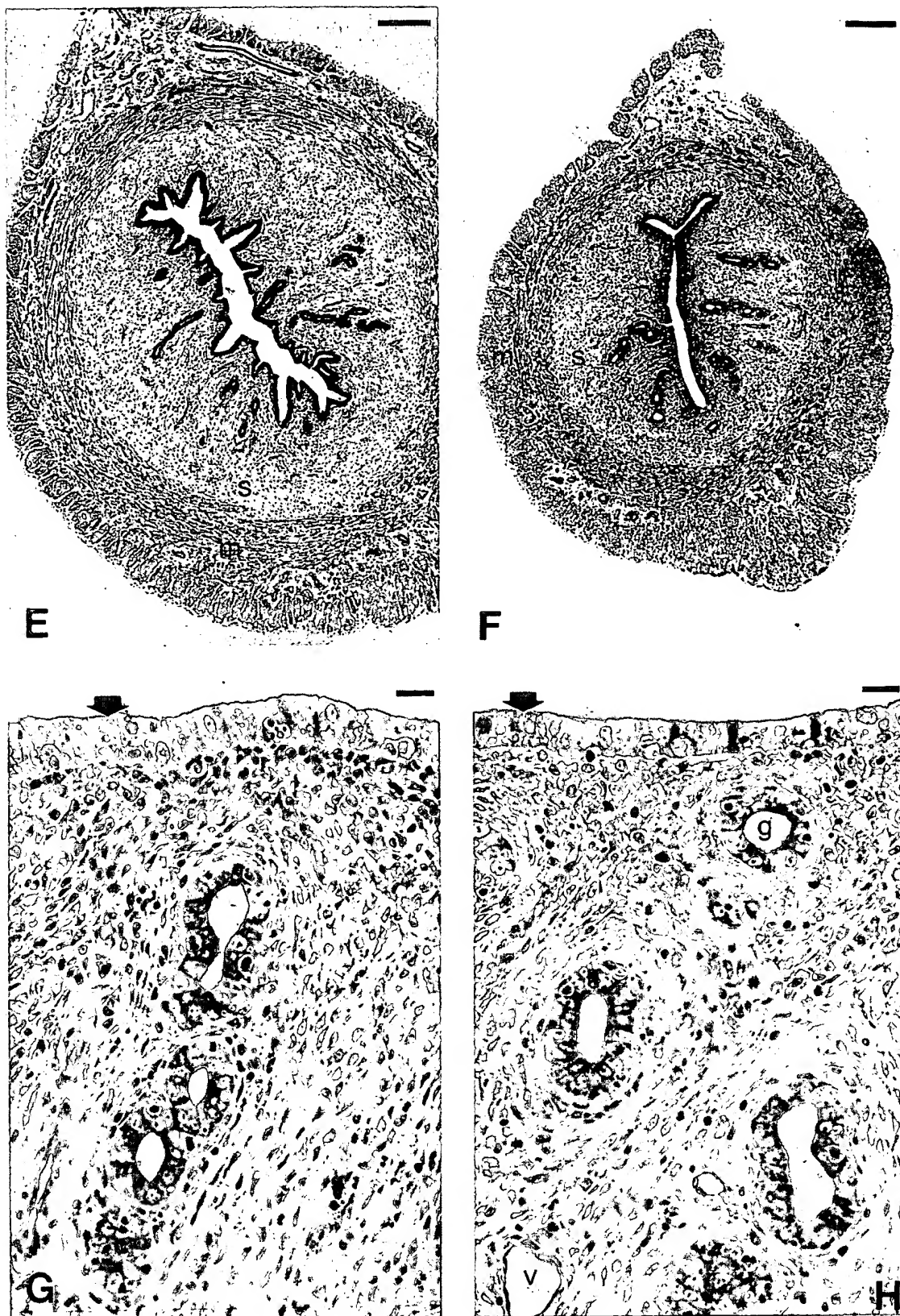


Fig. 2. (A) Normal rat thyroid gland composed of follicles of various sizes surrounded by cuboidal follicular cells (arrowhead). The lumina of the follicles contain colloid (c) rich in thyroglobulin. Blood vessels (V) were numerous. Bar, 20 μ m. (B) Thyroid gland from methimazole treated rat. The follicular architecture of the gland is much disrupted. There is an almost total absence of colloid in the lumina of the follicles. Follicular cells (arrowhead) became columnar, and mitotic figures (arrow) were common amongst them. Bar, 20 μ m. (C) Middle region of uterine horn (euthyroid). The horn consists of a columnar surface epithelium, a stroma (s) containing tubular glands, and circular and longitudinal muscle layers (m). The surface epithelium is thrown into folds, thereby increasing the luminal perimeter. Bar, 20 μ m. (D) High



power view of the uterine horn in (C) showing columnar surface epithelium (short arrow). Mitotic figures (long arrow) are also commonly seen amongst the epithelia. g, gland. Bar, 20 μ m. (E) Middle region of uterine horn in hypothyroid rat given thyroxine (MMI + T₄). Note also the folded nature of surface epithelium here as in (C). Bar, 200 μ m. (F) Middle region of uterine horn in hypothyroid rat. Note the flattened surface epithelium. s, stroma; m, muscle layer. Bar, 200 μ m. (G) High power view of the uterine horn in (E) showing columnar surface epithelial cells (short arrow). Bar, 20 μ m. (H) High power view of the uterine horn in (F). The surface epithelial cells (short arrow) are shorter than in (D) and (G) above. g, stromal gland; v, blood vessel. Bar, 20 μ m.

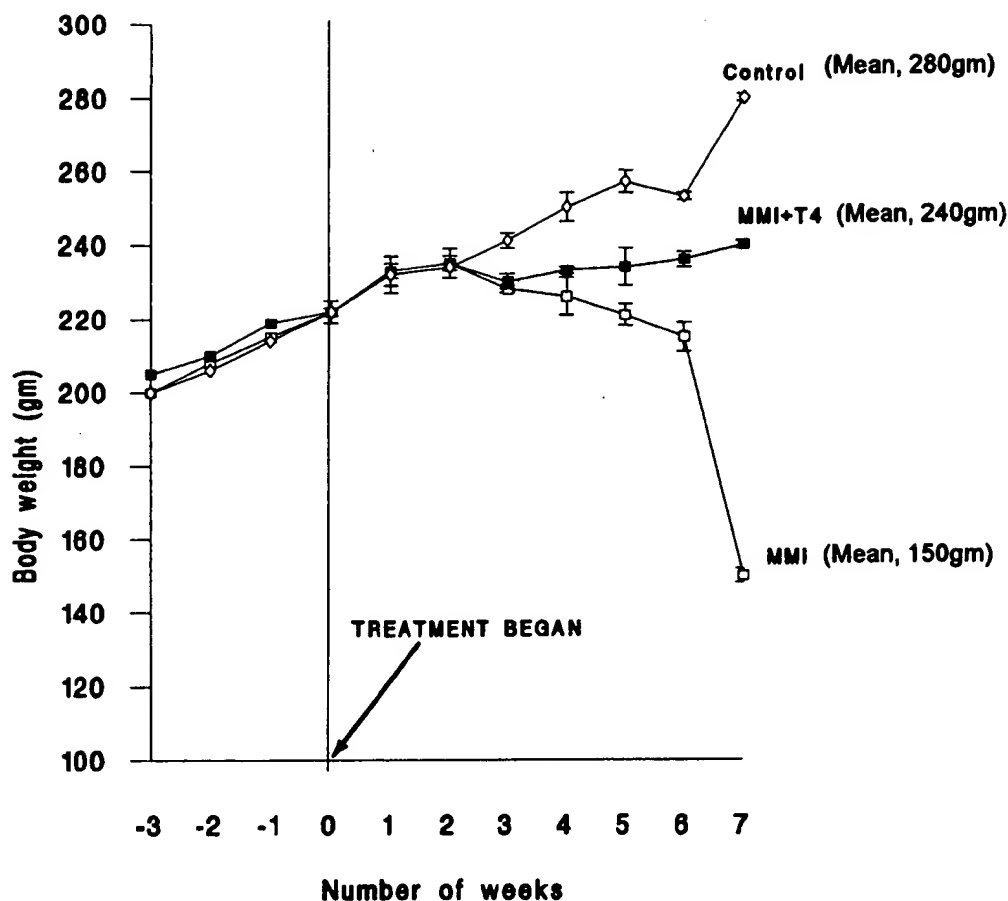


Fig. 3. Body weight and body weight change (mean \pm S.E.M.) in euthyroid (control), hypothyroid (MMI) and hypothyroid rats given thyroxine (MMI + T4) during the experiment. Rats in each group were weighed weekly and the mean \pm S.E.M. weight calculated.

Hypothyroid rats progressively lost weight, developed dry fur, and were observed to be less active than euthyroid (control) or hypothyroid rats given thyroxine (MMI + T4). Their weight loss was more pronounced from the 4th week of treatment (see Fig. 3). Hypothyroid rats were found to have disrupted oestrus cycles with a large proportion of the days (40.0%) spent in dioestrus, whilst only 12.3% was spent in oestrus. The euthyroid rats spent 26.3% of the days in oestrus stage with fewer days (22.7%) in the dioestrus stage of the oestrus cycle (see Fig. 4).

Uterine horn morphology

The uterine horn is made up of 3 distinct structural entities: the luminal epithelium, the stroma and 2 layers of smooth muscle. The stroma is composed of blood vessels and connective tissue cells. The luminal epithelium and stroma are collectively referred to as the endometrium. There is an inner circular and an outer longitudinal smooth muscle layer. A thin layer of connective tissue and mesothelium covers the

external surface of the longitudinal muscle layer (see Fig. 2c, e, f). The luminal epithelium is simple columnar and rests on a thin basement membrane. It is thrown into folds, thereby increasing the surface area of the lumen (see Fig. 2d, g, h).

Uterine horn morphometry

The morphometric parameters determined in the uterine horn were the absolute volume of the uterine horn, the relative and absolute volumes of various compartments of the horn, thickness of the endometrium, and the length of the uterine horn. The results are given in Tables 2 and 3. The volume density of endometrium was significantly greater in euthyroid and hypothyroid rats given thyroxine (MMI + T4) when compared with that of hypothyroid rats. The cross-sectional area of the uterine horn was also significantly reduced in hypothyroid rats. The absolute volume of the uterine horn was reduced in hypothyroid rats as compared with euthyroid ones ($P < 0.05$). However, in hypothyroid rats given

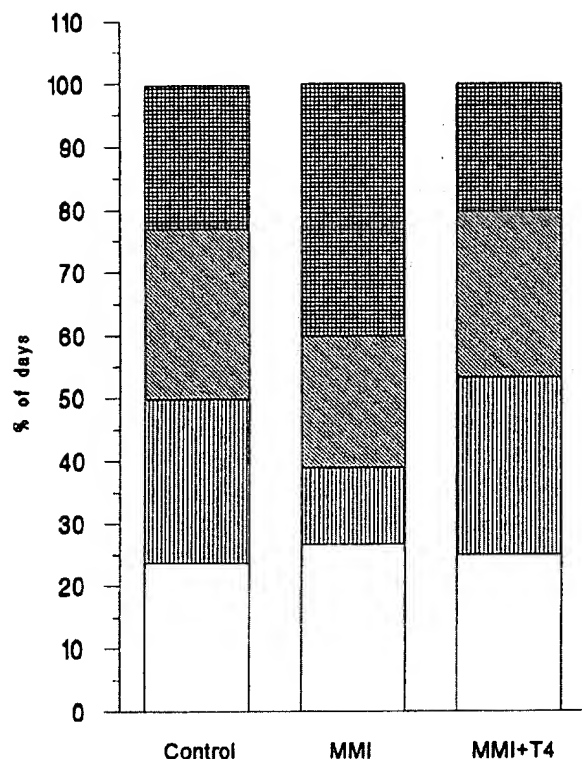


Fig. 4. Mean percentage of days spent on various stages of the oestrus cycle by each group of rats. Control, euthyroid; MMI, hypothyroid; MMI + T4, hypothyroid rats given thyroxine. The stage of oestrus cycle was determined by daily vaginal smears. ■ = dioestrus, ▨ = metoestrus, ▤ = oestrus, □ = proestrus.

thyroxine (MMI + T4), the volume was significantly higher ($P < 0.05$) as compared with hypothyroid rats. The decrease in volumes of different compartments of the uterine horn in hypothyroidism appear to be nonuniform. Whilst the endometrial volume had decreased by 45.1%, the muscle volume had decreased by 33.6% (see Table 4).

The thickness of the endometrium from the luminal surface to the stroma-muscle junction was found to be

Table 5. Morphometric variables for uterine horn in euthyroid (control), hypothyroid (MMI), and hypothyroid rats given thyroxine (MMI + T4)†

Variable	Control	MMI	MMI + T4
Endometrial thickness (mm)	0.72* (7.5)	0.54 (6.3)	0.62** (12.5)
Length of uterine horn (mm)	46* (6.5)	42 (8.5)	44 (7.1)
Cross-sectional area of horn (mm ²)	4.24* (1.6)	2.91 (1.7)	3.55** (1.7)
Luminal perimeter (mm)	0.959* (12.1)	0.725 (6.3)	0.857** (10.8)

† For explanation of abbreviations and symbols, see footnote to Table 4.

significantly greater in euthyroid rats than in hypothyroid rats ($P < 0.05$). Length of the uterine horn from its junction with the body of the uterus at one end, to the horn-fallopian tube junction at the other, as well as its cross-sectional area had similarly decreased in hypothyroid rats. However, the length of the uterine horn had only decreased by 8% whilst the cross-sectional area had decreased by 31.3% (see Table 5).

DISCUSSION

This study has demonstrated the occurrence of significant alterations of uterine morphology in hypothyroidism. The absolute volume of the uterine horn in hypothyroid animals was significantly reduced as was the wet weight of the organ. These changes were evidently partly prevented by thyroxine administration to hypothyroid animals.

The rarity of pregnancy in hypothyroid women has generally been attributed to a high incidence of

Table 4. Mean (CV%) relative and absolute volumes of different compartments of the uterine horn in euthyroid (control), hypothyroid (MMI), and hypothyroid rats given thyroxine (MMI + T4)†

Compartment	Volume density Vv			Absolute volume (mm ³)		
	Control	MMI	MMI + T4	Control	MMI	MMI + T4
Uterine horn	—	—	—	195.04* (10.5)	122.22 (9.8)	156.2** (4.7)
Endometrium	0.32* (3.1)	0.28 (5.3)	0.30** (9.8)	62.41* (8.0)	34.22 (12.1)	46.86** (9.5)
Muscle	0.67* (5.9)	0.70 (6.4)	0.68** (7.7)	132.63* (5.9)	88.0 (8.8)	109.34** (11.2)

† Results are group means (CV%) for 6 rats. Endometrial thickness was measured from the luminal surface of horn to the stroma-muscle junction. Luminal perimeter was the length of the outline of luminal epithelium in cross section. Control, euthyroid; MMI, hypothyroid; MMI + T4, hypothyroid rats given thyroxine; * $P < 0.05$, euthyroid vs hypothyroid; ** $P < 0.05$ hypothyroid vs hypothyroid rats given thyroxine.

anovulation (Goldsmith et al. 1952). The observations made here suggest that, in addition to anovulation, altered uterine morphology may play a part in preventing pregnancy.

The hypothyroid rats exhibited physical features of hypothyroidism with a significant increase both in the weight and absolute volume of the thyroid gland. This increase was clearly due to both hypertrophy and hyperplasia of follicular cells as evidenced by an increase in their height as well as the presence of numerous mitotic figures. Hypothyroidism was further demonstrated by the morphometric assessment of gland structure which correlates quite well with the functional status of the gland as was suggested by Kalisnik (1981).

Normally functioning human and rat thyroid glands have follicles of various sizes whose walls are made up of cuboidal or squamous follicular cells. The lumen of each follicle contains thyroglobulin (colloid) which serves as a storage form of thyroxine. In long standing hypothyroidism caused by methimazole, the normal follicular structure of the thyroid gland is disrupted. The cuboidal follicular cells become columnar, obliterating the lumina of the follicles, and the colloid almost totally disappears. The specific gravity of thyroid gland is significantly increased in hypothyroid animals ($P < 0.01$) presumably due to a decrease in colloid content.

The improvement of uterine structure to near euthyroid values by thyroxine administration to hypothyroid animals suggests that in euthyroid animals the presence of the hormone contributes to the maintenance of normal uterine morphology. Indeed, DeCherney & Polan (1984) had already shown that patients suffering from habitual abortion caused by hypothyroidism respond favourably to thyroxine therapy. The decrease in uterine horn weight and volume in hypothyroid rats could be thus a direct effect, particularly since thyroid hormone is believed to exert its influence on tissues by facilitating the transcription of DNA resulting in new protein synthesis. Evans et al. (1983) and Mukku et al. (1983) have independently shown that the rat uterus is a specific site for thyroid hormone action by demonstrating the presence there of thyroid hormone receptors. It is known that thyroid hormone has a growth promoting action in rats, its absence leading to growth retardation (Evans et al. 1960). Absence of the hormone could thus slow down the normal processes of tissue growth and replacement resulting in a decrease in the size of the uterine horn. It appears, however, that the effect of hypothyroidism on the uterine horn was more pronounced on the endo-

metrium than the smooth muscle layer. This could be as a result of unequal levels of metabolic activity, or due to a disproportionate distribution of thyroid hormone receptors in these 2 compartments.

It could be argued that changes may also occur as indirect effects of hypothyroidism since it has been shown that hypothyroidism leads to a decrease in serum levels of the pituitary gonadotrophins FSH and LH (Akanke, 1975; Valle et al. 1985; Kirby et al. 1992). These could in turn lead to a decrease in ovarian stimulation and hence a decrease in ovarian steroid hormone levels, causing a drop in stimulation of uterine metabolism. These effects might also explain why there is a preponderance of dioestrus smears in the hypothyroid rats in contrast to euthyroid or hypothyroid rats given thyroxine (MMI + T₄). In fact, our findings on this aspect agree with those of others (Vriend et al. 1987; Ortega et al. 1990) who also found a persistence of dioestrus smears and a reduction of oestrus smears in hypothyroid rats. As the dioestrus stage in rats is characterised by low serum levels of gonadotrophins, this observation suggests that hypothyroidism does have influence on the levels of these hormones.

This study therefore has provided quantitative data which suggest that the structure of the rat uterine horn was altered in hypothyroidism, and that this alteration was reversible with thyroxine administration. Further studies on the effect of hypothyroidism on protein metabolism and cell kinetics in the uterine horn, as well as ovarian enzyme histochemistry are being planned.

REFERENCES

- AKANKE EO (1975) Plasma concentration of gonadotrophins, oestrogen and progesterone in hypothyroid women. *British Journal of Obstetrics and Gynaecology* **82**, 552-556.
- BALEN AH, KURTZ AB (1990) Successful outcome of pregnancy with severe hypothyroidism. *British Journal of Obstetrics and Gynaecology* **97**, 536-539.
- BOYLAND P, DRURY MI (1979) Pregnancy in untreated hypothyroidism. *Irish Journal of Medical Science* **148**, 10-11.
- BURROWS GN (1972) Maternal hypothyroidism. In *The Thyroid Gland in Pregnancy*, vol. 3, pp. 55-68. Philadelphia: W. B. Saunders.
- DECHERNEY A, POLAN ML (1984) Evaluation and management of habitual abortion. *British Journal of Hospital Medicine* **3**, 261-262.
- DISTILLER LA, SAGEL J, MORLEY JE, OXENHAM E (1975) Assessment of pituitary gonadotrophin reserve using luteinizing hormone-releasing hormone (LRH) in states of altered thyroid function. *Journal of Clinical Endocrinology and Metabolism* **40**, 512-515.
- EVANS ES, ROSENBERG LL, SIMPSON ME (1960) Relative sensitivity of different biological responses to thyroxine. *Endocrinology* **66**, 433.
- EVANS RW, FARWELL AP, BRAVERMAN LE (1983) Nuclear thyroid hormone receptors in the rat uterus. *Endocrinology* **113**, 1459-1463.

- FISH LH, MARIASH CN (1988) Hyperprolactinemia, infertility, and hypothyroidism—a case report and literature review. *Archives of Internal Medicine* **148**, 709–711.
- GOLDSMITH RE, STURGIS SH, LERMAN J (1952) The menstrual pattern in thyroid disease. *Journal of Clinical Endocrinology and Metabolism* **12**, 846.
- GUNDERSEN HJG, JENSEN EB (1987) The efficiency of systematic sampling in stereology and its prediction. *Journal of Microscopy* **147**, 229–262.
- HARDY MP, KIRBY JD, HESS RA, COOKE PS (1993) Leydig cells increase their numbers but decline in steroidogenic function in the adult rat after neonatal hypothyroidism. *Endocrinology* **132**, 2417–2420.
- HEMADY ZS, SILER-KHODR M, NAJJAR S (1978) Precocious puberty in juvenile hypothyroidism. *Journal of Pediatrics* **92**, 55–59.
- HEYBURN PJ, GIBBY OM, HOURIHAN M, HALL R, SCANLON MF (1986) Primary hypothyroidism presenting as amenorrhoea and galactorrhoea with hyperprolactinaemia and pituitary enlargement. *British Medical Journal* **292**, 1660–1661.
- IMAMURA Y (1982) Uterine response to estrogen in the rat of hypothyroidism. *Nippon Naibunpi Gakkai Zasshi* **58**, 867–875.
- KALISNIK M (1981) Morphometry of the thyroid gland. *Stereologica Jugoslavia* **3**, Suppl. 1, 547–569.
- KENNEDY AL, MONTGOMERY DAD (1978) Hypothyroidism in pregnancy. *British Journal of Obstetrics and Gynaecology* **85**, 225–230.
- KIRBY JD, JETTON AE, COOKE PS, HESS RA, BUNICK D, ACKLAND JF et al. (1992) Developmental hormonal profiles accompanying the neonatal hypothyroidism-induced increase in adult testicular size and sperm production in the rat. *Endocrinology* **131**, 559–565.
- KROHN PL, WHITE HC (1950) The effect of hypothyroidism on reproduction in the female Albino rat. *Journal of Endocrinology* **6**, 375.
- MEISAMI E, SENDERA TJ, CLAY LB (1992) Paradoxical hypertrophy and plasticity of the testis in rats recovering from early thyroid deficiency: a growth study including effects of age and duration of hypothyroidism. *Journal of Endocrinology* **135**, 495–505.
- MONTORO M, COLLEA JV, FRASIER SD (1981) Successful outcome of pregnancy in women with hypothyroidism. *Annals of Internal Medicine* **94**, 31–34.
- MUKKU VR, KIRKLAND JL, HARDY M, STANCEL GM (1983) Evidence for thyroid hormone receptors in uterine nuclei. *Metabolism* **32**, 142–145.
- ORTEGA E, RODRIGUEZ E, RUIZ E, OSORIO C (1990) Activity of the hypothalamo-pituitary ovarian axis in hypothyroid rats with or without triiodothyronine replacement. *Life Science* **46**, 391–395.
- RAMSAY I (1986) The thyroid. In *Scientific Foundations of Obstetrics and Gynaecology*, 3rd edn (ed. E. Phillip, J. Barnes & L. Newton), pp. 462–465. London: Heinemann.
- RITCHIE JWK (1986) Diabetes and other endocrine diseases in pregnancy. In *Dewhurst's Textbook of Obstetrics and Gynaecology for Postgraduates*, 4th edn, pp. 293–294. Oxford: Blackwell Scientific Publications.
- SILVER JE, LEONARD JL (1985) Regulation of rat cerebrocortical and adenohipophyseal type II 5'-deiodinase by thyroxine, triiodothyronine, and reverse triiodothyronine. *Endocrinology* **116**, 1627–1635.
- SMITH CS, GUTTMANN L (1953) Measurement of internal boundaries in three dimensional structures by random sectioning. *Transactions of American Institute of Mineral and Metallurgical Engineers* **197**, 1561.
- VALLE LB, OLIVEIRA-FILHO RM, ROMALDINI JH, LARA PF (1985) Pituitary-testicular axis abnormalities in immature male hypothyroid rats. *Journal of Steroid Biochemistry* **23**, 253–257.
- VRIEND J, BERTALANFFY FD, RALCEWICZ TA (1987) The effects of melatonin and hypothyroidism on oestradiol and gonadotropin level in female Syrian hamster. *Biology of Reproduction* **36**, 719–728.
- WILLIAMS MA (1977) Quantitative methods in biology. In *Practical Methods in Electron Microscopy*, vol. 6, part II (ed. A. M. Glauret), pp. 36–38. Amsterdam: North Holland Publishing Company.

COPYRIGHT © 1974, BY ACADEMIC PRESS, INC.
ALL RIGHTS RESERVED.

NO PART OF THIS PUBLICATION MAY BE REPRODUCED OR
TRANSMITTED IN ANY FORM OR BY ANY MEANS, ELECTRONIC
OR MECHANICAL, INCLUDING PHOTOCOPY, RECORDING, OR ANY
INFORMATION STORAGE AND RETRIEVAL SYSTEM, WITHOUT
PERMISSION IN WRITING FROM THE PUBLISHER.

ACADEMIC PRESS, INC.
111 Fifth Avenue, New York, New York 10003

United Kingdom Edition published by
ACADEMIC PRESS, INC. (LONDON) LTD.
24/28 Oval Road, London NW1

Library of Congress Cataloging in Publication Data
Main entry under title:

Biomembranes, part A-

(Methods in enzymology, v. 31-

Includes bibliographies.

1. Cell membranes. 2. Cell fractionation. 3. Cell
organelles. I. Fleischer, Sidney, ed. II. Packer,
Lester, ed. III. Estabrook, Ronald W., ed.

[DNLM: 1. Cell membrane. W1ME9615K v. 31 / QH601
B6193]

QP601.C733 vol. 31
ISBN 0-12-181894-2

[QH601]
74-11352

574.1'925'08s

[574.8'75]

PRINTED IN THE UNITED STATES OF AMERICA

preparations contain other sugar transferases, such as *N*-acetylglucosaminyl and sialyltransferase, and suggested that the Golgi apparatus in liver is equipped with a multienzyme system for the synthesis of the terminal sugars in glycoproteins.

Acknowledgments

The author would like to thank Mr. Akitsugu Saito for the electron micrographs used in this paper and Dr. Theodore Peters, Jr., of The Mary Imogene Bassett Hospital, Cooperstown, New York, for the determination of rat serum albumin in the Golgi fractions. This work was supported in part by Grant AM-14632 of the U.S. Public Health Service.

[18] Isolation of Rough and Smooth Microsomes—General

By GUSTAV DALLNER

Definition. The isolated total microsomal fraction in most tissues consists of two major components: rough and smooth microsomes, the former having attached ribosomes on the outer surface. The definition of this fraction is based not on its content but on the result of the centrifugation procedure employed to isolate it. By this definition, the microsomes are those elements of a tissue homogenate that can be sedimented by ultracentrifugation from the mitochondrial supernatant. Whereas the rough microsomes originate from the rough-surfaced endoplasmic reticulum (ER), the smooth microsomes, depending on the tissue and isolation conditions, vary in origin. Smooth microsomes isolated from the liver derive either almost exclusively or to a great extent from the smooth ER¹; when isolated from the pancreas² and testis,³ the same fraction contains mainly Golgi elements; and at subfractionation of kidney,⁴ Ehrlich ascites tumor cells,⁵ or fibrocytes,⁶ parts of the plasma membranes are recovered as smooth microsomes. In most of the other organs, the microsomes may still contain additional elements.

Another complication facing those wishing to isolate rough and smooth microsomes is the variation in size and density even among particles deriving from the same origin. Unlike many other cellular organelles, none of the lamellar and cisternal structures of the rough and smooth ER can be

¹ G. Dallner and L. Ernster, *J. Histochem. Cytochem.* 16, 611 (1968).

² J. D. Jamieson and G. E. Palade, *J. Cell Biol.* 34, 597 (1967).

³ E. L. Kuff and A. J. Dalton, in "Subcellular Particles" (T. Hayashi, ed.), p. 114. Ronald Press, New York, 1959.

⁴ J. Rostgaard and O. J. Møller, *Exp. Cell Res.* 68, 356 (1971).

⁵ D. F. H. Wallach and V. B. Kamat, this series, Vol. 8, p. 164.

⁶ C. G. Gahmberg and K. Simons, *Acta Pathol. Microbiol. Scand. B*, 78, 176 (1970).

separated in the intact form.⁷ The new morphological structure appearing after homogenization acquires a spectrum of physical properties which to a great extent mirror the conditions employed. There is a consequence of this which is unfortunately not always recognized: the method used for the separation of rough and smooth microsomes in one tissue almost invariably cannot be used for another tissue.⁸ Indeed, when a procedure found successful for one type of animal is used on another type of animal, even in the case of the same organ, radical modifications are often necessary.

Recovery and Purity. The clash between high yield and absence of contamination is greatly accentuated during the isolation of rough and smooth microsomes. These two basic requirements of all subfractionation work cannot be reconciled at present. In simple terms, this clash means that we must choose between high quantitative recovery plus high impurity, and partial recovery plus high purity. Since extensive contamination of a subfraction runs counter to the very purpose of the procedure, the investigator in most cases must choose the second alternative. A high recovery would be desirable, certainly, but at present such an objective belongs in the realm of wishful thinking. The basic condition for a high yield of both rough and smooth microsomes is effective homogenization. The extensive homogenization of liver, for example, results in the breakage of plasma membranes⁹ and Golgi cisternae,¹⁰ it releases outer mitochondrial membranes,¹¹ and ruptures lysosomes,¹² all of which contribute to a high degree of impurity of smooth and in some instances even of rough microsomes. Furthermore, connective tissue cells and cells of erythropoiesis, particularly in the newborn—cell types that possess plasma membranes more resistant to shearing forces—also break up and contribute to a false heterogeneity.^{13,14} Prolonged homogenization leads to an increased release of bound ribosomes, modified vesicle structure and composition, and also interference with enzyme activities. It does not seem, at least in the case of the liver, that the ER portion lost in the first centrifugation represents a specific and unique part of the system. It is very probable that the loss is caused by the presence of unbroken or incompletely broken cells of random origin.

⁷ G. E. Palade and P. Siekevitz, *J. Biophys. Biochem. Cytol.* 2, 671 (1956).

⁸ Y. S. Kim, J. Perdomo, and J. Nordberg, *J. Biol. Chem.* 246, 5466 (1971).

⁹ R. Coleman, R. H. Michell, J. B. Finean, and J. N. Hawthorne, *Biochim. Biophys. Acta* 135, 573 (1967).

¹⁰ B. Fleischer, S. Fleischer, and H. Ozawa, *J. Cell Biol.* 43, 59 (1969).

¹¹ W. E. Criss, *J. Biol. Chem.* 245, 6352 (1970).

¹² R. L. Deter and C. de Duve, *J. Cell Biol.* 33, 437 (1967).

¹³ I. T. Oliver, W. F. C. Blumer, and I. J. Witham, *Comp. Biochem. Physiol.* 10, 33 (1963).

¹⁴ G. Dallner, P. Siekevitz, and G. E. Palade, *J. Cell Biol.* 30, 73 (1966).

Consequently, the isolated rough and smooth microsomes, at least in qualitative respects, represent the true picture.

Medium. Practically all fractionation procedures are performed in sucrose solutions.¹⁵ For homogenization, 0.25 *M* or 0.44 *M* solutions are used in most cases; 0.88 *M* sucrose is better able to keep an elongated, tubulelike structure among the rough microsomes,⁷ but this increases centrifugation time, which is a drawback for the separation procedure itself. Under the conditions of ultracentrifugation, the liver microsomal vesicle is completely permeable to sucrose,¹⁶ a property that seems to be shared by peroxisomes alone.¹⁷ Thanks to this property, sucrose has a less damaging effect on microsomal vesicles than many other suspension media. The vesicles do not display any osmotic response, and their high equilibrium density—mainly provided by the solid membrane material plus hydration water—is advantageous in the separation procedure. High polymer dextran, glycogen, and Ficoll, being nonpermeable solutes, lend low density to both rough and smooth microsomes to such an extent that their isolation in a discontinuous gradient is more difficult.

Influence of Surface Charge. The microsomal membranes possess a high net negative surface charge density, rough microsomes being more negative than the smooth variety.¹⁸ This property can be utilized for effective and rapid separation, and it is also important for a number of other reasons. During the isolation procedure, a significant amount of cytoplasmic basic proteins becomes attached to the particle surfaces, contributing in this way about 30% of the total microsomal protein.¹⁹ The extremely common finding that microsomal vesicles aggregate during the isolation procedure, at times as early as during homogenization, is a very unfortunate consequence of the surface charge, invariably leading to incomplete separation. Purity of all glassware as well as the absence of cations in the distilled water are of basic importance in the subfractionation of microsomes. Foreign charged substances ingested with food or drinking water accumulate in the liver, particularly on the surface of the ER. A well-documented finding is the influence of detergents used, for example, for cleaning cages.

¹⁵ The major disadvantage of sucrose is the steep rise in viscosity with increasing concentration and the very sensitive relationship between the viscosity of sucrose and temperature. To give an example: an increase in temperature from 5° to 10° (which frequently occurs during long centrifugations) will decrease the viscosity by 20% and consequently increase the sedimentation velocity by 20%.

¹⁶ R. Nilsson, E. Peterson, and G. Dallner, *J. Cell Biol.* 56, 762 (1973).

¹⁷ F. Leighton, B. Poole, H. Beaufay, P. Baudhuin, J. W. Coffey, S. Fowler and C. de Duve, *J. Cell Biol.* 37, 482' (1968).

¹⁸ G. Dallner and A. Azzi, *Biochim. Biophys. Acta* 255, 589 (1972).

¹⁹ G. Dallner, in "Proceedings of the 4th International Congress of Pharmacology" (R. Eigenmann, ed.), Vol. 4, p. 70. Schwabe, Basel, 1970.

It is no exaggeration to say that all these factors are decisive for the ultimate physicochemical properties of the microsomal membranes and certainly constitute one of the explanations why different laboratories obtain different results. It has also been suggested that the inner surfaces of several membranes have a different structure and consequently a different charge,²⁰ which may contribute toward a selective change of particle density when divalent cations are present in low amounts in a polymer gradient. All these considerations indicate how important it is not to use buffers in the gradient medium without controlling side effects. In most cases, the proteins present during subfractionation have a large enough buffering capacity to keep the pH around 7.

Stability. Microsomes have a great tendency to aggregate, often even in the absence of cations. This statement is valid for both subfractions, but smooth microsomes are decidedly more sensitive and unstable.²¹

The stability involving both an existence in nonaggregated form and an uninfluenced enzyme activity requires either high protein or high sucrose concentration or, in the most ideal case, both. It is not advisable to use a particle concentration of less than 5 mg of protein per milliliter or a sucrose concentration of less than 0.25 M. If it is difficult to obtain a high protein concentration, stabilization can be achieved by adding protecting colloids, such as albumin,²² spermine, or spermidine.²³ Stability may be increased by using a high sucrose concentration (30–40%), but this is not often practicable. Isolated subfractions tolerate sedimentation badly and aggregate in many cases. If smooth microsomes are pelleted, they always aggregate independently of the protein or sucrose concentration.

If isolated subfractions must be concentrated and aggregation is deleterious (for example, in the case of further subfractionation) a suitable concentration may be obtained by layering the suspension above a 2–4 ml sucrose cushion (~ 1.6 M) in an angle-head or swinging-bucket rotor and collecting the particles at the interface after short centrifugation (~ 30 minutes) at 60,000–80,000 g. A high sucrose concentration and high centrifugal force lead to aggregation of the particles at the interface and are no more advantageous than pelleting.

The simplest way to test for aggregation is to filter microsomes (4–5 mg of protein per milliliter) by suction pump through a filter of 0.45 μ m (Millipore Corp., Bedford, Massachusetts) followed by an additional volume of sucrose for washing.²³ In the nonaggregated state, about 90% of both rough and smooth microsomes appear in the filtrate.

²⁰ T. L. Steck and D. F. H. Wallach, *Methods Cancer Res.* 5, 93 (1970).

²¹ H. Glaumann and G. Dallner, *J. Cell Biol.* 47, 34 (1970).

²² G. Dallner and R. Nilsson, *J. Cell Biol.* 31, 181 (1966).

²³ P. H. Jellinck and G. Perry, *Biochim. Biophys. Acta* 137, 367 (1967).

In the isolated state, microsomes can be damaged by their own enzymes in the membrane (e.g., PLPase A,^{24,25} enzymatic lipid peroxidation²⁶) or in the lumen (e.g., trypsin, lipase²⁷). Specific inhibitors may counteract this: absence of cations and low temperature (PLPase A), small amounts of antioxidants or chelating agents (lipid peroxidation), trypsin inhibitor (trypsin), Zn^{2+} or Ag^+ (pancreatic lipase), etc.

Centrifugal Force and Rotors. It is very tempting to use high centrifugal forces to sediment microsomes, since their small size often requires a long centrifugation time, but this should be avoided. Microsomal vesicles in the usual concentration and in 0.25 M sucrose centrifuged in an angle-head rotor (26°) in the Spinco-Beckman ultracentrifuge at more than 40,000 rpm show signs of damage such as increased permeability and an oval rather than round form in the electron microscopical picture. Naturally, much higher speeds may be employed when the particle is moving in a high concentration of medium and does not hit the bottom of the tube. In most gradient centrifugation, swinging-bucket rotors are required. In the case of microsomal fractions, particularly when the sedimentation velocity of rough microsomes is increased by the addition of monovalent cations, angle-head rotors with a large tube angle of inclination to the axis of rotation may be used for the discontinuous sucrose gradient.²⁸ Actually, this can be advantageous, since the convections set up during centrifugation decrease centrifugation time without causing mixing of the two main components in the surface layer and in the pellet.

Isolation of Rough and Smooth Microsomes

Rat Liver

Rats weighing around 180–200 g give the most reproducible preparations. Starvation for 20 hours before sacrifice decreases the liver glycogen content to about 1 mg/g (wet weight). Starvation induces increased glucose-6-phosphatase (G6Pase) activity,²⁹ but in nonfasted rats the loss of both rough and smooth microsomes during the preliminary centrifugation is increased by 30–40%. Constituents from broken erythrocytes (e.g., hemoglobin) are easily adsorbed on the surface of microsomes,³⁰ and, if this is undesirable, perfusion with 0.25 M cation-free sucrose may be

²⁴ P. Bjørnstad, *Biochim. Biophys. Acta* 116, 500 (1966).

²⁵ M. Waite and L. L. M. van Deenen, *Biochim. Biophys. Acta* 137, 498 (1967).

²⁶ P. Hochstein and L. Ernster, *Cell. Inj., Ciba Found. Symp.*, 1963 p. 123 (1964).

²⁷ J. Meldolesi, J. D. Jamieson, and G. E. Palade, *J. Cell Biol.* 49, 130 (1971).

²⁸ A. Bergstrand and G. Dallner, *Anal. Biochem.* 29, 351 (1969).

²⁹ W. J. Arion and R. C. Nordlie, *Biochem. Biophys. Res. Commun.* 20, 606 (1965).

³⁰ M. L. Petermann and A. Pavlovic, *J. Biol. Chem.* 236, 3235 (1961).

performed. Livers are minced into small pieces with a pair of scissors and rinsed several times with cold sucrose solution. Homogenization is performed in the commercially available Teflon homogenizer in a volume that roughly corresponds to the volume of liver. In the motor-driven homogenizer, run at a speed not exceeding 400–500 rpm, four strokes are used. Complete homogeneity of the suspension is not obtained and is, in fact, not to be desired.

Cation-Containing Sucrose Gradient

Principle. Rough microsomes display a high binding affinity for Cs^+ in comparison with smooth microsomes.³¹ In the presence of a limited amount of Cs^+ , the net negative surface charge density selective for rough membranes decreases, with consequent abolishment of repelling forces. Extensive aggregation of rough microsomes follows,³² and the mean radius of the sedimenting particles is at least doubled or trebled; this increases the sedimentation velocity by 4–9-fold.²²

Beckman-Spinco Centrifuge. Practical. 40.2 ROTOR.²⁸ Homogenization of the liver is performed in 0.25 M sucrose followed by dilution to a tissue concentration of 25% (w/v). The homogenate is centrifuged at 10,000 g for 20 minutes, either in an ultracentrifuge or in a low-speed cooled centrifuge. The supernatant (10,000 g supernatant) is decanted to the last drop into a graded cylinder and is not diluted. In order to obtain a final CsCl concentration of 15 mM, the suspension is mixed with 0.15 ml of 1 M CsCl per 10 ml; 4.5 ml of CsCl-containing “10,000 g supernatant” is layered over 2 ml of 1.3 M sucrose–15 mM CsCl.^{33,34} After centrifugation in a 40.2 rotor (tube angle 40°) at 102,000 g for 120 minutes,³⁵ the clear reddish upper phase can be removed either with a pipette provided with a rubber aspirator or with a water pump. This portion is discarded. The fluffy double layer (upper: reddish, lower: light brown) at and under the gradient boundary is collected.³⁶ This fraction, *the total smooth microsomes*, contains some soluble cytoplasmic protein. If no further subfractionation is planned and aggregation has no importance, the fraction can

³¹ G. Dallner, L. Ernster, and A. Azzi, *Chem.-Biol. Interactions* 3, 254 (1971).

³² G. Dallner, *Acta Pathol. Microbiol. Scand.*, Suppl. 166 (1963).

³³ Layering may be done either with a pipette or with a peristaltic pump.

³⁴ For standardization, all sucrose solutions should be made up first by warming followed by cooling in an ice water bath with subsequent volume adjustment with cool water.

³⁵ Starting from a 20% homogenate, 90 minutes of centrifugation is sufficient.

³⁶ The intermediate layer may be removed with an ordinary or Pasteur pipette, but ideal is a syringe with a long needle whose tip has been bent into an L shape. The syringe is clamped above the tube, which rests on a variable stand that can raise it to the desired level.

be recentrifuged at 105,000 g for 90 minutes in order to obtain a pellet. The 1.3 M sucrose layer above the pellet is removed with a pipette or a syringe, except for the last few drops, which contain the fluffy layer. This layer with 15% of the total microsomal protein is discarded except when rough III microsomes are prepared (see below). The pellet with the few drops immediately covering it is resuspended by hand homogenization after the addition of water (*total rough microsomes*). The yield is ~12 and 5 mg of protein per gram of liver for rough and smooth microsomes, respectively.

SW 39 AND SW 40 ROTORS. Swinging-bucket rotors giving high g values can also be utilized for subfractionation.¹⁴ The decrease of convection in these rotors, however, increases centrifugation time in spite of the high centrifugal forces employed. Using a SW 39 rotor, 3 ml of Cs⁺-containing 10,000 g supernatant is layered above 2 ml of 1.3 M sucrose-15 mM CsCl; after 3 hours of centrifugation with the highest speed for this rotor (39,000 rpm), the two microsomal subfractions are separated. In the case of SW 40 rotor, 9 ml is layered above a 4-ml cushion. Centrifugation for 3 hours is still required for separation of rough and smooth microsomes in spite of the high centrifugal force employed (198,000 g).

40 ROTOR. Low tube angle to the axis of rotation increases convections to an extent incompatible with the successful separation of microsomal subfractions. The 40 rotor of the Spinco has a tube angle of 26°, but if 7 ml of Cs⁺-containing 10,000 g supernatant are layered above a 4-ml Cs⁺-containing cushion, after 140 minutes of centrifugation rough and smooth microsomes are separated. The result of this, however, probably because of side wall impaction, is that about 15% of smooth microsomes are recovered in the pellet.³⁷

Christ Omega and International B-60 Ultracentrifuge. Angle-head rotors with large tube angles (34° in the 60 rotor of Christ Omega and 35° in the A-321 rotor of International B-60 ultracentrifuge) can be spun at 60,000 rpm, which in both cases provides a force of 250,000 g. The conditions created in these rotors are close to ideal for the separation of rough and smooth microsomes by the method described above.³² In both centrifuges, 3.5 ml of 1.3 M sucrose-15 mM CsCl in the lower layer and 10,000 g supernatant with 15 mM CsCl in the full upper layer gives after 60 minutes of centrifugation at 60,000 rpm in both centrifuges an almost complete separation of rough and smooth microsomes with only limited amounts of particulate material in the 1.3 M sucrose phase.

Separation of Rough I, II, and III Microsomes. Rough vesicles with

³⁷ T. E. Gram, L. A. Rogers, and J. R. Fouts, *J. Pharmacol. Exp. Ther.* 155, 479 (1967).

few ribosomes remain in an intermediate position on a Cs^+ -containing discontinuous sucrose gradient and can be separated with a simple one-step centrifugation procedure.³⁸ Liver from starved rat is homogenized in 0.44 M sucrose at a tissue concentration of 20% (w/v). After centrifugation at 10,000 g for 20 minutes, the supernatant is mixed with 0.15 ml of 1 M CsCl /10 ml; 3.5 ml of the suspension is layered over 3 ml of 1.3 M sucrose–15 mM CsCl and centrifuged in a 40.2 rotor (Spinco) at 102,000 g for 90 minutes. The clear upper phase and the smooth microsomes at the gradient boundary are removed, and the 1.3 M sucrose layer down to the upper edge of the pellet is sucked off (*rough III microsomes*). The remaining sucrose solution above the pellet is taken up with a Pasteur pipette (*rough II microsomes*), and the pellet is suspended in 0.25 M sucrose (*rough I microsomes*). The two former subfractions may be pelleted after dilution with water or sucrose.

*Separation of Smooth I and II Microsomes.*³⁸ After centrifugation in the 40.2 rotor, total smooth microsomes from two tubes are combined, diluted dropwise with distilled water to 4.5 ml, mixed with 1 M MgCl_2 to give a final concentration of 7 mM, and layered over 2 ml of 1.15 M sucrose–7 mM MgCl_2 . After centrifugation at 102,000 g for 45 minutes in the 40.2 rotor, the clear upper phase is removed and discarded. The fluffy layer at the gradient boundary is collected, diluted with 0.25 M sucrose, and recentrifuged at 105,000 g for 90 minutes (*smooth II microsomes*). The pellet formed on the Mg^{2+} -sucrose gradient represents the *smooth I microsomes*.

Discontinuous Sucrose Gradient

Principle. The majority of rough microsomes possess a higher equilibrium density than smooth microsomes and on a suitably designed discontinuous sucrose gradient they will sediment, while the smooth microsomes remain in the vicinity of the interface.³⁹ The attainment of isopycnic equilibrium is not necessary; in fact, it is not even possible because of the type of gradient and the continuous density spectrum of the microsomal vesicles.

Practical. The following procedure⁴⁰ is a modification of the original one,³⁹ designed to abolish aggregation of the vesicles in the subfractions. Homogenization is performed in 0.44 M sucrose (2 g/10 ml). After centrifugation at 10,000 g for 20 minutes, the supernatant is diluted with 0.44 M sucrose to restore the original volume. Of this suspension, 8 ml is layered over 3 ml of 1.3 M sucrose and centrifuged at 105,000 g for 7

³⁸ L. C. Eriksson and G. Dallner, *FEBS (Fed. Eur. Biochem. Soc.) Lett.* 19, 163 (1971).

³⁹ J. Rothschild, *Biochem. Soc. Symp.* 22, 4 (1963).

⁴⁰ G. Dallner, A. Bergstrand, and R. Nilsson, *J. Cell Biol.* 38, 257 (1968).

hours 40 minutes in a 40 rotor (Spinco). The upper 0.44 M sucrose phase is sucked off. The milky layer localized in the upper part of the 1.3 M sucrose layer, which is in the process of sedimenting down, is removed. If the fraction is not used for further subfractionation, it may be recentrifuged after dilution with 0.25 M sucrose (*smooth microsomes*). The 1.3 M sucrose layer is removed and discarded, but the fluffy layer just above the pellet is left behind and rehomogenized by hand together with the pellet, after the addition of a few drops of water (*rough microsomes*). The 1.3 M sucrose layer, which is discarded, contains a mixture of rough and smooth microsomes (~10–15% of both). The yield after recentrifugation is ~10 and 4 mg of protein per gram of liver for rough and smooth microsomes, respectively.

Mouse, Rabbit, and Guinea Pig Liver

The isolation of rough, smooth I, and II microsomes from mouse liver, as well as rough and total smooth microsomes from rabbit liver, is carried out in the same way as described for rat liver. In the case of the rabbit, however, the density gradient with Mg^{2+} for subfractionation of smooth microsomes is composed of 0.25 M/1.00 M sucrose rather than 0.25 M/1.15 M sucrose. Because of the frequent aggregation of smooth microsomes from guinea pig liver, the soluble supernatant must be removed during the isolation procedure by a three-layered gradient. Over 2 ml of 1.3 M sucrose–15 mM Cs^+ , and 1 ml of 0.5 M sucrose–15 mM Cs^+ , 3.5 ml of 15 mM $CsCl$ containing 10,000 g supernatant is layered and centrifuged at 102,000 g for 90 minutes in a 40.2 rotor. The double-layered total smooth microsomes in the 0.5 M sucrose may be further subfractionated by centrifugation after dilution with 0.25 M sucrose and layering over 1.00 M sucrose, both containing 7 mM $MgCl_2$.

Guinea Pig Pancreas

Continuous Gradient^{41,42}

Pancreas from 20-hour-starved guinea pig is passed through a stainless steel tissue press and homogenized in 0.3 M sucrose (1 g/10 ml) by 30 strokes in a hand homogenizer fitted with a rubber pestle. After filtration through 110-mesh nylon cloth, the homogenate is centrifuged at 11,000 g for 15 minutes in a Spinco 40.3 rotor. The upper two-thirds of the supernatant is removed, centrifuged at 115,000 g for 60 minutes, and the pellet is resuspended in 0.3 M sucrose to a concentration of ~6 mg of protein per milliliter. Of this suspension, 0.2–0.3 ml is layered in a Spinco SW 39

⁴¹ J. D. Jamieson and G. E. Palade, *J. Cell Biol.* 34, 577 (1967).

⁴² J. Meldolesi, J. D. Jamieson, and G. E. Palade, *J. Cell Biol.* 49, 109 (1971).

tube on a 5-ml linear sucrose density gradient (1.04 to 2.00 M) and centrifuged for 5 hours at 115,000 g. This results in the appearance of 3 bands on the gradient: the upper band close to the top represents smooth microsomes; the band in the middle contains both rough and smooth microsomes as well as free ribosomes; and the third band, in the lower part, is made up of rough microsomes.

Cation-Containing Sucrose Gradient⁴³

Cleaned pancreas from 48-hour-starved guinea pig is homogenized in 0.44 M sucrose (2 g/10 ml) with a Teflon-glass homogenizer (400–500 rpm, 10 strokes). Twice during homogenization the adherent tissue clumps are removed from the pestle. After centrifugation at 15,000 g for 20 minutes, the supernatant is supplied with CsCl (final concentration 10 mM). Of this suspension, 3.5 ml is placed on a double layer consisting of 2 ml 1.05 M sucrose–15 mM CsCl and 1 ml of 0.6 M sucrose–10 mM CsCl. Centrifugation is performed in a 40.2 rotor (Spinco) at 102,000 g for 120 minutes. The double layer in the 0.6 M sucrose represents smooth microsomes (in this case deriving from the Golgi complex). The pellet together with the adherent fluffy layer consists of rough microsomes.

Remarks

Choice of Method. The simplicity of a method is often decisive, and it is understandable that many laboratories still employ differential centrifugation techniques for the isolation of the two main subfractions⁴⁴ in spite of the apparent cross contamination. Cation-containing gradients are effective and also fulfill one of the most important requirements in work on membrane structure: rapid, time-saving separation. On the other hand, they require a cation-free laboratory environment as well as relatively high quality laboratory animals, which are not readily available everywhere. Because of the heterogeneity of both rough and smooth microsomes, further subfractionation employing gradient technique is of great importance in studying microsomal membranes. Subfractionation of total microsomes by continuous gradients in general gives poor results, which may be explained by electrostatic interaction among differently charged particles. On the other hand, appreciable heterogeneity can be demonstrated by using isolated rough or smooth microsomes as starting fractions. Rough microsomes isolated in the presence of monovalent cations are in aggregated form and therefore cannot be used for further subfractionation.

Chemical Markers. The isolated microsomal particle contains not only membranous proteins but also adsorbed (~30% of the total) and

⁴³ G. Dallner and H. Glaumann, *Abstr. Int. Congr. Biochem.*, 7th 5, 933 (1967).

⁴⁴ Y. Moulé, C. Rouiller, and J. Chauveau, *J. Biophys. Biochem. Cytol.* 7, 547 (1960).

luminal ($\sim 15\%$) proteins, and in many studies these must be removed. Adsorbed basic proteins are removed most simply by suspending the pellet in a sucrose-free medium consisting of 0.15 M Tris-buffer, pH 8.0, followed by recentrifugation.^{30,45} The majority, if not all, of excretory blood proteins in the lumen can be extracted by incubation in distilled water (~ 0.5 mg of protein per milliliter) at 30°C for 15 minutes followed by chilling in an ice-water bath and recentrifugation.^{46,47} In the case of pancreas, the suspension of microsomes in alkaline buffers also extracts most of the secretory proteins.⁴³ The consecutive buffer and water treatments also remove most of the bound ribosomes. The PLP:protein ratio in nonwashed smooth microsomes is ~ 0.34 and in rough microsomes ~ 0.26 . The corresponding ratios for RNA:protein are ~ 0.07 and 0.25, respectively.⁴⁸ The cholesterol content on a PLP basis also differs, being $\sim 12\%$ in smooth, and 7% in rough, microsomes.

Enzymatic Markers. Most of the enzymes studied are more or less evenly distributed during steady-state conditions in total rough and total smooth microsomes¹ (but not in later subfractions of these two main divisions). One of the few exceptions is GDP-mannosyltransferase, which is present mainly or exclusively in rough microsomes.^{49,50} This is true only if GDP-mannose is used as substrate and endogenous protein as acceptor. On the other hand, during dynamic conditions, such as in newborn⁴⁵ and drug-induced animals,⁵¹ the enzymatic composition of the two subfractions differs greatly.

⁴⁵ G. Dallner, P. Siekevitz, and G. E. Palade, *J. Cell Biol.* 30, 97 (1966).

⁴⁶ M. Schramm, B. Eisenkraft, and E. Barkai, *Biochim. Biophys. Acta* 135, 44 (1967).

⁴⁷ H. Glaumann and G. Dallner, *J. Lipid Res.* 9, 720 (1968).

⁴⁸ A part of the free ribosomes, present in the 10,000 g supernatant, remain in the smooth microsomal fraction and contribute to its RNA content.

⁴⁹ J. Molnar, M. Tetas, and H. Chao, *Biochem. Biophys. Res. Commun.* 37, 684 (1969).

⁵⁰ C. M. Redman and M. G. Cherian, *J. Cell Biol.* 52, 231 (1972).

⁵¹ S. Orrenius, *J. Cell Biol.* 26, 725 (1965).

[19] Nondestructive Separation of Rat Liver Rough Microsomes into Ribosomal and Membranous Components

By M. R. ADELMAN, G. BLOBEL, and D. D. SABATINI

Preparation of Rough and Smooth Microsomes

Most fractionation procedures designed to obtain purified microsomes involve the preparation of a postmitochondrial supernatant (PMS) from which smooth (SM) and rough microsomes (RM) and free ribosomes are

EXHIBIT I

PHARMACY LIBRARY
SCHOOL OF PHARMACY

Methods in Enzymology

Volume XXXI

Biomembranes

Part A

EDITED BY

Sidney Fleischer

DEPARTMENT OF MOLECULAR BIOLOGY
VANDERBILT UNIVERSITY, NASHVILLE, TENNESSEE

Lester Packer

DEPARTMENT OF PHYSIOLOGY-ANATOMY
UNIVERSITY OF CALIFORNIA, BERKELEY, CALIFORNIA

Advisory Board

Ronald W. Estabrook
H. Ronald Kaback
Stephen C. Kinsky

Arnost Kleinzeller
George Laties
George E. Palade



ACADEMIC PRESS New York San Francisco London 1974

A Subsidiary of Harcourt Brace Jovanovich, Publishers

COPYRIGHT © 1974, BY ACADEMIC PRESS, INC.

ALL RIGHTS RESERVED.

NO PART OF THIS PUBLICATION MAY BE REPRODUCED OR TRANSMITTED IN ANY FORM OR BY ANY MEANS, ELECTRONIC OR MECHANICAL, INCLUDING PHOTOCOPY, RECORDING, OR ANY INFORMATION STORAGE AND RETRIEVAL SYSTEM, WITHOUT PERMISSION IN WRITING FROM THE PUBLISHER.

ACADEMIC PRESS, INC.

111 Fifth Avenue, New York, New York 10003

United Kingdom Edition published by

ACADEMIC PRESS, INC. (LONDON) LTD.

24/28 Oval Road, London NW1

Library of Congress Cataloging in Publication Data

Main entry under title:

Biomembranes, part A-

(Methods in enzymology, v. 31-

Includes bibliographies.

1. Cell membranes. 2. Cell fractionation. 3. Cell
organelles. I. Fleischer, Sidney, ed. II. Packer,
Lester, ed. III. Estabrook, Ronald W., ed.

[DNLM: 1. Cell membrane. W1ME9615K v. 31 / QH601
B6193]

QP601.C733 vol. 31

[QH601]

574.1'925'08s

[574.8'75]

ISBN 0-12-181894-2

74-11352

PRINTED IN THE UNITED STATES OF AMERICA

luminal ($\sim 15\%$) proteins, and in many studies these must be removed. Adsorbed basic proteins are removed most simply by suspending the pellet in a sucrose-free medium consisting of $0.15\text{ }M$ Tris-buffer, pH 8.0, followed by recentrifugation.^{30,45} The majority, if not all, of excretory blood proteins in the lumen can be extracted by incubation in distilled water (~ 0.5 mg of protein per milliliter) at 30°C for 15 minutes followed by chilling in an ice-water bath and recentrifugation.^{46,47} In the case of pancreas, the suspension of microsomes in alkaline buffers also extracts most of the secretory proteins.⁴⁸ The consecutive buffer and water treatments also remove most of the bound ribosomes. The PLP:protein ratio in nonwashed smooth microsomes is ~ 0.34 and in rough microsomes ~ 0.26 . The corresponding ratios for RNA:protein are ~ 0.07 and 0.25 , respectively.⁴⁸ The cholesterol content on a PLP basis also differs, being $\sim 12\%$ in smooth, and 7% in rough, microsomes.

Enzymatic Markers. Most of the enzymes studied are more or less evenly distributed during steady-state conditions in total rough and total smooth microsomes¹ (but not in later subfractions of these two main divisions). One of the few exceptions is GDP-mannosyltransferase, which is present mainly or exclusively in rough microsomes.^{49,50} This is true only if GDP-mannose is used as substrate and endogenous protein as acceptor. On the other hand, during dynamic conditions, such as in newborn⁴⁵ and drug-induced animals,⁵¹ the enzymatic composition of the two subfractions differs greatly.

⁴⁵ G. Dallner, P. Siekevitz, and G. E. Palade, *J. Cell Biol.* 30, 97 (1966).

⁴⁶ M. Schramm, B. Eisenkraft, and E. Barkai, *Biochim. Biophys. Acta* 135, 44 (1967).

⁴⁷ H. Glaumann and G. Dallner, *J. Lipid Res.* 9, 720 (1968).

⁴⁸ A part of the free ribosomes, present in the $10,000\text{ }g$ supernatant, remain in the smooth microsomal fraction and contribute to its RNA content.

⁴⁹ J. Molnar, M. Tetas, and H. Chao, *Biochem. Biophys. Res. Commun.* 37, 684 (1969).

⁵⁰ C. M. Redman and M. G. Cherian, *J. Cell Biol.* 52, 231 (1972).

⁵¹ S. Orrenius, *J. Cell Biol.* 26, 725 (1965).

[19] Nondestructive Separation of Rat Liver Rough Microsomes into Ribosomal and Membranous Components

By M. R. ADELMAN, G. BLOBEL, and D. D. SABATINI

Preparation of Rough and Smooth Microsomes

Most fractionation procedures designed to obtain purified microsomes involve the preparation of a postmitochondrial supernatant (PMS) from which smooth (SM) and rough microsomes (RM) and free ribosomes are

prepared, discontinuous sucrose density gradients being used. It is known that the RNA of membrane-bound ribosomes amounts to ~60% of the total RNA of rat liver.¹ Usually, 50% or more of the total RNA is sedimented with the nuclei and mitochondria, and most of this reflects the loss of RM.¹⁻⁸ Furthermore, the bound ribosomes in the PMS are only partially recovered in the purified RM fraction. Such losses of RM elements during cell fractionation should be avoidable, however. It is known that mitochondria can be washed relatively free of contaminating RM if simple sucrose solutions are used,^{4,5} but that the addition of mono- or divalent cations must be avoided since these cause clumping and aggregation of membranous organelles.^{6,7} Nuclei, on the other hand, cannot be washed extensively in salt-free media, since they tend to swell and produce a nucleoprotein gel.^{8,9} Rather pure nuclei can be separated from total homogenates, however, by sedimentation through dense sucrose solutions.^{9,10} The following fractionation scheme,¹¹ which yields RM preparations representing nearly 50% of the membrane-bound ribosomes of rat liver, has been devised following the above considerations. The method is in no way a radical departure from previously published ones. Procedures in common use involve sedimentation through concentrated sucrose media to purify nuclei,^{9,10} washes with simple sucrose media to reduce the microsomal contamination of mitochondria,^{4,5} and sedimentation through discontinuous sucrose density gradients to separate SM, RM, and free ribosome fractions.¹²⁻¹⁵ The scheme described here simply represents one convenient

¹ G. Blobel and V. R. Potter, *J. Mol. Biol.* 26, 279 (1968).

² R. R. Howell, J. N. Loeb, and G. M. Tomkins, *Proc. Nat. Acad. Sci. U.S.* 52, 1241 (1964).

³ A. Bergstrand and G. Dallner, *Anal. Biochem.* 29, 351 (1969).

⁴ C. de Duve, B. C. Pressman, R. Gianetto, R. Wattiaux, and F. Appelmans, *Biochem. J.* 66, 1955 (1955).

⁵ A. Amar-Costesec, H. Beaufay, E. Feytmans, D. Thinès-Semploux, and J. Berthet, in "Microsomes and Drug Oxidations" (J. R. Gillette, A. H. Conney, G. J. Cosmides, R. W. Estabrook, J. R. Fouts, and G. J. Mannering, eds.). Academic Press, New York, 1969.

⁶ W. C. Schneider and G. H. Hogeboom, *Cancer Res.* 11, 1 (1951).

⁷ G. H. Hogeboom, W. C. Schneider, and G. E. Palade, *J. Biol. Chem.* 172, 619 (1948).

⁸ R. M. Schneider and M. L. Peterman, *Cancer Res.* 10, 751 (1950).

⁹ M. Muramatsu, in "Methods of Cell Physiology" (D. M. Prescott, ed.), Vol. IV, p. 195. Academic Press, New York, 1970.

¹⁰ G. Blobel and V. R. Potter, *Science* 154, 1662 (1966).

¹¹ M. R. Adelman, G. Blobel, and D. D. Sabatini, *J. Cell Biol.* 56, 191 (1973a).

¹² E. Reid, in "Enzyme Cytology" (D. B. Roodyn, ed.), p. 321. Academic Press, New York, 1967.

¹³ G. Dallner and L. Ernster, *J. Histochem. Cytochem.* 16, 611 (1968).

¹⁴ G. Blobel and D. D. Sabatini, *J. Cell Biol.* 45, 130 (1970).

¹⁵ D. D. Sabatini and G. Blobel, *J. Cell Biol.* 45, 146 (1970).

combination of these techniques designed especially to maximize the yield of membrane bound ribosomes.

All solutions are prepared using deionized distilled water, Millipore filtered ($0.45\ \mu\text{m}$ for most, $1.2\ \mu\text{m}$ for concentrated sucrose stock solutions), and stored in the cold. All operations, unless otherwise specified, are carried out in an IEC B-60 centrifuge (International Equipment Co., Needham Heights, Massachusetts). In the figures, the notation "30 min-44K-A211 (200,000)" is used to denote a 30-minute centrifugation at 44,000 rpm in the A211 rotor under which conditions $g_{\text{max}} \sim 200,000$. In Spinco centrifuges (Beckman Instruments, etc.) rotors A211 and SB110 can be replaced with Spinco rotors 42.1 or Ti 60 and SW 27, respectively. All pH's are those measured at room temperature.

Male Sprague-Dawley rats (~ 120 – $150\ \text{g}$) starved for about 18 hours are sacrificed between 9:00 and 10:00 AM by decapitation with guillotine (Harvard Apparatus Co., Inc., Millis, Massachusetts). Livers are quickly excised, immersed into ice-cold $0.25\ M$ sucrose and cut into three to five large pieces. All subsequent operations are carried out in the cold room. Pieces of liver are blotted on absorbent paper and forced through a tissue press consisting of a piston and a stainless steel plate with 1-mm perforations. The pulp is weighed, slurried with 2 ml of $1.0\ M$ sucrose solution per gram, and homogenized (8–10 passes) with a Teflon pestle, motor-driven tissue grinder (Arthur H. Thomas Co., Philadelphia, Pennsylvania size C, pestle rotating at 1000–2000 rpm). Slightly more or less vigorous homogenization does not affect the fractionation significantly.

The fractionation scheme is described below with reference to the numbered steps in flow diagrams I and II (Figs. 1 and 2). The scheme essentially involves first removing nuclei from a liver homogenate, the density of which is adjusted so that most other membranous organelles either float, are isopycnic, or sediment very slowly during the appropriate centrifugation. No ionic components (KCl, Tris, MgCl_2 , etc.) are introduced into the homogenate. The postnuclear supernatant is then diluted to a density low enough to allow sedimentation of mitochondria which are washed with relatively ion-free sucrose solutions. The combined PMS is then fractionated on a discontinuous sucrose density gradient (which essentially contains no ions) into smooth and rough microsome and free ribosome fractions.

Flow Diagram I (Fig. 1)

Step a. The liver pulp is homogenized in 2 volumes of $1.0\ M$ sucrose (2 ml/g): a higher sucrose concentration makes homogenization more difficult, while a lower concentration necessitates a greater dilution of the homogenate in the subsequent density adjustment step. The homogenate is filtered through a single layer of Nytex cloth (No. 130, Tobler, Ernest

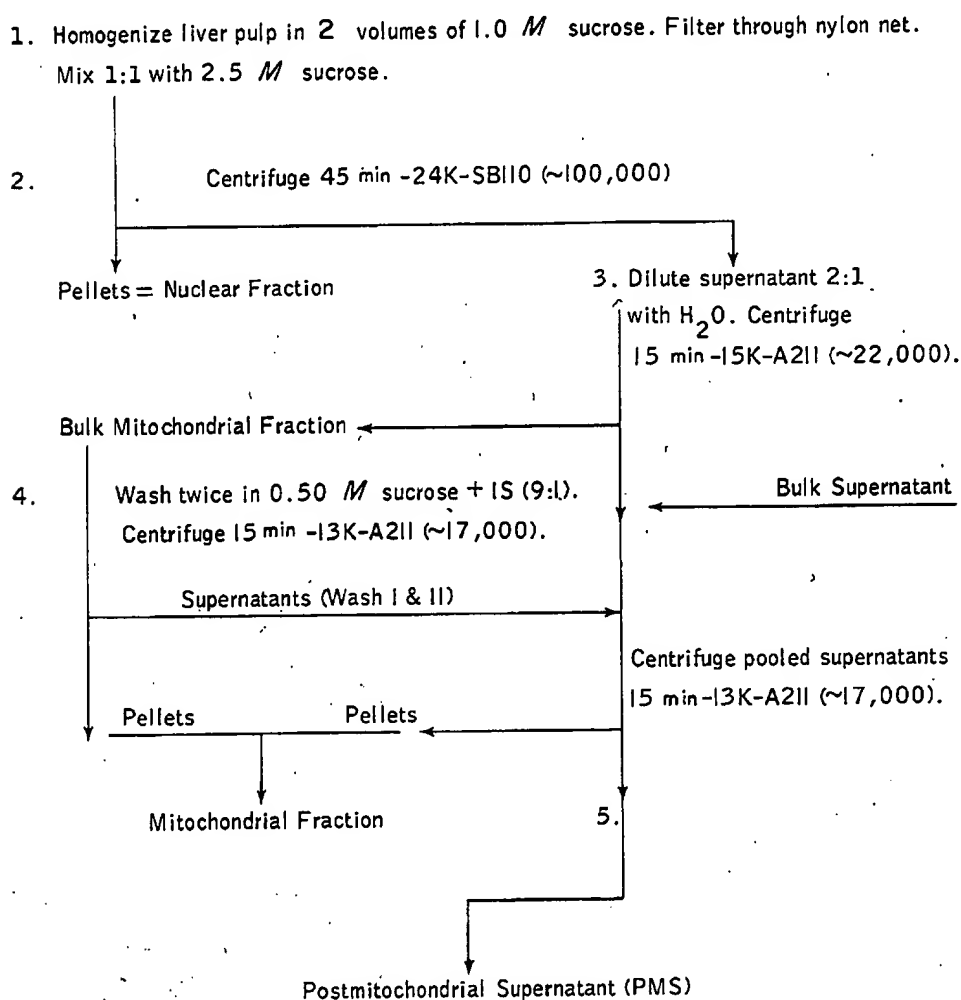


FIG. 1. Flow diagram I.

and Traber, Inc., New York); this removes connective tissue debris and improves the subsequent separation of nuclei. To the filtered homogenate, an equal volume of 2.5 *M* sucrose is added, followed by thorough mixing (repeated inversion in a stoppered measuring cylinder) thus producing a mixture of suitable density. Normally, 50 ml of filtered homogenate (representing ~17 g of liver pulp derived from four or five rats) are processed in this manner.

Step b. The 100 ml of density-adjusted homogenate are transferred to four SB 110 tubes and each is overlaid with 1 ml of 1.0 *M* sucrose to assure that material which floats to the top during the ensuing centrifugation is not exposed to an air-water interface. After centrifugation [45 minutes at 24,000 rpm in the IEC rotor SB 110 (~100,000 *g*)], each tube contains a well-packed, mottled, pinkish-gray pellet, a tan supernatant, and a thick, reddish-tan pellicle. Shorter centrifugation (15–30 minutes) often

fails to give well packed pellets; longer centrifugation does not increase the yield of nuclei. Recentrifugation of the rehomogenized supernatant (see below) gives a small pellet with only marginal increase in the overall yield of nuclei. Separation of nuclei under these conditions of minimal ion content does lead to some swelling and gelation. However, since the elimination of ions lessens the aggregation of membranous organelles, this disadvantage is deemed acceptable. Attempts to remove nuclei by step gradient centrifugation of the entire homogenate¹⁵ have been unsuccessful in that, with the large volumes used, considerable DNA is trapped at the lower interface and does not sediment further, even after prolonged centrifugation. This trapping occurs whether or not the underlay contains ion components (e.g., TKM: 0.050 M Tris·HCl, pH 7.5, 25 mM KCl, 5 mM MgCl₂).

Step c. The pellicle is dislodged from the walls of the centrifuge tube with a metal spatula, and, together with the viscous supernatant, carefully transferred into the tissue grinder and homogenized (two or three passes) to disperse all clumps. To the ~100 ml of this dispersed postnuclear supernatant 50 ml of water are added, with thorough mixing, to achieve a dilution sufficient to allow subsequent sedimentation of the mitochondria. The mixture is divided into six portions and centrifuged for 15 minutes at 15,000 rpm in the IEC rotor A211 (~22,000 g).

Step d. The pink, turbid supernatant is decanted and stored in a beaker (to which the mitochondrial washes are subsequently added). The pellets, tan with a small red bottom layer (presumably erythrocytes), are suspended and homogenized in 25 ml of a mixture of 9 parts 0.50 M sucrose and 1 part inhibitory supernatant (IS).¹⁶ The inclusion of IS at this point is a precaution to minimize nuclease attack on bound polysomes. The mitochondrial suspension is placed in two centrifuge tubes and sedimented for 15 minutes at 13,000 rpm in the IEC rotor A211 (~17,000 g). The supernatant is decanted and saved and the entire mitochondrial washing is repeated. The pellets obtained after each wash show a dark tan, tightly packed lower layer and a lighter tan, less tightly packed upper layer. In addition, an appreciable amount of pinkish, fluffy material is found which is only lightly packed and is decanted with the supernatants. Further washes of the mitochondrial fraction are ineffective in removing residual RNA. If the two washes are carried out with 0.25 M STKM, (0.25 M

¹⁶ IS: Inhibitory supernatant. Homogenize rat liver in 2 ml of 0.25 M per gram of sucrose. Centrifuge for 15 minutes at 20,000 rpm in the IEC rotor A211 to remove large debris. Recentrifuge the supernatant 2 hours at 44,000 rpm in the IEC rotor A211 (200,000 g). Remove the clear red supernatant (avoiding the floating milky scum as well as the loosely pelleted material. This supernatant, referred to as IS, stored frozen until use is a source of RNase inhibitor.¹⁷

¹⁷ G. Blobel and V. R. Potter, *Proc. Nat. Acad. Sci. U.S.* 55, 1283 (1966).

sucrose with the ionic composition of TKM) the contamination of the mitochondrial fraction with RNA is even greater.

Step e. The combined mitochondrial supernatants are put into 8 tubes and centrifuged for 15 minutes at 13,000 rpm in the IEC rotor A211 ($\sim 17,000 g$). Each tube contains a tiny two-layer pellet (as in step d above) and a large layer of loosely packed, pinkish, fluffy material. The supernatants are decanted with gentle swirling to assure transfer of the pinkish fluff, and then gently homogenize to disperse any clumps. The pooled supernatants constitute the final postmitochondrial supernatant (PMS). All the two-layer pellets (steps d and e) are combined and suspended for analysis as the "mitochondrial" fraction.

Flow Diagram II (Fig. 2)

The PMS (~ 180 – 190 ml, derived from ~ 17 g of liver) is used to separate free ribosomes, rough, and smooth microsomes on a discontinuous sucrose gradient.

Step a. The total PMS is distributed evenly in 8 centrifuge tubes, and, with a syringe and large steel cannula, underlaid with: (i) 4 ml of a mixture of 3 parts $2.0 M$ sucrose plus 1 part IS, and (ii) 1 ml of $2.0 M$ STKM. Layer i serves to separate rough (RM) from relatively smooth (SM) microsomes, and is approximately equivalent in density to $1.5 M$ sucrose. While the choice of this density cutoff results in an appreciable loss of

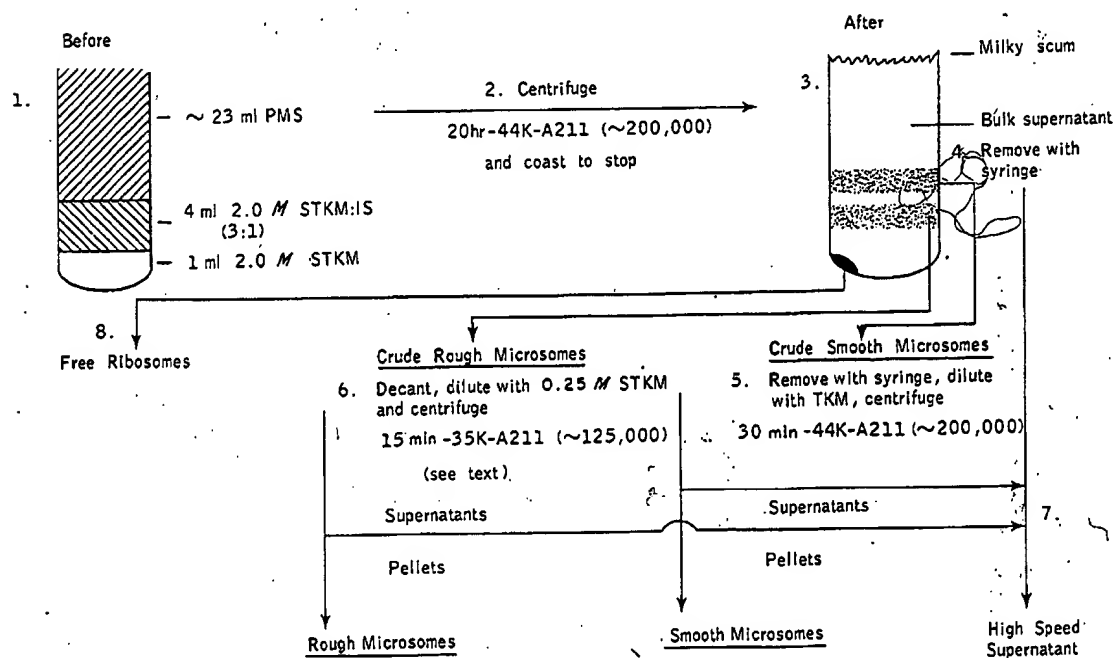


FIG. 2. Flow diagram II.

membrane-bound RNA to the SM fraction, it serves to minimize the extent to which mitochondrial fragments contaminate the RM. The addition of ions (e.g., TKM) to the underlay is avoided, since this leads to poorer separation of RM from SM (as shown by the RNA distribution). If IS is not present in the 1.5 M sucrose underlay, free polysomes are more extensively degraded, sediment more slowly, and therefore heavily contaminate the RM fraction.

Layer ii serves to separate RM from free ribosomes, which sediment through the 2.0 M STKM into a pellet. Addition of IS to the 2.0 M STKM layer does not improve the yield of preservation of free polysomes, so long as IS is present in layer i, above. Use of 2.0 M sucrose (without TKM) gives low yields of free ribosomes.

Step b. The step gradients are centrifuged 20 hours at 44,000 rpm in the IEC rotor A211 ($\sim 200,000$ g), and the rotor is allowed to coast to a stop. Shorter centrifugation times greatly decrease the yield of free ribosomes, and, if short enough (>4 –8 hours), result in poor separation of RM from SM. Even after 20 hours' centrifugation, sedimentation of free ribosomes is only two-thirds to three-fourths complete. These incompletely sedimented free ribosomes (mostly monomers) are easily removed from the RM during the subsequent differential centrifugation (step f, below).

Step c. As indicated in flow diagram II (Fig. 2), after centrifugation, each tube contains a clear, pink-to-red supernatant above which floats a thin, milky scum. Membranous material accumulates in the lower part of the tube. Upon close examination, it can be seen that there are two reddish-brown membranous bands, one at each interface, with a small, relatively clear zone between them. Under these conditions of separation, the upper band (crude smooth microsomes) is uniform, with no sign of clumping or adherence to the tube walls. If TKM is present in the ~ 1.5 M sucrose underlay (or if the microsomes in the PMS are first sedimented and re-suspended to allow application of a more concentrated sample to the discontinuous gradient), the upper membrane band is not uniform. Clumping of material in this band was found to be always associated with higher contamination of SM with RM and lower yields of purified RM. The lower membrane band contains crude rough microsomes which, having been in contact with the 2.0 M STKM, are somewhat clumped. Free ribosomes sediment through the 2.0 M STKM form a small, pale-orange pellet, the orange color being due to contaminating ferritin.

Step d. A syringe with a large steel cannula is used to remove the bulk clear supernatant (including the floating scum) from each tube and to transfer this to a beaker.

Step e. Using the same syringe and cannula, the upper membrane layer

is removed and transferred to a graduated cylinder, care being taken not to disturb the lower membrane layer. Including the residual supernatant fluid removed with this layer, a total of 50–60 ml of crude SM suspension is obtained. This is diluted with TKM to ~150 ml, distributed in six tubes, and centrifuged 30 minutes at 44,000 rpm in the IEC rotor A211 (~200,000 g). The clear supernatants are then added to the bulk supernatant (step d) while the pellets constitute the SM fraction.

Step f. The residual fluid contents of the step gradient tubes are decanted into a graduated cylinder. Each tube is then gently rinsed with ~5 ml of 0.25 M STKM, and the rinses added to the same cylinder, care being taken to maximize transfer of the turbid fluid while minimizing disturbance of the ribosome pellets. This crude RM suspension is brought to a volume of ~100 ml with 0.25 M STKM, gently homogenized, and centrifuged (in six tubes) 15 minutes at 35,000 rpm in the IEC rotor A211 (~125,000 g). The supernatant is added to that stored from steps d and e. The pellets are homogenized in 100 ml of 0.25 M STKM and recentrifuged (6 tubes) 15 minutes at 30,000 rpm in the IEC A211 (~95,000 g). The supernatants are saved as above, while the pellets constitute the fraction.

Step g. The combined supernatants (steps d–f) constitute the high-speed supernatant.

Step h. The small, pale-orange, slightly opalescent pellets left in the step gradient tubes constitute the free ribosome fraction. The pellets of free ribosomes, RM and SM can be frozen and stored at -20°C . Since RM and SM stored in this way form aggregates it is better to store the samples after resuspension in 0.25 M STKM (one pellet in ~2.0 ml) to which 4–6 ml of glycerol are added. The suspensions are kept at -20°C . RM and SM can be recovered from such glycerol suspensions by dilution (at least 5-fold) with the appropriate solution and centrifugation.

Analytical data on the various cell fractions are presented in Table I. The nuclear fraction, which accounts for ~80% of the total DNA, is only slightly contaminated with mitochondria, as judged by the low cytochrome oxidase activity. The small amount of RNA present, being not much higher than that found in nuclei purified by other procedures,¹⁸ suggests minimal trapping of ribosomal and/or rough microsomal elements. The mitochondrial fraction, which accounts for ~85% of the recovered cytochrome oxidase, contains the bulk of the residual DNA. In addition, this fraction contains ~20% of the total RNA. The assumption that this RNA reflects the presence of RM is supported by the observation that treatment of the mitochondrial fraction with puromycin, under appropriate ionic conditions, leads to release of ribosomal subunits and “stripped” membranes

¹⁸ A. Fleck and H. N. Munro, *Biochim. Biophys. Acta* 55, 571 (1960).

TABLE I
ANALYTICAL DATA ON RAT LIVER CELL FRACTIONS

Fraction	% RNA	% DNA	% Protein	% Cytochrome oxidase	Mg PLP mg protein	Catalase (% units recovered)	Acid phosphatase (% units recovered)
Homogenate	^a	^a	^a	^a	0.248	^b	^c
Nuclei	7.7	80.5	9.2	4.0	0.170	3.3	4.3
Mitochondria	20.4	16.2	33.9	85.9	0.219	7.6	32.9
SM	5.6	0.6	7.8	4.8	0.660	3.4	18.4
RM	28.3	1.3	7.3	4.5	0.679	5.4	10.8
Ribosome	17.8	0.3	1.4	0.05	0.078	0.9	0.3
Supernatant	19.8	1.1	40.5	0.81	0.071	80.5	33.4

^a The amount in each fraction is expressed as a percent of the sum of the amounts recovered in all fractions. Expressed as a percent of the contents of the homogenate, recoveries of RNA, DNA, protein, and cytochrome oxidase were 92, 103, 97, and 141%, respectively. The apparent overrecovery of cytochrome oxidase presumably reflects the difficulty of accurately assaying the activity in the homogenate.

^b Homogenate contained 810 U. Total recovered = 1033.

^c Homogenate contained 167 U. Total recovered = 196.

(see next section). The significance of and the reasons for the persistent contamination of the mitochondrial fraction with RM remain unclear; numerous modifications of the fractionation scheme have failed to minimize the contamination. About 28% of the RNA in rat liver, is recovered in the RM fraction while the SM and RM fractions jointly contain ~35% of the total RNA. Virtually all the RNA in these RM is due to ribosomes tightly bound to the membranes (i.e., contamination with free ribosomes is negligible). Assuming that 60% of all liver RNA is the ribosomal RNA of membrane-bound ribosomes,¹ the RM fraction contains nearly 50% of all the membrane-bound ribosomes. The RNA:protein ratio of these RM (0.20–0.25 mg/mg) is in good agreement with results of others. The RM contain ~5% of the cytochrome oxidase and a small amount of DNA, the significance of which remains obscure.¹⁹

The free ribosome fraction contains slightly less than the expected 20% of the total RNA,¹ because some of the free ribosomes fail to sediment through the 2.0 M STKM layer of the step gradient and are left in the crude RM layer. However, during the washing of the RM these free ribosomes, along with some small RM elements, are transferred to the combined high-speed supernatant fraction. Prolonged centrifugation of the supernatant leads to sedimentation of one-third to one-half of the RNA in this fraction, primarily as a mixture of free and bound ribosomes.

Phospholipid phosphorus analysis indicates the expected distribution of lipids.^{12,13} Both SM and RM fractions contain 0.6–0.7 mg of PLP per milligram of protein. Analysis of catalase, as a peroxisomal marker,²⁰ reveals ~80% of the activity in the supernatant fraction, which suggests (as might be expected in view of the repeated homogenization involved in this procedure) extensive rupture of peroxisomes. However, since a rather large fraction of rat liver catalase may exist in nonparticulate form²¹ the exact extent of peroxisome rupture is difficult to assess. The RM fraction contains ~5% of the recovered catalase activity. Damage to lysosomes seems less extensive, since only ~33% of the acid phosphatase activity is released to the supernatant, while an equal amount was found in the mitochondrial fraction (which is equivalent to the M + L fraction of de Duve *et al.*⁴). The RM account for ~10% of the recovered acid phosphatase activity. Electron microscopic examination of the SM and RM fractions corroborates these biochemical analyses. The SM consist of a fairly heterogeneous population of membranous vesicles most of which are smooth-surfaced, although occasional ribosome-studded vesicles are found. In addition,

¹⁹ W. C. Schneider and E. L. Kuff, *J. Biol. Chem.* 244, 4843 (1969).

²⁰ F. Leighton, B. Poole, H. Beaufay, P. Baudhuin, J. W. Coffey, S. Fowler, and C. de Duve, *J. Cell Biol.* 37, 482 (1968).

²¹ R. S. Holmes and C. J. Masters, *Arch. Biochem. Biophys.* 148, 217 (1972).

mitochondrial fragments, presumptive lysosomes, and large, flattened sheets (presumably plasma membrane) are present. The RM fraction is considerably more homogeneous, consisting primarily of ribosome-studded vesicles, which, when sectioned tangentially show a fairly high density of attached ribosomes.

The ribosomes in the RM and free ribosome fractions have been shown to be active in an *in vitro* amino acid incorporation mixture with endogenous messenger and to be stimulated by the addition of polyuridylic acid.

Separation of Ribosomes from Membranes of Rough Microsomes

It is known that ribosomes interact with microsomal membranes via the large (60 S) subunit²² and that the nascent polypeptide chain, which grows within a protected region in this subunit,^{14,23} enters into close relationship with the membrane immediately upon emerging from the ribosome.¹⁵ Chelating agents²² and concentrated salt solutions²⁴ devoid of magnesium ions can be used to release some or most of the bound ribosomes from rough microsomes (RM), but such treatments produce a mixture of intact membranes and damaged or denatured ribosomes. On the other hand, detergents, which have been extensively used to release functional ribosomes from RM,²⁵ are effective only by greatly altering or destroying membrane structure. Recent developments²⁶ have made it possible to nondestructively separate RM into the component parts, viz., ribosomes and membranes. These developments are based on the finding²⁷ that treatment of free polysomes with puromycin in solutions of high ionic strength leads to the disassembly of the polysomes into functionally viable ribosomal subunits.

Examination of the effect of puromycin on the stability of ribosome-membrane interaction has shown²⁶ that the combined action of this aminoacyl tRNA analog and appropriate high KCl conditions can be used to produce an efficient release of almost all the bound ribosomes from RM. Exposure of RM to a solution containing high KCl but no puromycin, results in release of some ribosomes (Fig. 3), the exact extent of release and state of the ribosomes being a function of the KCl and MgCl₂ concentrations, as well as of the time and temperature of treatment. It does not appear possible, however, to remove all ribosomes from RM by alterations in ionic constituents alone, unless conditions are used which lead to unfolding

²² D. D. Sabatini, Y. Tashiro, and G. E. Palade, *J. Mol. Biol.* 19, 503 (1966).

²³ L. I. Malkin and A. Rich, *J. Mol. Biol.* 26, 329 (1967).

²⁴ T. Scott-Burden and A. O. Hawtrey, *Biochem. J.* 115, 1063 (1969).

²⁵ J. K. Kirsh, P. Siekevitz, and G. E. Palade, *J. Biol. Chem.* 235, 1419 (1960).

²⁶ M. R. Adelman, D. D. Sabatini, and G. Blobel, *J. Cell Biol.* 56, 206 (1973).

²⁷ G. Blobel and D. Sabatini, *Proc. Nat. Acad. Sci. U.S.* 68, 390 (1971).

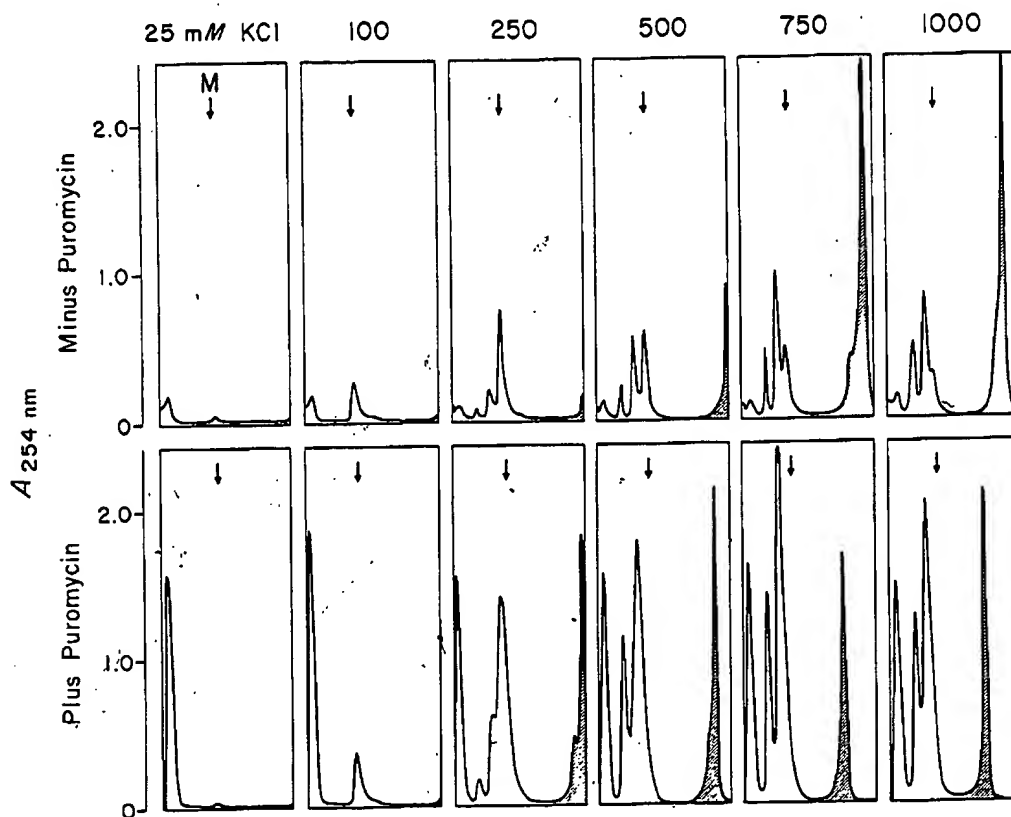


FIG. 3. Release of ribosomes from rough microsomes (RM) by combined action of high KCl and puromycin. Equal amounts of RM were incubated in S 250, Mg 5, T 50 plus 25, 100, 250, 500, 750, or 1000 mM KCl in the absence (upper panels) or in the presence (lower panels) of 0.79 mM puromycin. Samples were incubated for 70 minutes at 0°C, 10 minutes at 37°C, and then 10 minutes at room temperature. Samples (0.45 ml, 0.37 mg RNA) were applied to 15–40% sucrose gradients containing the appropriate K, Mg, T buffer. Sedimentation was at 20°C: 1¼ hours 40K-SB283 (~270,000). All profiles are presented with top of gradient at left, and the direction of sedimentation is from left to right. The small arrow (M) indicates the position of the ribosomal monomer (80 S). Gradients run at $[KCl] \geq 250$ mM also show small (40 S) and large (60 S) subunit peaks. The shading in the lower portions of these gradients is added to indicate that the UV absorption corresponded to a region in which membranes were visible (turbidity) but no attempt is made to indicate the exact extent of the turbidity. Membranous bands are designated with the symbol Mb. From ref. 26.

—hence denaturation—of the ribosomal subunits. But, under ionic conditions where partial release of functional ribosomes (or subunits) occurs, puromycin strongly enhances the extent of release. It is possible (see below) to remove up to 85% of all bound ribosomes by the combined action of puromycin and high KCl under conditions where ribosome, as well as membrane, integrity is maintained.

Those membrane bound ribosomes which are released solely in response to elevated ionic strength appear to be a mixture of inactive ribo-

somes and of ones bearing relatively short nascent chains. Experiments with [^3H]puromycin and/or [^3H]leucine pulse-labeled RM have shown that the puromycin releasable ribosomes react with the drug at low KCl and release their nascent chains vectorially to the microsomal membrane. However, at low ionic strength, some as-yet-unspecified interaction between the large ribosomal subunit and the membrane is maintained and only when the KCl concentration is elevated are the ribosomes released. Thus all membrane-bound ribosomes are attached via a large subunit-membrane interaction. In addition, some, but not all, ribosomes are tightly held to the RM by an interaction involving the nascent polypeptide chain. Only when both interactions are destabilized, by the combined action of high KCl and puromycin can the bound ribosomes be released in a nondestructive manner.

For routine disassembly RM (prepared as described in the preceding section) are suspended in 0.25 M sucrose, 0.75 M KCl, 5 mM MgCl_2 , 50 mM Tris·HCl, pH 7.5 plus 1 mM puromycin at a final concentration of 1–2 mg RNA/ml (5–10 mg protein/ml). The suspension is then incubated for 1–2 hours at room temperature. A shorter incubation time (15–30 minutes) at 37°C is also effective but variable results, some suggestive of large subunit breakdown, have been found using the high temperature. The reaction mixture can be directly separated into large and small subunits and stripped membrane fractions by zone sedimentation in sucrose density gradients (see legend to Fig. 3). The appropriate zones are collected separately, diluted with a suitable buffer (e.g., TKM) and centrifuged: 15 minutes at 30,000 rpm in the IEC rotor A211 ($\sim 90,000$ g) for the stripped membranes; 3 hours at 44,000 rpm in the IEC rotor A211 ($\sim 200,000$ g) for the ribosomal subunits. It should be noted that density gradient analyses such as those in Fig. 3 are considerably facilitated by the tendency to aggregate of RM (or stripped membranes therefrom) which have been stored frozen in pellet form. When RM which are freshly prepared or have been stored after suspension in glycerol are used, the membranes aggregate less, form broader bands in the gradients (because they take longer to reach their isopycnic position) and are thus less well resolved from the ribosomal subunits. When stripped membranes, but not ribosomal subunits, are required the reaction mixtures can be subjected directly to differential centrifugation 15 minutes at 30,000 rpm in the IEC rotor A211 ($\sim 90,000$ g) and the membrane pellets may be washed as desired by repeated suspension (gentle homogenization) in and resedimentation from a suitable washing medium, such as 0.25 M sucrose containing 50 mM Tris·HCl pH 7.5, 25 mM KCl, and 5 mM MgCl_2 .

By subjecting RM to the above protocol, it is possible to prepare stripped membranes which have released $\sim 85\%$ of their bound RNA (Table II). The exact nature of the residual 15% is not clear; these resid-

TABLE II
CHEMICAL ANALYSIS OF ROUGH (RM) AND SMOOTH (SM) MICROSOMES BEFORE AND AFTER
STRIPPING OF RIBOSOMES WITH KCl AND PUROMYCIN^a

Sample	Protein (mg/ml)	RNA (mg/ml)	PLP (mg/ml)	[³ H]RNA (cpm/mg RNA)	RNA/protein (mg/mg)	RNA/PLP (mg/mg)	PLP/protein (mg/mg)
RM	9.66	2.07	5.31	25,400	0.214	0.389	0.550
Stripped RM	6.57	0.358	5.20	21,600	0.054	0.069	0.791
SM	12.2	0.498	7.10	24,500	0.041	0.070	0.581
Stripped SM	7.95	0.063	5.46	12,600	0.008	0.012	0.687

^a Both rough microsomes and smooth microsomes were prepared at the same time from rats which had received an injection of [³H]-orotic acid (200 μ Ci, 2.5 mCi/mol) ~40 hours before sacrifice. RM and SM pellets were resuspended in S 250, K 25, Mg 5, T 50. Samples of each were incubated for 2 hours at room temperature in the presence of (final concentrations) S 250, K 750, Mg 5, T 50, and 0.63 mM puromycin. The samples were diluted with an excess of room temperature K 750, Mg 5, T 50 and centrifuged at room temperature 15 minutes, 30K-A211 (~90,000). The pellets were resuspended in cold buffer and recentrifuged. Each pellet was then resuspended in S 250, K 25, Mg 5, T 50 to the same volume as the original sample. Samples of the untreated RM and SM, as well as the KCl-puromycin-treated microsomes, were analyzed for protein, phospholipid phosphorus, RNA, and ³H cpm in the RNA hydrolysate.

ual ribosomes may be removed (in denatured form) by washing the membranes with 1.0 M KCl (no MgCl_2). It must be reemphasized, however, that total removal of all bound ribosomes has been achieved only under conditions leading to extensive unfolding of the subunits. With the nondestructive procedure presented here, ~85% of all bound ribosomes are recovered as subunits which are at least partially active in translating polyuridylic acid in an *in vitro* amino acid incorporating system. The stripped membranes are recovered as closed, apparently intact vesicles. The data of other workers indicate that the ionic conditions employed do not markedly affect characteristic membrane enzymes.

[20] Procedure for the Selective Release of Content from Microsomal Vesicles without Membrane Disassembly

By G. KREIBICH and D. D. SABATINI

Preparation of Microsomes

Rough microsomes (RM) and smooth microsomes (SM) are prepared by the procedure of Adelman *et al.*¹ (see this volume, 19a) from male albino rats of the Sprague-Dawley strain. Microsome pellets (10–30 mg protein per fraction) are stored at -20°C to -40°C for up to 2 months. Alternatively, and to reduce aggregation,² freshly prepared microsomes can be resuspended in 0.25 M sucrose, 25 mM KCl, 50 mM Tris·HCl pH 7.4, 5 mM MgCl_2 , mixed with 2 volumes of glycerol and kept at -20° to -40°C . Before use, the microsomes stored in glycerol are diluted four times with a solution containing 0.25 M sucrose, 0.5 M KCl, 50 mM Tris·HCl pH 7.5, 10 mM MgCl_2 , and recovered by sedimentation (15 minutes at 40,000 rpm in the IEC rotor A321). Microsomes stored as pellets are washed once (20 minutes at 20,000 rpm in the IEC A211 or in the Ti 60 Spinco rotors) in a medium of high ionic strength (HSB) (25 mM sucrose, 50 mM Tris·HCl pH 7.5, 0.5 M KCl, 10 mM MgCl_2).

From 22 g of rat liver (4–5, 120–150 g rats) an average of 180 mg protein is recovered in RM and 190 mg protein in SM.

Detergent Treatment

Table I lists five detergents of different polarity which can be used to release the content of microsomes without producing membrane disassem-

¹ M. R. Adelman, G. Blobel, and D. D. Sabatini, *J. Cell Biol.* 56, 191 (1973).

² D. Borgese, G. Blobel, and D. D. Sabatini, *J. Mol. Biol.* 74, 415 (1973).

Methods in Enzymology

Volume LII

Biomembranes

*Part C: Biological Oxidations
Microsomal, Cytochrome P-450, and Other
Hemoprotein Systems*

EDITED BY

Sidney Fleischer

DEPARTMENT OF MOLECULAR BIOLOGY
VANDERBILT UNIVERSITY, NASHVILLE, TENNESSEE

Lester Packer

MEMBRANE BIOENERGETICS GROUP
DEPARTMENT OF PHYSIOLOGY-ANATOMY
UNIVERSITY OF CALIFORNIA, BERKELEY, CALIFORNIA

Editorial Advisory Board

Lars Ernster
Ronald W. Estabrook
Frank Gibson

Youssef Hatefi
Martin Klingenberg
David F. Wilson



ACADEMIC PRESS New York San Francisco London 1978

A Subsidiary of Harcourt Brace Jovanovich, Publishers

COPYRIGHT © 1978, BY ACADEMIC PRESS, INC.
ALL RIGHTS RESERVED.
NO PART OF THIS PUBLICATION MAY BE REPRODUCED OR
TRANSMITTED IN ANY FORM OR BY ANY MEANS, ELECTRONIC
OR MECHANICAL, INCLUDING PHOTOCOPY, RECORDING, OR ANY
INFORMATION STORAGE AND RETRIEVAL SYSTEM, WITHOUT
PERMISSION IN WRITING FROM THE PUBLISHER.

ACADEMIC PRESS, INC.
111 Fifth Avenue, New York, New York 10003

United Kingdom Edition published by
ACADEMIC PRESS, INC. (LONDON) LTD.
24/28 Oval Road, London NW1 7DX

Library of Congress Cataloging in Publication Data

Main entry under title:

Biomembranes.

(Methods in enzymology, v. 52)

Includes bibliographical references.

Pt. C has special title: Biological oxidations: Microsomal,
cytochrome P-450, and other hemoprotein systems.

1. Cell membranes. 2. Cell fractionation.
3. Cell organelles. I. Fleischer, Sidney, ed.
II. Packer, Lester, ed. III. Series.
[DNLM: 1. Cell membrane. W1 ME9615K v. 31 /
QH601 B6193]
QP601 M49 vol. 31-32 [QH601] 574.1'925'08s
ISBN 0-12-181952-3 (v. 52) [574.8'75] 54-9110

PRINTED IN THE UNITED STATES OF AMERICA

gradient. Centrifugation is performed in an SW 27 rotor (Beckman) at 80,000 g for 48 hr. At the end of centrifugation, 5 visible bands are apparent (Fig. 8). The relatively narrow band 1 has a white flaky appearance (density 1.085 g/cm^3). Bands 2 and 3 are finely dispersed, white, and equilibrated at 1.11–1.12 and 1.14–1.15 g/cm^3 , respectively. Fractions 4 and 5 are gray, grainy, and localized at densities 1.18 and 1.20 g/cm^3 , respectively. The enzyme compositions of the five bands are different and show separation of a number of enzyme groups; in these groups the enzymes are functionally related to each other. The first band contains adenosine monophosphatase, inosine diphosphatase, and some glucose-6-phosphatase; band 2 is enriched in the NADH-linked, and band 3 in the NADPH-linked, electron transport enzymes; bands 4 and 5 have glucose-6-phosphatase as their main enzyme component. Deoxycholate inactivates a part of the enzyme activities, and total recoveries cannot be obtained by this procedure. The phospholipid:protein ratio decreases from band 1 to 5 and is 2.51, 1.37, 1.01, 0.38, and 0.11, respectively.

It is not clear what the mechanism of particle formation in detergent-containing gradient is. It appears that deoxycholate liberates membrane fragments, which upon gradient centrifugation equilibrate in different bands. The presence of similar fragments in high concentration within the same band may result in aggregation of these fragments to larger particles.

[6] Preparation of Microsomes with Calcium

By JOHN B. SCHENKMAN and DOMINICK L. CINTI

Isolation of the microsomal fraction of the hepatic cell generally employs a procedure of differential ultracentrifugation.¹⁻³ The usual method normally consists of homogenization of the tissue in a medium such as 0.25 M sucrose, followed by sequential centrifugations at 600 g , 8000–12,000 g , and 105,000 g , the last yielding a pellet designated the microsomal fraction. This method, which had been developed for mammalian liver tissue, has also been employed to obtain "microsomal"

¹ G. H. Hogeboom, W. C. Schneider, and G. E. Palade, *J. Biol. Chem.* 172, 619 (1948).

² W. C. Schneider and G. H. Hogeboom, *J. Biol. Chem.* 183, 123 (1950).

³ G. H. Hogeboom, this series, Vol. 2, p. 16.

fractions from a variety of tissues, such as lung,⁴⁻⁶ kidney,^{7,8} spleen,⁹ adrenals.¹⁰

Other procedures used to isolate microsomes have been developed to replace ultracentrifugation for two main reasons: (1) differential ultracentrifugation requires an expensive ultracentrifuge; (2) it is time consuming, requiring 2 hr of ultracentrifugation. Two methods that have been used to isolate microsomes from the postmitochondrial fraction are acid precipitation¹¹ and gel filtration.¹² The former procedure, while circumventing the above two problems, results in the inactivation of a number of microsomal enzymes, namely, cytochrome P-450, glucose-6-phosphatase, NADH-cytochrome *b₅* reductase, and NADPH-cytochrome *c* reductase. In the latter procedure, i.e., gel filtration, the main disadvantages include the need for several columns, much gel material (Sephadex 2B) and a fraction collector. In addition, time is consumed in the washing and equilibration of the gel, in the preparation of the column(s), and in the elution of the microsomal fraction.

In recent years one of the procedures for microsomal isolation which has been extensively studied and is gaining acceptance in mammalian liver studies is a method involving aggregation of microsomes with calcium.¹³⁻¹⁷ Basically, this involves the addition of Ca^{2+} ions to the postmitochondrial supernatant followed by a short centrifugation at speeds obtainable with most refrigerated centrifuges, such as the Sorvall RC-2B. The microsomal pellet can then be resuspended and washed or used immediately. The use of Ca^{2+} ions to prepare microsomes greatly reduces the time necessary for isolation of this fraction and eliminates the need for an ultracentrifuge.

⁴ D. Garfinkel, *Comp. Biochem. Physiol.* **8**, 367 (1963).

⁵ W. W. Oppelt, M. Zange, W. E. Ross, and H. Remmer, *Res. Commun. Chem. Pathol. Pharmacol.* **1**, 43 (1970).

⁶ J. R. Bend, G. E. R. Hook, R. E. Easterling, T. E. Gram, and J. R. Fouts, *J. Pharmacol. Exp. Ther.* **183**, 206 (1972).

⁷ A. Ellin, S. V. Jakobsson, J. B. Schenkman, and S. Orrenius, *Arch. Biochem. Biophys.* **150**, 64 (1972).

⁸ R. Grundin, S. Jakobsson, and D. L. Cinti, *Arch. Biochem. Biophys.* **158**, 544 (1973).

⁹ R. Tenhunen, H. Marver, N. R. Pimstone, W. F. Trager, D. Y. Cooper, and R. Schmid, *Biochemistry* **11**, 1716 (1972).

¹⁰ D. Y. Cooper, R. W. Estabrook, and O. Rosenthal, *J. Biol. Chem.* **238**, 1320 (1963).

¹¹ R. Karler and S. A. Turkanis, *Arch. Int. Pharmacodyn.* **175**, 22 (1968).

¹² O. Tangen, J. Jonsson, and S. Orrenius, *Anal. Biochem.* **54**, 597 (1973).

¹³ S. A. Kamath, F. A. Kummerow, and K. Ananth Narayan, *FEBS Lett.* **17**, 90 (1971).

¹⁴ J. B. Schenkman and D. L. Cinti, *Life Sci.* **11**, 247 (1972).

¹⁵ S. A. Kamath and K. Ananth Narayan, *Anal. Biochem.* **48**, 53 (1972).

¹⁶ D. L. Cinti, P. Moldéus, and J. B. Schenkman, *Biochem. Pharmacol.* **21**, 3249 (1972).

¹⁷ D. Kupfer and E. Levin, *Biochem. Biophys. Res. Commun.* **47**, 611 (1972).

Reagents

Sodium chloride, 0.9%

Sucrose, 250 mM–10 mM Tris-chloride, pH 7.4

Calcium chloride

Potassium chloride 150 mM–10 mM Tris-chloride, pH 7.4

Procedure

The method to be described applies to livers obtained from rats; application of the Ca^{2+} procedure to other tissues will be discussed separately. Livers from fed or starved (24 hr) Sprague-Dawley rats (200–300 g) are removed and immediately perfused with 0.9% saline to remove the bulk of blood, since hemoglobin interferes with spectral analysis of the microsomal hemoproteins, and has been reported to catalyze certain hydroxylations.^{18,19} The livers are then minced and homogenized in 0.25 M sucrose containing 10 mM Tris-chloride, pH 7.4; the concentration of the liver homogenate can vary from 10% to 25% without any significant effects on the microsomal activities. We have observed that the more dilute the homogenate, the greater is the yield of microsomal protein (Cinti and Schenkman, unpublished observations). The 10–25% homogenate is then centrifuged as shown in Fig. 1 to obtain the postmitochondrial (12,000 g) supernatant. Addition of solid CaCl_2 (8.0 mM final concentration) to the postmitochondrial supernatant allows complete sedimentation of the microsomes at 25,000 g in 15 min. The pellet is then washed by resuspending in an equal volume of 150 mM KCl containing 10 mM Tris-chloride, pH 7.4, by rehomogenization and is resedimented at 25,000 g for 15 min. The resultant pinkish, opalescent pellet of microsomes overlies a small translucent glycogen pellet (in fed rats), from which it is readily separated by tapping the test tube. Shortcuts in this procedure can be taken; for example, if livers are well perfused with NaCl and one is interested only in obtaining microsomes, the liver homogenate may be immediately centrifuged at 12,000 g for 15–20 min; to the resulting supernatant, 8 mM CaCl_2 is added directly, followed by centrifugation at 25,000 g for 15 min.

One can readily modify these procedures further to accommodate centrifuges of lesser speeds by diluting the postmitochondrial supernatant 10-fold from 0.25 M sucrose after addition of calcium. The decrease in viscosity allows the microsomes to sediment out in about 15 min in a flask on ice.¹⁶

¹⁸ J. J. Mieyal, R. S. Ackerman, J. L. Blumer, and L. S. Freeman, *J. Biol. Chem.* **251**, 3436 (1976).

¹⁹ J. R. Gillette, B. B. Brodie, and B. LaDu, *J. Pharmacol. Exp. Ther.* **119**, 32 (1957).

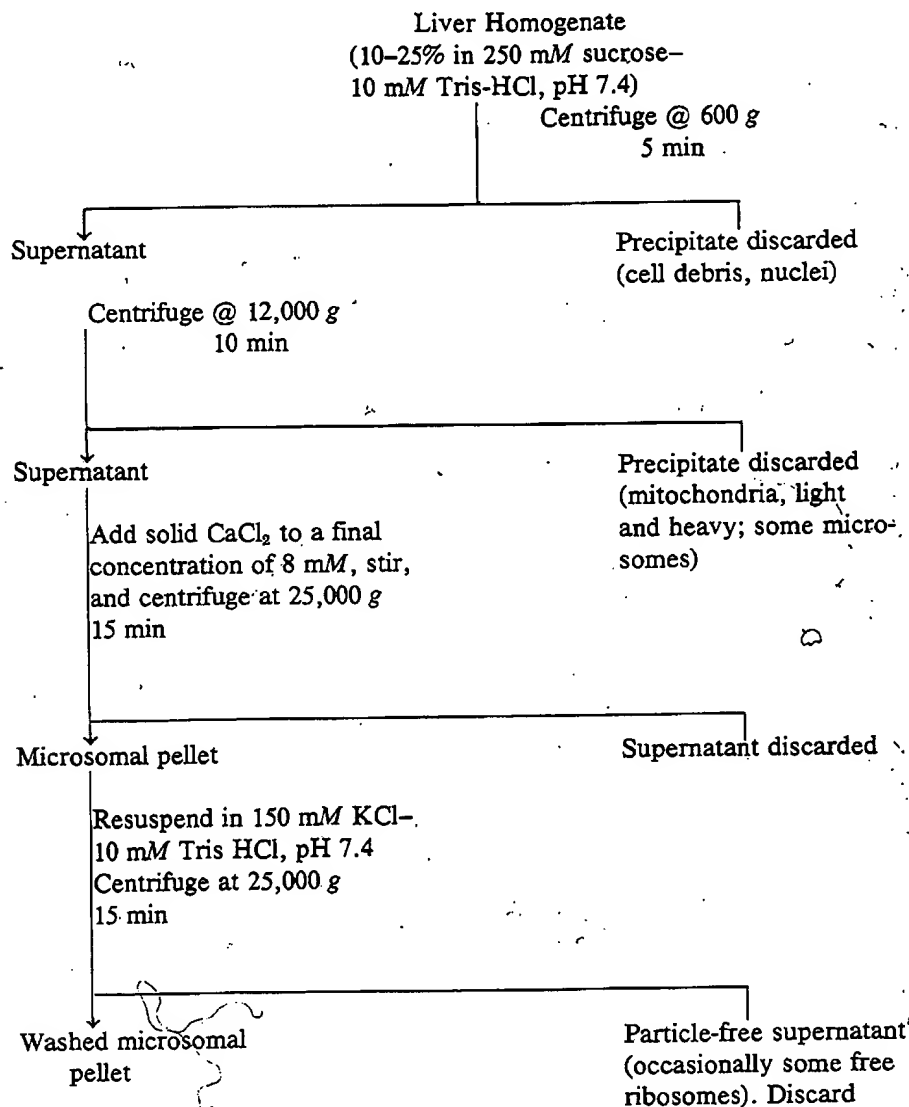


FIG. 1. Flow diagram of procedure for the calcium sedimentation of microsomes. All steps are carried out at 0°-4°.

Role of Ca²⁺ Ions in the Isolation of Subcellular Membranes

The use of divalent cations, such as Ca²⁺, in the isolation of membrane fractions was first reported more than 25 years ago. Schneider and Petermann²⁰ employed Ca²⁺ ions to isolate mouse spleen nuclei, which appeared to be morphologically intact and apparently free of cytoplasm; this was extended to isolation of calf thymus nuclei by

²⁰ R. M. Schneider and M. L. Petermann, *Cancer Res.* 10, 751 (1950).

Allfrey and Mirsky.²¹ The Ca^{2+} ion is particularly effective in preventing nuclear fragmentation and clumping. Sarcoplasmic reticulum vesicles of skeletal muscle also respond to Ca^{2+} , rapidly accumulating it from the medium through the action of a Ca^{2+} -stimulated ATPase.^{22,23}

In 1958, Gross and Pearl²⁴ obtained a pentose nucleoprotein-rich fraction of microsomal origin, upon addition of Ca^{2+} to a rat liver homogenate. Carvalho *et al.*²⁵ reported hepatic microsomes bind both Ca^{2+} and Mg^{2+} . They found that the extent of binding was a function of the cation concentration, with saturation of the microsomal binding sites above 2 mM concentration. These investigators suggested, on the basis of pK_a values, that imidazolium and secondary phosphate groups could be the binding sites for the divalent cations. This cation-binding ability may be the basis for the Ca^{2+} -aggregation of microsomes.¹⁴⁻¹⁷ It has been reported¹⁵ that other divalent cations, like Mg^{2+} , Fe^{2+} , Ba^{2+} , Hg^{2+} , and Zn^{2+} , are also capable of aggregating microsomes, while monovalent and trivalent cations have very little aggregating ability.

Recent studies have shown that rat liver microsomes have the ability to accumulate Ca^{2+} in a manner similar to mitochondria²⁶; this sequestering mechanism appears to differ from the process that causes aggregation, since the former mechanism appears to be energy dependent, requiring specifically ATP and Mg^{2+} ; whereas aggregation does not.

Effect of Ca^{2+} Ions on Microsomal Enzyme Systems

An extensive number of enzymic activities have been examined in microsomes prepared by Ca^{2+} aggregation and compared with the activities in microsomes prepared by older ultracentrifugation procedures. In the table is a list of enzymic activities and other microsomal membrane constituents that are unaffected by the Ca^{2+} aggregation method. Kamath and Narayan¹⁵ reported that aniline hydroxylase and ethylmorphine demethylase activities were somewhat higher in Ca^{2+} -prepared microsomes; however, we have found no differences in these two activities.^{14,16} Montgomery *et al.*²⁷ recently reported that ferritin,

²¹ V. G. Allfrey and A. E. Mirsky, *Proc. Natl. Acad. Sci. U.S.A.* 43, 589 (1957).

²² S. Ebashi, and F. Lipmann, *J. Cell Biol.* 14, 389 (1962).

²³ G. Meissner, *Biochim. Biophys. Acta* 298, 906 (1973).

²⁴ P. R. Gross and W. Pearl, *J. Cell. Comp. Physiol.* 52, 147 (1958).

²⁵ A. P. Carvalho, H. Sanui, and N. Pace, *J. Cell. Comp. Physiol.* 62, 311 (1963).

²⁶ L. Moore, T. Chen, H. R. Knapp, Jr., and E. J. Landon, *J. Biol. Chem.* 250, 4562 (1975).

²⁷ M. R. Montgomery, C. Clark, and J. L. Holtzman, *Arch. Biochem. Biophys.* 160, 113 (1974).

RAT LIVER MICROSOMAL ENZYME ACTIVITIES AND MICROSOMAL MEMBRANE
CONSTITUENTS SHOWN TO BE UNAFFECTED BY Ca^{2+} AGGREGATION

Component	Percent conventional activity	References
Glucose 6-phosphatase	97	15
Inosine diphosphatase	96	15
5'-Nucleotidase	92	^a
Mg^{2+} - Na^{+} - K^{+} -dependent ATPase	98	15
Cytochrome b_5	101	16
NADH-cytochrome b_5 reductase	100	^b
NADH-cytochrome c reductase	102	^b
Cytochrome P-450	107	16
NADPH-cytochrome c reductase	100	16
NADPH-cytochrome P-450 reductase	99	16
Aminopyrine demethylase	96	14
Aniline hydroxylase	106	14
<i>p</i> -Chloro- <i>N</i> -methylaniline demethylase	145, 98	17, 31
Biphenyl-4-hydroxylase	90	31
UDP-glucuronyl transferase	98	31
Tetrahydrocannabinol hydroxylase	145	17
Total lipids	93	15
Phospholipids	101	15
Cholesterol	103	15
RNA	95	15

^a S. A. Kamath and E. Rubin, *Biochem. Biophys. Res. Commun.* **49**, 52 (1972).

^b D. L. Cinti and J. Ozols, *Biochim. Biophys. Acta* **410**, 32 (1975).

which is the major source of nonheme iron, was largely removed from microsomes prepared by Ca^{2+} aggregation. This would agree with our observation (Cinti and Schenkman, unpublished) that lipid peroxidase activity is virtually absent in microsomes prepared by calcium aggregation in the absence of an iron chelate, and would suggest a greater stability to storage of such microsomes. Microsomes precipitated with Ca^{2+} reportedly give lower protein values with two of nine protein assay procedures,²⁸ apparently owing to the inability of dilute NaOH (less than 0.3 N) to adequately dissociate the microsomes.

Application of the Ca^{2+} -Aggregation Method to Other Tissues and Species

The calcium aggregation method cannot be universally applied to all tissues and species. Although mouse hepatic microsomes show the same

²⁸ P. W. Albro, *Anal. Biochem.* **64**, 485 (1975).

p-nitroanisole *O*-demethylase activity, NADPH oxidase activity, and cytochrome P-450 content²⁹ when prepared by this method, as compared with ultracentrifugation techniques, and adrenal, ovaries, and testes microsomal steroid metabolizing activity is likewise unaltered,³⁰ the same is not true with all preparations. For example, microsomes prepared from the abdomen of insecticide-resistant and susceptible house flies, and from the midgut of the southern armyworm, showed significant differences when the two isolation procedures were compared; *O*-demethylation activity, NADPH oxidase activity, and cytochrome P-450 content were greatly diminished in the Ca^{2+} -aggregated preparation.²⁹ Rat and rabbit lung microsomal preparations are apparently also susceptible to harm by Ca^{2+} -aggregation,³¹ since the treatment diminished microsomal NADPH-cytochrome *c* reductase activity, *p*-chloro-*N*-methylaniline demethylase, and biphenyl-4-hydroxylase; these same activities were unimpaired in rat and rabbit kidney.³¹ These observations indicate that, before adapting the calcium aggregation procedure to preparation of microsomes of another tissue or species, it is necessary to first determine whether the method is deleterious.

²⁹ R. C. Baker, L. B. Coons, and E. Hodgson, *Chem.-Biol. Interactions* 6, 307 (1973).

³⁰ A. Warchol and R. Rembiesa, *Steroids Lipids Res.* 5, 113 (1974).

³¹ C. L. Litterst, E. G. Mimnaugh, R. L. Reagan, and T. E. Gram, *Life Sci.* 17, 813 (1975).

[7] Purification and Properties of NADPH-Cytochrome P-450 Reductase¹

By HENRY W. STROBEL and JOHN DAVID DIGNAM

NADPH-cytochrome P-450 reductase, a flavoprotein component of the endoplasmic reticulum of liver and other organs, catalyzes the transfer of electrons from NADPH to cytochrome P-450. Cytochrome P-450 is the terminal oxidase of the drug metabolism system which hydroxylates a variety of compounds, such as alkanes, fatty acids, drugs, and steroids.² Several forms of this hemoprotein have been purified to homogeneity, differing in minimum molecular weight and substrate specificity.^{3,4}

¹ Supported by Grant CA 19621 from the National Cancer Institute and DRG 1258 from the Damon Runyon Memorial Fund.

² B. B. Brodie, J. R. Gillette, and B. N. LaDu, *Annu. Rev. Biochem.* 27, 427 (1958).

³ D. Ryan, A. Y.-H. Lu, S. West, and W. Levin, *J. Biol. Chem.* 250, 2157 (1975).

⁴ D. A. Haugen, T. A. van der Hoeven, and M. J. Coon, *J. Biol. Chem.* 250, 3567 (1975).